PhD thesis

THE MIDBRAIN ORIGIN OF AUDITORY PREDICTIVE PROCESSING AND HOW DOPAMINE MODULATES EARLY PERCEPTION OF SURPRISING SOUNDS

Guillermo Varela Carbajal

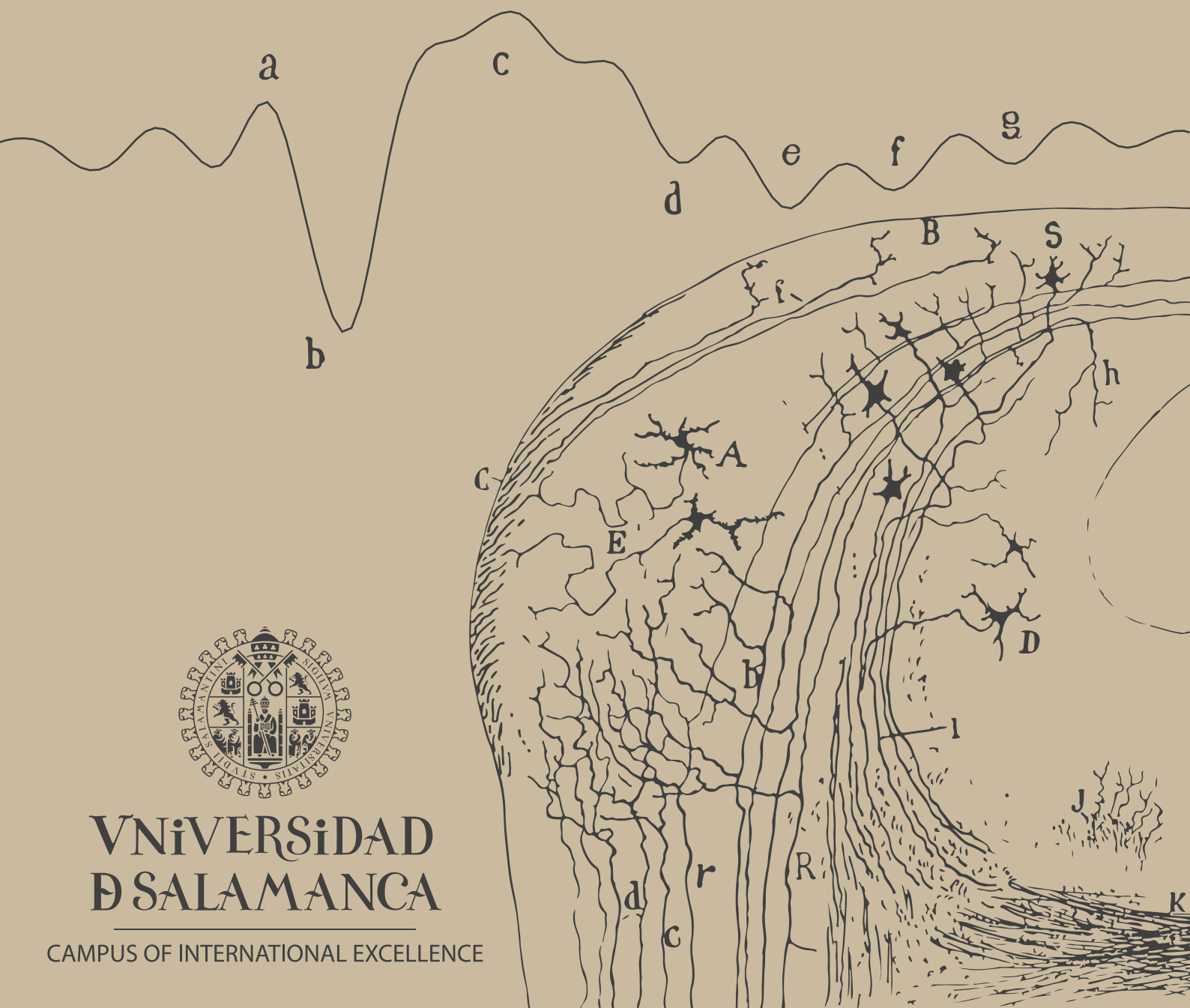

VNiVERSiDAD D SALAMANCA

CAMPUS OF INTERNATIONAL EXCELLENCE

University of Salamanca
Institute of Neuroscience of Castile and Leon
Auditory Cognitive Neuroscience Laboratory

THE MIDBRAIN ORIGIN OF AUDITORY PREDICTIVE PROCESSING AND HOW DOPAMINE MODULATES EARLY PERCEPTION OF SURPRISING SOUNDS

El origen mesencefálico del procesamiento predictivo en la audición y cómo la dopamina modula tempranamente la percepción de los sonidos inesperados

Thesis submitted by

GUILLERMO VARELA CARBAJAL

to obtain the degree of

Doctor in Neuroscience

and the

International Doctor Mention

Supervised by
Prof. Malmierca S. Malmierca, M.D., Ph.D.
David Pérez González, Ph.D.

Supported by:

GOBIERNO DE ESPAÑA
MINISTERIO DE CIENCIA E INNOVACIÓN

Erasmus Mundus

Salamanca, May 2021

Dr. Manuel Sánchez Malmierca, catedrático del Departamento de Biología Celular y Patología de la Universidad de Salamanca y director del Instituto de Neurociencias de Castilla y León.

Dr. David Pérez González, investigador postdoctoral del Instituto de Neurociencias de Castilla y León.

CERTIFICAN

que la tesis doctoral titulada:

The midbrain origin of auditory predictive processing
and how dopamine modulates early perception of surprising sounds

ha sido redactada en inglés y contiene un resumen en español que describe el trabajo de investigación realizado por D. Guillermo Varela Carbajal bajo nuestra dirección durante los últimos 4 años.

Esta memoria recoge un análisis detallado y exhaustivo de la contribución mesencefálica al procesamiento predictivo en la audición, así como de la modulación que sobre este ejerce el sistema dopaminérgico. Los datos presentados en esta memoria constituyen una aportación original y podemos afirmar que ponen de manifiesto un gran avance y progreso en el área de la Neurociencia.

Por todo ello, consideramos que esta tesis reúne la calidad y rigor científico necesarios para que sea defendida en la Universidad de Salamanca como requisito para que D. Guillermo Varela Carbajal opte al título de 'Doctor con mención de Doctor Internacional' por la Universidad de Salamanca.

Y para que así conste, firmamos el presente certificado.

En Salamanca, a 24 de mayo de 2021,

Dr. Manuel Sánchez Malmierca Dr. David Pérez González

e il naufragar
m'è dolce
in questo mare

a Ana

A quienes me alentaron, guiaron, asistieron, ampararon y acompañaron durante parte o toda esta ardua trinquetada por los confines del conocimiento...

· GRACIAS · MERCI · THANKS ·

A mis abuelas y abuelos, por legarnos su cultura del esfuerzo y su apuesta por el saber.

A mi madre y mi padre, por su inquebrantable fe en mis capacidades y mis decisiones.

A mi tío Antonio, por tejer las alas de mis proyectos más arriesgados.

A mi hermana, Carlos y Drusco, los guardianes de las esencias.

A Elías Monreal y Óscar Lecuona, los flotadores en un barco que hace aguas.

A Eduardo García-Garzón y Alberto Angosto, los acicates de mi pundonor.

A Alba Espina, por mostrarme lo verdaderamente importante.

Au Dr Alexandre Lehmann, pour m'avoir internationalisé.

À Marjorie Ludet, Alexis Myr, Marie-Anne Prud'homme, Ignacio Spiousas et Marcel Farrés, amis dans un pays étranger.

A la buena gente de INNOVA Salamanca, FJI-Precarios y Eurodoc, por resistir siempre.

To Drs Eva Hnatkova and Giulia Malaguarnera, for showing their empathy and kindness when it is most desperately needed.

Al Dr Enrique Saldaña, por enseñarme a escribir mejor ciencia.

A los Drs Flora Antunes y Camilo J Morado-Díaz, por compartir conmigo su veteranía.

A María Torres y Antonio Rivas, por su diligente y muy apreciado apoyo técnico.

Al Dr Javier Nieto-Diego, por guiar mis primeros pasos e inspirar los siguientes.

A los Drs David Pérez-González, Catalina Valdés-Baizabal y Gloria G Parras, por descubrirme mis talentos y compensar mis debilidades.

A mi compañera de fatigas, Lorena Casado-Román, por su complicidad.

A mi compañera de vida, Ana Peleteiro-Vigil, por el plan.

Y por último, a mi maestro, el Dr Manuel S Malmierca, por confiarme esta oportunidad.

* * * * * GRACIAS A TODOS * * * * *

TABLE OF CONTENTS (click & go)

ABSTRACT

The predictive processing framework comprises neurobiologically-informed models of cortical function. These models consist of hierarchical neural networks arranged in several levels of processing. Higher-order levels develop expectations that try to predict and inhibit the input from lower-order levels. In turn, lower-order levels signal prediction errors to higher levels when their expectations about incoming input are not met. The main aim of this thesis is to demonstrate that predictive processing in the auditory system does not begin at the level of the cerebral cortex, but as deep as in the midbrain. Auditory oddball paradigms, in combination with no-repetition controls, were presented to anesthetized rats and awake mice while performing extracellular recordings in the inferior colliculus, in order to find traces of prediction error signaling that could not be accounted for by sheer stimulus-specific adaptation. In addition, dopaminergic agonists and antagonists were applied by means of microiontophoresis in order to test how D_2-like receptors mediate the modulation of surprise responses in the neurons of the cortex of the inferior colliculus. Results confirmed that auditory midbrain neurons generate genuine prediction error signals, which expected precision is encoded by dopaminergic projections from the subparafascicular nucleus of the thalamus to the cortex of the inferior colliculus. Hence, the inferior colliculus is the first station capable of implementing predictive processing in the ascending auditory pathway.

KEYWORDS

MMN/mismatch negativity, SSA/stimulus-specific adaptation, IC/inferior colliculus, dopamine, deviance detection, repetition suppression, prediction error, predictive processing, novelty perception, surprise processing

LIST OF ABBREVIATIONS

4V: fourth ventricle
A1: primary auditory field
AAF: anterior auditory field
ABR: auditory brainstem response
AC: auditory cortex
AEP: auditory evoked-potential
AMPA: α-amino-3-hydroxy-5-methyl-4-isoxazolepropionic acid
ANOVA: analysis of variance
Aq: aqueduct of Sylvius
Cb: cerebellum
cic: commissure of the inferior colliculus
CN: cochlear nucleus
CNIC: central nucleus of the inferior colliculus
CSI: common stimulus-specific adaptation index
DCIC: dorsal cortex of the inferior colliculus
DCN: dorsal cochlear nucleus
DEV: deviant condition
DNLL: dorsal nucleus of the lateral lemniscus
DRN: dorsal raphe nucleus
ECIC: external cortex of the inferior colliculus
EEG: electroencephalography
Ep: ependyma
FDR: false discovery rate
FFR: frequency following responses
fMRI: functional magnetic resonance imaging
FRA: frequency response area
GABA: γ-aminobutyric acid
IC: inferior colliculus
ICx: inferior colliculus cortex
iMM: index of neuronal mismatch
INLL: intermediate nucleus of the lateral lemniscus
iPE: index of prediction error
iRS: index of repetition suppression
LC: locus coeruleus
LCIC: lateral cortex of the inferior colliculus
LDT: laterodorsal tegmental nucleus
LFP: local field potential
LFP: local field potential
LLR: long-latency responses
LSO: lateral superior olive
MGB: medial geniculate body
MGD: dorsal division of the medial geniculate body
MGM: medial division of the medial geniculate body
MGV: ventral division of the medial geniculate body
MLR: middle-latency responses
MMN: mismatch negativity
MSO: medial superior olive
MUA: multiunit activity
n.s.: non-significant

NLL: nucleus of the lateral lemniscus
NMDA: N-methyl-d-aspartate
NRC: no-repetition control/condition
PAF: posterior auditory field
PAG: periaqueductal grey
PE: prediction error
PE-LFP: prediction error potential
PFC: prefrontal cortex
PP: predictive processing
PPT: pedunculopontine tegmental nucleus
PSTH: peristimulus histogram
RCIC: rostral cortex of the inferior colliculus
ReIC: recess of the inferior colliculus
SC: superior colliculus
SEM: standard error of the mean
SFD: spike-density function
SFR: spontaneous firing rate
SNR: signal-to-noise ration
SOC: superior olivary complex
SPF: subparafascicular nucleus
SPL: sound pressure level
SPO: superior paraolivary nucleus
SRAF: suprarhinal auditory field
SSA: stimulus-specific adaptation
STD: standard condition
SUA: single-unit activity
VAF: ventral auditory field
VCN: ventral coclear nucleus
VNLL: ventral nucleus of the lateral lemniscus
VTz: ventral nucleus of the trapezoid body

I.- INTRODUCTION

Why do surprising sounds automatically stand out from others in our perception? Modern cognitive neuroscience has been pursuing the answer for at least half a century now, addressing the question from a prevailingly corticocentric approach. After 4 years of intense scientific work and several publications on the matter (Carbajal & Malmierca, 2018a, 2020, 2018b; Casado-Román, Carbajal, et al., 2020; Malmierca, Carbajal & Escera, 2019; Parras et al., 2017; Pérez-González et al., 2020; Valdés-Baizabal, Carbajal, et al., 2020), I here propose a thesis that aims to shift our current understanding on how the brain identifies novelty in what we hear, zooming out from the cerebral cortex in order to afford more focus to subcortical players. Furthermore, my thesis implicates dopamine in the sensory process that bestows novelty on auditory percepts, thereby extending the classic interpretation of dopaminergic function, traditionally defined in hedonic terms of pleasure and reinforcement. All these aspirations will be substantiated under the somewhat neo-Kantian notion of predictive processing (PP; Friston, 2005; Rao & Ballard, 1999). On the foundations of cybernetic theory (Ashby, 1960), the PP framework regards the brain as a Helmholtz machine (Dayan et al., 1995), driven by a constant endeavor to generate the most accurate representation of the world by means of Bayesian inference (Clark, 2016; Friston et al., 2006; Hohwy, 2013).

In this opening block, I will provide the reader with a gentle introduction to all the core tenets and concepts necessary to understand the full extent and scope of my proposal. First, I will explore from a neurological standpoint the challenging task of transducing acoustic waves into auditory sensations, and then transforming those into useful auditory percepts. Then, I will describe the general characteristics of the 2 main biomarkers of novelty perception: the large-scale mismatch negativity (MMN) and the microscopic stimulus-specific adaptation (SSA). Finally, I will discuss the 3 major currents of thought regarding novelty perception: (1) the *Detection Hypothesis*, a cognitive approach derived from the study of the MMN (Näätänen, 1990; Näätänen & Michie, 1979); (2) the *Adaptation Hypothesis*, a neurophysiological interpretation based on SSA data (May & Tiitinen, 2010; Mill et al., 2011); and (3) the *Expectation Hypothesis*, a recent integrative explanation offered by the PP framework (Carbajal & Malmierca, 2020; Garrido et al., 2009). Ultimately, this thesis can be understood as an effort to assess the eligibility of these 3 theoretical accounts attempting to explain how we perceive novelty in the sound.

I.1.- THE AUDITORY SYSTEM: A GENERAL OVERVIEW

Before we fully delve into the neural mechanisms that encode surprise in audition, I estimate convenient to provide the reader with a hitchhiker's guide to the auditory system. Speaking in the most practical terms, if right now a dog barked in our surroundings, which would be the obligatory body parts that acoustic signal would need to traverse, and what basic processing those barks would need to undergo in order to be heard by us?

I.1.a.- Auditory sensation: from mechanical energy to electrochemical signals

Each bark produces a sound that travels through the air in all directions in the form of a pressure wave. Unlike light, this mechanical energy that requires a medium to travel, something that determines the design of the 3 functional divisions of the peripheral auditory system that lie inside the temporal bone of our skull: the outer, middle and inner ear. In the outer ear, the pinna or auricle and the external auditory canal steer the propagation of the pressure wave through the air towards the tympanic membrane or eardrum, which lays at the end of the ear canal (Figure 1A). When the pressure wave from the bark hits the tympanic membrane, it starts vibrating a certain number of times per second with a certain magnitude of displacement. The number of eardrum vibrations per time units encodes the frequency of the sound wave, what we will eventually perceive as pitch. The magnitude of each vibration encodes the amplitude of the sound wave, what we will eventually perceive as loudness.

Within the middle ear, this mechanical energy is conveyed by 3 tiny bones known as the ossicles. The malleus or hammer is attached to the tympanic membrane, passing the vibration to the incus or anvil, which in turn relays it to the stapes or stirrup (Figure 1A). At the end of the middle ear, the stapes is attached to the oval window, a membrane-covered opening to the liquid-filled cochlea of the inner ear. As every diver has experienced, most of the sound travelling through the air is just reflected when it comes into contact with a liquid medium. Therefore, if the tympanic membrane were directly connected to the cochlea instead of via ossicles, the sound energy transmitted to the inner ear would be very scarce, and every hearing being would be losing a great proportion of acoustic information. At best, we would hear the bark very muffled, as if we had our heads submersed in water. The action of the ossicles can be understood as those of two interconnected levers —malleus and incus— and a piston —stapes— that transmit sound energy from a vibrating tympanic membrane to an oval window 15 times smaller. The resultant pressure gain in the middle ear ensures that the acoustic

impedance of the air in the outer ear matches to that of the liquid in the inner ear, thus implementing an efficient transfer of sound energy from the former medium to the latter.

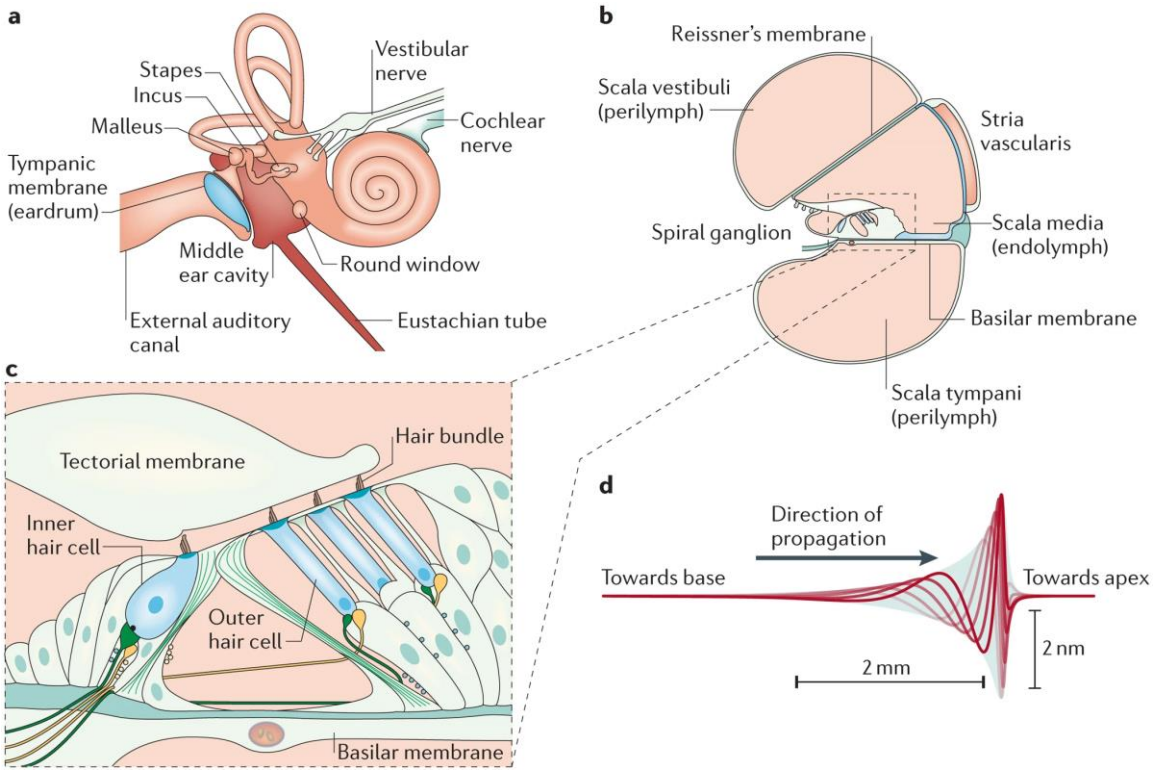

Figure 1. Essential anatomy of auditory sensation. A. Schematics of the peripheral auditory system. **B.** Cross-section diagram of the cochlea showing the 3 scalae, which are separated by 2 elastic partitions: Reissner's membrane and the basilar membrane. The somata of the afferent neurons that innervate hair cells lie in the spiral ganglion. **C.** Organ of Corti. **D.** When the cochlea is excited by sound, the back-and-forth motion of the stapes produces alternate increases and decreases in the pressure of the liquid at the base of the scala vestibuli. The pressure difference across the basilar membrane elicits a series of travelling waves that progress along the cochlea. Reproduced from Hudspeth (2014).

The inner ear houses the cochlea, a coiled structure of progressively diminishing diameter akin to the shell of a snail that contains 3 liquid-filled ducts: the scala vestibuli on top, the scala tympani at the base, and the scala media in between (Figure 1B). The scala vestibuli goes from the oval window to the helicotrema, where it communicates with the scala tympani, slightly below the cochlear apex. The scala tympani goes from the helicotrema to the round window of the cochlea. The round window is sealed by a membrane that vibrates with opposite phase to the vibrations entering the inner ear through the oval window, due to the displacement of the perilymph that fills both vestibuli and tympani scalae. The thin Reissner's membrane

separates the scala vestibuli from the scala media, and the elastic basilar membrane separates the scala media from the subjacent scala tympani (Figure 1B). The stiffness of the basilar membrane varies in a continuum along the length of the cochlea, endowing each section with a distinct resonant frequency, i.e., the frequency at which the membrane can oscillate at maximum amplitude (Robles & Ruggero, 2001; Slepecky, 1996). At the base of the cochlea, the basilar membrane is thicker and tauter, so it resonates with higher frequencies. As the basilar membrane becomes increasingly floppier towards the cochlear apex, it resonates with correspondingly lower frequencies, in a pattern akin to an inverted piano (von Békésy, 1960). This spatial arrangement of frequencies results in a hydromechanical frequency analyzer, i.e., a biological mechanism to perform a Fourier transform, decomposing complex pressure waves into a sum of simple harmonic functions (Nobili et al., 1998). In plain words, the resultant tonotopic map allows the cochlea to compute the sound of the bark as a distribution of pure tones of one frequency and amplitude each (Figure 1D). Henceforth, this tonotopy will become a central principle in the organization of the auditory nervous system (Merzenich et al., 1975; Merzenich & Reid, 1974).

The true auditory receptor organ can be found in the scala media, submersed in potassium-rich endolymph (Figure 1C). The organ of Corti is an epithelial ridge extending over the basilar membrane that performs an mechanoelectrical transduction of the perilymphatic pressure waves (Dallos, 1992; Slepecky, 1996). The human organ of Corti contains 3 rows of outer hair cells and 1 row of inner hair cells, all of which present characteristic stereocilia at their apical end. Stereocilia in adjacent rows are connected by cadherin filamentous structures called tip links, which are attached to stretch-gated cation channels in the hair cell membrane (Müller, 2008). Over them, a gelatinous strip called tectorial membrane is attached at its bottom surface to the tips of the longest stereocilia in the hair bundles of outer hair cells. Movement of the tectorial membrane relative to the bundles accordingly deflects the outer hair cell bundles. The hair bundles of inner hair cells are instead deflected by motion of the liquid beneath the tectorial membrane (Russell, 1983). When —and where— the basilar membrane resonates with the perilymphatic pressure waves, oscillations move the stereocilia, pulling or loosening the tip links, which in turn open or close the stretch-gated cation channels, thereby producing changes in the membrane potential of both types of hair cells (Figure 2). On the one hand, the outer hair cells contain a transmembrane protein called prestin that confers electromotility on their cellular membrane, which elongates or contracts longitudinally due to changes in the membrane potential. When the outer hair cells depolarize, prestin shortens and pulls on the

basilar membrane, increasing its action on the inner hair cells. Conversely, when the outer hair cells hyperpolarize, prestin lengthens and eases tension on the inner hair cells (Howard et al., 1988; Markin & Hudspeth, 1995; Pickles & Corey, 1992). Thus, the outer hair cells work as a dynamic amplifier that enhances the amplitude and frequency selectivity of basilar vibrations using electromechanical feedback. In this way, the organ of Corti can modify the auditory input signal before it reaches the brain (Hudspeth, 1997, 2014). On the other hand, potassium and calcium ions flowing into the inner hair cells open their voltage-gated calcium channels. At the basolateral end of the inner hair cells, the resultant receptor potential releases glutamate to ribbon synapses with the afferent fibers of the cochlear nerve (Dallos, 1992; Hudspeth, 2014; Slepecky, 1996). Now, the acoustic information of the bark has been completely transduced into electrochemical signals, the code that the neurons of our brain use to process and represent the external world. But we are not *hearing* the bark yet, we have just *sensed* it.

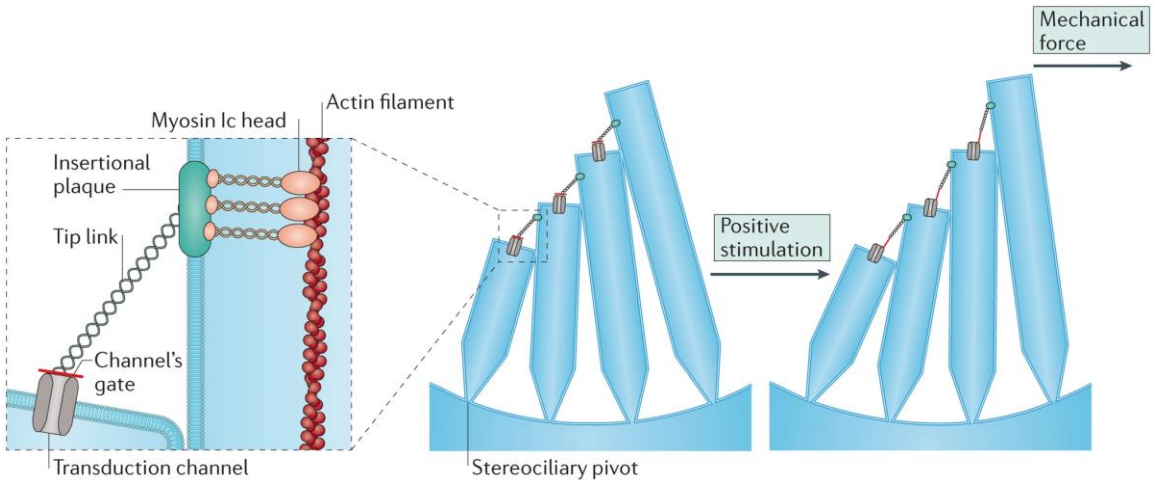

Figure 2. Hair cell bundle movement. At the top of the hair bundle there is a transduction element connected by a tip link to adjacent stereocilia (left diagram). The lower end of the link is connected to mechanically sensitive channels, while the upper end terminates at the insertional plaque. When a mechanical stimulus deflects a hair bundle in the positive direction (right diagram) towards its longest stereocilia, the stereocilia pivot at their basal insertions but remain in contact with one another near their tips. The resultant shearing motion between contiguous stereocilia increases the tension in the tip link that extends from the top of each short stereocilium to the insertional plaque on the side of the tallest adjacent stereocilium. This enhanced tension increases the probability that the channels at the link's lower insertion will open. Ionic current, carried predominantly by potassium but including calcium cations, then enters the stereocilium, depolarizes the hair cell and triggers the release of glutamate at the ribbon synapses on the cell's basolateral surface. Reproduced from Hudspeth (2014).

I.1.b.- Auditory perception: from electrochemical signals to hearing

A dog has barked in our surroundings, and the pressure wave it produced in the air has been mechanically caught by our sensors. Those physical signals were transduced into electrochemical impulses operable by the brain, in a process called *sensation*. However, we have not *perceived* the bark yet. At this stage, we are not hearing anything, as our brain has merely received the electrochemical output signal of a Fourier transform performed by the cochlea. Could you distinguish a bark from any other sound, or locate where the dog is barking from, just by looking at its spectrogram? That is precisely the function of *perception*: to make sense out of the incoming sensory signal. Perception organizes inputs, identifies patterns and interprets our sensations, establishing which action potential corresponds to each acoustic element and which of those are meaningful to our states and goals.

Auditory perception in particular is an extremely complex process due to the very nature of the sound and the demanding requirements of auditory scene analysis. This complexity becomes apparent when we inspect the high degree of specialization that can be found in the neuroanatomy of the auditory central nervous system. As the subcortical processing of sound will be the main topic of this thesis, let me illustrate my point by comparing the number of stations that sensory information must go through from receptor to the corresponding cortex in 3 different sensory modalities. Despite vision being our dominant sense, the retina and the visual cortex connect via just 1 relay: the lateral geniculate body of the thalamus. Between the mechanoreceptors of our skin and the somatosensory cortex there are 2 subcortical nuclei: the cuneate nucleus and the ventral posterior thalamus. In contrast, between the cochlea and the auditory cortex (AC) there are no less than 5 major processing centers: the cochlear nuclear complex (CN), the superior olivary complex (SOC), the nuclei of the lateral lemniscus (NLL), the inferior colliculus (IC) and the medial geniculate body (MGB) of the thalamus. Moreover, the auditory central nervous system is comprised of many parallel processing pathways forming manifold routes of information convergence and divergence, with ascending and descending projections that implement feedback loops. Evolutionary logic dictates that natural selection would have favor a more efficient, direct fiber connection instead of this intricate network in case any of these extra stages of subcortical processing were not absolutely essential to hear properly. An exhaustive review of the morphology and function of the auditory central nervous system is beyond the scope of this thesis, as all the original data I will present later were obtained in the IC. Nevertheless, since the IC is but one piece within a

holistic processing machine, having the big picture will be very helpful down the line to better understand the full significance of my results. Hence, let me quickly render a flavor of how our brain transforms a meaningless deluge of electrochemical signals into the coherent representation of a dog barking in a specific position within our surroundings.

I.1.c.- Multiple specialized processing pathways in the auditory brainstem

The auditory system differs from most other sensory modalities in that the location of stimuli is not conveyed by the spatial arrangement of the afferent pathways. Instead, the location and identification of sounds is constructed from patterns of frequencies mapped at the 2 ears as well as from their relative intensity and timing. The auditory system is endowed with an exquisite temporal sensitivity, capable of detecting time differences as small as 10 μs. This enables our brain to locate the direction of the sound with precisions of 1º. As our heads usually screens one of our ears from the sound —i.e., head shadowing—, the auditory system can also use intensity differences between our 2 ears to locate the origin of the pressure wave in the horizontal plane. Regarding sounds with wavelengths that are close to or smaller than the dimensions of our head, our shoulders and our characteristically-shaped auricles interact with those body parts to produce constructive and destructive interferences. With the information from 1 ear, the auditory system can apply spectral filtering to locate the source of those sound in the vertical plane. The auditory nuclei of the brainstem are endowed with specialized neuronal types and neuroanatomical arrangements necessary to perform the refinement of the signal that will allow us to locate almost instantly where the dog is barking from.

After the transduced auditory signal leaves the cochlea, the first station of the ascendint auditory pathway is the CN (Irvine, 1986b; Malmierca, 2015). The cochlear nerve spreads in a tonotopic organization as soon as it enters the CN (Lorente de No, 1926, 1933; Ramón y Cajal, 1904), innervating different types of neurons with very characteristic and well-defined morphologies and physiologic properties (Figure 3). Each neuronal type processes a separate aspect of the signal and relay it to the next processing stage in the ascending auditory pathway (Harrison & Feldman, 1970). In the ventral division of the CN (VCN), the transduced auditory input from the bark reaches 3 major types of neurons, all intermingled (Harrison & Irving, 1965, 1966; Harrison & Warr, 1962). The *bushy cells* are involved in the detection of interaural intensity differences and project bilaterally to the SOC. Thanks to their tonotopic arrangement, the *stellate cells* are able to encode the spectral properties of the signal and relay them to the

ipsilateral dorsal division of the CN (DCN), the contralateral ventral division of the NLL (VNLL) and other auditory nuclei. The *octopus cells* detect onset transients and periodicity in the auditory signal, conveying that information to the contralateral VNLL in a process that is critical for the eventual recognition of sounds. In the laminated DCN , *fusiform cells* integrate

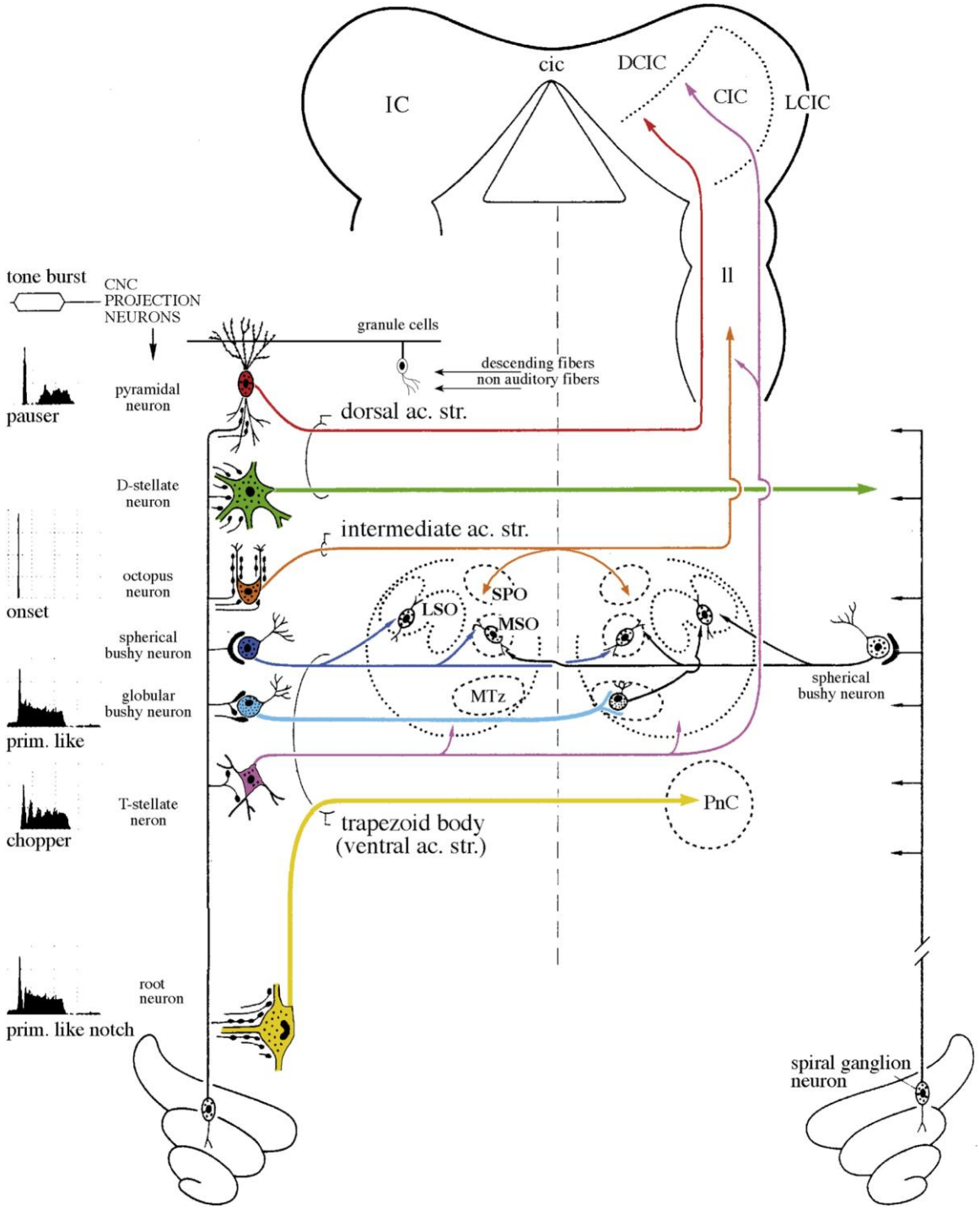

Figure 3. Main projecting cell types of the rat CN. Each cell type exhibits a characteristic response pattern, which is represented in the left. Reproduced from Malmierca (2015).

somatic information from the vestibular system with auditory input from the cochlea to identify spectral cues for localizing sounds (Brawer et al., 1974; Osen, 1969).

The SOC comprises multiple auditory nuclei that combine information from both ears to locate the source of the sound applying distinct methods in 2 separated main circuits (Irvine, 1986c; Malmierca, 2015). In order to pin down the location of lower-frequency sounds, the medial superior olive (MSO) computes the interaural time differences (Grothe et al., 2019), whereas for higher frequencies, the lateral superior olive (LSO) detects the interaural intensity differences resulting from head shadowing (Friauf et al., 2019). Besides contributing to sound location, the circuit formed between the superior paraolivary nucleus (SPO) and the medial nucleus of the trapezoid body is capable of encoding episodes of diminished stimulus energy, such as gaps and the falling flanks of an amplitude modulation, by producing short and precisely timed bursts of inhibition that presumably impose a temporal structure on neural activity in the IC and MGB (Kadner et al., 2006; Kadner & Berrebi, 2008). The SPO is particularly well suited to encode rhythmic sound patterns and information on temporal periodicity that is likely important for detecting communication cues, such as the acoustic envelopes of vocalizations and speech signals (Felix et al., 2011). The SOC receives significant descending projections from the IC, which mainly target the ventral nucleus of the trapezoid body (VTz) in the periolivary region (Warr & Beck, 1996). These descending projections from the IC may be involved in the activation of SOC neurons that innervate the hair cells of the cochlea (Rajan, 1990; Vetter et al., 1993). Olivocochlear projections create a feedback loop from the SOC to the hair cells that balances the excitability of the cochlear nerve, thereby adjusting the auditory input signal (Elgoyhen et al., 2019).

The NLL also form 3 distinctive streams of auditory information (Felmy, 2019). The VNLL processes information coming mainly from the contralateral ear, so it is considered to perform monaural processing of temporal features of the sound. It is important to mention that the VNLL is a major supplier of inhibition to the ipsilateral IC (González-Hernández et al., 1996), releasing both glycine and γ-aminobutyric acid (GABA), although it contains excitatory neurons as well (Figure 4; Kelly et al., 2009; Riquelme et al., 2001). The intermediate NLL (INLL) hosts both monoaural and binaural auditory neurons that integrate information across different sound frequencies. The INLL target the ipsilateral IC with both excitatory and inhibitory projections (Felmy, 2019). The dorsal NLL (DNLL) receives information from both ears, playing a role in the binaural location of the sound (Felmy, 2019). The DNLL sends

mainly GABAergic projections to both the ipsilateral and contralateral IC (Figure 4; González-Hernández et al., 1996; Kelly et al., 2009).

In conclusion, the CN origins many parallel ascending pathways dedicated to process different aspects of sound: frequency composition, loudness, spectral patterns, temporal patterns, position in space, etc. This parallel processing continues in the SOC and the NLL combining information from both ears, before all the aforementioned streams converge and integrate in the IC of the midbrain (Irvine, 1986a, 1992; Malmierca, 2015).

I.1.d.- The Inferior Colliculus (IC): convergence and integration in the midbrain

In the dorsal portion of the midbrain, located just rostral to the cerebellum, there are 4 rounded swellings arranged in pairs, collectively known as the corpora quadrigemina. The rostral pair is called the superior colliculi (SC), which are involved in multisensory integration, exchanging sound location information with the IC, as well as with the visual and somatosensory systems (Doubell et al., 2000). There, binaural sound cues and the monaural spectral cues merge with visual and somatosensory information to create an auditory map in which neurons are tuned to specific sound directions. Hence, the SC is critical form reflexive orienting movements of the head and eyes to acoustic and visual cues in space (Oliver & Huerta, 1992). The caudal pair is known as the inferior colliculi, and constitutes an almost obligatory station for auditory input in its way to the cortex. All major ascending auditory pathways converge in the IC before innervating the MGB and the AC (Malmierca, 2004). However, the IC is much more than a simple relay. A great deal of excitatory, inhibitory and neuromodulatory projections coming from lower and higher auditory nuclei and some extra-auditory nuclei (Figure 4), together with an extensive intrinsic connectivity, make the IC a prominent center for convergence, processing and integration (Malmierca, Carbajal & Escera, 2019). Since the IC provides the electrophysiological data for my thesis, this section will explore the neuroanatomical characteristics of the IC with finer detail and more specificity than for the rest of auditory nuclei.

In the case of rodents, the model species chosen for my experiments, the IC is the largest structure of the auditory system. Each rat IC counts half a million glutamatergic, glycinergic and GABAergic neurons contained in an ellipsoid shape of 3.5 mm by 2 mm diameters, slightly tilted towards the caudomedial direction (Figure 5). More precisely, the long axis is oriented from ventral, lateral and rostral to dorsal, medial, and caudal, forming an angle of about 15º in

the frontal plane and 45º in the sagittal plane (Faye-Lund & Osen, 1985). The IC receives direct ascending projections from most of the lower auditory nuclei (J. C. Adams, 1979), such as the CN (Malmierca et al., 2005; Oliver, 1984b, 1987), the SOC (Shneiderman & Henkel, 1987;

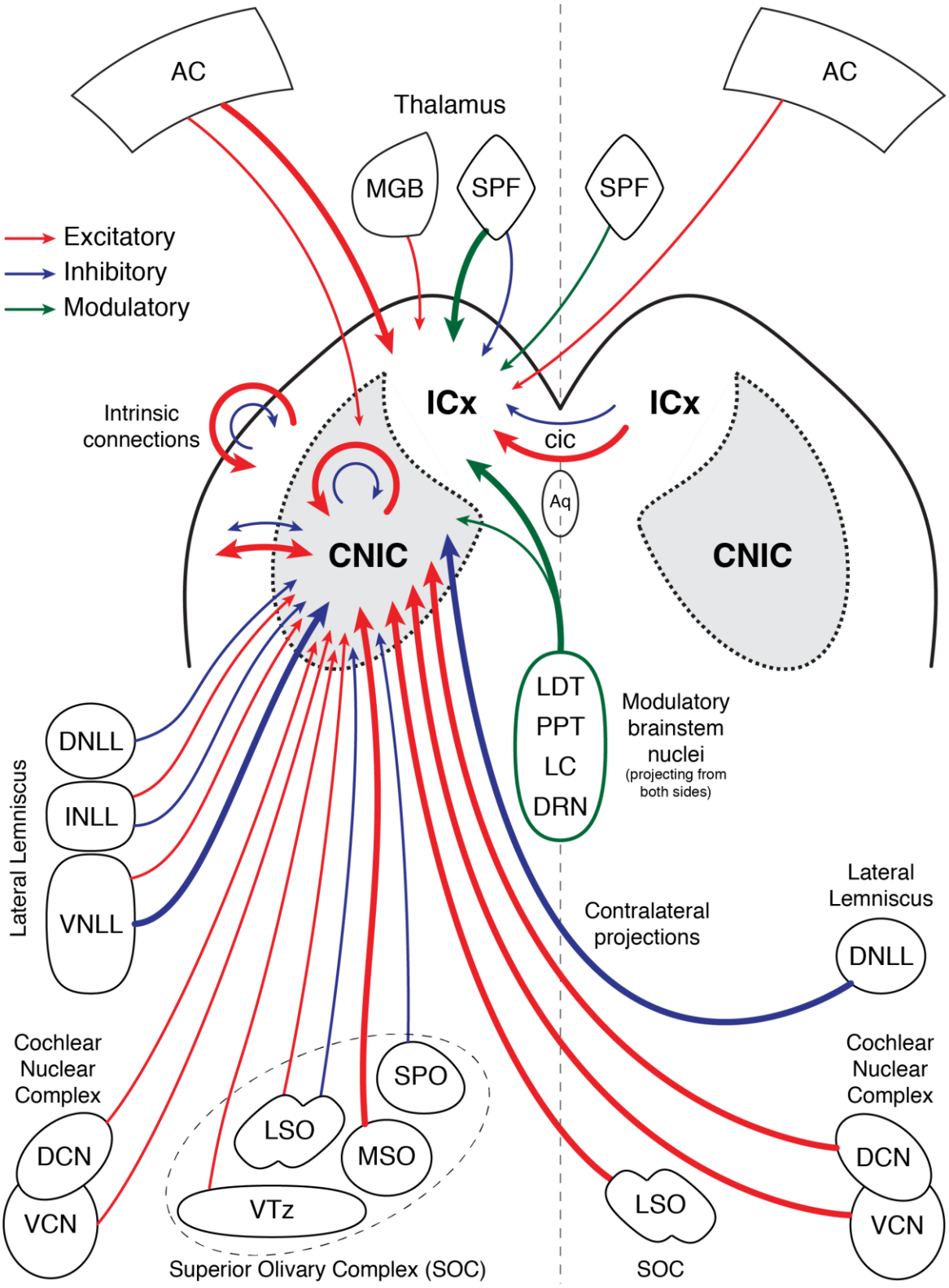

Figure 4. Main afferences of the IC. Thicker arrows represent relatively denser innervation.

Warr & Beck, 1996) and the NLL (Malmierca et al., 1998; Merchán et al., 1994; Merchán & Berbel, 1996), as well as rich cortical and thalamic projections (Figure 4; Andersen, Snyder, et al., 1980; Bajo et al., 2007; Bajo & Moore, 2005; Beyerl, 1978; Coleman & Clerici, 1987; Diamond et al., 1969; Druga et al., 1997; Druga & Syka, 1984; Faye-Lund, 1985; Games & Winer, 1988; Herbert et al., 1991; Krieg, 1947; Malmierca & Ryugo, 2011; Saldaña et al., 1996; W. H. Thompson, 1901; Vaudano et al., 1991; Winer et al., 1998, 2002). The IC also presents dense intrinsic connections (Ito et al., 2018; Malmierca et al., 1995; Saldaña & Merchán, 1992), and connects to the contralateral IC by a commissure (cic) that crosses the midline over the aqueduct of Sylvius (Aq; Figure 4; L. M. Aitkin & Phillips, 1984; Coleman & Clerici, 1987; Malmierca et al., 1995; Rees & Orton, 2019; Saldaña & Merchán, 1992). From the lateral part of each IC emerges a tract of fibers that innervates the MGB (Oliver, 1984a) via which the thalamus receives most of its ascending auditory input (Malmierca et al., 2002). There are also some descending projections from the IC to the lower auditory nuclei of the brainstem (Caicedo & Herbert, 1993; Herbert et al., 1991; Malmierca et al., 1996; Malmierca & Ryugo, 2011).

In line with the original description by Ramón y Cajal (1902; Figure 6), the IC is commonly divided in a central nucleus (CNIC) and a peripheral region or cortex (ICx). Most morphology studies have focused in the CNIC, so its neuronal types and inputs are better understood than those of the ICx (Ito et al., 2018; Malmierca et al., 2011; Oliver, 2005). Neurons in the CNIC receive massive tonotopic innervation from the lower auditory nuclei in the brainstem (Figure 4), thereby receiving mostly ascending auditory information (Beyerl, 1978; Coleman & Clerici, 1987). In consequence, CNIC neurons show very sharply-tuned receptive fields, most of which display V-shaped frequency response areas (FRA) akin to those of the cochlear nerve fibers (Figure 7A). The neurons contained in the CNIC can be roughly categorized into 2 major types (Morest & Oliver, 1984; Oliver et al., 1991; Rockel & Jones, 1973). The most characteristic are the *disc-shaped neurons*, whose flat dendritic fields have about 50 μm of average thickness. These disc-shape neurons, together with their afferent tonotopic fibers, are arranged into approximately 150 thin fibrodendritic laminae, stacked and inclined from dorsomedial to ventrolateral, and showing smooth undulations (Malmierca et al., 1993, 1995, 2008; Wallace et al., 2012). They are usually referred to as *isofrequency laminae* because each lamina is dedicated to process one narrow frequency band. Hence, these isofrequency laminae constitute the structural basis for the tonotopic organization of the CNIC (Friauf, 1992; Malmierca et al., 2008; Pierson & Snyder-Keller, 1994), inherited from the

cochlea (Merzenich & Reid, 1974). The neurons included in the dorsal laminae respond to lower frequencies, while the neurons in the more ventral laminae respond to progressively

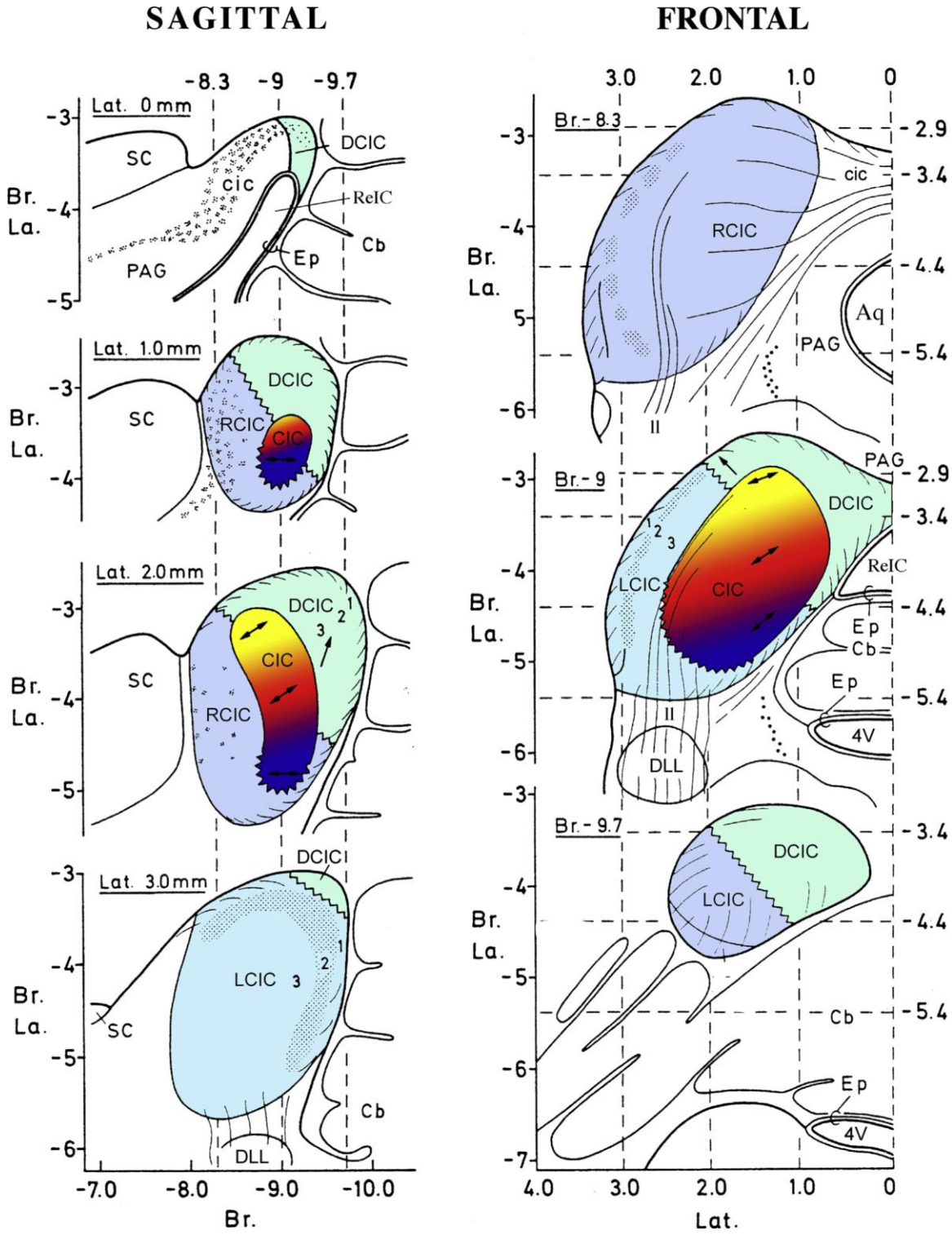

Figure 5. Serial schematic sections of the rat IC. Drawings are arranged by stereotaxic coordinates in Paxinos & Watson (2007). Arrows in the CNIC indicate the orientation of the fibrodendritic laminae, while the color gradient reveals the tonotopy. Arrows in the DCIC indicates the preferred orientation of dendritic arbors. Reproduced from Malmierca (2015).

higher frequencies (Figure 5, color gradient). Located in the interlaminar spaces there are *stellate neurons*, whose elliptic dendritic fields have about 100 μm of average thickness (Faye-Lund & Osen, 1985; Malmierca et al., 1993; Morest & Oliver, 1984; Reetz & Ehret, 1999). The presence of stellate neurons connecting isofrequency laminae implies integration across frequencies, part of a complex spectral processing of the sound. Additionally, the CNIC also have rich intralaminar connections, which could be related to the processing of some temporal features of sound (Miller et al., 2005). The CNIC constitutes the neuroanatomical origin of the so-called *lemniscal pathway* (Figure 8), an ascending line of tonotopically organized projections that covey primary auditory information from the midbrain to the AC (Hu, 2003).

The ICx of rodents is commonly divided in at least 2 cortical regions: a dorsal cortex (DCIC) covering the caudal and dorsomedial regions of the CNIC, and an external cortex (ECIC) surrounding the lateral, rostral, ventral and ventrocaudal regions of the CNIC (Faye-Lund & Osen, 1985; Malmierca et al., 2011). The DCIC is the division of the IC that receives the densest innervation from primary and nonprimary AC, followed by the ECIC, although the CNIC also receives some tonotopic projections from primary AC (Bajo et al., 2007; Bajo & Moore, 2005; Druga et al., 1997; Games & Winer, 1988; Herbert et al., 1991; Saldaña et al., 1996; Vaudano et al., 1991; Winer et al., 1998). In the case of the rat, modern authors oftentimes regard the lateral (LCIC) and rostral (RCIC) regions of the ECIC as separate cortical divisions (Figure 5; Loftus et al., 2008; Malmierca, 2015). This is because the LCIC presents a layered structure where multipolar neurons exhibit a dendritic orientation perpendicular to the pial surface, whereas no clear signs of layering or anisotropy are discernible in the RCIC (Malmierca, 2015). The ICx receives much input from the CNIC (Malmierca et al., 1995; Saldaña & Merchán, 1992), but they serve as multisensory integration regions that concentrate projections from heterogeneous sources and also receive massive influence from the AC (Figures 4 and 8; Bajo et al., 2007; Bajo & Moore, 2005; Beyerl, 1978; Druga et al., 1997; Druga & Syka, 1984; Games & Winer, 1988; Herbert et al., 1991; Krieg, 1947; Malmierca & Ryugo, 2011; Saldaña et al., 1996; Vaudano et al., 1991; Winer et al., 1998). This integrative, higher-order nature is reflected in the broadly-tuned receptive fields that neurons commonly exhibit in the ICx (Figure 7C), as well as in their distinctive response properties. Since ICx neurons have considerably wider FRAs than those of the CNIC, their tonotopic organization becomes diffused, despite continuing the laminar organization of the CNIC. The dorsomedial-to-ventrolateral orientation of the CNIC laminae extends into the DCIC, but it bends in the ECIC along an opposite ventromedial-to-dorsolateral inclination. These two different slopes

meet at the border between the CNIC and the ECIC, creating the shape of two convergent lines, which sometimes meet to form a 'V' or even a 'Y' shape, with the vertex laying in the border between the subdivisions. The ECIC receives projections from the ipsilateral cerebral cortex rostral to primary AC and from other extra-auditory nuclei, such as the subparafascicular nucleus (SPF) of the thalamus, the cuneatus and trigeminal nuclei, the lateral nucleus of the substantia nigra, the parabrachial region, the periaqueductal grey (PAG), the periventricular nucleus and the globus pallidus (Tokunaga et al., 1984; Yasui et al., 1992; Yasui, Kayahara, Kuga, et al., 1990; Yasui, Kayahara, Nakano, et al., 1990). Consistent with this variety of afferents, it has been shown that ECIC neurons respond not only to auditory stimuli, but also to somatosensory stimuli (Aitkin et al., 1981). In turn, the ECIC projects to the dorsal (MGD) and medial (MGM) subdivisions of the MGB. It is also noteworthy that ICx neurons are under heavier modulatory influence those in the CNIC, given that the ICx receives denser serotonergic, noradrenergic and dopaminergic fibers (Fyk-Kolodziej et al., 2015; Hormigo et al., 2012; Klepper & Herbert, 1991; Nevue, Elde, et al., 2016; Papesh & Hurley, 2016). From the ICx emerges the *nonlemniscal pathway* (Figure 8), which is part of an integrative system that plays an important role in multisensory integration, temporal pattern recognition and certain sophisticated forms of learning (Hu, 2003).

The ICx is organized in 3 layers of neural tissue that wraps around the CNIC (Ramón y Cajal, 1902). Layer 1 consists of thin fibrocellular tissue that encapsulates the whole IC. It contains scattered, small, flattened neurons (Faye-Lund & Osen, 1985; Malmierca et al., 2011). This superficial layer receives the densest serotoninergic fibers, whereas noradrenergic input is relatively sparse (Klepper & Herbert, 1991). Layer 2 is slightly thicker than layer 1, while layer 3 constitutes about two thirds of the maximum thickness of the ICx. Contrary to layer 1, layer 3 receives the densest noradrenergic fibers, whereas serotoninergic input is relatively sparse (Klepper & Herbert, 1991). These distinctive modulatory patterns suggest layer-specific, complementary functions of the different types of modulatory projections that innervate the IC (Hurley, 2018). In the DCIC, layer 1 receives some descending input from the nonprimary AC (Saldaña et al., 1996). Layer 2 of the DCIC contains smaller, mainly multipolar neurons, while layer 3 contains more medium-sized neurons. Besides, at the border of the DCIC with the CNIC, there are large multipolar neurons with elongated dendritic arbors that parallel the orientation of the fibrodendritic laminae of the CNIC. Bilateral projections from primary AC and ipsilateral projections from the sagulum provide the main afferences to the DCIC, which in turn projects to the dorsal division of the MGB (MGD). In the ECIC, layer 2 is characterized

by dense clusters of many small and a few medium-sized neurons partly aggregated in myelin-dense neuropil. The neural domains within these aggregates are under rich cholinergic and GABAergic input (Chernock et al., 2004; Lesicko et al., 2016; Ottersen & Storm-Mathisen, 1984). Layer 3 of the ECIC, consists of relatively scattered, small, medium and large neurons exhibiting 3 types of morphologies: bitufted, pyramidal-like and chandelier (Malmierca et al., 2011). The most characteristic element of this internal layer are the large multipolar neurons with coarse Nissl granules and extensive dendritic arbors, whose axis is perpendicular to the

Figure 6. Drawing of a frontal slice of the IC by Ramón y Cajal in 1902. This neural tissue was taken from an 8-days old mouse, as Golgi's method requires axons to be unmyelinated in order to stain the neurons. In spite of its immature stage, the distinction between the CNIC and the ECIC is evident, and the layering in ECIC can also be identified (notations in red).

pial surface (Faye-Lund & Osen, 1985; Malmierca et al., 2011; Ramón y Cajal, 1902; P. H. Smith, 1992). As already noted in Cajal's pioneering works already in 1902 (Figure 6), the exquisite and sophisticated neuroarchitecture of the ICx features some neuronal morphologies and arrangements that somewhat resembles to some organizational properties of the cerebral cortex (Ramón y Cajal, 1902). This hints at the higher-order processing capabilities of the ICx circuitry, to the point that electroencephalography (EEG) data from the rat suggests that the ICx modulates sensorimotor integration in neonates, prior to the assumption of this function by the mature cerebral cortex (McCown & Breese, 1991).

The interaction between excitation and inhibition plays an important role in shaping the response of the IC neurons to the acoustic stimuli. Glutamate is the main excitatory neurotransmitter in the IC of rodents (J. C. Adams & Wenthold, 1979; Ottersen & Storm-Mathisen, 1984), which expresses 2 types of glutamatergic receptors. N-methyl-d-aspartate (NMDA) selectively activate NMDA receptors, whereas α-amino-3-hydroxy-5-methyl-4-isoxazolepropionic acid (AMPA) selectively activate AMPA receptors (Caicedo & Eybalin, 1999; Gaza & Ribak, 1997; Kelly & Caspary, 2005; Schmid et al., 2001). NMDA receptors are more abundant in the ICx than in the CNIC (Ohishi et al., 1993), coinciding with the distribution pattern descending projections. In fact, corticocollicular innervation induces long-lasting changes in the neuronal responses of the IC. Such neuronal plasticity may be caused by top-down stimulation of NMDA receptors (Clarkson et al., 2010a, 2010b, 2012; Suga et al., 2000), which can induce long-term potentiation in IC neurons (Hosomi et al., 1995; Y. Zhang & Wu, 2000). AMPA receptors are critical to initiate the neuronal response, and both types of glutamatergic receptors are involved in maintaining action potentials during the stimulus (H. Zhang & Kelly, 2001). On the other hand, about 25% of IC neurons are GABAergic, and both glycinergic and GABAergic presynaptic boutons have also been found, so the IC is under strong inhibitory influence by both GABA and glycine (Kelly et al., 2009; Kelly & Caspary, 2005; Merchán et al., 2005; Oliver et al., 1994; Roberts & Ribak, 1987). The interaction between excitatory and inhibitory input from ascending, descending and intrinsic projections in each neuron determines its response properties and the shape of its FRA (Oliver et al., 1994). In fact, non-V-shaped FRAs appear to be generated de novo in the IC (Figure 7B-D), since most of them change to V-shaped (Figure 7A) when applying antagonists of inhibitory neurotransmitters (Le Beau et al., 2001). Hence, V-shaped FRAs seem to be inherited by the IC neurons from lower auditory nuclei, and in turn inhibition sculpts those receptive fields into

new shapes: O-shaped or closed, I-shaped or narrow, W-shaped or multi-peaked, low-tilt, high-tilt and disorganized FRAs (Hernández et al., 2005).

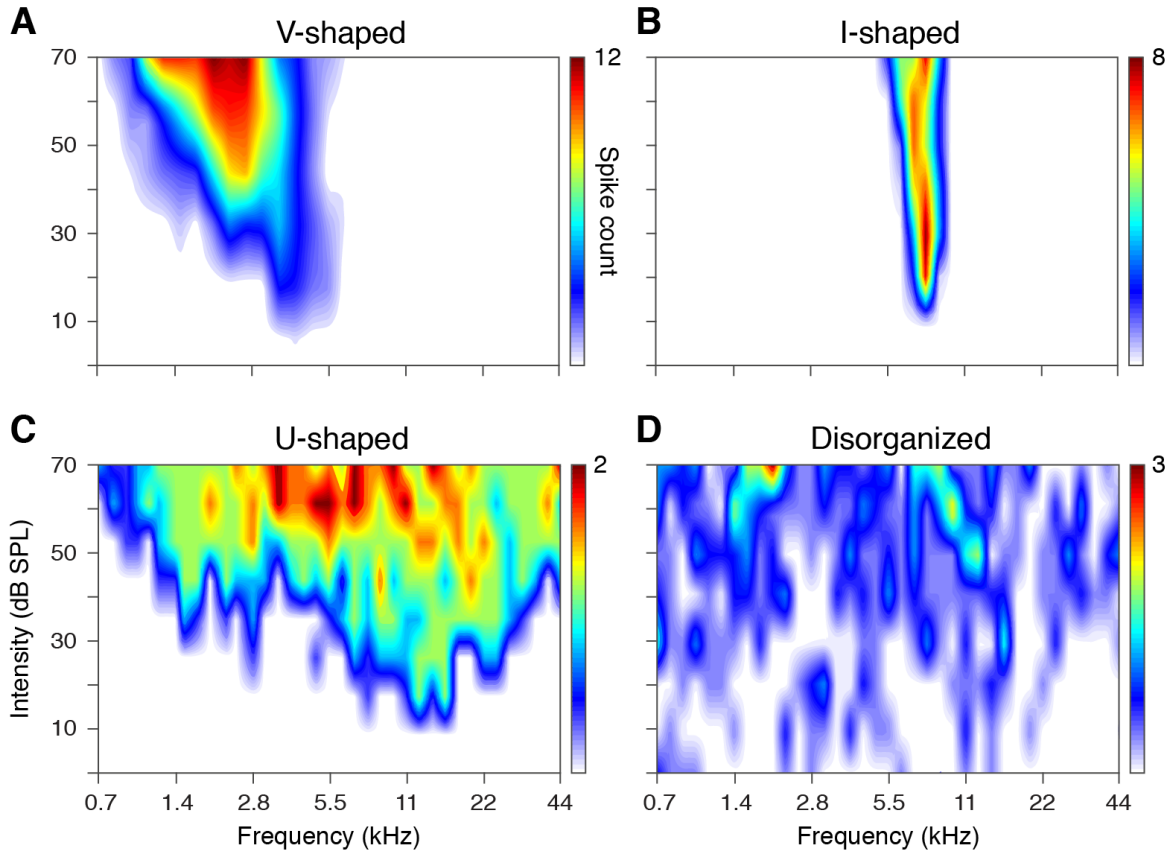

Figure 7. FRAs of IC neurons. A-B. 2 types of narrowly-tuned receptive fields. **C.** Broadly-tuned receptive field. **D.** Untuned receptive field, with no apparent characteristic frequency.

The balance between excitation and inhibition not only determines the receptive field of IC neurons and the shape of their FRAs, but also the shape of the peristimulus time histograms (PSTH) and their discharge patterns (Faingold et al., 1989, 1991; Kelly & Zhang, 2002; Le Beau et al., 1996; Palombi & Caspary, 1996; Vaughn et al., 1996; H. Zhang & Kelly, 2001, 2003). Both extrinsic and intrinsic factors determine the temporal response of any neuron. On the one hand, the relative proportion and timing of the excitatory and inhibitory projections that a neuron receives will initiate, maintain or modulate changes of the membrane potential that eventually may give rise to action potentials (Le Beau et al., 1996, 2001; Tan et al., 2007). On the other hand, the membrane properties conferred by the expression of ion channels determines the excitability of the neuron and the final shape of its action potentials. Different receptors for the same neurotransmitter sometimes have quite different kinetics, resulting in different outputs. The multiple types and subtypes of many ion channels, specially

the family of voltage-gated potassium channels, are going to offer a great range of variability in the neuronal response (Peruzzi et al., 2000; Sivaramakrishnan & Oliver, 2001). Besides, each region of the neuronal membrane contains varied ion channels in different proportions. Resulting from the interaction of these extrinsic and intrinsic factors, IC neurons show 5 prototypic response pattern tendencies: onset, sustained, chopper, pauser and offset (Figure 3, left margin), although combinations of those patterns are common (Le Beau et al., 1996; Peruzzi et al., 2000; Rees et al., 1997).

Neuromodulation reconfigures processing midbrain neural circuitries by regulating the action of neurotransmitters —glutamate, GABA and glycine—, thereby modifying the excitatory and inhibitory balance of IC neurons. The IC receives prominent diffuse projections from centralized neuromodulatory systems (Figure 4, in green), which target the ICx with much denser fibers (Fyk-Kolodziej et al., 2015; Hormigo et al., 2012; Klepper & Herbert, 1991; Nevue, Elde, et al., 2016; Papesh & Hurley, 2016). Neuromodulatory input to the IC originates in extra-auditory clusters of cholinergic neurons in the laterodorsal tegmental (LDT) and pedunculopontine tegmental (PPT) nuclei (Dautan et al., 2016; Motts & Schofield, 2009) as well as in the rostral ventrolateral medullary region (Stornetta et al., 2013), noradrenergic neurons in the locus coeruleus (LC; Klepper & Herbert, 1991; Mulders & Robertson, 2001), serotonergic neurons in the dorsal raphe nucleus (DRN; Klepper & Herbert, 1991; G. C. Thompson et al., 1994) and dopaminergic neurons in the thalamic SPF (Nevue, Elde, et al., 2016; Nevue, Felix, et al., 2016). Although these modulatory nuclei are not explicitly part of the auditory system, they receive projections from primary auditory regions and are responsive to acoustic stimuli. This bidirectional influence suggests the existence of auditory-modulatory feedback loops. A characteristic of neuromodulatory centers is that they integrate inputs from anatomically widespread and functionally diverse sets of brain regions. This connectivity gives neuromodulatory systems the potential to import information into the auditory system on situational variables that accompany acoustic stimuli, such as context, internal state, or experience.

Once released, neuromodulators functionally reconfigure auditory circuitry through a variety of receptors expressed by IC neurons. The effects of neuromodulation on their intrinsic properties and sound-evoked responses depend on the types of receptors expressed in their membrane (Hurley & Sullivan, 2012). Many neuromodulators have suppressive effects on neural firing for some IC neurons in spite of showing facilitatory effects for others, as reported

for acetylcholine (Habbicht & Vater, 1996), serotonin (Hurley & Pollak, 1999) and dopamine (Gittelman et al., 2013). This range of selective modulatory mechanisms results in the transformation of functional response properties. Commonly, neuromodulators can alter the spontaneous or evoked firing rates of IC neurons in response to stimuli (Curtis & Koizumi, 1961; Gittelman et al., 2013; Hurley et al., 2004; Hurley & Pollak, 1999), firing patterns (Gittelman et al., 2013; Habbicht & Vater, 1996), latency or latency jitter (Gittelman et al., 2013; Hurley, 2007; Hurley & Pollak, 2005b) and frequency tuning (Hurley & Pollak, 2001). These types of changes can contribute to shifts in neural selectivity for spectrotemporally divergent sounds, such as tones versus frequency-modulated sweeps (Hurley & Pollak, 1999), sounds of different frequency (Hurley et al., 2004; Hurley & Pollak, 2001) or different species-specific vocalizations (Hurley & Pollak, 2005a). In addition to shaping ascending auditory information to the local auditory context (Ayala & Malmierca, 2015; Valdés-Baizabal et al., 2017; Valdés-Baizabal, Carbajal, et al., 2020), neuromodulation within the IC influences behaviors that arise subcortically (Petersen & Hurley, 2017). Neuromodulatory systems therefore provide a route for integrative behavioral information to access auditory processing from its earliest levels (Hurley, 2018).

In conclusion, the IC works as a main integration center able to performs complex spectral, temporal and multisensory processing thanks to: (1) a sophisticated neuroanatomical organization (Figures 5 and 6), (2) a wide variety of neuronal types endowed with specialized response properties, and (3) a rich excitatory, inhibitory and neuromodulatory innervation provided by both ascending and descending projections, as well as dense intrinsic connections (Figures 4 and 8). For these reasons, the role of the IC in the auditory system has even been compared to that of the primary visual cortex in the visual system (King & Nelken, 2009).

I.1.e.- Lemniscal and nonlemniscal pathways: primary vs nonprimary representation

As we have seen in the previous section, the CNIC is tonotopically organized and mainly driven by ascending input from the auditory periphery, whereas the ICx work under much heavier influence of descending and neuromodulatory fibers from higher auditory and integrative regions of the brain. Such neuroanatomical dichotomy in the IC between ‘core’, first-order structures and ‘belt’, higher-order structures find a correlate in the next stations of the ascending auditory pathway, the MGB and the AC. Consequently, the IC constitutes the

neuroanatomical origin of two parallel lines of processing in the auditory system: the lemniscal and nonlemniscal pathways (Andersen, Roth, et al., 1980; C. C. Lee & Sherman, 2011). The auditory centers comprised in each pathway share some common characteristics in their neural structure and function, so the distinction of lemniscal and nonlemniscal structures provide some general insights about how the auditory system processes sensory input.

On the one hand, the *lemniscal pathway* initiates in the CNIC, goes by the thalamic MGV and finishes in the primary fields of AC. Lemniscal subdivisions constitute the neural core of their respective auditory stations. These cores tend to contain sharply-tuned neurons in tonotopic arrangement, creating isofrequency laminae in the CNIC and the MGV, as well as isofrequency bands in primary AC. Most of the neurons in each isofrequency lamina project to their corresponding homologous lamina or band in the next station of the lemniscal pathway (Malmierca, 2015), shaping a straightforward line that conveys sensory input in bottom-up fashion (Figure 8). Relative to their nonlemniscal pairs, lemniscal neurons exhibit more consistency in their response to the sound, narrower receptive fields reflected in V-shaped FRAs, shorter latencies, higher firing rates, more overall spikes fired per stimulus, and a tendency to show a strong sustained component in their response that follows the stimulus until it ends (e.g., Figures 12B-C, 28A and 34A). As a rule of thumb, the lemniscal pathway hosts first-order auditory neurons that obtain their input mainly from lower auditory stations and respond fundamentally driven by the physical features of the sound. Therefore, the information stream conveyed throughout the lemniscal line carries rather primary representations of the sound in progressive levels of complexity (Carbajal & Malmierca, 2020, 2018b).

On the other hand, the *nonlemniscal pathway* is built around the lemniscal line, comprising the shell of the IC, the MGD and the MGM of the thalamus, and the nonprimary regions of AC (Figure 8). Nonlemniscal divisions are akin to capsules or belts, wrapping the lemniscal core from where nonlemniscal neurons obtain part of their input. The rest of their input is provided by other nonlemniscal divisions and by the AC, besides receiving relatively denser projections from non-auditory sources. Subcortical nonlemniscal neurons project to the next nonlemniscal division in the pathway, while cortical neurons send back descending projections mainly the nonlemniscal divisions of the MGB and the IC (Figure 8; Arnault & Roger, 1990; Bajo et al., 2007; Bajo & Moore, 2005; Bartlett et al., 2000; Beyerl, 1978; Diamond et al., 1969; Games & Winer, 1988; Hazama et al., 2004; Herbert et al., 1991; Kimura et al., 2005, 2007; Krieg, 1947; Malmierca & Ryugo, 2011; Saldaña et al., 1996; Shi & Cassell,

1997; W. H. Thompson, 1901; Vaudano et al., 1991; Winer & Larue, 1987). Nonlemniscal neurons are broadly tuned, which diffuses or even effaces any trace of tonotopic organization in nonlemniscal divisions. Their response properties are also more heterogeneous than those of

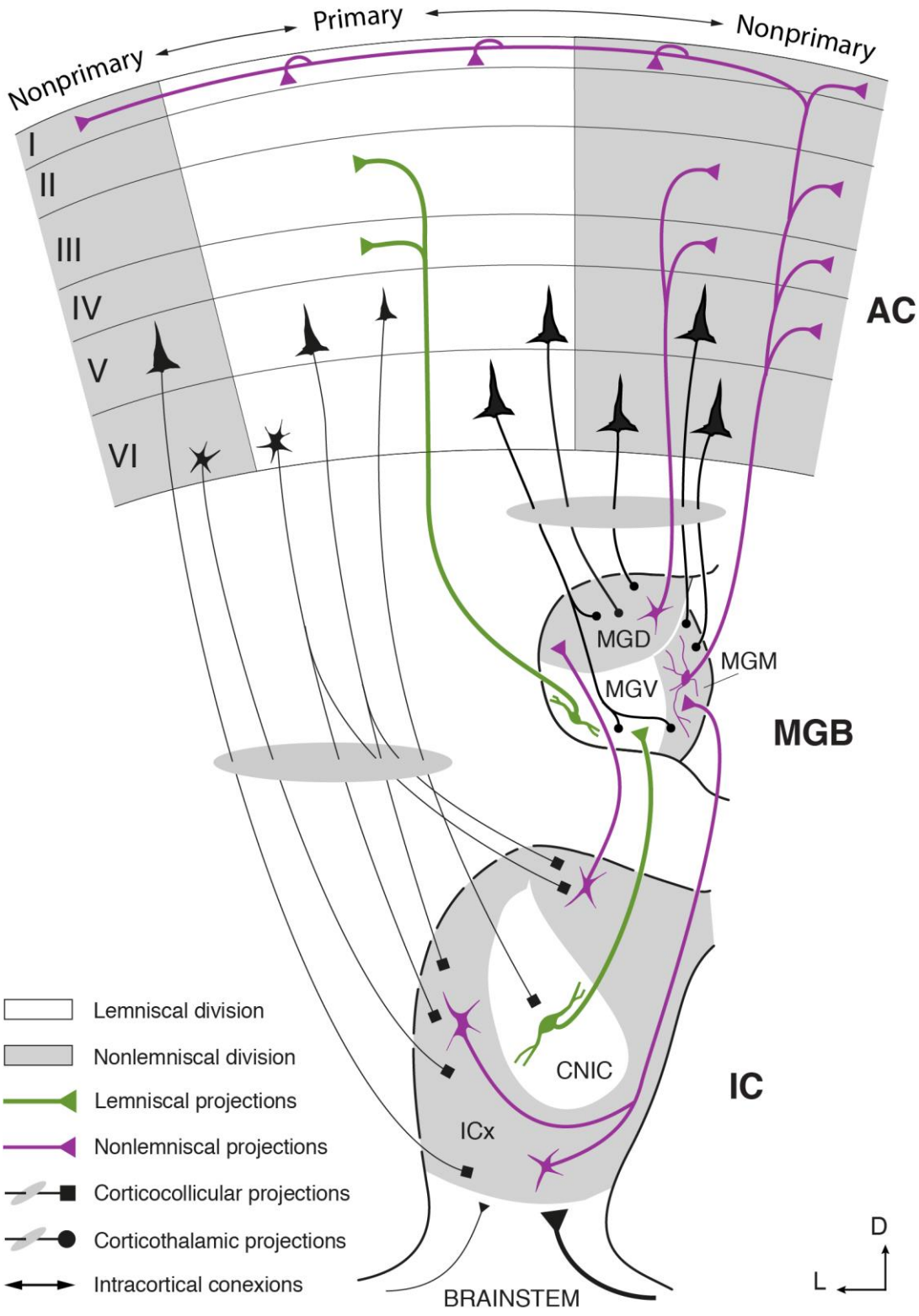

Figure 8. Lemniscal and nonlemniscal pathways. Adapted from Malmierca (2015).

the lemniscal neurons, although onset components signaling relevant acoustic events tend to predominate in nonlemniscal responses (e.g., Figures 12D-E, 28B and 34B). The neuroanatomical position adjunct to the lemniscal line, the loop-like connectivity with the heavy cortical influence, the extensive receptive fields and the longer latencies characteristic of nonlemniscal neurons, as well as their multisensory afferences, strongly suggest that they perform higher-order integrative functions. Therefore, the nonlemniscal pathway progressively generates an elaborate representation of the sound that eventually results in a proper auditory object relative to its auditory context (Carbajal & Malmierca, 2020, 2018b). In other words, the end product of nonlemniscal processing will finally be perceived as a bark over a sound landscape.

Following both ascending pathways, auditory information leaving the IC is funneled into the ipsilateral thalamus (Figure 8). The thalamus is known to actively regulate the flow of information from periphery to cortex (Sherman, 2007), as well as between cortical areas (Guillery & Sherman, 2002; Llano & Sherman, 2008). And like every other thalamic nucleus, the MGB is an obligatory relay station and the last stage of subcortical processing before the auditory signal enters the AC. With 1.2 mm long in the rostrocaudal dimension, 1.5 mm wide and 1 mm high, the MGB is a considerably smaller structure than the IC, prominent in the posterodorsal surface of the thalamus. Also in contrast with the IC, there are no intrinsic connections known between the different subnuclei or commissural projections interconnecting the 2 sides of the MGB (Malmierca, 2015), and only about 1% of its neurons are GABAergic in rodents (Winer & Larue, 1988). GABAergic input to the MGB is provided by the IC (Winer et al., 1996) and by the caudoventral portion of the thalamic reticular nucleus (Bartlett & Smith, 1999; Yu et al., 2009), which some authors consider an integral part of the auditory pathway (Cotillon et al., 2000; Kimura et al., 2007; Shosaku & Sumitomo, 1983; Yu et al., 2011). Thus, the thalamic reticular nucleus takes part in a feedback system that controls the transmission of information from the thalamus to the cortex, maybe playing a role in selective attention (Arcelli et al., 1997).

Lemniscal and nonlemniscal divisions of the MGB show clear anatomic and physiological differences at the cellular level (Bartlett & Smith, 1999). In the middle of the lemniscal line, the MGV receives projections from the CNIC and in turn projects to the primary AC in tonotopic manner (Figure 8, green lines; Donishi et al., 2006; Kimura et al., 2003). The MGV contains large, bitufted relay neurons (Clerici et al., 1990; Clerici & Coleman, 1990;

Winer, Kelly, et al., 1999; Winer, Larue, et al., 1999; Winer, Sally, et al., 1999), which respond transiently in typically lemniscal fashion (Aitkin & Webster, 1972; Bordi & Ledoux, 1994; Bordi & LeDoux, 1994). Similar to the organization of the CNIC, these neurons have highly oriented dendritic arbors arranged in the direction of the afferent fibers, forming isofrequency laminae that constitute the basis of tonotopic organization of the MGV. Frequency representation follows a dorsoventral gradient from low to high frequencies (Aitkin & Webster, 1971; Bordi & Ledoux, 1994; Bordi & LeDoux, 1994; Imig & Morel, 1985). The MGV is reciprocally connected with the AC in tonotopic fashion (Clerici & Coleman, 1990; Hazama et al., 2004; Kimura et al., 2003, 2005; Ryugo & Killackey, 1974; Shi & Cassell, 1997; Storace et al., 2010, 2011; Winer, Sally, et al., 1999; Winer & Larue, 1987). The nonlemniscal divisions of the MGB, i.e., the MGD and MGM, find their major source of input in the ICx, and their main target is the nonprimary AC. They are anatomically and functionally distinct from the MGV. Their heterogeneous nonlemniscal neurons are reciprocally connected to nonprimary AC, and also receive driving glutamatergic input from the lemniscal fields of AC (Figure 8, purple lines). The MGD contains tufted and stellate neurons, whose cell bodies and dendrites are not oriented in any particular fashion. There are no traces of a tonotopic organization in the MGD. Compared to the MGV, MGD neurons are less responsive to acoustic stimuli and show longer latencies, preferring complex sounds than pure tones (Bordi & Ledoux, 1994; Bordi & LeDoux, 1994). The MGM is a narrow disc of tissue, with large, sparsely distributed cell bodies. It comprises a diverse population of neurons, the most unusual ones being the ‘magnocellular’ neurons (Clerici & Coleman, 1990; Winer, Kelly, et al., 1999). The anterior portion of the MGM displays some tonotopy, but much less ordered than in MGV. Whereas the MGV processes essentially acoustical features (LeDoux et al., 1987), nonlemniscal thalamic divisions subserve advanced, higher-order functions such as multisensory processing and auditory learning (Bordi & Ledoux, 1994; Bordi & LeDoux, 1994; Spreafico et al., 1981). The MGD and the MGM are implicated in multisensory integration, processing of communication signals, auditory learning and emotional significance of sounds (C. C. Lee, 2015). This is especially true for the MGM, but both nonlemniscal thalamic nuclei send and receive feedforward and feedback projections among a wide constellation of midbrain (LeDoux et al., 1987; Malmierca et al., 2002), cortical (Shi & Cassell, 1997; Winer & Larue, 1987), and limbic sites (Doron & Ledoux, 1999; Ottersen & Ben-Ari, 1979), which support potential conduits for auditory information flow to higher auditory cortical areas, mediators for transitioning among arousal states, and synchronizers of activity across expansive cortical territories.

Finally, ascending auditory information reaches the AC, in the temporal lobes of our human brains, where the highest-order level of processing and integration within the auditory system will take place. Subcortical auditory nuclei have already completed an essential spectrotemporal analysis, so powerful and efficient indeed that animals do not even need the AC to accomplish simple perceptual or audiomotor tasks, such as frequency discrimination or sound localization (Gimenez et al., 2015; Kelly & Kavanagh, 1986). Therefore, the processing resources of the AC are available to deal with the most abstract aspects of the auditory signal, recognizing complex patterns, and attaining elaborate auditory percepts with behavioral affordances (Li et al., 2017; Nelken, 2004; Sutter & Shamma, 2011). In addition, the AC is the site of highest neuronal plasticity for learning and memory about the objects that populate the complex structure of the auditory world (Weinberger, 2004).

The AC is a specialized area of the mammalian neocortex, a highly modular structure resulting from the extensive repetition of a common pattern, suggesting a shared underlying computational principle (Mountcastle, 1997). In the horizontal dimension, the neocortex is organized in 6 layers extending about 1.2 mm. This number can vary between areas, but 6 is the most common for sensory cortices (Figure 9). The middle layers, mainly layer IV —but also lower layer III in AC—, are dense in cell bodies of small stellate cells with smooth dendrites that project only to local tissue, thus presenting a gritty aspect from which they take the name *granular layer*. Layers I-III, called *supragranular layers*, are dense in small pyramidal cells with regular spiking firing profiles that project locally and to higher-order cortical areas. Layers V-VI, called *infragranular layers*, contain larger pyramidal cells with intrinsically bursting firing patterns that project to manifold subcortical targets. Besides, Layer VI also presents abundant bitufted and multipolar neurons (Krieg, 1946a, 1946b; Malmierca, 2015).

In the vertical dimension, neurons are grouped in a columnar system of intrinsic fibers perpendicular to the surface, each column spanning 200-800 µm in width and made up of terminal axons that extend through all cortical layers. Neurons along the column tend to show similar receptive field properties (Mountcastle, 1997), but the modular organization of the AC goes beyond small columns. Different properties such as spectral bandwidth, intensity tuning or binaural interactions seem to be organized in columnar patches or complex metagradients that, unlike tonotopic gradients, extend beyond the limits between cortical fields (Polley et al., 2007). Like other cortical regions, the AC is rich in a large variety of GABAergic interneurons

with many potential roles in controlling and synchronizing neuronal activity (DeFelipe et al., 2013). But in the particular case of the AC, inhibitory influences may have an even more important role in shaping receptive fields and encoding temporal information (Bendor, 2015; Schinkel-Bielefeld et al., 2012).

Lastly, a third common principle of cortical organization is the functional division in areas, specialized in carrying out different types of information processing. Whereas subcortical divisions and their reciprocal connectivity tends to be relatively well preserved across species, the neocortex displays great interspecific variations. For example, the AC comprises 5 different fields in rodents, 10–12 fields in primates, and around 30 fields in humans (Malmierca, 2015). Nevertheless, all species present a core of primary auditory fields, surrounded by —and connected to— a belt of nonprimary auditory fields, which in turn connect to higher-order multisensory association areas (Kaas, 2011; Read et al., 2002; Winer & Lee, 2007). Those are respectively the high end of the leminscal and nonlemniscal pathways that emerged in the IC (Hu, 2003; Malmierca & Hackett, 2010). The lemniscal AC contains a dense granular layer that receives strong, direct tonotopic input from the MGV, and contains one or more complete tonotopic representations of the audible frequency range of the animal (Polley et al., 2007; Reale & Imig, 1980). In rats, the lemniscal AC comprises 3 fields: the primary auditory cortex (A1), the anterior auditory field (AAF) and the ventral auditory field (VAF). By contrast, the nonlemniscal AC lacks a thick granular layer, receiving their ascending input from nonlemniscal divisions of the MGB and from the supragranular layers of primary AC without forming a clear tonotopic organization. In rats, the nonlemniscal AC comprises at least 2 nonprimary fields in the belt regions: the posterior auditory fields (PAF) and the suprarhinal auditory field (SRAF; Donishi et al., 2006; Doron et al., 2002; Kimura et al., 2003; Polley et al., 2007; Rutkowski et al., 2003). The lemniscal fields of AC are reciprocally connected to lemniscal MGV through tonotopic ascending and descending projections (Read et al., 2002). However, whereas MGV follows a laminar tonotopy, cortical fields are organized in isofrequency bands, so a whole isofrequency lamina of MGV neurons must converge into each cortical column (Imaizumi & Lee, 2014). Each isofrequency band of A1 receives input from the rostral half of an isofrequency lamina of MGV, whereas VAF receives from the caudal MGV (Storace et al., 2010). A1 project to both nonlemniscal divisions of AC, PAF reciprocally connects with the MGD and the MGM, and SRAF connects back with the MGM (Kimura et al., 2003, 2005; Philip H. Smith et al., 2012; Storace et al., 2010). Finally, PAF and SRAF also send out projections beyond the classic boundaries of the auditory system, targeting a wide

variety of cortical areas —e.g., the prefrontal cortex (PFC), the limbic cortex, etc— and subcortical nuclei —e.g., the amygdala, the striatum, the basal ganglia, the SC, etc— that will keep adding nuances to our auditory perception (Kaas et al., 1999; Krieg, 1947; Paula-Barbosa & Sousa-Pinto, 1973; Read et al., 2002; Romanski & Ledoux, 1993; Shi & Cassell, 1997; W. H. Thompson, 1901; Winer, 2005). Now, we are finally *hearing* the bark.

I.1.f.- Descending projections: iterating towards auditory perception

So far, I have introduced the organization of the auditory pathway as it is usually done: following a sequential order from the cochlear to the AC. Although such a systematic description in ascending manner is very convenient for presenting the main neuroanatomical elements involved in auditory processing, it may not provide the best representation of *how* auditory information is actually processed. At this point, a neophyte reader could have an impression on the auditory system as a forward processor, where information bits are treated like pieces within a Fordian assembly line. However, as mentioned throughout the previous sections, there is a portion of descending afferences at every step of the way. All along the auditory system, there are many nuclei where ascending and descending pathways can cross and integrate their input. In fact, the connectivity of the auditory system would be better described as a series of nested loops of reverberating ascending and descending information, each next loop surrounding the previous one to add the next layer of auditory processing (Malmierca, 2015; Malmierca & Ryugo, 2011; Winer, 2005).

Going back on our steps from the AC, we find that the MGB works under heavy cortical feedback (Figure 8). Descending corticothalamic projection is around 10 times denser than ascending thalamocortical projection (Malmierca, 2015). There are 2 main types of corticothalamic projection, one arising from the pyramidal —glutamatergic— neurons of layer VI and the other emerging from layer V. In the lemniscal fields of AC, the projection from layer VI innervates back the MGV in a highly tonotopic manner, terminating in small terminal boutons of putative modulatory nature. The projection from layer V reaches the nonlemniscal MGB, terminating in large terminals of putative driver nature (Bartlett et al., 2000; Llano & Sherman, 2008). This driver projection creates an indirect connection between lemniscal and nonlemniscal fields of AC mediated by thalamic gating (Sherman & Guillery, 2011). In the nonlemniscal fields of AC, the modulatory projection from layer VI arrives at both

nonlemniscal MGB divisions, whereas the driver projection from layer V target mainly to the MGM (Figure 8; Kimura et al., 2005).

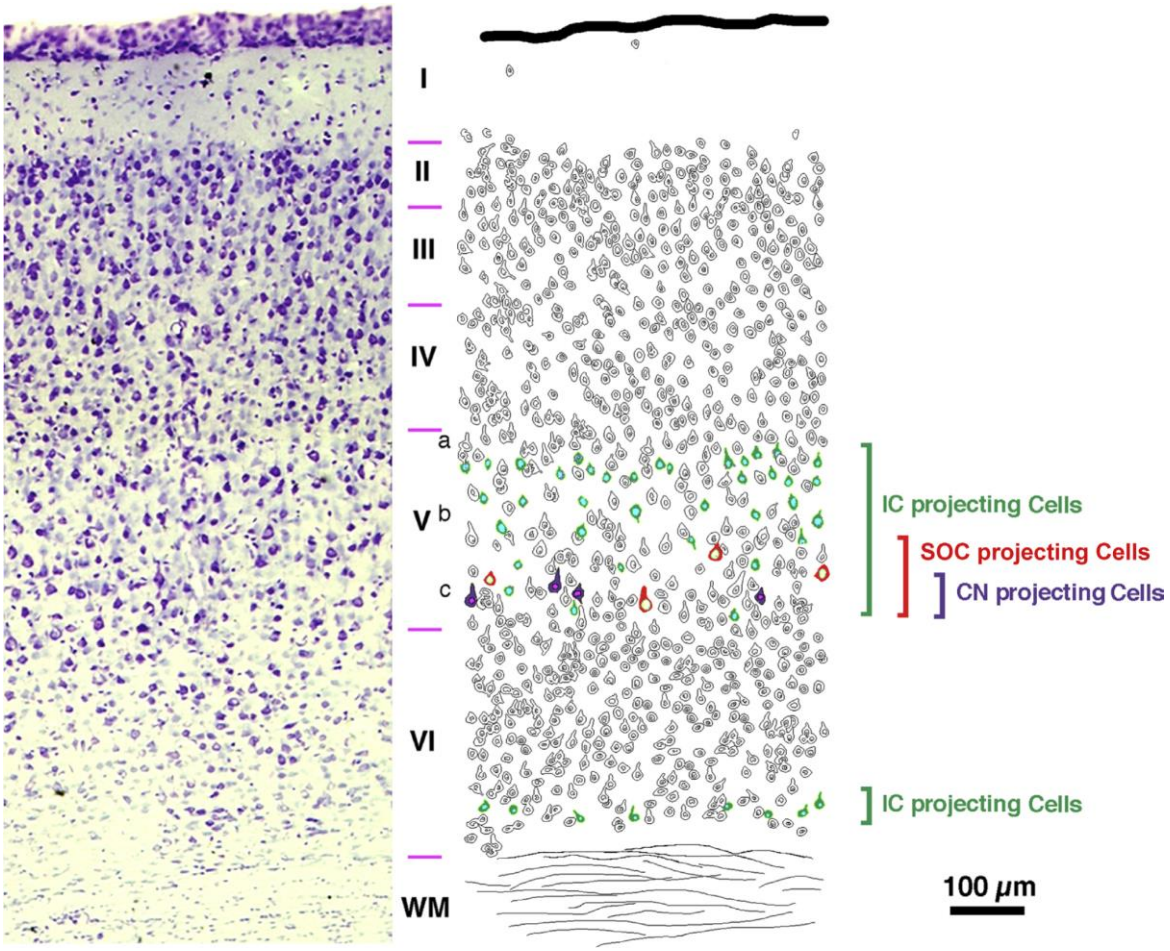

Figure 9. Auditory corticofugal projections in the rat. On the left, a photomicrograph displaying a Nissl-stained section through A1. The surface of cortex is at the top of the figure. On the right is a schematic of layers V and VI that illustrates the distribution of neurons projecting to the IC, SOC, and CN. A small number of corticocollicular neurons are located near the border of layer VI and white matter, but most are distributed within layer V. All three distributions overlap. However, notice that the cortical neurons projecting to more distant targets are more narrowly distributed and centered in deeper regions of layer V. Reproduced from Malmierca (2015).

The AC also sends important direct projections to the IC (Schofield & Beebe, 2019), bypassing the MGB (Figures 8 and 9). The heaviest corticocollicular projection arises from the large pyramid neurons in layer V of A1. This projection is mostly ipsilateral and tonotopic, such that low-frequency regions of A1 innervate the dorsolateral region of the IC, and the high-frequency regions of A1 innervate the ventromedial region of the IC. Nevertheless, some

corticocollicular projections emerge from other AC fields, and there are small neurons at the bottom of layer VI that also innervate the ICx (Figures 8 and 9). Most corticocollicular projections from both primary and nonprimary fields of AC target the ICx (Herbert et al., 1991), although the CNIC also receives a smaller, weaker projection from A1 (Beyerl, 1978; Diamond et al., 1969; Saldaña et al., 1996). Corticofugal projections arise from pyramidal cells, and are therefore glutamatergic (Feliciano & Potashner, 1995). However, electrical stimulation of AC produces both excitation and inhibition of IC neurons (Mitani et al., 1983), and AC deactivation yielded both types of effects as well (Anderson & Malmierca, 2013; Nwabueze-Ogbo et al., 2003), which implies that the AC exerts inhibitory influences over IC neurons through the activation of inhibitory connections within the local circuitry of the IC (Malmierca, 2015). The ICx also receives some descending excitatory projections from the MGB, and some inhibitory projections from the SPF of the thalamus (Moriizumi & Hattori, 1992). Not only the AC sends descending projections to subcortical auditory nuclei (Figure 8), but important descending projections emerge also from the IC to the lower brainstem, and from the SOC to the cochlea (Malmierca, 2015).

Thus, descending afferences constitute an elaborate feedback system in the auditory pathway. Judging from their size, descending projections must play a fundamental role in auditory processing, modulating or gating ascending auditory responses, shaping neuronal receptive fields (Sillito et al., 2006) and assisting in higher-order processes, such as figure-ground separation (Hupé et al., 1998). Most importantly for this thesis, descending projections seem to play a role in identifying the novelty of sensory input. Some authors even consider that these descending projections carry the *feedforward* signal of the modeling activity of our brain, while the lesser ascending information would be used as a *feedback* to confirm that incoming signals are consistent with the current internal representation of the external world (Friston, 2005). According to the PP proposal that I will introduce in Section I.3, the auditory system would not simply extract and add together spectrotemporal cues to build a representation of the bark. Instead, our brain may already hold an active representation of what a bark entails in terms of evoked neuronal activity and what it implies: a dog. Our brain just uses those spectrotemporal cues it needs to confirm or update the current model of the auditory scene: ‘There is a dog nearby, barking’.

In conclusion, more than the sum of the separated activity of the ascending and descending auditory pathways, it is the continuous looping interaction between forward and

backward information streams in the auditory system what establishes the physiological foundations of auditory perception. Contrary to the widespread corticocentric understanding of perception, we do not hear the bark with the cortex, but with our whole brain. Auditory perception is a very complex multi-step process that requires much more from subcortical auditory nuclei than their traditionally-given role of basic spectrotemporal analysers, relay stations and reflex organizers. Whether the perception of the bark eventually enters our consciousness or not may be decided even before the auditory signal leaves the brainstem, as I will demonstrate in the following.

I.2.- NOVELTY PERCEPTION: BIOMARKERS AND HYPOTHESES

A dog nearby barked and we have heard it, but most likely that was not the only thing taking place in our surroundings. Imagine we are taking a walk across an urban park. There are always countless events simultaneously happening around us, generating a profuse amount of physical changes in the environment that are mechanically caught by our sensors: dogs barking, birds chirping, the breeze blowing the leaves of nearby trees, our own footfalls on the gravel, distant traffic noise, people talking passing by, kids playing and laughing, a ball bouncing around, skates rolling, etc. A continuous flow of fine air-pressure oscillations coming from myriad sources hits our eardrum at every fraction of a second of every second of our life. But apart from the effects that natural selection has exerted in the evolution of our sensors, the importance of the transduced physical signals for our purposes or our survival is fundamentally disregarded by sensation (see Section I.1.a). Each vibration is mechanically transduced by the organ of Corti into action potentials without any distinction of utility, ceaselessly pouring sensory input into our central nervous system even at the risk of overloading its metabolic capacity.

The prime task of every sensory system is to winnow the useful bits of information in a deluge of sensory input and organized them into perceptual objects, or percepts. And this selection must be carried out as fast as possible, since the resultant percepts must serve as the building blocks of more complex cognitive and motor operations that enable our adaptive behavior. Hence, our central nervous system has neither the time nor the resources as to meticulously evaluate the content of each sensation in full. Instead, there is mounting evidence that perception is biased by the *probability* of sensations. This has a logical explanation:

uncommon changes in our environment tend to be more informative and critical for our survival than usual events. Therefore, the most efficient strategy to craft useful percepts is to automatically allocate the limited processing resources to the most improbable sensory input (Barlow, 1961). To maintain an efficient processing and avoid saturation, our central nervous system must implement basic network mechanisms that automatically downplay the repetitive and irrelevant *'standard'* aspects of the auditory scene in favor of the more infrequent and informative *'deviant'* events.

We have all experienced the result of this kind of sensory processing. Sometimes we become so accustomed to certain background noises that it feels like we are not hearing them anymore, as if our ears had shuttered for the sounds we already know that are there. However, novel and arresting sounds keep popping up in our minds here and there, without any conscious effort, and whether we want it or not. This sensory discrimination reliant on probability is pre-attentive and escapes volitive control, which makes sense from a self-preservation standpoint. When we stroll through the park, maybe trying to concentrate on our own thoughts, we would likely be most pleased when our auditory system tones down monotonous and potentially annoying noises. But if a bark suddenly sounds behind us, that unusual event would immediately trigger our attention. It could be just someone walking with a leashed dog, but it could also be an unleashed, unattended dog stalking us. In this context, whereas fully processing every redundant noise around us would be a waste of resources, and could saturate our perception with irrelevant information, getting an early alert of the risk of being bitten by a dog is worth the metabolic cost of instantly detecting the deviant sound of a bark.

The effects of such pre-attentive sensory discrimination based on input probability are evident at phenomenological level, but their neurobiological substrate is more elusive. The last half century of neuroscientific research has formulated several theoretical proposals for the functioning and implementation of the neural mechanisms and networks that could automatically bestow salience and novelty on deviant auditory percepts. These proposals have tended to derive from specific areas of expertise and methodologies and can be grouped into 3 major currents of thought, which I will introduce along the ensuing sections. But from an empirical standpoint, what all 3 hypotheses have in common is the *oddball paradigm* (Figure 10A), the most quintessential experimental design for the study of novelty perception. An oddball paradigm consists of a sequence of stimuli, where the repetitive presentation of a *standard* stimulus is randomly interspersed with a rare *deviant* stimulus, usually featuring in

around 10% of the trials. This deviant stimulus is different in certain physical features. In the case of an auditory oddball sequence, the deviant stimulus may vary from the standard in its frequency composition, intensity, duration, amplitude modulation, interstimulus interval, etc. Then, in a *reversed* oddball sequence (Figure 10A), the two stimuli switch conditions to control for the physical characteristics of the sound in the evoked response. Hence, when an auditory stimulus evokes different responses in the *standard condition* (STD) and the *deviant condition* (DEV), this difference can only be due to the uneven probability of each presentation condition. During electrophysiological recordings, the usual finding is that the neural responses to DEV are considerably larger than those to STD, yielding a *differential response* (*DEV – STD*) to the oddball paradigm. Depending on the recording technique, this differential response manifests at the macroscopic scale, in the form of a *mismatch negativity* (MMN) within the auditory evoked potential (AEP); or at the microscopic level, in the form of *stimulus-specific adaptation* (SSA) of the neuronal firing rate. Despite their resemblance, the physiological connection between these two signs of novelty perception has been a matter of debate for decades.

I.2.a.- The Mismatch Negativity (MMN) and the Detection Hypothesis

The MMN is the most iconic neurosignal reflecting the perceptual process by which novel stimuli pop out in our mind over the redundant ones. In the four decades since it was first described (Näätänen et al., 1978), the MMN has become a central research tool in cognitive and clinical neuroscience (Bartha-Doering et al., 2015; Kujala et al., 2007; Sussman et al., 2014). Several features have granted unmatched relevance to the MMN as an objective biomarker of automatic novelty processing: it is technically accessible, quite affordable, non-invasive, very versatile, and most importantly, it is an obligatory change-related component of the human AEP. The MMN can be recorded simply by presenting an oddball paradigm to a human participant while recording EEG through scalp electrodes. By subtracting the STD-elicited AEP from the DEV-elicited AEP, the MMN arises as a slow negative deflection within the *long-latency responses* (LLRs, >80 ms), peaking around 100–250 ms after stimulus onset (Figure 10D and E).

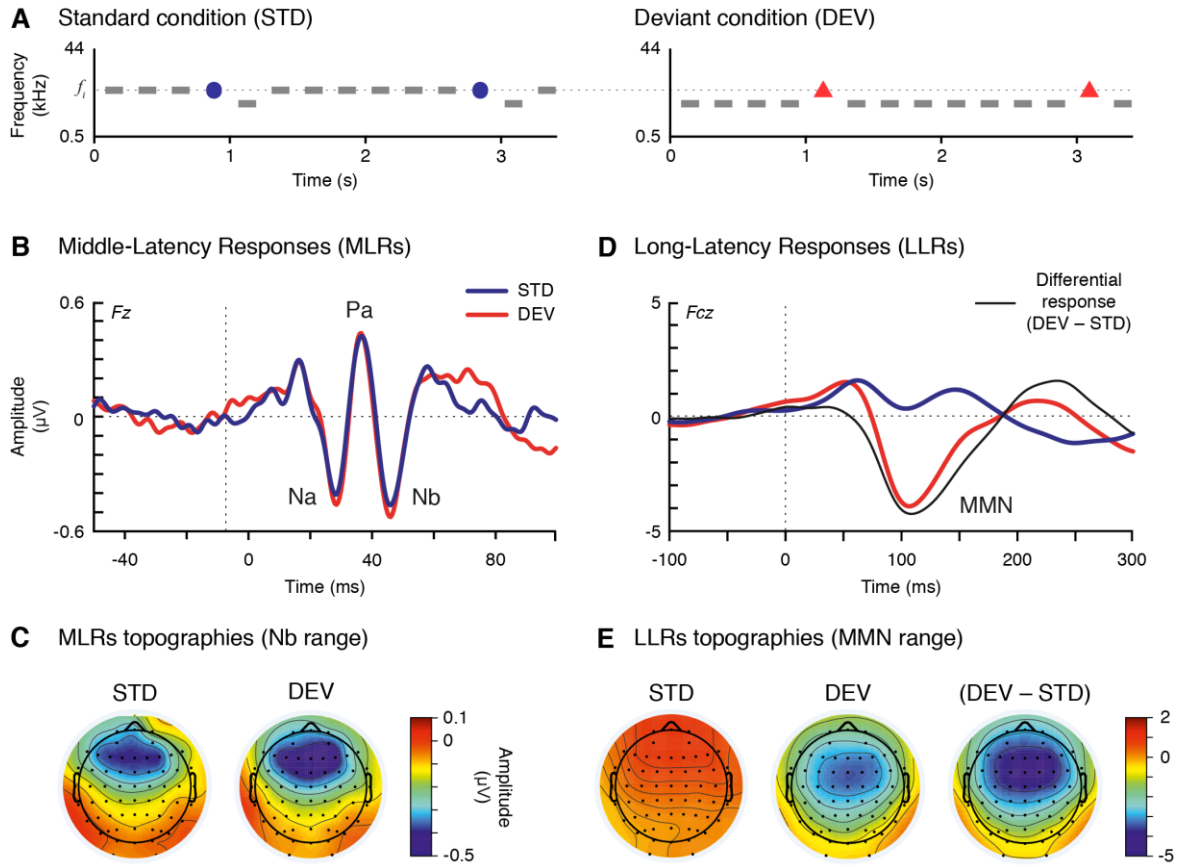

Figure 10. Human AEP under oddball stimulation. **A.** Oddball sequence comprising two tones of different frequency. The unbalanced probability of appearance defines the DEV (red triangle) and STD. Only the last STD (blue circle) previous to a DEV tone is used to calculate the differential response (DEV – STD). **B.** MLRs with its typical morphology waveforms disclosing larger amplitude for DEV (red) than for STD (blue) stimuli. **C.** Scalp distribution of the Nb latency range for DEV and STD. **D.** LLRs for STD (blue) and DEV (red), and the differential response (black) revealing the mismatch negativity (MMN). **E.** Scalp distribution of the MMN latency range for STD (left) and DEV (center), as well as the differential response (right), which reveals the topography of the MMN. Adapted from Althen et al. (2013).

The MMN is the largest and last obligatory differential response in the human AEP. On the one hand, there are AEP modulations related to pre-attentive novelty processing already present in the *middle-latency responses* (MLRs, 10–80 ms). MLRs are thought to correspond to the earliest responses of the AC, mostly from its primary regions (Yvert et al., 2001, 2005). Those differential MLRs (Figure 10B and C), however, then enlarge by one order of magnitude within the MMN time frame, when auditory information has reached the *nonprimary regions* of the AC and the frontal cortex. On the other hand, there are other large responses related to novelty processing after the MMN. However, subsequent LLRs involve higher cognitive functions, such as attention (P3a; Comerchero and Polich, 1999), working memory (P3b; Kok,

2001), semantic (N400; Kutas and Hillyard, 1980) and syntactic processing (P600; Kaan et al., 2000), and are thus not obligatory components of the AEP (Duncan et al., 2009). Conversely, the MMN remains persistent during sleep (Nashida et al., 2000; Strauss et al., 2015), anesthesia (Koelsch et al., 2006; Quaedflieg et al., 2014) or coma (Morlet & Fischer, 2014; Rodríguez et al., 2014). Moreover, the MMN is present in the moment of birth (Carral et al., 2005; Winkler et al., 2003) and even before (Draganova et al., 2005, 2007). This led some renowned authors to interpret the MMN as the sign of a 'primitive intelligence' embedded in the auditory system (Näätänen et al., 2001); an early process of cognitive nature that serves as foundation and trigger of higher cognitive functions reflected by later LLRs (Näätänen et al., 2010), such as attention (Fritz et al., 2007) and memory (Ranganath & Rainer, 2003). The MMN is thus the signature of an automatic processing of sensory novelty, active even in the lack of consciousness, which makes it a perfect tool for basic cognitive research (Näätänen et al., 2007).

Patients suffering from neurodevelopmental and psychiatric conditions exhibit MMN disruptions (Lavoie et al., 2019; Näätänen et al., 2014). The MMN is characteristically and profoundly reduced in schizophrenia (Light & Näätänen, 2013; Michie et al., 2016; Näätänen et al., 2015, 2016; Todd et al., 2013), and it is also altered in other pathologies such as Parkinson's disease (Pekkonen, 2000; Seer et al., 2016), Alzheimer's disease (Horváth et al., 2018; Pekkonen, 2000), language impairments (Bishop, 2007; Kujala & Leminen, 2017) and autism spectrum disorders (Schwartz et al., 2018; Vlaskamp et al., 2017). Understanding these MMN disruptions can offer valuable insights for clinical research, and even possible diagnostic applications. A simple EEG screening protocol including an auditory oddball paradigm could objectively estimate affectations of the general brain function. This is true even for populations of neuropathological or psychiatric patients in non-collaborative conditions, thanks to the obligatory nature of the MMN (Schall, 2016).

The thorough study of MMN latencies and topographies in almost every imaginable experimental, developmental and clinical condition established that the MMN emerges from two underlying processes taking place in a frontotemporal cortical network: (1) a sensory-memory mechanism, related to temporal generators —i.e., nonprimary AC of the human brain—; and (2) an attention-switching mechanism, related to frontal generators (Alho, 1995). According to this cognitive hypothesis, a detector system pre-attentively compares the current sensory input with a sensory-memory trace of previously encoded auditory regularities. The

detection of a deviance prompts an involuntary attention switch towards the auditory change, and the sum of that neural activity reflects in the AEP as an MMN (Figure 11). Thus, the MMN constitutes a separately evoked *mismatch signal*, which corresponds to the functioning of a mechanism of *deviance detection* based on *regularity encoding* that mobilizes cognitive resources to further process deviant events (Näätänen & Winkler, 1999; Winkler et al., 1996).

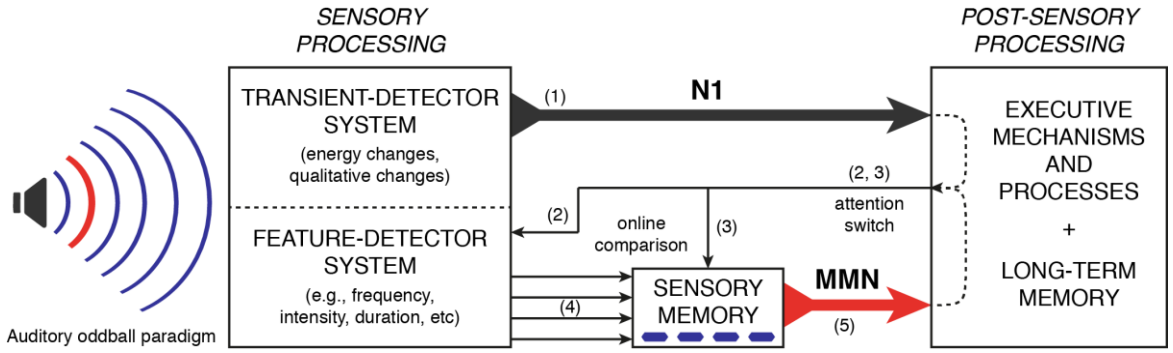

Figure 11. Auditory novelty perception according to the Detection Hypothesis (Näätänen, 1990; Näätänen et al., 2007). Transient-detector systems are activated by sudden changes of stimulus energy, such as onsets and offsets, without content information, bombarding the central executive mechanisms with interrupt signals that reflect in the AEP as a negativity between 80–120 ms, called N1 (1). Whether some momentary threshold is exceeded, this bombardment causes an attentional switch to the ongoing sensory processes (2) and to the results of previous sensory analysis stored in the sensory memory (3). The feature-detector system passes information extracted from the physical features of the acoustic stimuli to the sensory memory (4). Then, this information is encoded in precise stimulus representations or neuronal traces, which are strengthened by repetitions of an identical stimulus or by regular successions of thereof (in blue). After a solid memory trace has been encoded, however, DEV input (in red) yields another interrupt or mismatch signal to the executive mechanisms, which reflects within 100–250 ms of the AEP as an MMN (5). The attention switch occurs when the strength of the generator process exceeds some temporary limit (2, 3), enabling a conscious perception. Note that this model postulates different types of neurons in the AC: N1 generators, feature detectors, memory traces, online comparators, MMN generators, etc. However, electrophysiological data does not support such functional division, and direct evidence of neurons exclusively devoted to change detection and MMN generation is still lacking (May & Tiitinen, 2010). Adapted from Näätänen (1990).

The *Detection Hypothesis* enjoyed great acceptance for decades over other possible explanations (for a review from the time, see Näätänen and Alho, 1995). Yet, reports of cortical SSA under oddball stimulation (Ulanovsky et al., 2003) relaunched and bolstered an alternative interpretation of the MMN (Jääskeläinen et al., 2004; May & Tiitinen, 2004), which had been broadly discarded up to that moment (Cowan et al., 1993; Näätänen et al., 2005). Challenging the cognitive approach, there was a plausible chance that the MMN could be explained by simpler physiological mechanisms inducing synaptic adaptation.

I.2.b.- Stimulus-Specific Adaptation (SSA) and the Adaptation Hypothesis

It is possible to record the activity of single auditory neurons in animal models under oddball paradigm stimulation (Figure 12A). Some auditory neurons respond similarly to the STD and the DEV (Figure 12C), driven by the physical characteristics of each stimulus without being influence by its presentation probability. By contrast, other neurons progressively *adapt* or attenuate their response to the STD, while resuming their firing in response to the DEV (Figure 12E). The same happens when the tones switch conditions, implying that such differential response is due to their distinct probability of occurrence, and not to the different physical features of each tones. Unlike other mechanisms of adaptation present all over the auditory system, this one does not affect global responsiveness of the neuron, but exclusively the responsiveness to the repetitive stimulus. In other words, the physiological mechanisms behind this response adaptation are acting in a stimulus-specific manner.

Most types of adaptation can be understood as rather basic physiological mechanisms governed by the neuronal output. For example, spike-frequency adaptation depends on the discharge history of the neuron, accounted for by activation of voltage-dependent conductance (Sánchez-Vives et al., 2000b, 2000a) or tonic hyperpolarization (Carandini & Ferster, 1997). However, since these mechanisms operate at the level of the somatic membrane potential, they cannot be stimulus-specific (Ulanovsky et al., 2004), nor can they vary across the neuronal receptive field as SSA does (Duque et al., 2012). Considering that, SSA emergence must rely on physiological mechanisms operating at the input of the neuron, based on its synaptic history. Short-term plasticity mechanisms, such as synaptic depression and facilitation (Abbott et al., 1997; Tsodyks & Markram, 1997) or inhibition (L. I. Zhang et al., 2003) would differentially affect distinct regions of the dendritic tree, thereby exerting stimulus-specific effects over the eventual response of the neuron. Most interestingly, there is a positive correlation between the

width of the receptive field of the neuron the strength of its SSA (Duque et al., 2012). All of which suggests that SSA is not the result of intrinsic membrane properties of individual neurons, but it is rather an emergent functional property of the neural network. SSA likely develops from plastic mechanisms at neurons with extensive dendritic arbors, which converge manifold sensory input while depressing the synapses that get activated recurrently.

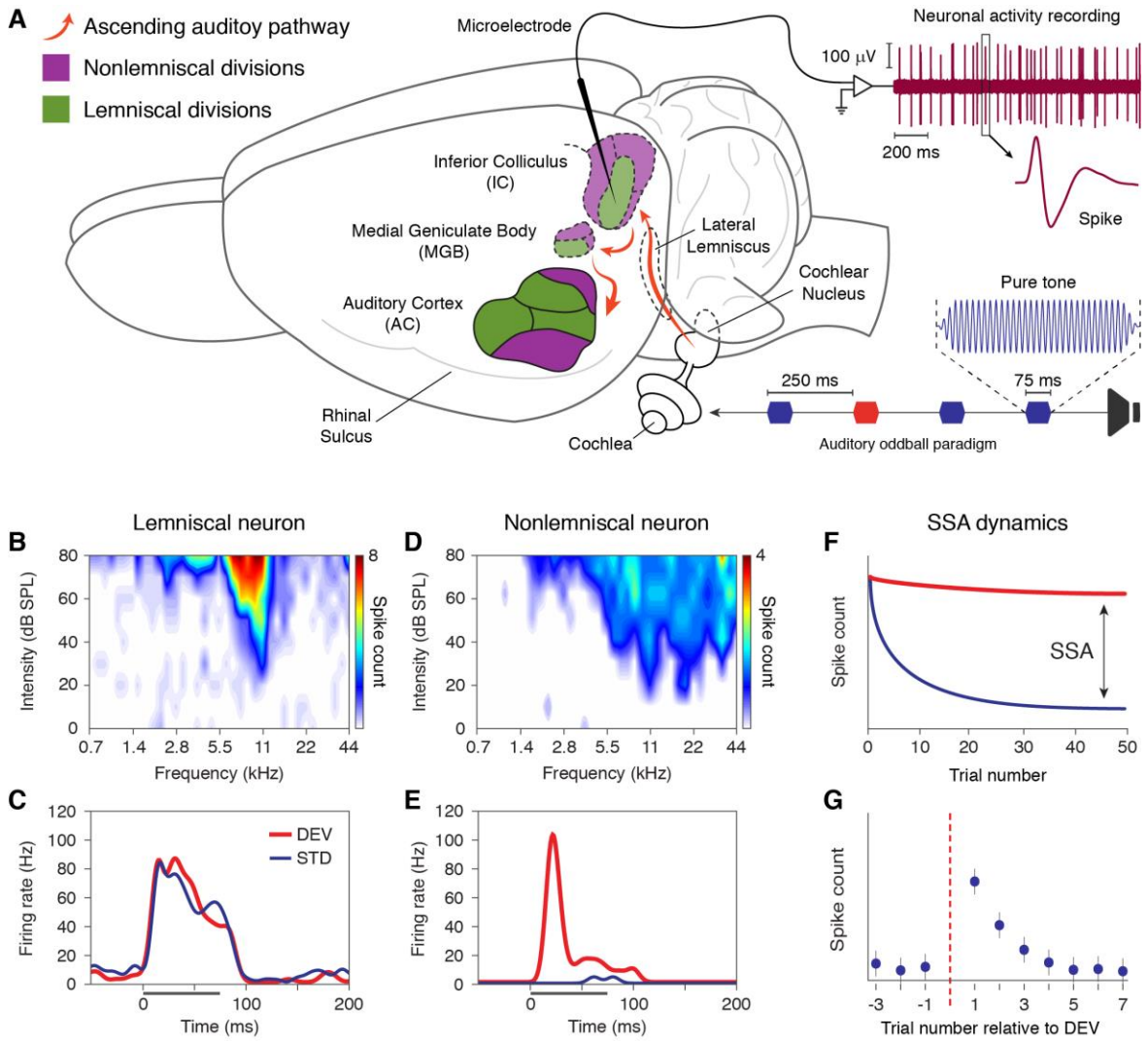

Figure 12. Recording SSA from a rat brain. **A.** Sketch of a typical experimental setup for extracellular recording. **B.** Example of a sharply tuned FRA, characteristic of lemniscal neurons. **C.** PSTH of that same neuron in B responding to an oddball paradigm. Note that both responses follow the tone (thick grey bar) and their vigorous firing rates are barely modulated by the experimental condition. **D.** Example of a broadly tuned FRA, characteristic of nonlemniscal neurons that can process and integrate a wider range of frequencies. **E.** PSTH of that same neuron in D responding to an oddball paradigm. Note that the response to STD is almost completely adapted. **E.** Long-term dynamic of SSA. **E.** Short-term dynamic of SSA. Reproduced from Carbajal & Malmierca (2020).

Only one repetition of a stimulus suffices to induct SSA. Consequently, SSA can emerge from a local effect prompted by the influence of the immediately preceding stimulus. Therefore, the response to a repeated stimulus A (r_{AA}) will always be weaker than if a different stimulus B would have come before A (r_{BA}), as it is been empirically observed ($r_{BA} > r_{AA}$) in the AC (Ulanovsky et al., 2004) and the IC (Zhao et al., 2011). According to this one-trial effect, it does not matter whether a stimulus is DEV or STD, just whether it is repeated or not. This one-trial effect is known as the *short-term dynamic* of SSA (Ulanovsky et al., 2004; Zhao et al., 2011). Notwithstanding, the short-term dynamic does not fully explain what can be observed in the context of the oddball paradigm. A stimulus will elicit a weaker response after several repetitions than after just one ($r_A > r_{AA} > r_{AAA} > r_{AAAA}$), implying an *n*-trial effect (Ulanovsky et al., 2004). Therefore, after enough presentations, the unbalanced probabilities of the oddball paradigm will have a great influence over the neuronal response. This global effect is referred to as the *long-term dynamics* of SSA (Ulanovsky et al., 2004; Zhao et al., 2011).

The long-term dynamic of SSA explains why the appearance of a deviant tone does not fully restore the response to the standard tone. SSA strength is determined by several preceding trials, not just the last one. Most strikingly, this accumulative effect can last for tens of seconds, which is beyond the time frame of passive plasticity mechanisms such as synaptic depression (Abbott et al., 1997; Ulanovsky et al., 2004). This has led some authors to speculate an involvement of additional PP mechanisms actively adjusting the synaptic efficiency of SSA neurons (Rubin et al., 2016), as I will discuss in Section I.3. Nevertheless, the STD response indeed recovers to some extent after each DEV presentation, indicating that SSA strength is not only determined by the global probability of each stimulus (Ulanovsky et al., 2004; Zhao et al., 2011). Whether this were the case, after enough repetitions of the STD tone, a STD tone coming after the DEV tone would subdue similar SSA as the last STD tone before that deviant tone. Conversely, the response to the STD tone partially remerges after a DEV tone, implying that the one-trial effect is still at play throughout the whole oddball sequence (Figure 12G). Thus, the magnitude of the SSA that a neuronal response undergoes at each stimulus presentation is determined by both short-term and long-term dynamics, which represent two time scales of integration in SSA (Ulanovsky et al., 2004).

The magnitude of SSA effects over the firing rate of a neuron are positively correlated with (1) the probability of the stimulus, (2) the physical contrast with the other stimulus in the

oddball paradigm and (3) the stimulus presentation rate (Antunes et al., 2010; Ayala & Malmierca, 2013; Malmierca et al., 2009). As a rule of thumb, faster rates tend to induce stronger SSA, but only up to the point where the rapid succession of stimuli begins to induce temporal masking effects in the recorded auditory center (Faure et al., 2003). Additionally, slow presentation rates reveal that significant SSA can last for several seconds or even minutes, a time frame that weakens its connection to short-term plasticity mechanisms, whereas it allows to link SSA with the habituation observed in behavioral approaches (Gutfreund, 2012; Netser et al., 2011). Minding the differences between techniques and species, these functional characteristics of SSA dovetail with those of the MMN (Ulanovsky et al., 2003).

Based on their conspicuous functional resemblance, cortical SSA was proposed as the neuronal correlate of the MMN (Jääskeläinen et al., 2004; Ulanovsky et al., 2003), sparking a prolific debate in the MMN literature (Näätänen et al., 2005). According to the *Adaptation Hypothesis*, neurons tuned the repeated STD stimulus simply adapt due to passive plasticity processes such as synaptic depression, while neighboring neurons remain fresh and respond strongly when a DEV stimulus makes an entrance (Mill et al., 2011; Taaseh et al., 2011). Thus, the MMN would correspond to a delayed and attenuated STD response, which appears to be a separated component of the AEP only when it is subtracted from the DEV response.

The Adaptation Hypothesis provided a more parsimonious and neurobiologically grounded interpretation of the MMN, as compared to the intricate cognitive interplay of sensory processors, memory tracers, and online comparators proposed by the Detection Hypothesis (Näätänen et al., 2007). A detector system seemed plausible at the massive scale of brain imaging, but it stumbled upon some serious difficulties when trying to pin down its correlates at the neuronal scale (Fishman, 2014; May & Tiitinen, 2010). By contrast, the Adaptation Hypothesis considered that the MMN recorded by surface electrodes was essentially the sum of many SSA processes occurring throughout all the auditory regions of the cortex (Jääskeläinen et al., 2004; Ulanovsky et al., 2003). Whether that were correct, SSA would offer an exceptional model to investigate the physiological mechanisms affected in the neuropathological and psychiatric conditions accompanied by MMN impairments. Accordingly, SSA studies in animal models have substantially thriven since the connection between SSA and the MMN was formally proposed (Ulanovsky et al., 2003).

In spite of this, there were some remnant incongruities between the SSA and the MMN, mostly due to the impossibility of recording human neurons as we do in animal models. In

essence, cellular recordings consist in inserting a microscopically thin electrode in one area of interest of the brain and record the activity of one neuron at a time —i.e., single-unit activity

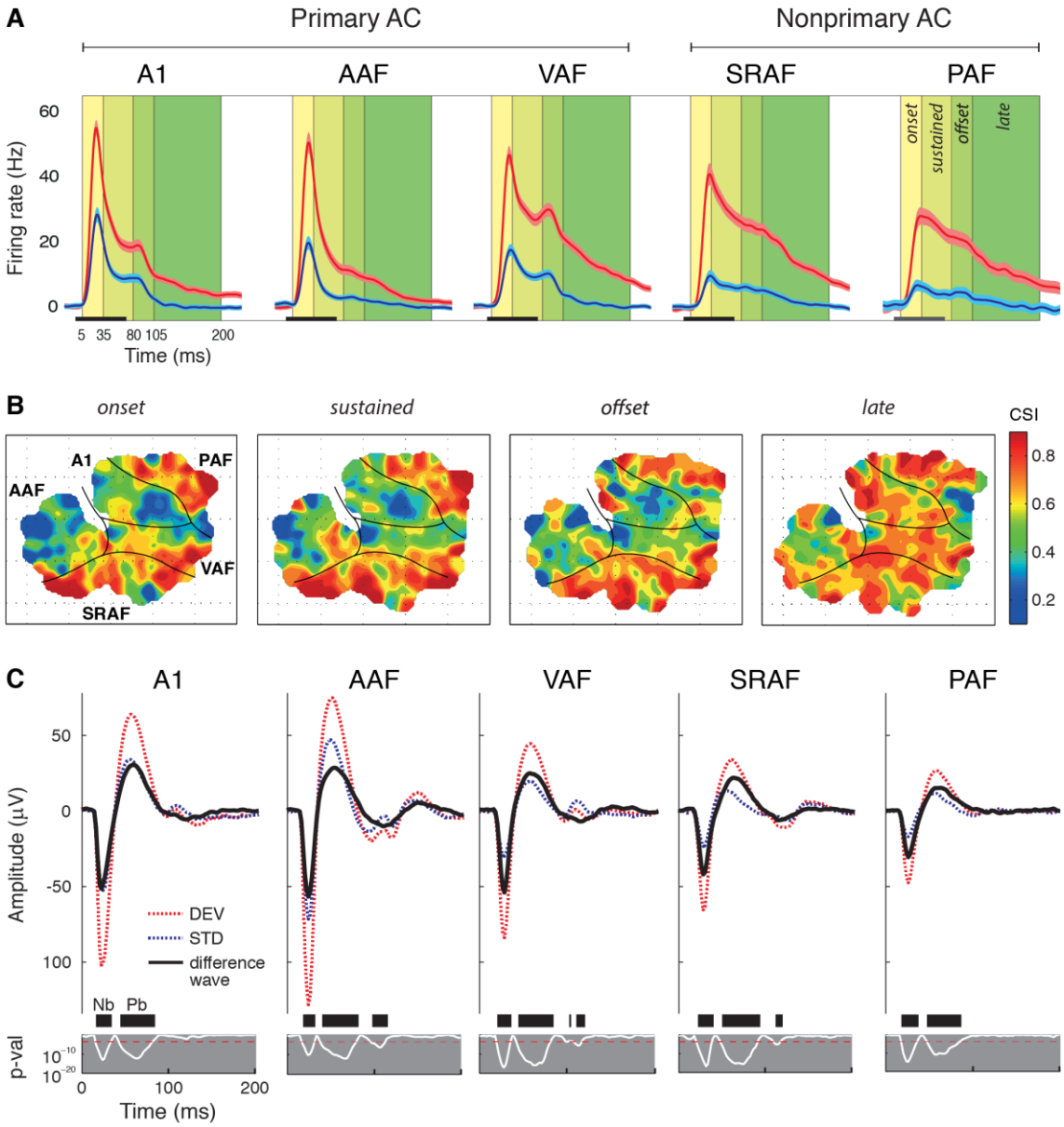

Figure 13. CSI variation across time and cortical fields of the rat AC. **A.** Grand-average MUA to STD (blue) and DEV (red) within each field and throughout 4 time windows. **B.** Topographic distribution of the CSI in 4 different time windows. Note that only the late component of the CSI is high throughout the entire AC. **C.** Grand-average LFPs. The difference wave described 2 components: a fast Nd and a slower Pd. An additional small but significant deflection of the LFP was identified at longer latencies (>100 ms) in anteroventral fields (AAF, VAF, and SRAF). The thin white line below represents the p value of the difference wave, with a thick black bar marking the time intervals containing significant differences. Adapted from Nieto-Diego & Malmierca (2016)

(SUA)— or several of them in a close range —i.e., multi-unit activity (MUA). Moreover, by widening the filter of the recorded signal, it is possible to gather the activity of a whole neural region of several millimeters around the tip of the electrode, obtaining a local-field potential (LFP). These techniques yield extraordinarily detailed information from the electrophysiological and neuroanatomical standpoints, but they require invasive surgical procedures that damage the neural tissue irreversibly (Figure 12A). Therefore, cellular recordings are not suited for investigating the human brain.

Notwithstanding, the presence of SSA to auditory stimulation has been demonstrated in the primary (Harpaz et al., 2021; Parras et al., 2017; Pienkowski & Eggermont, 2009; Taaseh et al., 2011; Ulanovsky et al., 2003) and nonprimary regions of AC (Nieto-Diego & Malmierca, 2016; Parras et al., 2017), in the MGB (Anderson et al., 2009; Antunes et al., 2010; Harpaz et al., 2021; Kraus et al., 1994; Parras et al., 2017) and the IC (Harpaz et al., 2021; Lumani & Zhang, 2010; Malmierca et al., 2009; Parras et al., 2017; Pérez-González et al., 2005), as well as in extra-auditory regions such as the thalamic reticular nucleus (Jia et al., 2021; Yu et al., 2009), the amygdala (Camalier et al., 2019), the hippocampus (Rummell et al., 2016) or the PFC (Casado-Román, Carbajal, et al., 2020; Srivastava & Bandyopadhyay, 2020). SSA has been vastly confirmed in several mammalian species, such as cats (McKenna et al., 1989; Ulanovsky et al., 2003), guinea pigs (Condon & Weinberger, 1991; Kraus et al., 1994), gerbils (Bäuerle et al., 2011; Malone & Semple, 2001), rats (Nieto-Diego & Malmierca, 2016; Pérez-González et al., 2005), mice (Anderson et al., 2009; Duque & Malmierca, 2015), bats (Thomas et al., 2012) and monkeys (Fishman & Steinschneider, 2012; Malone et al., 2002). Moreover, SSA of auditory responses have been reported also in animal models from other classes: in avian species, such as songbirds (Chew et al., 1995; Gill et al., 2008) and barn owls (Netser et al., 2011; Reches & Gutfreund, 2008); in amphibian species such as marsh frogs (Bibikov, 1977) and leopard frogs (Ponnath et al., 2013); and even in an insect like the katydid (Prešern et al., 2015; Schul et al., 2012; Triblehorn & Schul, 2013). Thus, the physiological mechanisms that enable SSA seem to be evolutionarily old and well preserved across species. Consequently, it is safe to assume that SSA also happens in the human brain, and it could indeed be the neural substrate of the MMN.

I.2.c.- The MMN and SSA: 2 scales of the same phenomenon?

Despite their striking functional resemblance, it has not been easy to reliably link cortical SSA with the human MMN. Originally, and for more than a decade, all the available oddball-evoked MUA data was recorded within primary AC (Khouri & Nelken, 2015; Ulanovsky et al., 2003), whereas the MMN source in the human brain is located within nonprimary AC, besides other frontal generators (Alho, 1995). Thus, the cortical topographies of SSA and the MMN were not fitting. Moreover, SSA in primary AC seemed to emerge and decay prematurely as compared to the relatively long latency and slow deflection described by the MMN. These incongruities have casted doubt on the plausibility of the Adaptation

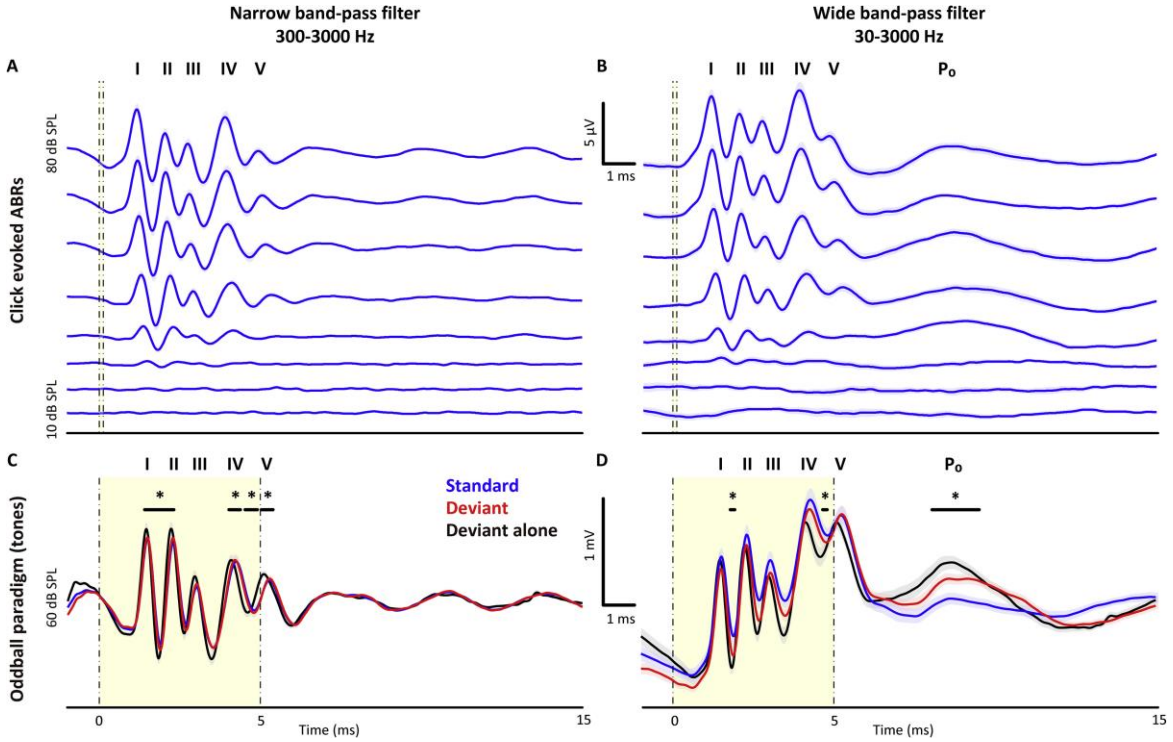

Figure 14. ABRs with narrow band-pass filters vs. wide band-pass filters. **A-B.** Click-evoked ABRs from 24 different CBA/J mice recorded with a narrow band-pass filter (A, 300–3000 Hz) and with a wide band-pass filter (B, 30–3000 Hz). A slow positive wave P_0 can be identified 8–9 ms after sound onset when using a wide band-pass filter. Yellow shaded band shows the 100 µs click duration. **C-D.** ABRs to pure tones in an oddball paradigm recorded with a narrow band-pass filter (C, 300–3000 Hz) and with a wide band-pass filter (D, 30–3000 Hz). ABRs to pure tones presented as STD (80% occurrence: blue) and DEV (20% occurrence: red) are shown. ABRs in a deviant alone condition (infrequent presentation: black) are also shown. Black lines over the ABRs show regions where there are statistical differences (* $p < 0.05$) between STD and DEV waves. Shadowed yellow band shows the 5 ms tone duration. Reproduced from Duque et al. (2018).

Hypothesis. However, nowadays copious AEP data confirm the presence of early mismatch signals all over the AC of humans and animals (Grimm et al., 2016). Oddball paradigms using location (Aghamolaei et al., 2016; Grimm et al., 2012; López-Caballero et al., 2016; Sonnadara et al., 2006), interaural time difference (Cornella et al., 2012), temporal (Leung et al., 2013), intensity (Althen et al., 2011, 2016), modulation (Shiga et al., 2015) and frequency deviants (Althen et al., 2016; Grimm et al., 2011; Recasens, Grimm, Capilla, et al., 2014; Recasens, Grimm, Wollbrink, et al., 2014; Slabu et al., 2010) consistently elicit mismatch responses within the human MLRs, besides a subsequent MMN. AEP studies in animal models have identified MMN-like potentials generated from the nonprimary AC of cats (Pincze et al., 2001) and rats (Shiramatsu et al., 2013), coinciding with the temporal generators of the human MMN (Alho, 1995). Additionally, a MUA study from our lab proved that SSA is stronger and lasts well over 200 ms in nonprimary AC neurons (Figure 13A and B; Nieto-Diego & Malmierca, 2016). This study also analyzed the LFPs to provide a mesoscopic measurement in between the neuronal SSA and the mass activity reflected by the MMN. The LFPs conveyed mismatch signals that that correlated in time and space with the SSA, and were likewise larger and more persistent in nonprimary AC (Figure 13C; Nieto-Diego & Malmierca, 2016). The difference wave of the DEV-evoked LFPs and the STD-evoked LFPs showed the same morphology in all AC regions, with a fast, negative deflection (Nd) followed by a positive one (Pd). However, Nd and Pd presented variations between cortical areas. On the one hand, the Nd was larger and tended to peak earlier in primary AC. While the Nd peaks as early as 24 ms in primary AC, in the nonprimary regions the Nd takes more than 31 ms to peak. The Nd time frame could correspond to that of the modulations observed in the human MLRs, which suggests a correlation between the onset component of the SSA in the rat AC, the Nb of the rat LFP and the differential responses of the human MLRs. On the other hand, the Pd peaks rather homogeneously along all AC regions around 60 ms, which is well within the range of the MMN-like potentials in the rat (50–100 ms; Jung et al., 2013; Shiramatsu et al., 2013; Harms et al., 2014; Harms, Michie and Näätänen, 2016), thus connecting cortical SSA to the MMN (Nieto-Diego & Malmierca, 2016). One of the aims of my thesis is to establish a similar connection at the level of the auditory midbrain between large-scale mismatch signals and SSA data.

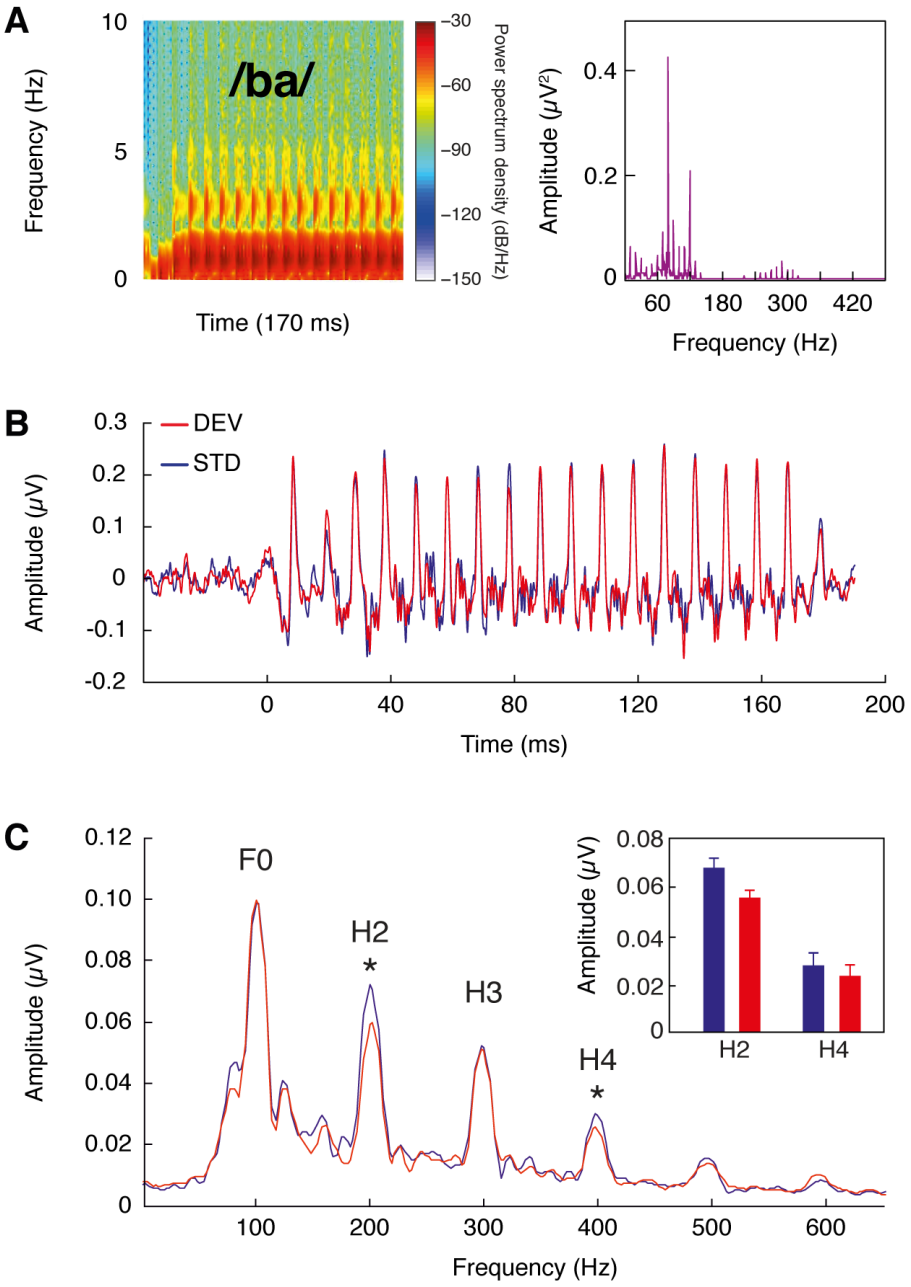

Figure 15. Differential responses to complex stimuli in the human auditory brainstem response. A. Spectrogram (left) and frequency spectrum (right) of the /ba/ syllable used in an oddball sequence together with different /wa/ vocalisations (not shown). **B.** Grand-average of the FFR elicited by STD and DEV presentations of the syllable /ba/. **C.** FFR spectrum of the /ba/ syllable, showing a significant difference between conditions in the amplitude of the second (H2) and forth (H4) harmonics. Adapted from Cacciaglia et al. (2015).

Few studies have actively pursued to correlate SSA in the IC with the earliest mismatch signals detectable in the human brain, as pinning down the precise anatomical source of potentials originated in deep parts of the brain when recording from scalp electrodes entails a

formidable technical challenge. Inasmuch as auditory neurons from lower brainstem nuclei do not exhibit any SSA (Ayala et al., 2013), the IC is the earliest anatomical source of SSA in the mammalian auditory system. Midbrain-level SSA should be ideally reflected within the early latencies of the AEP, in the *auditory brainstem responses* (ABR, <10 ms). Simple stimuli, such as clicks or noise bursts, evoke ABRs displaying a prominent wave V, which is thought to reflect the activity of the IC (Picton, 2010; Stockard et al., 1979). More complex sounds, such as amplitude-modulated tones or vocalizations, elicit *frequency-following responses* (FFR) after wave V, which encode the spectral and periodicity information of complex stimuli. Mismatch responses have been confirmed within the rat ABR (Figure 14; Duque et al., 2018), but none have been clearly identified in the human wave V thus far (Althen et al., 2011; Slabu et al., 2010). This discrepancy could be due to how the huge neuroanatomical differences between the two species affect the conductance of the mismatch signal from its deep source to the superficial recording electrodes. Notwithstanding, when the oddball paradigm uses consonant–vowel vocalizations (e.g., /ba/ and /wa/), mismatch signals become visible in the human FFR (Figure 15; Shiga et al., 2015; Skoe et al., 2014; Slabu et al., 2012). Additionally, mismatch responses have been observed in the IC of rats (Gao et al., 2014) and humans (Cacciaglia et al., 2015) using fMRI (Figure 16).

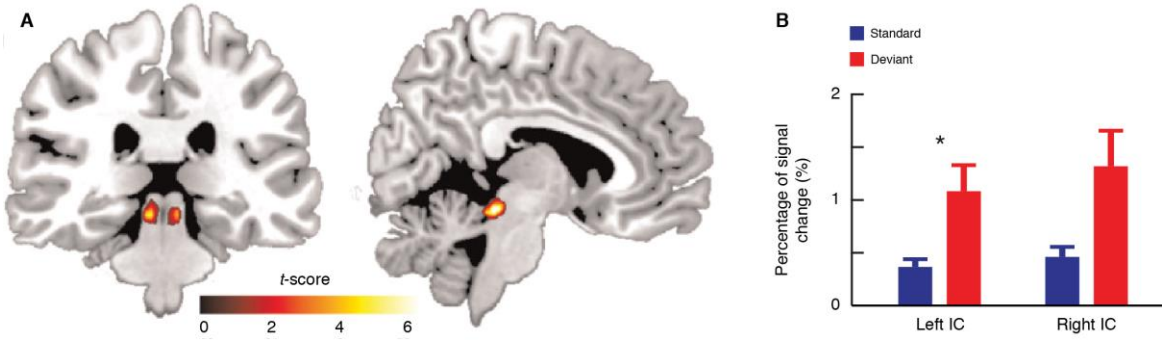

Figure 16. Response to the oddball paradigm in the human IC shown in fMRI. A. The region of interest analysis revealed a significant activation of the IC in the contrast between STD and DEV. **B.** Percentage of signal change. Adapted from Cacciaglia et al. (2015).

In summary, the mismatch signals that become very prominent within the time frame of the MLRs and LLRs of humans and animals, are already observable at the ABR, hinting at a midbrain-level generator. This seems to coincide with the distribution of SSA across the auditory pathway, in the IC, MBG and all over the AC. Such an anatomical and temporal coincidence between SSA and the MMN makes the Adaptation Hypothesis plausible. From this neuronal perspective, the MMN would not result from an active cognitive process of

deviance detection, and it would not really be a *genuine* mismatch signal. Conversely, STD responses become adapted passively while DEV responses simply remain fresh. Each stimulus repetition induces inhibition or short-term plasticity via mechanisms like synaptic depression, automatically conferring saliency to rare stimulus, given that those processing channels are not adapted (Mill et al., 2011; Taaseh et al., 2011). Thus, pre-attentive novelty processing would emerge from passive *adaptation*, instead of from active *detection*.

I.2.d.- Detection or adaptation? The no-repetition controls (NRC)

Both Detection and Adaptation Hypotheses account for the differential response to the oddball paradigm, but their functional explanations are conflicting. On the one hand, the Detection Hypothesis involves a system comparing the current sensory input with a memory trace of STD repetition, where the nonconformity of DEV generates a mismatch signal to adjust that memory trace. Thus, the MMN constitutes a *separated* mismatch response, emerging from an active process of deviance detection based on regularity encoding. On the other hand, according to the Adaptation Hypothesis, neurons simply adapt their responsiveness specifically to the repetitive STD via passive processes such as synaptic depression and lateral inhibition. Thus, the MMN is just the result of subtracting an attenuated and delayed STD response from the non-adapted AEP elicited by DEV. There is no separate mismatch signal, no active deviance detection, just passive SSA. The two hypotheses understand automatic novelty processing in qualitatively distinct manners. Going back to our walk through the park, the Detection Hypothesis posits that our brain actively detects a deviant bark within the stream of random noises, whereas the Adaptation Hypothesis posits that our brain just abates standard noise, clearing processing channels for deviant sounds such as nearby barks. Abiding by the law of parsimony, the simpler and more neurobiologically grounded SSA is apparently better than deviance detection for explaining the MMN elicited in the context of the oddball paradigm (Fishman, 2014; May & Tiitinen, 2010). Notwithstanding, SSA struggles to account for responses yielded during stimulation paradigms where there is not an acoustically constant STD (Winkler et al., 2009).

In the detection-vs-adaptation debate, the widely-used oddball paradigm has a major methodological limitation: it cannot distinguish the effects of deviance detection from the effects yielded by SSA. In order to control for the passive adaptation effects that could contribute to MMN, some experimental designs began to incorporate controls for the repetition

of the STD. Such *no-repetition controls* (NRC) are stimulation sequences that must meet 3 criteria: (1) featuring the same stimulus of interest with the same presentation probability as that of the DEV; (2) inducing an equivalent state of refractoriness in the auditory system —e.g., presenting the same rate of stimulus per second, etc—, which implies that presenting the stimulus of interest solo, over a background of silence, does not set a proper NRC; and (3) presenting no recurrent repetition of any individual stimulus. Thus, it is possible to assess the portion of the differential response that could have been induced by SSA. In other words, the NRC provides an estimation on how well the Adaptation Hypothesis can account for the MMN elicited by the oddball paradigm (Figure 17C). Whether the differential response equates to the difference between the response evoked to the NRC and to the STD, then the differential response can be attributed entirely to passive adaptation (i.e.: DEV = NRC; Figure 17D). Otherwise, a process of active detection cannot be discarded. Moreover, without rejecting a possible contribution of SSA to the MMN, many authors have considered that a stronger response to DEV that to NRC unveils a component of so-called *genuine* deviance detection (i.e.: DEV > NRC; Figure 17E).

There are 2 designs meeting the aforementioned criteria that have been widely accepted as suitable NRC for the oddball paradigm: the many-standard sequence and the cascade sequences (Figure 17B). The *many-standards NRC* (Schröger & Wolff, 1996) presents the stimulus of interest embedded in an aleatory sequence of assorted stimuli, where each tone shares the same presentation probability as the DEV in the oddball paradigm. However, some authors have argued that the many-standards NRC is not fully comparable with the oddball paradigm, inasmuch as the random succession of tones never allows to form the sensory-memory trace of a proper regularity, unlike the STD. Moreover, the chaotic succession of stimuli might elicit mismatch responses, which would underestimate the genuine deviance detection in the comparison of DEV against NRC. The cascade NRC (Ruhnau et al., 2012) tries to overcome these alleged caveats by arranging stimuli in regular fashion, following an increasing or a decreasing frequency succession. Thus, the stimulus of interest conforms to a regularity —as opposed to the DEV—, but not a regularity established by repetition —contrary to the STD—, making the cascade NRC more fitted and less conservative than the many-standards. There is not consensus in the literature about which of these NRCs is more adequate, so this thesis will make use of both.

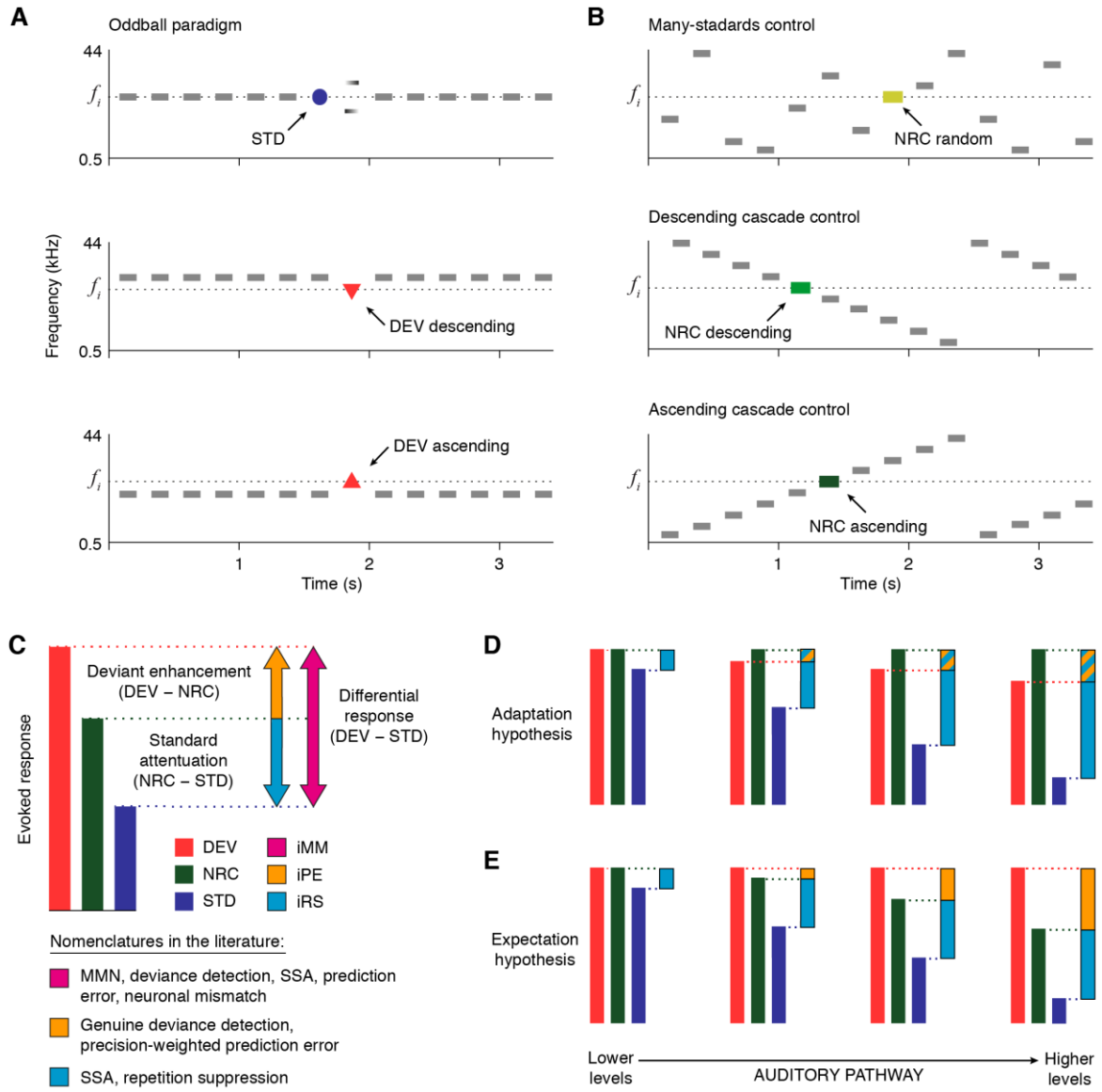

Figure 17. Interpretation of the no-repetition controls (NRCs). **A.** Oddball paradigm displaying 3 possible experimental conditions for a given f_i tone. **B.** NRC sequences highlighting the f_i tone. **C.** Decomposition of the differential response by means of the NRC. **D.** According to the Adaptation Hypothesis, there should be an increasing adaptation to the STD from lower to higher processing levels. Due to cross-frequency adaptation of the DEV relative to the NRC, the iPE should turn increasingly negative (orange bar mixed with cyan). **E.** According to the Expectation Hypotheses, repetition suppression of the STD should increase from lower to higher-order levels, while DEV responses should become higher than NRC responses as auditory information moves up in the processing hierarchy, leading to growing positive iPE values (orange bars). Adapted from Carbajal & Malmierca (2020).

The introduction of NRCs in the experimental designs along the oddball paradigm has demonstrated that the Adaptation Hypothesis cannot fully account for the MMN elicited by

frequency (Jacobsen et al., 2003; Jacobsen & Schröger, 2001), intensity (Jacobsen et al., 2003), duration (Jacobsen & Schröger, 2003) and location DEV (Schröger & Wolff, 1996); nor for the early signs of novelty processing present in the MLRs to frequency (Grimm et al., 2011; Slabu et al., 2010), intensity (Althen et al., 2011) and location DEV (Grimm et al., 2012). Furthermore, EEG and fMRI analysis of subcortical nuclei under oddball and NRC stimulation revealed a component of genuine deviance detection in the differential response of the MGB and the IC (Cacciaglia et al., 2015; Slabu et al., 2012). Other more complex experimental designs that do not confound the effects of SSA and deviance detection have also exposed the shortcomings of the Adaptation Hypothesis beyond the oddball paradigm (Carbajal & Malmierca, 2020). Considering the evidence, the Adaptation Hypothesis cannot fully replace Detection Hypothesis, but just complement it. And the same holds true for the Detection Hypothesis, inasmuch as the cognitive notion of genuine deviance detection is not readily applicable to subcortical processing. At this point, 2 hypotheses would be needed to account for novelty perception, which is far from ideal. In the next block, I will introduce the third contestant hypothesis, an integrative proposal under the PP framework.

I.3.- THE PREDICTIVE PROCESSING FRAMEWORK

The challenge of attaining perception is not only that our sensors are providing much more input than the nervous system can fully process. The true challenge comes when such a deluge of sensory input is not even representing the external world as it is. To put it in straightforward terms: How can we see a 3D world with a 2D retina? Regarding audition, there is always a plethora of sounds travelling through the air and other matters, often been partially blocked by objects in the way, bouncing on every surface, and mixing into an acoustic jumble were some load sounds may mask others, everything before eventually hitting our little tympanic membrane all at once. For a moment, bring back to mind our walk through the urban park, where we could hear every event that is taking place in our surroundings, all at the same time, just by tracing the vibration of your eardrums. How is it possible to perceive individual auditory objects, like the bark, relatively neat and separated from other background sounds, like the wind, the traffic, the people… based on such a chaotic signal? Since our sensors are very limited in number and mechanic capacity, our brain is forced to come up with useful percepts out of an overwhelming amount of incomplete, noisy and ambiguous sensory information (Carbajal & Malmierca, 2020).

More than two centuries ago, Kant (1781) already advised us that we never have a direct experience of the events taking place in our environment, since our mind can only access the events that occur within our nerves. The information we obtain about the external world is introduced into our nervous system via sensation, so the characteristics of sensory input depend more on the nature of our own sensory organs than on the nature of the external objects themselves (see Section I.1.a). For example, when someone talks to us, we never directly experience that speech. We do not even have direct access to the vibrations that human voice yields in our tympanic membrane. Our brain can only operate with the electrochemical impulses that the Organ of Corti has transduced those vibrations into. It is our brain who must first estimate whether the organization of those electrochemical impulses meet the conditions of possibility of a human voice, better than any other plausible auditory object. And then, it must establish what ensembles of impulses correspond to specific words of a language we know, instead of any other word in our lexicon. Thus, our brain must apply some prior beliefs —expectations about human voices, about language, etc— to organize our sensations, and thereby represent what might have interacted with our sensors. But those prior beliefs or expectations are constructs that do not really exist as such in the external world; they are just mere conditions of possibility already established in our minds before the object has been experienced. Therefore, the actual external objects that interacted with our sensors remains always *hidden* to us. The task of perception is to *infer* them (Carbajal & Malmierca, 2020).

Instead conceiving perception as mostly governed by bottom-up processes, Kantian thought emphasized top-down influences, where our own prior beliefs meet sensory input to generate useful percepts. A century later, Helmholtz (1867) incorporated those Kantian notions to the scientific study of vision, concluding that perception was indeed a process of unconscious inference about the causes of the sensory neural activity based on our prior beliefs. Another century had passed when Neisser (1976) turned this idea into a general operative loop of analysis by synthesis. The so-called *perceptual cycle* constituted a fundamental pillar of the newly founded Cognitive Psychology. Nowadays, the latest computational advances on data processing and cybernetic theory (Ashby, 1960; Dayan et al., 1995) have granted us a renewed theoretical framework which, nonetheless, inherits this classic but pivotal idea that *perceiving* is in fact *inferring* —the cause of our sensations—. Thus, most recent and interesting attempts to explain perception as an inferential process are coming from the application of the Bayes' Theorem (Equation 1) to the brain function (Aitchison & Lengyel, 2017), within the so-called PP framework (Friston, 2003, 2005, 2010, 2018). In fact, the PP framework is currently

engendering the most influential and comprehensive theories of neural function addressing how the brain makes sense of the world (Heilbron & Chait, 2018).

$$P(cause|input) = \frac{P(cause) \cdot P(input|cause)}{P(input)}$$

Equation 1. Bayes' Theorem applied to a process of perceptual inference. $P(cause|input)$ is the conditional probability of our perceptual hypothesis (cause) given the sensation (input). In Bayesian Statistics, this is known as the posterior belief, which would correspond to our mental representation or percept. $P(cause)$ is the marginal probability of our perceptual hypothesis. This prior belief works as a prediction in PP. $P(input|cause)$ is the likelihood or conditional probability of the sensory input given our perceptual hypothesis, serving as evidence to update our beliefs. $P(input)$ is the marginal probability of our sensation. For a graphic representation, see Figure 18.

PP emerged as a coding strategy developed for data compression, enabling a computational system to efficiently process complex information by predicting its content. Instead of encoding all the information, PP would only encode the values of the *prediction error* (PE), i.e., the difference between the expected value of a variable and the actual value of that variable in the input signal (Clark, 2013). We can find an illustrative example in the way computers store video files. Videos contain loads of redundant information from one frame to the next, so instead of encoding every pixel in each frame, computers just encode the differences between adjacent frames to compress the data. In the same vein, our brain could *expect* the content of one sensation based on the content of previously processed sensations. Each sensory receptor responding in a *surprising* manner will be encoded in a PE value that the perceiving system must consider for properly predicting the next sensation. Therefore, to represent the whole sequence of events, our brain would just have to process the PE values, i.e., the divergence between our sensations and our expectations. As those PEs are used to update the perceptual model and generate more fitted expectations, the load of PEs to process gets reduced. Hence, low PE values flag an optimized processing of information. This is the driving principle of the PP framework: *PE minimization*.

I.3.a.- Hierarchical Minimization of Prediction Error (PE)

A perceptual system could carry out PE minimization by implementing within its neural network a hierarchical generative model, where bottom-up sensory input is compared to top-

down predictions across multiple levels of processing that are highly interdependent. Each level uses PEs forwarded from the level below as *evidence* to update its *prior beliefs* by means of Bayesian inference. Posterior beliefs at one level serve as prior beliefs for the subordinate level, constituting the *expectation* at those levels. Divergences between that expectation and the actual evidence —i.e., the *surprising* portion of sensory input—, gets encoded as a PE value and forwarded to the level above. In turn, that PE value serves as evidence to update the prior belief at the superior level, yielding a new posterior belief. This posterior belief is then conveyed back, top-down, as the new expectation. And this cycle keeps iterating, trying to *explain away* the PE, i.e., trying to reduce the *surprise* by fitting expectations to the actual sensory input from lower levels (Figure 18A). Hence, perception emerges from a hierarchy of causal inferences, where each level constrains the processing of their nested levels (Carbajal & Malmierca, 2020).

In order to illustrate in a simple manner how the PP framework understands perceptual inference, imagine we are watching a video. Prior beliefs at low levels of the processing hierarchy tend to be rather overfitted, i.e., too specific, short-term and mutable. A (hypothetical) first level of processing can cast predictions on very simple stimulus features, such as expecting to find the pixels of one frame colored the same in the next frame. These overfitted predictions are very prone to error, so this first level will forward a PE signal accounting for each pixel changing color between frames. Top-down predictive influences are inhibitory, such that the expected features of the sensory input are suppressed. Hence, only the surprising input is transmitted to the higher levels in the form of PEs. In other words, higher levels only work with portions of evidence that could not be predicted at its nested levels. This means that the sensory input generated by the pixels remaining the same color is suppressed at the first level of processing, so the next level up in the hierarchy only ‘sees’ the pixels which color has changed between frames (Carbajal & Malmierca, 2020).

As PEs are progressively explained away level after level, beliefs at higher levels become more abstract, global and stable. Higher-order expectations show an increasing sensitivity to complex regularities and long-term interactions of multiple causes. Hence, instead of just seeing pixels flickering from one frame to the next, successive levels of processing begin to dissociate background (relatively stable pixels) from figure (rapidly changing pixels), identify objects (sensory ensembles that tend to appear or change together and coherently

across pixels and frames), trace their movements throughout a span of many frames, and eventually form a perceptual model of the scene in the video (Carbajal & Malmierca, 2020).

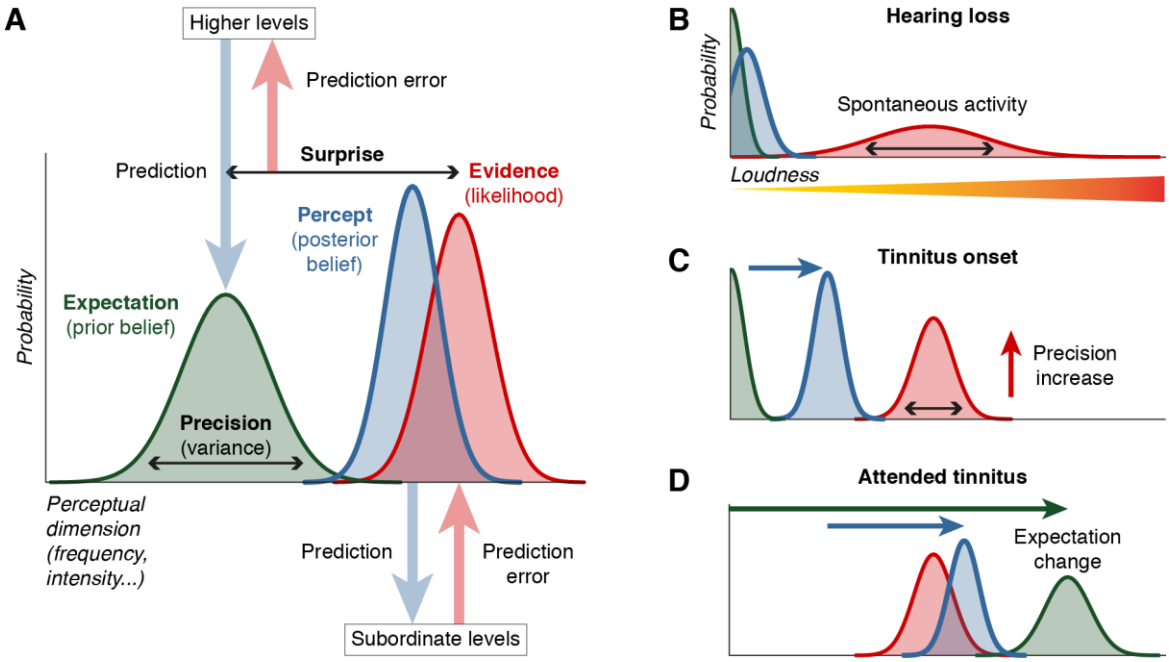

Figure 18. Perception as a process of Bayesian inference. **A.** Representation of the probability densities of prior beliefs (green), posterior beliefs (blue) and evidence (red) as Gaussian distributions over a perceptual dimension, where the heights indicate the prediction probabilities and the widths (variance) account for the expected precision (inverse of variance). In the bottom, a legend indicates the role of those Bayesian statistics in the PP framework. **B.** A hypothetic representation of the perception of sound intensity in a condition of tinnitus predisposition. After suffering hearing loss, spontaneous activity yields 'fake' PEs (red), but its low precision is not sufficient to override the strong expectation of silence (green) that is currently dominating auditory perception (blue). **C.** Whether a maladaptive adjustment increased the expected precision of the 'fake' PE, it could update the posterior belief and the tinnitus would become audible. **D.** Whether the patient paid attention to the tinnitus, the expectation would change drastically from silence to sound (green), so the tinnitus would become even more intense and clear. Reproduced from Carbajal & Malmierca (2020).

Higher levels can then cast more general predictions about upcoming sensory input over longer timescales, although not in a very detailed manner. Imagine the video is showing a person wearing a jogging outfit and running through a park. In the hierarchical generative model trying to account for the scene in the video, higher levels can expect the jogging pace to remain relatively slow and regular. That is a very useful prior belief to keep overall PE value at minimum, as it would be surprising to see a jogger suddenly sprinting. Conversely, higher-

order expectations will be completely different if the video presents a person wearing a business suit and running with a suitcase through an airport. To optimize sensory processing in this case, a very irregular pace, with sudden sprints and obstacles in the way, must be somewhat expected. But the generalist nature of higher-order processing cannot precisely account for each speed fluctuation, every twitch of a limb, each abrupt change in direction, etc. For this reason, the role of the higher-order predictive activity is to impose a top-down contextual constraint on the subordinate levels to hyperparameterize lower-order processing. Thereby, the overfitted expectations at lower levels will suppress predictable input and sample the surprising bits of sensation more efficiently. This will generate PEs that are useful to keep our internal model updated, which in turn will minimize PE values in the long run. As a result, we perceive the content of the video through an optimized predictive sensory processing (Carbajal & Malmierca, 2020).

In summary, the lower levels of the perceptual hierarchy are relatively myopic, so their scrupulous processing must be guided by the hyperopic higher levels, which downplay the details to acquire the big picture (Hohwy, 2013). Hierarchical PE minimization, i.e., the convergence of expectations and sensory input throughout nested levels of causal inference, configure a multilevel representations or *percepts* of the surprising information in the environment. Thereby, perception arises at the minimum expense of processing resources (Carbajal & Malmierca, 2020).

I.3.b.- Expected Precision

The nervous system is always processing certain PE amounts, not only because the world is in constant change, but also because of the noisy functioning of our own nervous system. For example, when sensors have suffered impairments (e.g., macular degeneration, hearing loss) or operate under challenging conditions (e.g., to see amidst the dark or the fog; to make sense of speech during a takeoff, with intense noise and pressure changes within the ears), some of the transduced sensory input may not be reporting faithfully on real changes in the environment, which may lead to misinformative PEs. Furthermore, our own nervous system may introduce noise in properly transduced sensory input due to conduction problems, or even generate 'fake' PEs. For example, a nerve impingement results in referred pain, which is perceived at a location other than the site of the impingement. PEs are not infallible signals, but the product of an inferential process. Therefore, not all PE values can receive equal

treatment. The brain must discriminate the residue error related to ambiguity and uncertainty from the relevant PE which truly reports on incorrect beliefs and real changes in the environment. In the PP framework, such assessment is performed by means of expected *precision*, which ponderates the gain of synaptic messages according to their confidence. In plain English, precision amplifies reliable signals (Carbajal & Malmierca, 2020).

Formally, prior beliefs are expressed using Gaussian probability distributions over a given perceptual dimension; e.g., frequency, intensity, duration, etc. In that distribution, (1) the mode represents the most probable prediction of the prior belief, i.e., the *expectation*; and (2) the inverse of the variance defines the confidence on that expectation, called *precision*. A prior belief is thus defined by the expectation itself and the expected reliability of that prediction, which is its precision (Figure 18A). The precision describes the expected uncertainty associated to the predictions based in our hierarchical generative model. On the other hand, the sensory evidence is expressed in terms of *likelihood*, which is the conditional probability of observing the sensory input given the prior belief. Therefore, sensory evidence also has an expected precision of its own. Ultimately, the comparison between the prior belief and the acquired evidence results in the PE, which in turn also has a precision value. As a result, the influence that each factor has in perceptual inference is proportional to their own precision. Only sufficiently precise PEs will be able to significantly update the prior beliefs, thereby modifying the attained percept. When the precision is high, inputs are up-weighted and will dominate inference; when it is low, inputs are down-weighted, and the expectations of the established perceptual model will dominate inference (Figure 18B-D). Thus, perception results from the precision-weighted average of the sensory input and the prior belief (Sedley et al., 2016).

In terms of neurobiology, the PP proposes that neuromodulatory systems implement precision weighting through the regulation of postsynaptic gain (Bastos et al., 2012; Feldman & Friston, 2010; Parr et al., 2018). Some authors have theorized particularly about the involvement of the cholinergic (Moran et al., 2013) and dopaminergic systems (Friston et al., 2012, 2014) in the adjustment of expected precision. These proposals are very relevant for this thesis, given that the neural sources of acetylcholine and dopamine are also intrinsic components of auditory circuitry in the midbrain, and thereby modulate the early stages of auditory processing (Hurley 2018; Elgoyhen & Katz, 2012; Mulders & Robertson, 2004; Sherriff & Henderson, 1994). From a more cognitive standpoint, PP posits that attention is essentially a high-order process of precision weighting (Parr & Friston, 2019). Paying attention

to a feature amounts to expecting the related signals to be reliable or informative, so their processing should be prioritized (Clark, 2017; Feldman & Friston, 2010). Correct precision weighting is critical for the overall function of the perceptual system, as any mismanagement would result in a failure to distinguish between PEs that contain useful information from those that do not. Maladaptive adjustments of precision could be the origin of many signs and symptoms of neuropsychiatric disorders, such as auditory hallucinations or tinnitus (R. A. Adams et al., 2013; Hullfish et al., 2019).

I.3.c.- The neural implementation of predictive processing (PP)

According to the predictive coding framework, our brain minimizes PE (1) by representing the quickly changing states of the environment, (2) by accounting for the slower fluctuations in more general parameters, and (3) by applying positive gain to reliable signals. Each of these operations has a possible neuronal implementation: (1) the s*ynaptic activity* of the neural circuitry provides the hierarchical exchange of top-down expectations and bottom-up PE signals from which sensory representations or percepts emerge, in a process known as *perceptual inference*; (2) the *synaptic efficacy* regulates the way neurons connect by means of plasticity mechanisms, leading to *perceptual learning*; (3) the *post-synaptic gain* adjusted via neuromodulation regulates the intrinsic excitability of neurons according to their expected precision, facilitating or dampening message transmission (Hohwy, 2013). At play within each neural network and between each processing level of the hierarchical generative model, these neuronal mechanisms of synaptic activity, plasticity and neuromodulation can be measured via brain imaging and cellular recordings (Carbajal & Malmierca, 2020).

In addition to the neuronal mechanisms, the PP framework also affords to speculate about the neural circuitry and connections. The canonical microcircuits for the 'standard' implementation of PP use feedforward excitatory connections to convey bottom-up PE signals while feedback inhibitory connections convey top-down expectations (Bastos et al., 2012). Since forward connections originate in superficial (II/III) pyramidal neurons, and backward connections originate in deep (V/VI) pyramidal neurons (Felleman & van Essen, 1991) this asymmetry has a straightforward anatomical consequence: *prediction neurons* reside in deep layers, and *PE neurons* in superficial layers (Figure 19A). Although other PP models propose different neural arrangements (Figure 19C; Spratling, 2008b, 2008a, 2010; Wacongne, Changeux and Dehaene, 2012), all formulations assume that predictions and PEs are computed

by separate neurons in distinct cortical layers. Hence, expectations and PE responses are assumed to have empirically contrastable laminar profiles (Figure 19).

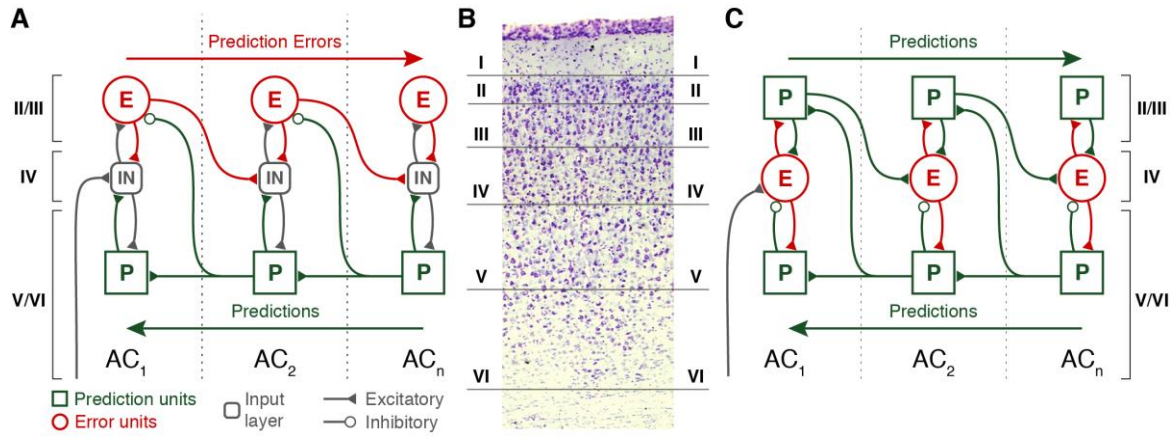

Figure 19. Simplified examples of neurobiological implementations of PP. Vertical dashed lines delimit cortical columns corresponding to hierarchically arranged AC areas. **A.** According to the standard PP model (Bastos et al., 2012), PE flow upwards (bottom-up) while predictions flow downwards (top-down). Error units (in red) are therefore should be located in superficial layers (II/III) above the input layer (IV), while prediction units (in green) should be found in the deep layers (V/VI) below the input layer (IV, in grey). Prediction units at higher levels can suppress error units at lower levels via top-down inhibitory connections. **B.** Laminar organization of the AC provided for reference. **C.** In other PP models (Spratling, 2008a, 2008b), however, predictions flow upwards in the supragranular layers (II/III) and downwards in the infragranular layers (V/VI) while PE is computed at the granular layer (IV). Prediction units (green) would suppress error units (red) via intracolumnar inhibition, and top-down connections are fully excitatory. Reproduced from Carbajal & Malmierca (2020).

The current theoretical implementations of PP only refer to the laminar profiles of the cerebral cortex, and modelling work does not usually include subcortical structures as key players in the hierarchical generative model, except maybe as providers of 'raw' sensory input. However, there are some EEG (Slabu et al., 2012), fMRI (Cacciaglia et al., 2015) and SSA data (see Section 1.2.b) that could be interpreted as evidence of PP activity starting at the level of the auditory midbrain. Although the possibility has never been explored, the IC is endowed with its own cortex of 3 layers (Figure 6), which exhibit varied neuronal specializations arranged in a complex and intricate local microcircuitry that remains not very well studied as of date (see Section I.1.d). In addition, all available models of cortical PP posit that the role of infragranular layers is to encode expectations. V/VI layers of the AC are the origin of corticocollicular projections, which could therefore potentially impose expectations on IC neurons. Moreover, the PPT and LDT nuclei of the brainstem (Ayala & Malmierca, 2015), and

the SPF of the thalamus provides the IC with dopaminergic input (Batton et al., 2018; C. Chen et al., 2018; Gittelman et al., 2013; Hurd et al., 2001; Nevue, Elde, et al., 2016; Nevue, Felix, et al., 2016; Weiner et al., 1991; Yasui et al., 1992). Theoretically, these neuromodulatory projections could be encoding expected precision in the auditory midbrain (Friston et al., 2012, 2014; Moran et al., 2013). Hence, the IC could potentially contain all the necessary elements to implement some level of early PP within the auditory system.

I.3.d.- The Expectation Hypothesis: the MMN and SSA as PP biomarkers

The PP framework was initially adopted in visual research (T. S. Lee & Mumford, 2003; Rao & Ballard, 1999) and it is gaining momentum in the study of auditory novelty perception as of late (Carbajal & Malmierca, 2018a, 2020; Garrido et al., 2009; Malmierca & Auksztulewicz, 2021). The core tenets of the PP framework offer great integrative potential to previous theoretical approaches to the study of automatic novelty processing, i.e., the Detection and the Adaptation Hypotheses. The PP framework proposes an *Expectation Hypothesis* particularly well suited to account for novelty responses and biomarkers such as the MMN and SSA (Garrido et al., 2009). In this section, I will discuss the Expectation Hypothesis in detail, since the main driver of this thesis is to provide evidence of its validity to explain midbrain-level auditory and novelty processing.

According to the Expectation Hypothesis, current sensory input is predicted from past events by means of a hierarchical generative model, which gets updated by encoding PE signals. This resembles to the Detection Hypothesis (see Section I.2.a), where the current sensory input was compared with a memory trace (Figure 11, blue dash train) by a detector system, which generates mismatch signals to induce memory updates (Figure 11, thick red arrow). PE signaling thus plays an analogous role to that of deviance detection (Schröger et al., 2014, 2015; Winkler et al., 2009; Winkler & Czigler, 2012; Winkler & Schröger, 2015), although it would emerge from a discrepancy between incoming sensory input and *prospective expectation* (Figure 18), instead of *retrospective comparison* (Figure 11). Hence, contrary to the Adaptation Hypothesis (see Section I.2.b), both Detection and Expectation Hypotheses interpret differential responses as genuine mismatch signals. But contrary to the Detection Hypothesis, the Expectation Hypothesis does not consider those mismatch signals to be evoked *de novo* (Figure 11, thick red arrow) and separated from the input signal (Figure 11, thick black arrow). Conversely, the Expectation Hypothesis posits that the redundant portions of the

original input signal are suppressed, and only the remnant surprising bits constitute the mismatch signal (Figure 20), which is more in the vein of the Adaptation Hypothesis (Carbajal & Malmierca, 2020).

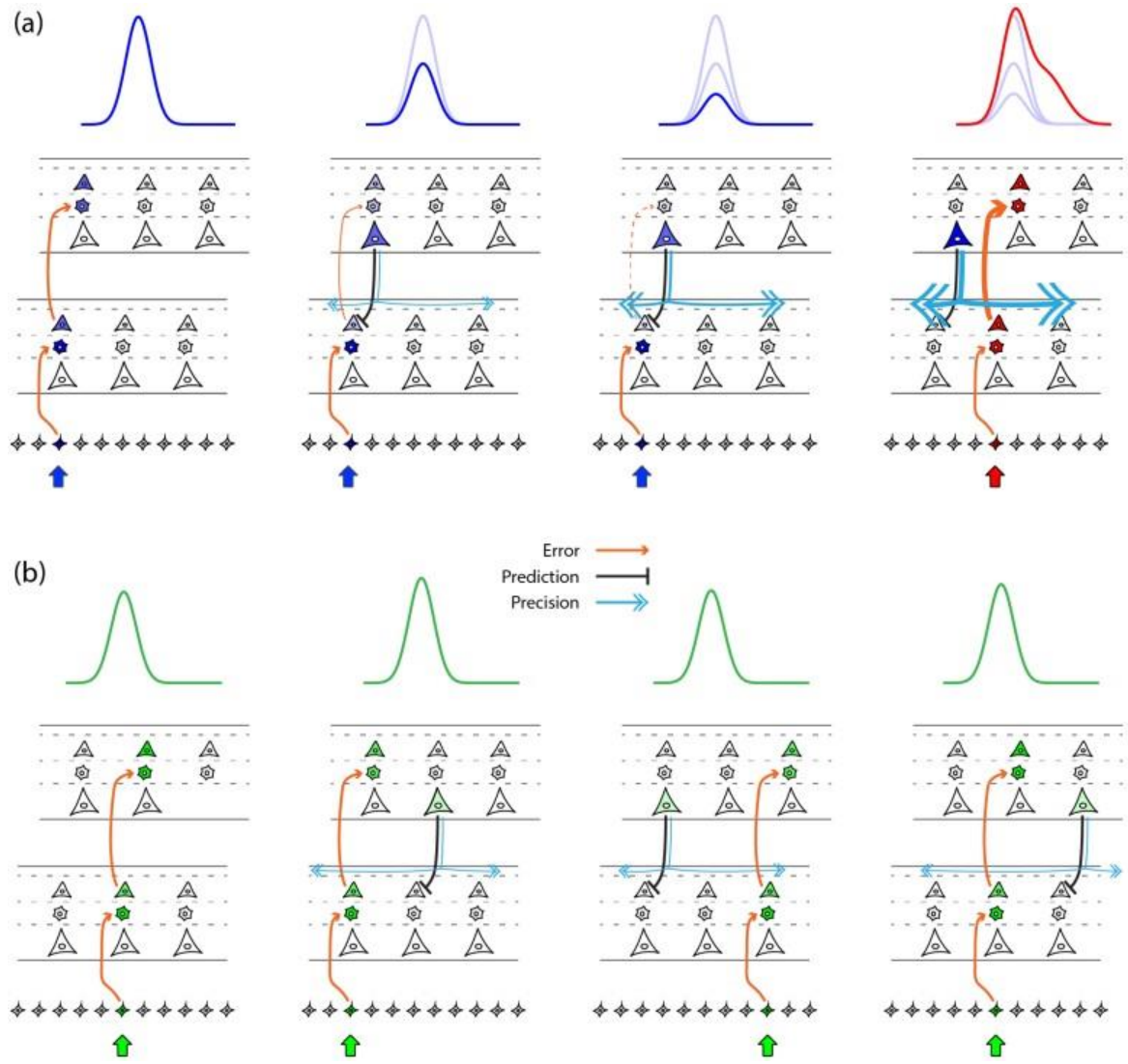

Figure 20. Emergence of mismatch responses according to the Expectation Hypothesis. Each schematic represents 2 reciprocally connected areas of AC, one hierarchically higher than the other. Granular layers receive ascending inputs, supragranular layers forward PEs, and infragranular layers send backward predictions (black connections) and the expected precision thereof (light blue connections). **A.** As STD tones are played, an expectation is generated with increasing precision. The expectation has an inhibiting effect, yielding repetition suppression. The expected precision is adjusted by means of a modulatory signal that will take effect only when a DEV tone is played, amplifying the PE generated, and thus leading to a strong mismatch response. **B.** When the NRCs are played, expectations are issued with low expected precision, and the PE generated by each tone is not as big as the mismatch response elicited by the DEV. Reproduce from Nieto-Diego (2017).

Consequently, differences between DEV and STD responses result from 2 distinct processes (Figures 18 and 20): (1) Expectations at a given processing level inhibit part of the sensory input or PE signals forwarded from lower levels, partially suppressing the neural response. During an oddball paradigm, such suppressive effect will strength with each repetition of the STD. Hence, SSA is indeed a form of perceptual learning, compatible with the generation of genuine mismatch signals. (2) The surprising bits of the input signal, those that could not be inhibited or explained away by expectations at the given level, are forwarded to higher processing levels in a PE signal which is susceptible to be amplified by its expected precision. During an oddball paradigm, all the information in DEV input contrasting with the expectation of STD is relayed as a PE signal to a higher processing level, and possibly amplified in the transmission (Carbajal & Malmierca, 2020). Hence, some authors from the PP framework have offered reinterpretations of the MMN as a sum of precision-weighted PE signals (Chennu et al., 2016; Garrido et al., 2008, 2009; Garrido, Kilner, Kiebel, & Friston, 2007; Garrido, Kilner, Kiebel, Stephan, et al., 2007; Phillips et al., 2015, 2016). Furthermore, the Expectation Hypothesis regards the MMN and SSA as respectively the macroscopic and microscopic signs of automatic novelty processing, offering a unified explanation to their emergence at both scales (Carbajal & Malmierca, 2018a; Garrido et al., 2009).

II.- SCIENTIFIC RATIONALE

The Detection Hypothesis provides a cognitive approach to the MMN based on an intricate interplay of sensory processors, memory tracers, and online comparators distributed along a cortical frontotemporal network (see Section I.2.a). Such complex formulation of a cortical detector system is plausible at the macroscopic scale of brain imaging techniques, but it falters when providing fine-grained neural implementations, and it excludes the evidence of subcortical novelty processing (Figure 11). Conversely, the Adaptation Hypothesis does provide better and more parsimonious implementations of automatic novelty processing at the microscopic scale based on SSA (see Section I.2.b). However, its simpler formulation struggles to account for empirical data beyond the oddball paradigm. The Expectation Hypothesis finds the middle ground and offers conspicuous advantages in relation to its predecessors. This hypothesis is very parsimonious, in the sense that with 1 simple mechanism at its core —i.e., PE minimization—, replicated throughout the neural hierarchy, it can explain how the brain performs perceptual inference and learning in general (Figure 18), and novelty perception in

particular (Figure 20). Furthermore, PP models offer richly detailed neural circuitries (Figure 19), which processing functions are elegantly grounded in concrete neurophysiological mechanisms of synaptic plasticity and neuromodulation, while accounting for the most complex characteristics of automatic novelty processing, from SUA to the mass activity of brain imaging (Figure 20). Hence, the Expectation Hypothesis can compete in explanatory power with the Detection Hypothesis, while somewhat retaining the parsimonious approach of the Adaptation Hypothesis. By virtue of integrating the strongest aspects of both preceding hypotheses under the PP framework, the Expectation Hypothesis regards the MMN and cortical SSA as respectively the macroscopic and microscopic signs of novelty perception, offering a unified explanation to their emergence at both scales (Carbajal & Malmierca, 2020). This link is of the upmost scientific importance considering the manifold applications in neurocognitive research and diagnosis of the MMN, as the SSA would provide a way to study such process down to the level of single neurons.

But there is still one piece of empirical evidence that does not fully dovetail with the Expectation Hypothesis. Most biologically-informed implementations of PP refer exclusively to a processing hierarchy established between cortical columns and areas (Bastos et al., 2012; Friston, 2005; Keller & Mrsic-Flogel, 2018). A more profound PP network would contravene the currently available PP models (Figure 19). And yet, the first auditory neurons to display SSA are not placed in the neocortex, but as deep as in the midbrain. In the auditory system, mismatch responses to the oddball paradigm first arise at the level of the IC, as reported in the human FFR (Figure 15; Shiga et al., 2015; Skoe et al., 2014; Slabu et al., 2012) and fMRI (Figure 16; Cacciaglia et al., 2015), as well as in the ABR (Figure 14; Duque et al., 2018), fMRI (Gao et al., 2014) and extracellular recordings (Ayala et al., 2013; Malmierca et al., 2009) of animal models (Figure 12). Extracellular recordings undoubtably point at the midbrain as the earliest source of SSA, as confirmed in the IC of gerbils (Malone & Semple, 2001), rats (Pérez-González et al., 2005), mice (Duque & Malmierca, 2015) and bats (Thomas et al., 2012), as well as in the optic tectum of barn owls (Reches & Gutfreund 2008) and in the torus semicircularis of lake frogs (Bibikov, 1977). The possibility of finding a subcortical circuitry capable of implementing hierarchical PP is not so far-fetched when considering the complex and sophisticated cytoarchitecture of the IC (see Section I.1.d). As the neuroanatomical origin of the lemniscal and nonlemniscal pathways (Figure 8), the IC has at least one lower-order processing level in its CNIC, and at least another higher-order processing level or more embedded within the 3-layered cortical circuitry of the ICx (Figures 5 and 6). Both levels are

reciprocally connected through a dense local network of intrinsic and commissural connections (Figure 4). Besides, nearly all ascending and descending auditory pathways converge in the IC. This creates a very loopy (Figure 8), iterative connectivity that integrates excitatory, inhibitory and neuromodulatory input coming from above and below (Figure 4), and where especially the ICx work under heavy cortical and modulatory influence. Such rich network of backward and forward connections between hierarchically arranged processing stations encompasses all the elements required to build a PP circuit: the top-down inhibitory flow of predictions, the bottom-up excitatory transmission of PE signals, and the neuromodulatory mechanisms needed adjust expected precision (Figures 18, 19 and 20).

Although the possibility of PP emerging within the microcircuitry of the IC has not been tested directly, previous reports provide a solid basis to speculate in this direction. As mentioned in Section I.2.b, SSA is not just dependent on short-term dynamics (Figure 12G), but also on long-term dynamics that surpass the time frame of short-term plasticity mechanisms such as synaptic depression (Figure 12F). This long-term dynamic was first revealed in the AC (Ulanovsky et al., 2004), and some modelling work postulated that other additional mechanisms should contribute to SSA emergence in AC (Taaseh et al., 2011; Yaron et al., 2012), including PE signaling (Rubin et al., 2016). However, the double sensitivity of SSA to recent and long-term past stimulus history was reported also the IC (Zhao et al., 2011), where SSA emerges even after cortical deactivation (Anderson & Malmierca, 2013). Moreover, EEG (Slabu et al., 2012) and fMRI (Cacciaglia et al., 2015) studies that presented the oddball paradigm along the many-standards sequence to human participants found midbrain-level DEV responses surpassing NRC responses, thereby refuting the Adaptation Hypothesis in the human IC. Given that the Detection Hypothesis is not readily applicable to subcortical processing (Figure 11), such evidence may speak in favor of the Expectation Hypothesis (Figure 20).

The rationale of the NRCs for the oddball paradigm can be easily reinterpreted under the optic of the PP framework (Figure 17C, see Section I.2.d). During the oddball paradigm (Figure 17A), STD repetition allows to set a very precise prediction —i.e., *'next tone will be the same'*—, which fails when DEV occurs. On the one hand, the ascending/descending cascade also generates a prediction —i.e., '*next tone will have higher/lower pitch*'— (Figure 17B), but neither such predictions are based on repetition expectation as in STD, nor are they broken by the stimulus of interest as in DEV. On the other hand, the many-standards creates a context of uncertainty that impedes expectations to be precise (Figures 17B and 20). At best,

the only prediction that the generative model could establish would be *'next tone will be different'*. When the DEV response surpasses the NRC response, i.e., when the Adaptation Hypothesis cannot account for the differential response to the 2 conditions of the oddball paradigm (DEV > NRC), the involvement of predictive mechanisms cannot be discarded (Figure 17E). From this standpoint, a mismatch signal in the AEP would not simply result from the sum of SSA across the auditory regions of the brain, but rather from PE signaling. Then, differences between NRC and STD responses to should not be ascribed to SSA, but to a low-level expectation yielding *repetition suppression* on the STD response (Auksztulewicz & Friston, 2016). The difference between DEV and NRC responses, interpreted by the Detection Hypothesis as *genuine deviance detection*, would presumably correspond to the amplification of the PE signal by the expected precision, with a possible contribution of PEs prompted by the failure of expectations other than repetition (Figure 17C). Therefore, the NRC of the oddball paradigm can be used in the IC to discard the Adaptation Hypothesis and provide support for the Expectation Hypothesis (Carbajal & Malmierca, 2020).

Studying the role of neuromodulation on SSA of IC neurons could provide additional evidence in favor of the Expectation Hypothesis. As previously mentioned, some authors from the PP framework have proposed that acetylcholine (Moran et al., 2013) and dopamine (FitzGerald et al., 2015; Friston et al., 2012, 2014; Nour et al., 2018; Schwartenbeck et al., 2015) adjust the expected precision of PE signals. Regarding cholinergic modulation, a previous study from our lab (Ayala & Malmierca 2015) used an in vivo microiontophoresis technique to locally apply cholinergic agonists and antagonists to neurons in the rat IC. The infusion of a cholinergic agonist provoked a general decrease in SSA levels, whereas cholinergic antagonists yield the opposite effect (Ayala & Malmierca 2015). By contrast, the possible neuromodulatory effects of dopamine on the SSA of IC neurons have not been explored so far, in spite of several studies indicating that the IC receives dopaminergic innervation from the SPF, especially dense in the ICx (Batton et al., 2018; C. Chen et al., 2018; Gittelman et al., 2013; Hurd et al., 2001; Nevue, Elde, et al., 2016; Nevue, Felix, et al., 2016; Weiner et al., 1991; Yasui et al., 1992). Furthermore, previous reports have detected mRNA coding for dopaminergic D_2-like receptors in the IC (Nevue, Elde, et al., 2016; Nevue, Felix, et al., 2016) and proved its functional expression as protein (Hoyt et al., 2019), while other studies demonstrated that dopamine modulates the auditory responses of IC neurons in heterogeneous manners (Gittelman et al., 2013; Hoyt et al., 2019).

In conclusion, there is a solid ground to explore scientifically the possible involvement of dopaminergic modulation of SSA in IC neurons. This can be done by applying the same microiontophoresis technique that allowed my colleagues to study the cholinergic influence on SSA of IC neurons (see Section III.4.a). Additionally, it is possible to present NRCs along with the oddball paradigm during the extracellular recording of well-isolated IC neurons in order to identify traces of PE signaling (see Section III.4.b). Finally, whether I can prove that dopamine modulates SSA in the IC and that SSA in the IC contains a PE component, the logical step to take would be trying to directly modulate that PE signaling of IC neurons by locally applying dopamine by means of microiontophoresis (see Section III.4.c). Meeting the aforementioned conditions would imply that the Expectation Hypothesis perfectly is applicable to the IC, which would entail that auditory PP first emerges at midbrain level.

II.1.- HYPOTHESES

All factors considered, I hypothesize that:

1. The Expectation Hypothesis is better fitted than the Adaptation Hypothesis to account for SSA in the IC.
2. SSA is a biomarker of early hierarchical PP in the auditory system.
3. Auditory PP first emerges in the midbrain, despite the rather corticocentric PP models currently available.
4. The CNIC acts as a low-order, primary input level, maybe receiving top-down predictions that help to induce SSA, but not elaborating and imposing predictions upon other lower processing levels.
5. The ICx meet the necessary conditions to fully implement a PP circuitry within its 3 layers. ICx neurons receive top-down predictions from higher processing levels in the auditory pathway, and maybe even from other higher-order neurons and regions within the ICx. In turn, ICx neurons can impose predictions on CNIC neurons.
6. Dopamine modulates SSA of IC neurons. Particularly, dopamine release adjusts the expected precision of PE signals generated by IC neurons.

II.2.- OBJECTIVES

Therefore, the main goal of this thesis is to demonstrate that the neuroanatomical origin of auditory PP is not the AC, but the IC. In order to test the abovementioned hypotheses, I will set the following objectives:

1. To investigate how the dopaminergic system modulates SSA in IC neurons by emulating local release of dopamine in the IC using microiontophoresis during extracellular recordings of the oddball paradigm.
2. To assess to what extent the dopaminergic modulation of SSA in IC neurons is mediated via the D_2-like receptors present in the IC by applying microiontophoretic injections of eticlopride, a selective antagonist of those receptors.
3. To confirm that IC neurons participate in hierarchical PP —i.e., the Expectation Hypothesis— by identifying a PE component within the mismatch response using no-repetition controls for the oddball paradigm.
4. To analyze the response differences between the CNIC and the ICx regarding PE signaling and repetition suppression levels.
5. To control for the possible effects of anesthesia in PE signaling by recording extracellular responses to the oddball paradigm and its no-repetition controls in the IC of awake animals.
6. To test to what degree dopamine regulates PE signaling by adjusting expected precision using microiontophoresis and no-repetition controls.

III.- MATHERIALS AND METHODS

Experiments were conducted on 67 female Long-Evans rats of 150–250 g aged 9–17 weeks and on 5 CBA/J mice of 27–30 g aged 8–12 weeks, in reciprocal collaboration with my colleagues, Drs Valdés-Baizabal, Parras and Nieto-Diego (Parras et al., 2017; Valdés-Baizabal, Carbajal, et al., 2020). All methodological procedures were approved by the Bioethics Committee for Animal Care of the University of Salamanca (USAL-ID-195) and performed in compliance with the standards of the European Convention ETS 123, the European Union Directive 2010/63/EU and the Spanish Royal Decree 53/2013 for the use of animals in scientific research.

III.1.- MANUFACTURING PROCEDURES

The recording consumables, i.e., the tungsten electrodes and the multibarrel pipettes for microiontophoresis, most critical tools for my research, were handcrafted in our laboratory using the referenced workstation setup (Bullock et al., 1988) in order to adequately meet our experimental requirements and high-quality standards in data acquisition.

III.1.a.- Tungsten microelectrodes

Tungsten microelectrodes used to record the extracellular activity of IC neurons were crafted with a tip impedance of 1.5–3.5 MΩ impedance at 1 kHz following the ensuing protocol (Merrill & Ainsworth, 1972). Tungsten wires were first placed in a custom-built alignment tool to assist cutting them to the desired length. This alignment tool consists of 30 needles (25 G) glued in parallel at 2 mm intervals, with a stop at one end to limit the length of the wires to ~40 mm. The loose ends of the wires were carefully attached to adhesive tape, and the wire end towering over the alignment tool is trimmed with strong scissors. The trimmed tungsten wires were removed from the alignment tool by gently pulling from the tape in order, making sure that all the wires remain attached.

The tape was rolled onto a polished brass spindle, pressing the wires firmly against the surface for an optimal electrical contact. The spindle was connected to a 5-rpm motor in the workstation, and ~1/3 of the protruding wire tips were introduced with a 45° angle into an etching solution (KNO_2, 90 g/80 mL) with a carbon rod electrode submersed inside to close the electrical circuit. The current passing through the electrodes and the etching solution was adjusted to 250 mA, and sharpening of the tips stopped when the current had dropped to 200 mA.

Sharpened wires were passed through a flame to remove any grease and adhesive residue and introduced (blunt end first) into a borosilicate glass capillary (1.5 mm outer diameter., 0.86 mm inner diameter) with its lower end blocked with modelling clay. This capillary was passed vertically through a coil (diameter 5 mm, depth 5 mm) and clamped vertically at the top and bottom. When turned on, the coil heated the glass while a suspended plunger pulled from the capillary gently. As the capillary was pulled down by the weight of the plunger, the molten glass formed a very fine coat around the sharpened tungsten wire.

The glass coat covering the sharp tip was removed by means of a molten bead of sodium tetraborate. This glass-removing tool was formed by mixing sodium tetraborate (~0.25 g) with a small amount of water (~0.5 mL) and slowly placing it on a heating holder, until it melts into a bead of approximately 2 mm in diameter. The bead was placed on focus under a microscope, with its heating holder mounted on a 3-axis manipulator arm and its temperature controlled by a potentiometer. On the other hand, the glass-covered wire was secured to a sliding holder under the microscope focus. The bead was heated until slightly melting, and the sliding holder was moved to plunge the sharpened wire tip into the bead approximately 10 to 15 µm. The heating potentiometer is then turned off, so as the bead cooled down and contracted, it removed the glass coat from the sharpened tip of the electrode, exposing the underlying tungsten. The resulting microelectrode is ready to record.

III.1.b.- Multibarrel glass pipettes

The multibarrel glass pipettes used for the microiontophoretic application of dopamine and eticlopride were crafted from 5-barrel glass capillaries in H configuration (World Precision Instruments, catalogue nº 5B120F-4) following the ensuing protocol. The ends of the 5-barrel capillaries were first protected with heat-shrink tubing, thereby affording some breakage protection and a better grip to the puller clamps. After being reinforced, the 5-barrel capillaries were placed in the vertical puller, heated and stretched (as described in the previous section) to obtain tip lengths of approximately 15 mm. The capillaries were pulled to obtain 2 pipettes with the tips occluded. Then pipette tips were broken using fine scissors or forceps under the microscope, until their outer diameter was 30–40 µm. Broken edges were refined using the tetraborate bead technique described in the previous section.

A tungsten microelectrode was placed in a holder made with a 20 G needle at the end of a 3-axis manipulator arm mounted on the microscope stage. Using forceps, the end of the electrode was bended 5–10°, around 30 mm away from the tip. Under the microscope, the tungsten microelectrode was aligned over the multibarrel tip. Once aligned, the microelectrode was lowered until it contacted the multibarrel, fitting in the groove between the two upper barrels. The microelectrode tip was then slided until it protruded 15–20 µm over the tip of the multibarrel. After ensuring that the angle between microelectrode and multibarrel was as small as possible for a better bonding and a thinner ensemble, a small drop of light-curable adhesive was applied around 5 mm away from the tips. Repeated cycles of application and curing with

a blue light LED lamp were usually needed to achieve a save bonding. In addition, the middle section of the piggyback microelectrode was wrapped in a short length of heat-shrink tube and rapid curing epoxy appropriate for glass was applied to further bond the tungsten microelectrode to the multibarrel. The resulting device is capable of applying drugs using the microiontophoresis technique while recording the extracellular activity of the IC neuron bathed with such drugs.

III.2.- SURGICAL PROCEDURES

All surgical procedures were approved by the Bioethics Committee for Animal Care of the University of Salamanca (USAL-ID-195) and performed in compliance with the standards of the European Convention ETS 123, the European Union Directive 2010/63/EU and the Spanish Royal Decree 53/2013 for the use of animals in scientific research.

III.2.a.- Anesthetized rats

Surgical anesthesia was first quickly induced with a mixture of ketamine (100 mg/Kg) and xylazine (20 mg/Kg) injected intramuscularly and then maintained it with urethane (1.9 g/Kg) injected intraperitoneally. To ensure a stable deep anesthetic level, supplementary doses of urethane (~0.5 g/Kg) were administrated intraperitoneally when the rat recovered corneal or pedal withdrawal reflexes. Urethane was chosen over other anesthetic agents because it preserves normal neural activity better, having a modest, balanced effect on inhibitory and excitatory synapses (Duque et al., 2016; Hara & Harris, 2002; Maggi & Meli, 1986; Sceniak & MacIver, 2006).

Normal hearing of rats was verified by recording the ABR was recorded via subcutaneous needle electrodes. An RZ6 Multi I/O Processor (Tucker-Davis Technologies, TDT) was used to acquire the ABR, which was immediately processed with BioSig software (TDT) before beginning each experiment. ABR stimuli consisted of 0.1 ms clicks at a rate of 21 clicks/s, delivered monaurally to the right ear in 10 dB steps, from 10 to 90 decibels of sound pressure level (dB SPL), in a closed system through a Beyer DT-770 earphone (0.1–45 kHz) fitted with a custom-made cone and coupled to a small tube (12 G) sealed in the ear.

Once normal hearing had been confirmed, a cannula was installed in the trachea to provide artificial ventilation to the rat with monitored expiratory CO_2, given that urethane

depresses respiratory function. Likewise, to maintain body temperature at 37±1 ºC, rats were introduced a rectal thermometer probe and placed on a homeothermic blanket system (Cibertec). The head was stabilized in a stereotaxic frame with a bite bar and 2 hollow specula replacing the ear bars. A sound delivery system was be accommodated within the right hollow speculum. Eyes were protected with a drop of ophthalmic gel. To prevent an excess of bronchial secretions, 0.1 mg/Kg of atropine sulfate was administrated subcutaneously. To ameliorate brain edema, 0.25 mg/Kg of dexamethasone was injected intramuscularly. To prevent dehydration, 5 mL of glucosaline solution was administrated subcutaneously. The scalp was shaved, and the revealed skin was disinfected with povidone-iodine. Using a scalpel, an incision was opened along the midline to expose the skull and the periosteum covering the parietal and the most rostral part of the occipital bones was retracted. Using an electric trephine (5 mm diameter), a round window was drilled in the caudal part left parietal bone, just rostral to the lambdoid suture and lateral to the sagittal suture, thereby exposing the cerebral cortex overlying the left IC. The exposed dura was removed and the tissue beneath it was covered with 2% agar to prevent desiccation during the recording session.

III.2.b.- Awake mice

In order to keep mice calmer and comfortable during the recording sessions, animals were handled, trained to stay in an adapted customized foam bed and placed into the stereotactic frame for 5–7 consecutive days. Mice were anesthetized using a mixture of ketamine (50 mg/Kg) and xylazine (10 mg/Kg) injected intramuscularly for the surgery. This dose induces a deep anesthesia for approximately 1 hour, and supplementary doses of one third of the initial dose were administrated if the mouse began to recover corneal or pedal withdrawal reflexes. Mice were introduced a rectal thermometer probe and placed on a homeothermic blanket system to maintain body temperature at 38±1 ºC (Cibertec). The head was stabilized in a stereotaxic frame by using 2 ear bars and a bite bar, avoiding excessive pressure that could affect the brain or pierce the tympanic membrane. Eyes were protected with a drop of ophthalmic gel. The scalp was shaved, and the revealed skin was disinfected with povidone-iodine. Using a scalpel, an incision was opened along the midline to expose the skull and the periosteum covering the parietal and the more rostral part of the occipital bones was retracted.

A comfortable fixation point for the mouse could be created by means of a lightweight duralumin headpost (weight ~0.65 g, length 30 mm) with a round and flat base (5 mm diameter)

glued on the skull. As a reference electrode for the electrophysiological recordings, a silver wire was glued to the middle of the headpost leaving its ends free. A thin layer of light-curable adhesive was applied on the skull and the base of the headpost, and after 10 s, the headpost was placed over the rostral area of the parietal bones, along the midline. The adhesive was exposed to a blue light for 20 s of curation. Around and behind the base of the headpost, 2 holes were drilled using an electric drill to place 2 watch screws (~2 mm length) that serve as additional contact points between the skull and the headstage. A third hole was drilled to insert the tip of the silver ground wire until it contacts the dura, applying a small drop of water-resistant cyanoacrylate glue to bind the wire to the skull. Using a small trephine (2.35 mm diameter), round window was drilled just caudal to the lambdoid suture and lateral to the midline, exposing the left IC. A small wall (~1 mm wide and ~1 mm high) of composite was built and light-cured around the window. The exposed skull and muscle were covered with antibiotic ointment, and the exposed surface of the left IC was covered by filling the well with a removable silicone elastomer (Kwik-Cast™ & Kwik-Sil™, WPI). Finally, the mice were kept on the heating blanket until they awoke.

After the surgery, each mouse was returned to an individual, enriched housing cage to recover for at least 3 days before recording sessions could begin. Buprenorphine (Buprex™, RB Pharmaceuticals Limited) was injected subcutaneously (0.03 mg/kg, diluted 1:10 in sterile saline) as an analgesic every 12 h after surgery. Daily, sawdust was changed to prevent infections and mice recovery was checked, looking for possible signs of discomfort. Mice were given time to acclimate to the recording environment and to having its head restrained by fixing the headpost to the holder while the mouse is sitting on a custom-made cushioned foam restrainer carved to its body shape. This will limit the movements of the mouse and will contribute to its calmness. This acclimatation began with sessions of 10 min and lengthen progressively up to 120 min, according to each mouse capability to remain calm. During the acclimatation sessions, mice were rewarded with sweet liquids (condensed milk, diluted 30:70 in water) at variable intervals. The same variable reward was provided during the fixation to the stereotactic frame, at the start and at the end of recording sessions, as well as between each recording of MUA.

For the recording session, awake mice were placed into the foam custom-made cushioned restrainer, the headpost was secured with a holder attached to the stereotactic frame, and the body was covered with a cotton blanket and loosely fasten with a plastic hemicylinder

and adhesive tape. If mice were not very excited after movement restriction, a reward was provided. Then, the silicone elastomer was removed from the window in the skell and rinsed with warm sterile saline so the recording session could begin. Only well-acclimated animals were used to collect data, and mild sedative acepromacine (2 mg/kg, Equipromacina, Fatro Iberica) was injected intraperitonially in case a mouse showed signs of apprehension during the recordings. Recording sessions were no longer than 3 h, during 2–3 consecutive days.

III.3.- DATA ACQUISITION PROCEDURES

Experiments were performed inside a sound-insulated and electrically shielded chamber. All sound stimuli were generated using the RZ6 Multi I/O Processor (TDT) and custom software programmed with OpenEx Suite (TDT) and Matlab™ (Mathworks). In search of evoked auditory neuronal responses from the IC, white noise bursts and sinusoidal pure tones of 75 ms duration with 5 ms rise-fall ramps were presented, oftentimes varying stimuli parameters manually to prevent overlooking SSA neurons.

Once the activity of a single neuron was clearly isolated, only pure tones were used to record the experimental stimulation protocols, which ran at 4 stimuli per second. In the experimental setup for anesthetized rats, stimuli were delivered monaurally in a close-field condition to the ear contralateral to the left IC through a speaker. We calibrated the speaker using a ¼-inch condenser microphone (model 4136, Brüel&Kjær) and a dynamic signal analyzer (Photon+, Brüel&Kjær) to ensure a flat spectrum up to 76 ± 3 dB SPL between 0.5 and 44 kHz, and that the second and third signal harmonics were at least 40 dB lower than the fundamental at the loudest output level. The experimental procedure for the awake mice was mostly similar to the anesthetized setup, but auditory stimulation delivered in a free-field condition to the contralateral ear (at ~1 cm) using an electrostatic loudspeaker (TDT-EC1) driven by a RZ6 processor. The output of the system was calibrated as described before and its maximum output was flat from 1 to 44 kHz up to $\sim 89 \pm 4.3$ dB SPL.

A new handcrafted glass-coated tungsten microelectrode was used for each recording session (see Section III.1.a). In the protocols that required dopaminergic manipulation procedures (see Section III.5), this microelectrode would be attached to a multibarrel (see Section III.1.b) when the experiments required to perform microiontophoresis during the recording of extracellular MUA from IC neurons. Hence, one individual microelectrode was used to record one single neuron at a time. The microelectrode was mounted on a holder over

the exposed cortex, forming an angle of 20° perpendicularly rostral to the coronal plane. Using a piezoelectric micromanipulator (Sensapex), the electrode was plunged into the brain while measuring the penetration depth until strong spiking activity synchronized with the train of searching stimuli could be identified.

Analog signals were digitized with a RZ6 Multi I/O Processor, a RA16PA Medusa Preamplifier and a ZC16 headstage (TDT) at 12 kHz sampling rate and amplified 251×. Neurophysiological signals from multiunit activity were band-pass filtered between 0.5 and 4.5 kHz. Stimulus generation and neuronal response processing and visualization were controlled online with custom software created with the OpenEx suite (TDT) and MATLAB. A unilateral threshold for automatic action potential detection was manually set at about 2–3 standard deviations of the background noise. Spike waveforms were displayed on the screen and overlapped on each other in a pile-plot to facilitate isolation of SUA. Only when all spike waveforms were akin and clearly separable form other smaller units and the background noise, the recorded action potentials were considered to belong to a SUA. Recorded spikes were considered to belong to a SUA when the spike-amplitude-to-noise-ratio (SNR) of the average waveform was larger than 5.

$$SNR = \frac{\max\left(\bar{x}(S)\right) - \min(\bar{x}(S))}{Std(S)}$$

III.4.- EXPERIMENTAL DESIGN

For all recorded IC neurons, a map of response magnitude for each frequency/intensity combination was first computed, representing the receptive field in an FRA (Figure 7). The stimulation protocol to obtain the FRA consisted of a randomized sequence of sinusoidal pure tones ranging between 0.7–44 kHz, 75 ms of duration with 5 ms rise-fall ramps, presented at a 4 Hz rate, randomly varying frequency and intensity of the presented tones (3–5 repetitions of all tones). After this common procedure, different stimulation protocols were tested along my 4 years of doctoral research, which I have grouped under 3 separated studies trying to answer 3 different but related questions.

III.4.a.- Protocol 1: Do D_2-like dopaminergic receptors modulate SSA in the IC?

This protocol used an oddball paradigm (Figure 17A) in combination with microiontophoresis to study the involvement of dopaminergic receptors in the modulation of SSA in IC neurons. Two frequencies (f_1 and f_2) were chosen within the excitatory region of the FRA, 10–40 dB above the threshold level, and were presented at a rate of 4 Hz in pseudo-random order forming sequences of 400 stimuli. First, f_1 appeared with high probability (P=0.9), establishing the STD, which repetition was randomly interrupted by f_2, presented with lower probability (P=0.1) to provide the DEV. The first 10 tones of the sequence were always STD, and a minimum of 3 STD always preceded each DEV.

After one presentation of that sequence, the relative probabilities of f_1 and f_2 were reversed, thereby becoming DEV and STD respectively. This will allow to control for the physical characteristics of the sound in the evoked response when looking for mismatch responses. Older MMN studies used only one oddball sequence and directly subtracted the STD-f_1 from the DEV-f_2 AEP, assuming that the evoked responses to f_1 and f_2 were identical, which is not usually the case. Using a 'flip-flop' or reversed control allows to compare the evoked responses to the same tone in both conditions, i.e., DEV-f_1 against STD-f_1 and DEV-f_2 against STD-f_2, such that the differential response between DEV and STD can only be due to their differential probability of appearance. Only the last STD tone preceding each DEV will be considered for the analysis (Figure 17A, top panel, highlighted in blue), so 40 measurements per condition were obtained for each oddball paradigm played. A separation of 0.28 octaves between frequencies was chosen in this round of experiments in order to allow result comparisons with previous SSA studies in the IC (Malmierca et al., 2009).

Following this design, one oddball paradigm was recorded for a *'control condition'* and another oddball was recorded after microiontophoretic injections of dopamine or eticlopride (see Section III.5).

III.4.b.- Protocol 2: Is SSA a biomarker of PP in the IC?

This protocol used the oddball paradigm and both NRC sequences. Here, 10 frequencies separated by 0.5 octave steps at a fixed sound intensity (usually 20–30 dB above minimal response threshold) were selected so that at least 2 consecutive tones fell within the excitatory region of the FRA (for examples, see Figures 28 and 34, top panels). These 10 tones were used

to generate the NRC sequences (Figure 17B), and each adjacent pair within the excitatory region of the FRA was used to create oddball sequences. All sequences were 400 tones in length and presented at a constant rate of 4 Hz. The first 10 tones were always STD, and a minimum of 3 STD preceded each DEV. Oddball sequences were labeled either 'ascending' or 'descending', depending on whether the DEV had a higher or lower frequency than the STD, respectively (Figure 17A).

To control for the overall presentation rate of the target tone, this study used 2 different NRC sequences, namely, the many-standards (Figure 17B, top panel) and the cascade sequences (Figure 17B, middle and bottom panels). The many-standards sequence was a random presentation of the 10 selected tones, such that each of them was played the same number of times in an unpredictable order but a single tone was never repeated. Besides, there were 2 cascade versions, one 'ascending' and the other 'descending' to control for the respective versions of the oddball sequence. The cascade sequence contained the same 10 tones but arranged in ascending (Figure 17B, bottom panel) or descending frequency (Figure 17B, middle panel). The tone immediately preceding a DEV is the same in the oddball and cascade sequences, enhancing its control capabilities. In fact, the cascade was designed as an improvement to the many-standards, by controlling for the state of refractoriness and for the potential sensitivity of the neuron to a rise or fall in frequency between 2 successive tones. Besides, the cascade sequence better mimics the regularity that emerges in the structure of the oddball sequence, with the key difference that now the cascade tone conforms to the rule, instead of being a DEV. Using this design, each given tone was played as DEV, NRC and last STD a total of 40 times. The order of presentation of these sequences was randomized across neurons, with a silent pause of ~30 s between sequences. If the neuron could be held for long enough, the same protocol was repeated at different sound intensities.

The objective of this design is to confirm or refute the Expectation Hypothesis proposed by the predictive processing framework, in the same vein that MMN studies did with the Detection Hypothesis. When the evoked response to DEV was equal or less than that evoked by the NRCs, then the Expectation Hypothesis could not be accepted in the IC, thereby defaulting to the Adaptation Hypothesis. Conversely, when the DEV response was significantly larger than the response elicited by the NRCs, then the Expectation Hypothesis would prove to provide a more suitable explanation for SSA generation in IC neurons. This experimental

design was used in anesthetized rats and in awake mice, in other to control for the possible effects of anesthesia.

III.4.c.- Protocol 3: Does dopamine modulate PE signaling in the IC?

In light of the preliminar data collected in Protocol 2, Protocol 1 was brought to a close and adapted to incorporate the NRC sequences (Ruhnau et al., 2012), constituting a third separated protocol. This protocol was designed to test, once the Expectation Hypothesis could be confirmed in the IC, whether dopaminergic receptors contributed to the precision weighting of PE signals forwarded by IC neurons. After computing the FRA (Figure 7), 10 evenly-spaced frequencies at a fixed sound intensity 10–40 dB above minimal response threshold were selected so that at least two tones fell within the excitatory region of the FRA. In order to make the results comparable to those of Protocol 2, the 10 frequencies were separated from each other by 0.5 octaves. These 10 tones were used to build the NRC sequences (Figure 17B), and the 2 tones that fell within the excitatory region of the FRA were used to generate the ascending and descending versions of just one oddball paradigm (unlike in Protocol 2, where multiple oddball paradigms were generated). The first 10 tones of the oddball paradigm were always STD, and a minimum of 3 STD preceded each DEV. All sequences were 400 tones in length, at the same, constant presentation rate of 4 Hz, thus obtaining 40 trials per condition (Figure 17A and B). The order of presentation of these sequences was randomized across neurons. After recording all the DEV, STD and NRC in a *'control condition'*, dopamine was applied microiontophoretically before running the protocol again with the same neuron, as detailed in the ensuing section.

III.5.- DOPAMINERGIC MANIPULATION PROCEDURES

In Studies 1 and 3, after completing the stimulation protocol once to record a *'control condition'* (i.e., before any dopaminergic manipulation), dopamine or the D_2-like receptor antagonist eticlopride (Sigma-Aldrich Spain) were microiontophoretically applied through a multi-barreled pipette attached to the recording micrelectrode (see Section III.1.b). The center barrel was filled with saline for current compensation (165 mM NaCl). The others were filled with dopamine (500 mM) or eticlopride (25 mM). Each drug was dissolved in distilled water and the acidity of the solution was adjusted with HCl to pH 3.5 for dopamine and pH 5 for eticlopride. The drugs were retained in the pipette with a –20 nA current and ejected using 90

nA currents (Neurophore BH-2 system, Harvard Apparatus). Thus, dopamine or eticlopride were released into the microdomain of the recorded neuron at concentrations that have been previously demonstrated effective in *in vivo* studies (Gittelman et al., 2013). About 5 minutes after the drug injection, the FRA and the stimulation protocol of the study were repeated continuously until the drug was washed away, leaving roughly 1–2 minutes between the end of one recording set and the beginning of the next one. The recording set showing a maximal SSA alteration relative to the control values was considered the *'drug condition'* of that neuron. We established the *'recovery condition'* when the spike count returned to levels that did not significantly differ from control values, never before 40 minutes post-injection.

Protocol 1 used both dopamine and eticlopride, whereas only dopamine was tested in Protocol 3. During Protocol 1, in a few cases where the recording was exceptionally stable, after the first recovery we performed a second injection using the other drug (Figure 27). This prolonged procedure was meant to test the consistency of dopaminergic effects (agonist versus antagonist) within individual neurons when possible.

III.6.- HISTOLOGY AND NEUROANATOMICAL LOCALIZATION

At the end of each experiment, electrolytic lesions were inflicted by applying an electric current of 5 μA during 5 s through the recording electrode along the recorded tract. If still alive, animals were sacrificed by injecting a lethal dose of pentobarbital, after which they were decapitated. Brains were immediately immersed in a mixture of 1% paraformaldehyde and 1% glutaraldehyde in 1 M PBS. After fixation, the neural tissue was cryoprotected in 30% sucrose and sectioned in the coronal plane at 40 μm thickness on a freezing microtome. Slices were stained with 0.1% cresyl violet to facilitate identification of cytoarchitectural boundaries. Finally, the recorded neurons were assigned to one of the main subdivisions of the IC using the standard sections from a rat brain atlas as reference (Paxinos & Watson, 2007).

III.7.- DATA ANALYSIS AND VISUALIZATION

All data analyses and data visualization were performed with SigmaPlot™ (Systat Software) and MATLAB™ (MathWorks) software, using the built-in functions, the Statistics and Machine Learning toolbox for MATLAB, and custom scripts and functions developed in

our laboratory. Unless indicated otherwise, all the measures of central tendency for trials and neurons are expressed as *median [quartile 1, quartile 3]* because the data did not follow a normal distribution (1-sample Kolmogorov-Smirnov test).

III.7.a.- Peristimulus histogram (PSTH), spike-density function (SDF) and baseline-corrected spike count

Taking the 40 trials available for each tone and condition, a PSTH was computed to represent the action potential density over time in spikes per second from −75 to 250 ms around stimulus onset (Figures 24, 26, 27, 28 and 34). This PSTH was smoothed with a 6 ms gaussian kernel (*ksdensity* function in MATLAB) in 1 ms steps to estimate the spike-density function (SDF) over time (Figures 31A and B, as well as 32C and D), and the baseline spontaneous firing rate was determined as the average firing rate (in spikes/s) during the 75 ms preceding stimulus onset. The excitatory response was measured as the area below the SDF and above the baseline spontaneous firing rate, between 0 and 180 ms after stimulus onset. This measure is referred to as the *baseline-corrected spike count*.

Only excitatory responses were analyzed, since my studies were looking for enhancements of DEV responses. Unit-frequency combinations with no significant excitatory response to at least one of the conditions (DEV, STD or NRC) were excluded from the analyses. To test for statistical significance of the baseline-corrected spike count, we used a Monte Carlo approach, a probability simulation that obtain numerical results from several random sampling. First, 1000 simulated PSTHs were generated using a Poisson model with a constant firing rate equal to the spontaneous firing rate. Then, a null distribution of baseline-corrected spike count was generated from this collection of peri-stimulus histograms, following these same steps. Finally, the *p* value of the original baseline-corrected spike count was empirically computed as $p = (g + 1)/(N + 1)$, where g is the count of null measures greater than or equal to baseline-corrected spike count and $N = 1000$ is the size of the null sample.

III.7.b.- Common SSA Index (CSI)

Replicating the methodology of previous studies of SSA neuromodulation in the IC (Ayala & Malmierca, 2015, 2018; Pérez-González et al., 2012; Valdés-Baizabal et al., 2017), the Common SSA Index (CSI; Ulanovsky et al., 2003) was chosen to analyze the data generated

in Protocols 1 (see Section III.4.a) and 3 (see Section III.4.c). One CSI was calculated for the frequency pair in each oddball paradigm as:

$$CSI = \frac{DEV_{f1} + DEV_{f2} - STD_{f1} - STD_{f2}}{DEV_{f1} + DEV_{f2} + STD_{f1} + STD_{f2}}$$

Where DEV_{fi} and STD_{fi} are spike counts in response to a frequency f_i when it was presented in deviant and standard conditions, respectively. The CSI ranges between -1 to +1, being positive if the response to the DEV was greater than to the STD. Rare cases of unit-frequency combinations exhibiting negative CSI values were excluded from further analyses, since these outliers are not performing novelty processing, and thus are out of the scope of this study.

III.7.c.- Indices of Neuronal Mismatch (iMM), Repetition Suppression (iRS) and Prediction Error (iPE)

In both Protocols 2 (see Section III.4.b) and 3 (see Section III.4.c), NRCs were introduced to control for the repetition effects of the oddball paradigm, allowing a dissociation of SSA into *PE* and *repetition suppression* components. In order to adequately compare between responses from different neurons, the spike count evoked by each tone in DEV, STD and NRC was normalized as follows:

$$DEV_N = \frac{DEV}{N} \;;\; STD_N = \frac{STD}{N} \;;\; NRC_N = \frac{NRC}{N}$$

Where,

$$N = \sqrt{DEV^2 + STD^2 + NRC^2}$$

From these normalized responses, we computed the indices of *neuronal mismatch* (iMM), *repetition suppression* (iRS) and *prediction error* (iPE) as:

$$iMM = DEV_N - STD_N$$

$$iRS = NRC_N - STD_N$$

$$iPE = DEV_N - NRC_N$$

These indices range between -1 and 1. The iMM is largely equivalent to the classic CSI as an index of SSA (see Supplementary Figure 2 in Parras et al., 2017). Nevertheless, please beware the CSI provides one index for each pair of tones in the oddball paradigm, whereas the iMM provides one index for each tone tested, and the same goes for the iPE and the iRS.

III.7.d.- Bootstrapping

SSA indices, both CSI and iMM, were calculated from the averages of the single-trial responses to DEV, STD, and NRC. Consequently, only one value of such indices could be obtained for each unit and condition. Therefore, a bootstrapping was required to test whether the microiontophoresis of dopamine or eticlopride had yielded significant changes on the SSA levels of each neuron from Protocols 1 (see Section III.4.a) and 3 (see Section III.4.c). The bootstrapping draws random samples (with replacement) from the spike counts evoked on each trial, separately for DEV and STD stimuli, and then applies either the CSI or the iMM formula. This procedure is repeated 10000 times, thus obtaining a distribution of expected CSI values based on the actual responses from a single recording. The *bootci* MATLAB function returned the 95% confidence interval for the SSA indices in the control condition. Dopaminergic effects were considered significant when the SSA index in the *drug condition* did not overlap with the confidence interval in the *control condition*.

III.7.e.- Local Field Potential (LFP) and PE Potential (PE-LFP)

For the analysis of the LFP signal, recorded wave was aligned to the onset of the stimulus for every trial, and the mean LFP was computed for every recording site and stimulus condition (DEV, STD and NRC), as well as 2 LFP difference waves: the *mismatch potential* ($LFP_{DEV} - LFP_{STD}$) and the *prediction error potential* (PE-LFP = $LFP_{DEV} - LFP_{NRC}$). For lemniscal (i.e., CNIC) and nonlemniscal divisions (i.e., the IC cortices) separately, grand-averages were computed for all conditions (DEV, STD NRC). The *p* value of the grand-averaged PE-LFP was determined for every time point with a two-tailed *t* test (Bonferroni-corrected for 200 comparisons, with family-wise error rate of less than 0.05), and then the time intervals where PE-LFP was significantly different from zero were computed (Figure 31).

In order to analyze and illustrate any possible coincidences between spiking and local field activity, the iMM and iPE of each unit and tone combination was recomputed and averaged within each IC division for 12 different time windows of 20 ms width, from −50 to

190 ms respect to stimulus onset. The index value for each window was then tested against zero (Wilcoxon signed rank test, FDR-corrected for 12 comparisons), revealing a significant time interval that could be compared with that of the corresponding LFP difference wave.

III.7.f.- Statistical hypothesis testing

Given that the data set was not normally distributed, statistical analyses were carried out using distribution-free, non-parametric tests. These included the Wilcoxon signed-rank test and Friedman test for baseline-corrected spike counts, normalized responses, indices of neuronal mismatch, repetition suppression and prediction error. Wilcoxon signed rank test (signrank function in MATLAB) was applied to check for differences at the population level between the control and drug CSI and firing rates. Only the difference wave for the LFPs (PE-LFP in Figure 31) was tested using a *t* test, since each LFP trace is itself an average of 40 waves, and thus approximately normal (according to the Central Limit Theorem). For multiple comparison tests, *p* values were corrected for false discovery rate (FDR = 0.1) using the Benjamini-Hockberg method. Linear models used to test significant median indices within each auditory stationand significant effects of intensity, direction, and interactions between them, were fitted using the 'fitlm' function in Matlab, with robust options (Figure 33). Then, an ANOVA was performed to identify the significant factors and interactions in the linear model using the function 'anova'. For Protocol 3 data, effects of dopaminergic manipulation were analyzed using a repeated-measures ANOVA with Dunn–Šidák correction (Figure 36A).

IV.- RESULTS

We performed a total of 368 SUA and MUA recordings, one at a time using a microelectrode, from 67 anesthetized Long Evans rats (Figure 21A and B) and 5 awake CBA/J mice (Figure 21C and D) using 3 different protocols. Approximately 3 quarters of the recorded units were well-isolated neurons, while the rest were MUA. However, this proportion was not equivalent across studies. Data obtained from Protocol 2 shows that more than 95% of the recorded spikes had at least 5 times more amplitude than the background noise, and more than 60% even achieved SNR > 10, whereas data from Protocols 1 and 3 barely surpass half of the former percentage. This inequity is undoubtably caused by the added technical challenge of maintaining a neuron well isolated during a prolonged recording session with a microelectrode

attached to a relatively bulky multibarrel pipette plunged into the neural tissue (see Section III.1.b).

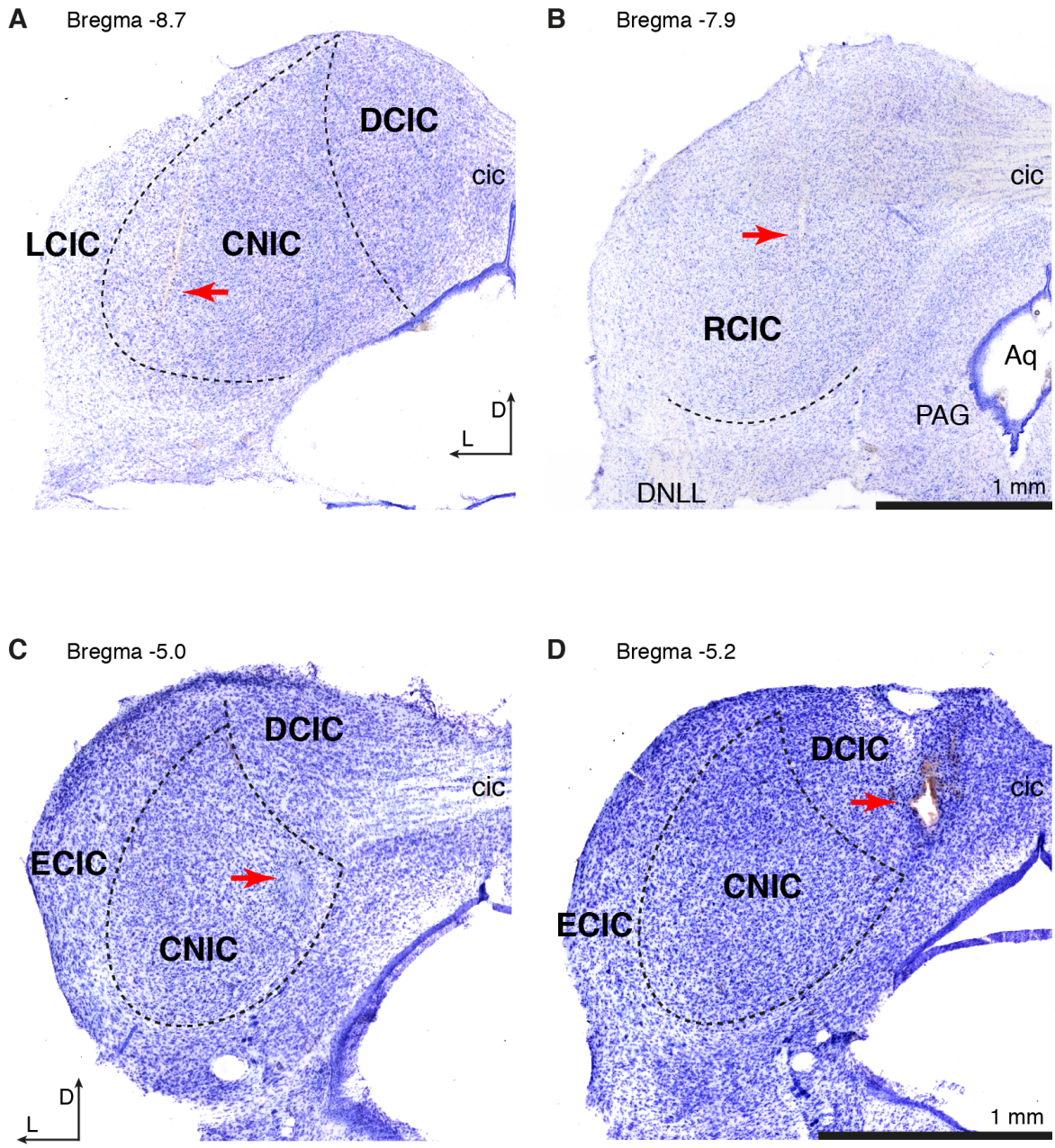

Figure 21. Examples of Nissl-stained histological slice showing an electrolytic lesion. A and B display coronal sections from the IC of 2 different rats, whereas B and C show coronal sections of the IC of 2 different mice. Red arrows point at the electrolytic lesions found in each section (see Section III.6). Scale bars: 1 mm in each pair.

In Protocol 1 (see Section III.4.a), neuronal responses to the oddball paradigm were recorded before, during and after the microiontophoretic application of dopamine (49 units), eticlopride (43 units) or both drugs in succession (5 units), in order to test whether dopaminergic modulation exerted significant changes on the CSI of IC neurons. Histological analysis revealed that all 97 units recorded during Protocol 1 were located in the ICx, where neurons tend to exhibit the highest CSI values (Malmierca et al., 2009).

In Protocol 2 (see Section III.4.b), the oddball paradigm was recorded along the NRCs in order to identify possible PE components within the neuronal responses of the IC. A first round of these experiments was performed in anesthetized rats, where 134 well-isolated SUAs were recorded. Histological analysis revealed that 99 neurons were located in the ICx and the other 35 neurons came from the CNIC. A second round of these experiments was performed in awake mice, yielding 47 MUA recordings. The aim of this second round was to provide a control for any possible effects of anesthesia, as well as to replicate the same experiments in a different rodent species. The many-standards sequence was not tested in the anesthetized preparations; only cascade sequences were presented as NRC. Histological analysis revealed that 27 MUA were recorded in the ICx and the other 20 MUA were recorded in the CNIC.

Finally, in Protocol 3 (see Section III.4.c), neuronal responses to both the oddball paradigm and the NRCs were recorded before, during and after the microiontophoretic application of dopamine, in order to test how dopamine modulate PE signaling in IC neurons. This protocol was tested after positive results had been confirmed in the 2 previous protocols, as an effort to combine and integrate both. Histological analysis revealed that the 43 units recorded during Protocol 3 were located in the ICx.

The data obtained from each protocol was not analyzed in isolation as 3 different studies. Instead, the samples obtained under each protocol were combined whenever they were methodologically compatible, in order to obtain more representative sample sizes to answer each research question. In the following, I will specify the exact composition of the sample at the beginning of each section.

IV.1.- Dopamine application tends to induce CSI reductions

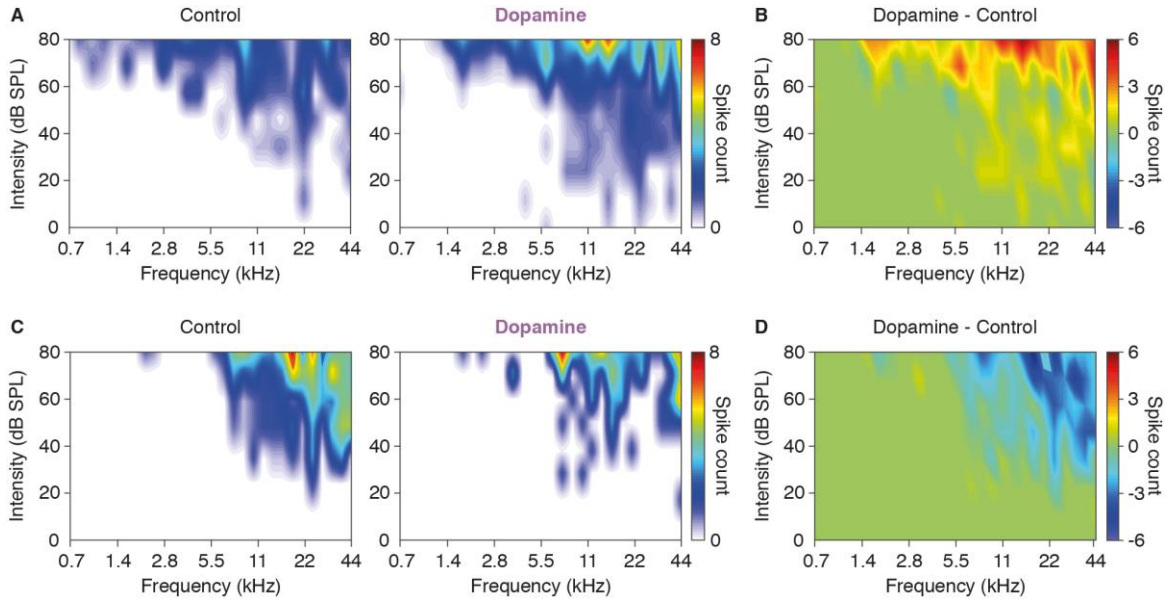

Figure 22. Dopamine effects on the FRA. A. FRA of a neuron in control condition (left panel) and after dopamine application (right panel). **B.** The subtraction of the control FRA from the FRA after dopamine application reveals that dopamine increased the excitability of this unit. **C.** FRA of another neuron in control condition (left panel) and after dopamine application (right panel). **D.** The subtraction of the control FRA from that after dopamine application in C reveals that dopamine decreased the excitability of this neuron.

To study the role of dopamine in shaping SSA in the IC, a total of 94 units from the ICx recorded during Protocols 1 and 3 were pooled together and analyzed collectively because, despite their dissimilar frequency contrast, their responses to the oddball paradigm did not differ significantly. The separation between f_1 and f_2 was 0.28 octaves the 49 units from Protocol 1 (see Section III.4.a) and 0.5 octaves in 45 units from Protocol 3 (see Section III.4.c), which is within the range of frequency separations used in other previous studies in the IC (Ayala et al., 2013, 2016; Ayala & Malmierca, 2015, 2018; Duque et al., 2012, 2016; Duque

& Malmierca, 2015; Malmierca et al., 2009; Valdés-Baizabal et al., 2017; Valdés-Baizabal, Casado-Román, et al., 2020).

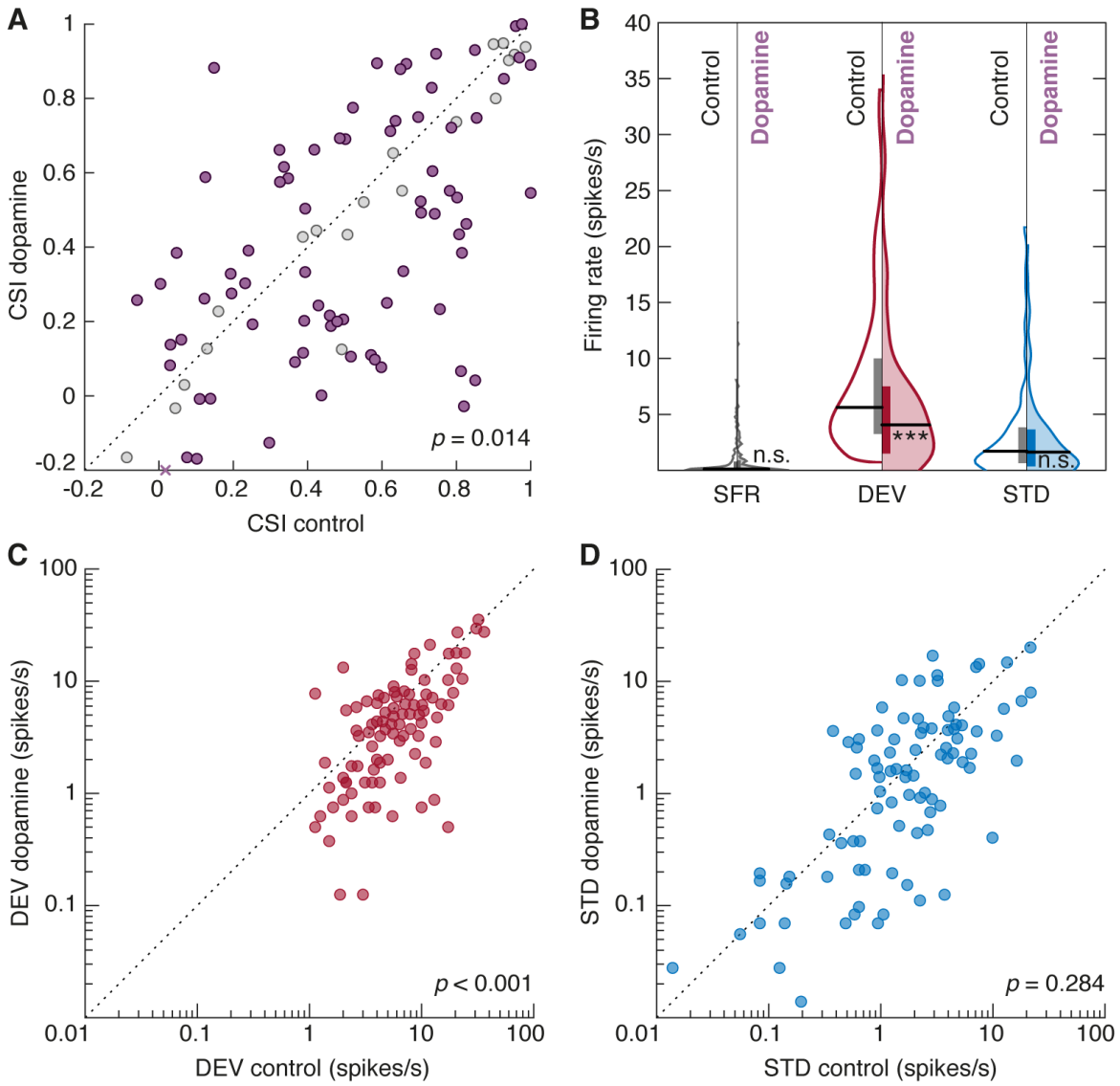

Figure 23. Dopamine effects on the CSI. A. Scatter plot of the CSI in control condition versus dopamine application. Units that underwent significant CSI changes are represented in purple, whereas the rest are marked as gray dots. The purple cross on the abscissa axis represents one CSI measurement which ordinate value falls out of scale (y = –0.59). **B.** Violin plots of the spontaneous firing rate (SFR), DEV and STD responses. Control conditions are represented in the left half of each violin (no color) while dopamine effects are on display in the right half (colored). Horizontal thick black lines mark the median of each distribution, while vertical bars cover the interquartile range (n.s. = non-significant; *** p < 0.001). **C.** Scatter plot of DEV responses in control condition versus dopamine application. **D.** Scatter plot of STD responses in control condition versus dopamine application.

The microiontophoretic application of dopamine induced changes in the firing rate and FRAs of the recorded units (Figure 22). As a general consequence, SSA indices decreased by 15% in this sample, falling from a median CSI of 0.51 [0.25, 0.78] in control condition to 0.43 [0.15, 0.73] after dopamine application (p = 0.014). Such average reduction was caused by a 25% drop in the median DEV response (control firing rate: 5.63 [3.25, 10.00]; dopamine firing rate: 4.19 [1.63, 7.63]; p < 0.001), while STD response remained stable (control firing rate: 1.71 [0.64, 3.83]; dopamine firing rate: 1.63 [0.36, 3.65]; p = 0.284). The spontaneous firing rate found in the IC cortices tended to be very scarce and did not change significantly with dopamine application (control spontaneous firing rate: 0.18 [0.05, 0.77]; dopamine spontaneous firing rate: 0.15 [0.03, 0.90]; p = 0.525; Figure 23).

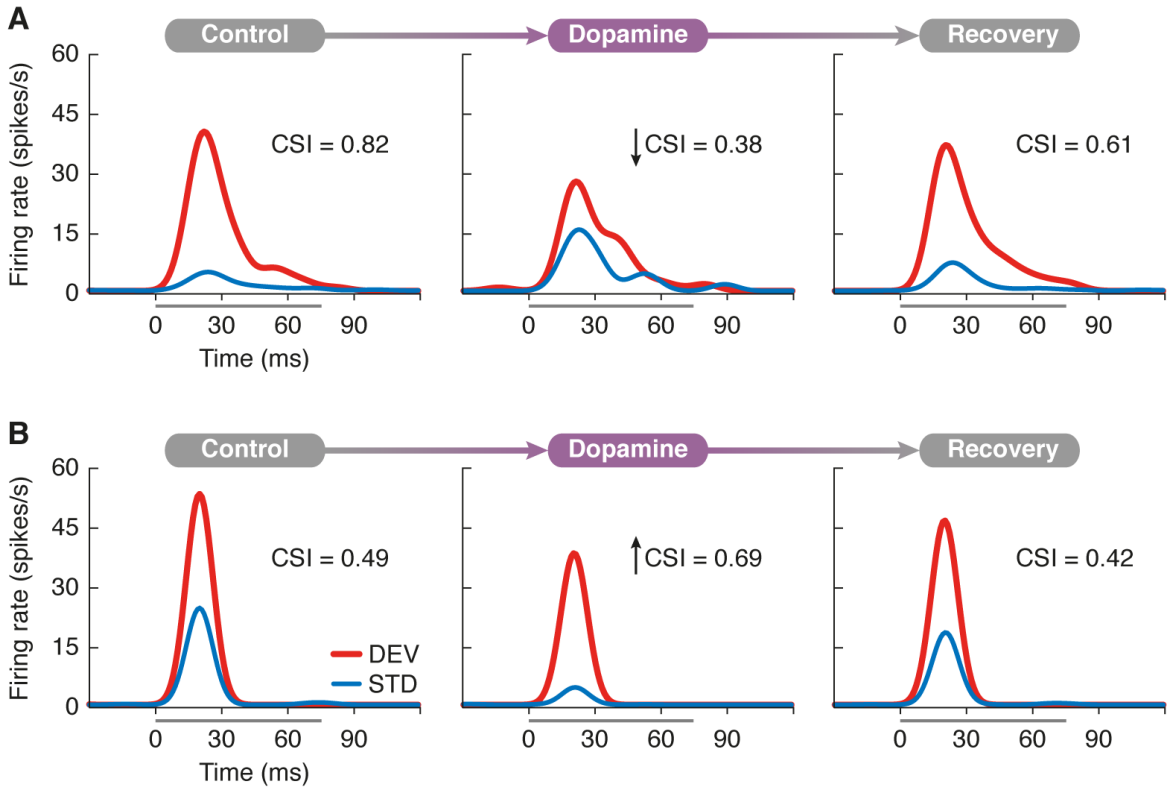

Figure 24. Examples of dopaminergic effects on different MUA recordings. A. PSTH of a neuron before (left panel), during (middle panel) and after (right panel) dopamine application (baseline-corrected spike counts, averaged within 0–180 ms after tone onset). In this case, dopamine reduced the CSI. **B.** Another example showing the opposite effects.

Previous studies had reported heterogeneous dopaminergic effects on the response of IC neurons (Gittelman et al., 2013; Hoyt et al., 2019), so a bootstrap analysis was performed to evaluate the statistical significance of CSI changes unit by unit (see Section III.7.d). Such

heterogeneity was evident across the sample, with 42 units following the population trend whereas 33 units increased their CSI under dopamine and other 19 units remained unaltered (Figure 23A). Figure 24A shows the response of a neuron to STD (blue) and DEV (red) in the control condition (left panel), during dopamine application (middle panel) and after recovery (right panel). The application of dopamine caused an increment of the STD response and a decrement of the DEV response, leading to a decrease of the CSI. In contrast, the example in Figure 24B showed a decrement of the response to both STD and DEV during the application of dopamine, thus resulting in an increase of the CSI. The effects of dopamine peaked around 8-10 minutes after microiontophoretic application, followed by a progressive recovery to baseline values that could take beyond 90 minutes (Figure 24, right panels).

IV.2.- Endogenous dopamine release modulates the CSI via D_2-like receptors

Previous reports (Nevue, Elde, et al., 2016; Nevue, Felix, et al., 2016) hinted at D_2-like receptors as the most probable mediators of the dopaminergic effects observed in the CSI of ECIC neurons. In order to test for a possible endogenous dopaminergic modulation on SSA mediated by D_2-like receptors, eticlopride, a D_2-like receptor antagonist, was applied to 43 units of the ICx following Protocol 1 (see Section III.4.a).

At sample level, no significant response changes were manifest (DEV firing rate: p = 0.609; STD firing rate: p = 0.769; spontaneous firing rate: p = 0.405; CSI change: p = 0.170). However, a bootstrap analysis to evaluate the statistical significance of CSI changes in each unit under eticlopride influence revealed that only 11 units remained unaffected (see Section III.7.d). Conversely, the CSI had significantly increased in 19 units and decreased in 13 units, implying that eticlopride was indeed antagonizing endogenous dopaminergic modulation mediated by D_2-like receptors on those units (Figure 25). Figure 26A shows the response of a neuron to STD (blue) and DEV (red) in the control condition (left panel), during eticlopride application (middle panel) and after recovery (right panel). The application of eticlopride caused an increment of the STD response and a decrement of the DEV response, leading to a decrease of the CSI. In contrast, the example in Figure 26B showed a decrement of the STD response STD and an increment of the DEV response during the application of eticlopride, thus resulting in an increase of the CSI. The effects of eticlopride peaked around 8-10 minutes after

microiontophoretic application, followed by a progressive recovery to baseline values that could take beyond 90 minutes (Figure 26, right panels).

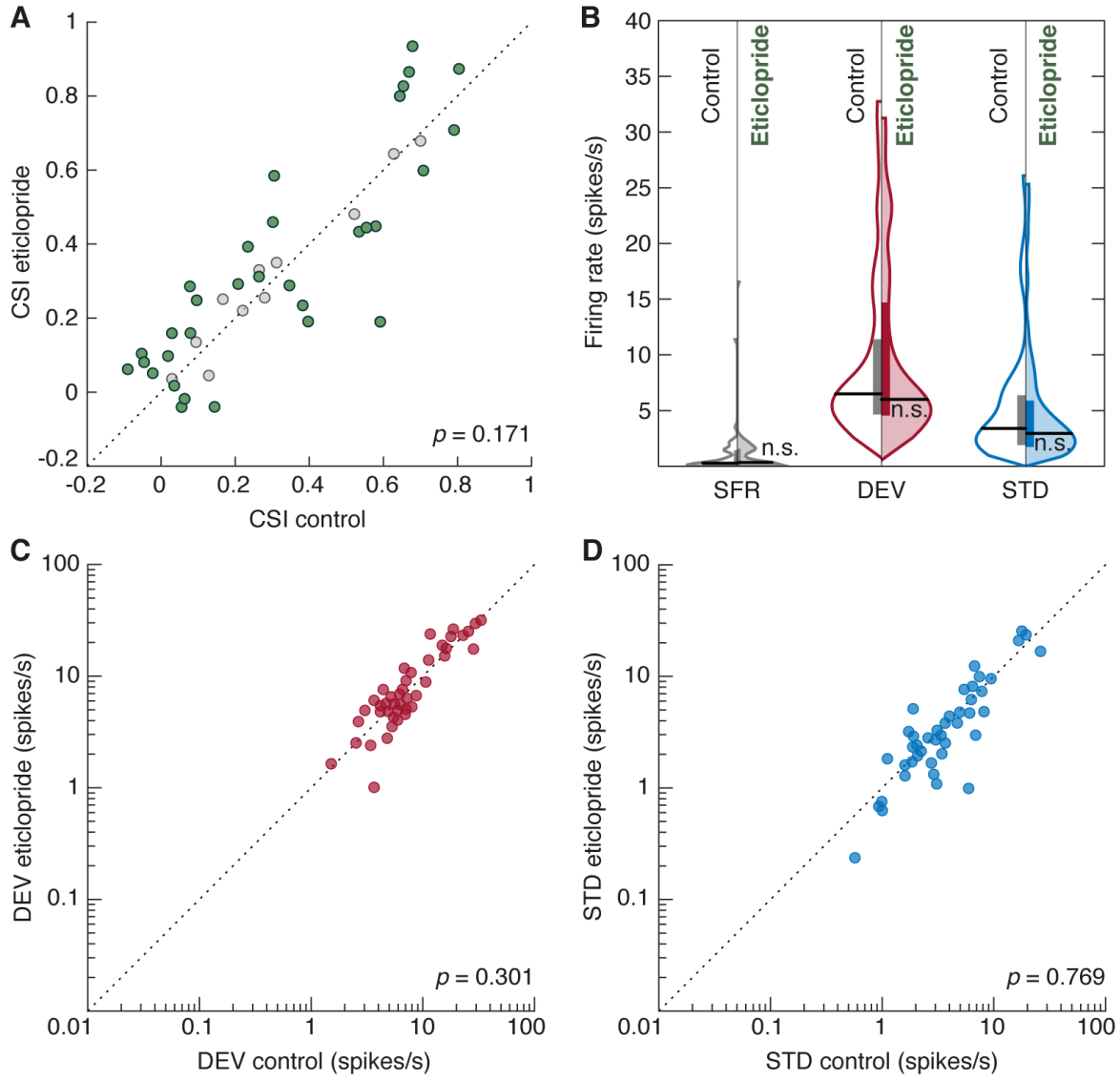

Figure 25. Eticlopride effects on the CSI. **A.** Scatter plot of the CSI in control condition versus eticlopride application. Units that underwent significant CSI changes are represented in green, whereas the rest are marked as gray dots. **B.** Violin plots of the spontaneous firing rate (SFR), DEV and STD response. Control conditions are represented in the left half of each violin (no color) while eticlopride effects are on display in the right half (colored). Horizontal thick black lines mark the median of each distribution, while vertical bars cover the interquartile range (n.s. = non-significant). **D.** Scatter plot of STD responses in control condition versus eticlopride application.

In addition, 5 units remained exceptionally stable during the recording session, so they were used to test whether dopamine and eticlopride yielded complementary effects on the same unit (Figure 26). We recorded the activity of these 5 units in control condition, and then during an application of either dopamine or eticlopride. After enough time had passed for the units to recover from the effects of the first drug (never less than 40 minutes post-injection), their activity was recorded again (Recovery 1) and the other drug was applied. The neuronal activity was recorded under the effect of the second drug, after which the neuron was let to recover and a final recording was performed (Recovery 2). In 4 of the 5 cases, dopamine was applied first and eticlopride second, and viceversa in the other case left.

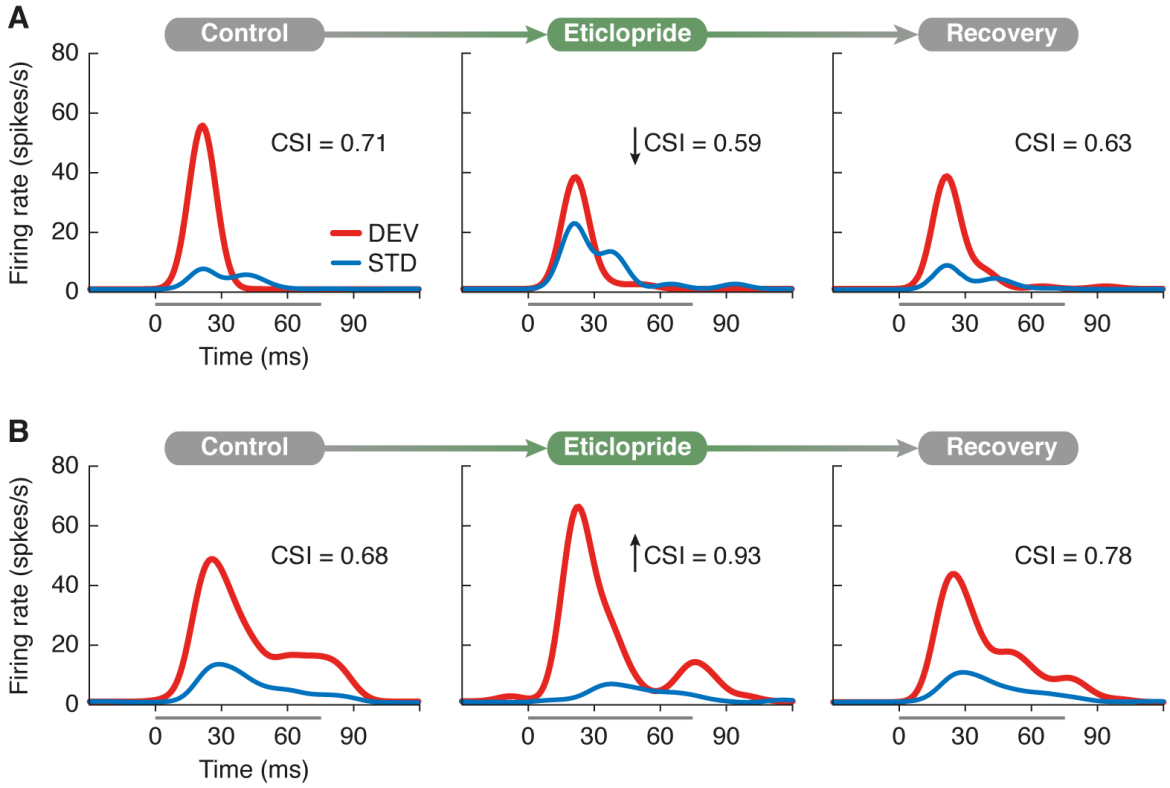

Figure 26. Examples of eticlopride effects on different MUA recordings. **A.** PSTH of a neuron before (left panel), during (middle panel) and after (right panel) eticlopride application (baseline-corrected spike counts, averaged within 0–180 ms after tone onset). In this case, eticlopride reduced the CSI. **B.** Another example a neuron showing the opposite effects.

This sequential protocol revealed that dopaminergic effects were specifically mediated by D_2-like receptors, as dopamine and eticlopride induced complementary effects in each neuron tested (Figure 27), although these response changes did not always reach statistical significance. Figure 27A and B show 2 units illustrating the effect of a dopamine injection (time after first injection: ~5 – 15 mins), followed by its recovery (~40 – 65 mins) and a

subsequent eticlopride injection (~65 – 80 mins) with its recovery (~120 – 140 mins). The CSI of the unit displayed in Figure 27A decreases with the dopamine injection and increases with eticlopride. Conversely, yet consistently, the unit illustrated in Figure 27B shows the opposite effects, increasing its CSI during the dopamine application and decreasing with eticlopride application. The bar plots in Figure 27C show the averaged effect of dopamine and eticlopride on the spontaneous activity, the CSI and the firing rate for both DEV and STD. These parameters tend to change in opposite directions depending on the application of dopamine or eticlopride.

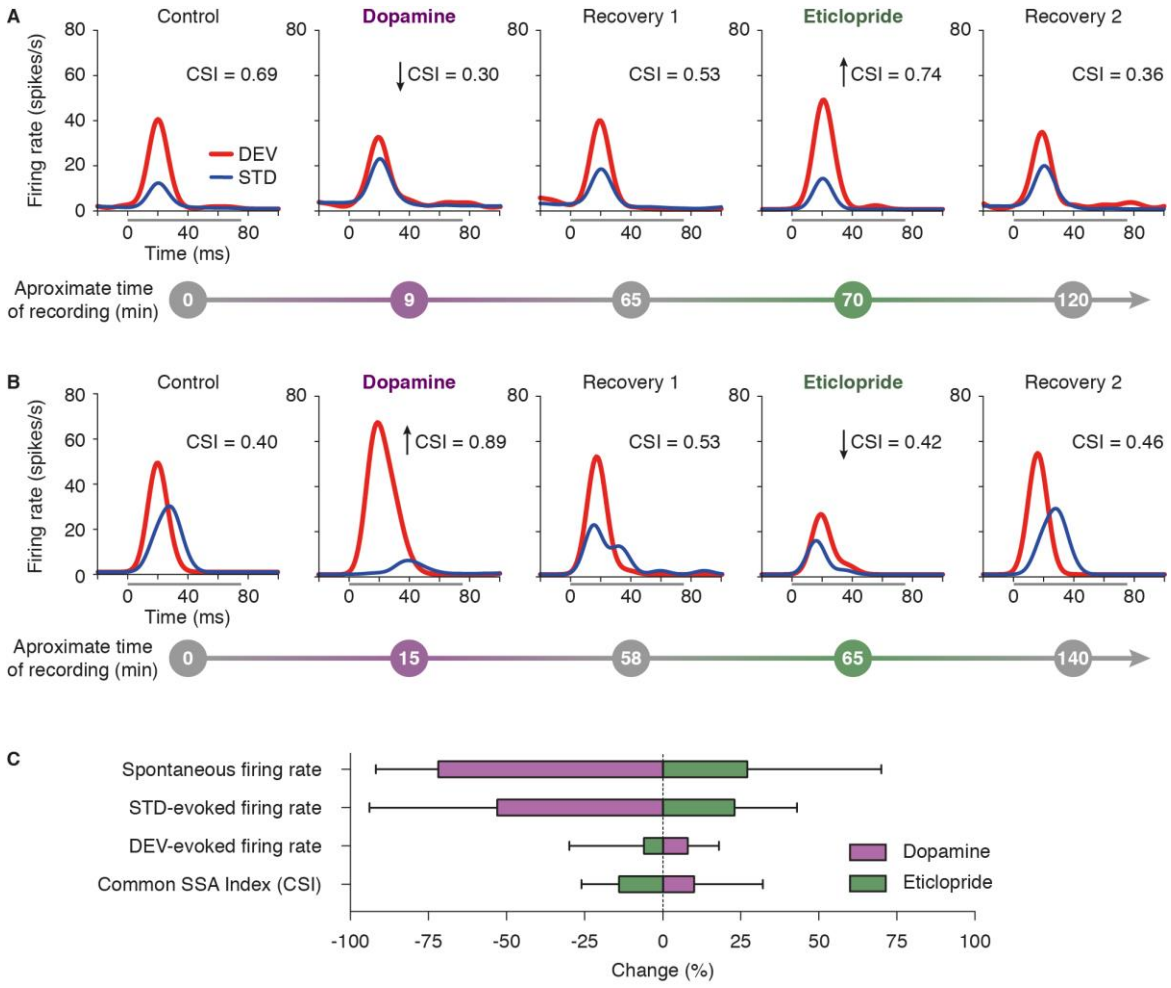

Figure 27. Antagonistic effects of dopamine and eticlopride application on the same neuron. A. PSTH examples of a neuron that underwent a sequential application of dopamine and eticlopride. **B.** PSTH examples of another neuron exhibiting the opposite effects. **C.** Bar plots represent the percent of change of spontaneous firing rate, first spike latency, firing rate and CSI caused by dopamine (purple bar) and eticlopride (green bar) for the 5 neurons tested, denoting changes in opposite directions for the 2 drugs in most cases.

IV.3.- Auditory PP begins in the IC cortex (ICx)

In order to settle which explanation of novelty perception accounts better for the mismatch signals recorded in the IC, i.e., the Adaptation Hypothesis (see Section I.2.b) or the Expectation Hypothesis (see Section I.3.d), a total of 177 units were recorded in the IC of the anesthetized under oddball and no-repetition stimulation. This sample comprises all the recordings performed in anesthetized rats following Protocol 2 (see Section III.4.b), and also includes the similar control condition of Protocol 3 (i.e., before dopamine application). Hence, this sample includes 142 units recorded from the ICx (e.g., Figures 21B and 28B) and the other 35 neurons came from the CNIC (e.g., Figures 21A and 28A). In addition, Protocol 2 was also applied to record 47 well-isolated SUAs in the IC of awake mice, 27 ICx neurons (e.g., Figures 21D and 34B) and 20 CNIC neurons (e.g., Figures 21C and 34A), in order to control for the influence of anesthesia over PE signaling.

Each recorded IC unit was presented a set of oddball sequences (Figure 17A), using tones selected from the FRA, to compute the iMM as the difference between DEV and STD responses, thus being equivalent to the CSI (see Section III.7.c). To determine whether this differential response (DEV > STD) reflected PP activity at the cellular level instead of sheer adaptation (Figure 17C), 2 cascade sequences, ascending and descending, and 1 many-standards sequence were presented as NRCs (Figure 17B, see Section I.2.d; Harms et al., 2014; Ruhnau et al., 2012). In these NRCs, each tone has the same 10% probability of occurrence as DEV in the oddball sequence, so it is not repetitive as the STD, so it is free from repetition effects. Besides, the NRC tone does not stand out from the statistical context as the DEV within an oddball sequence, and therefore it is not perceived as a deviant sound (Harms et al., 2014; Ruhnau et al., 2012). Hence, NRC responses can be used as a reference to dissociate repetition-induced suppression of the STD responses from any possible traces of genuine PE signaling within the DEV response (Figure 17C). Whether the neuronal mismatch response (DEV – STD) were caused entirely by SSA to the STD, as postulated by the Adaptation Hypothesis (see Section I.2.b), DEV and NRC responses should remain comparable across the whole sample (Figure 17D). Or, at most, some DEV responses could undergo a slightly stronger suppression than NRC responses due to cross-frequency adaptation (Mill et al., 2011; Taaseh et al., 2011). By contrast, according to the Expectation Hypothesis of the predictive processing framework (see Section I.3.d), PP based on Bayesian inference (Friston, 2009) would increase

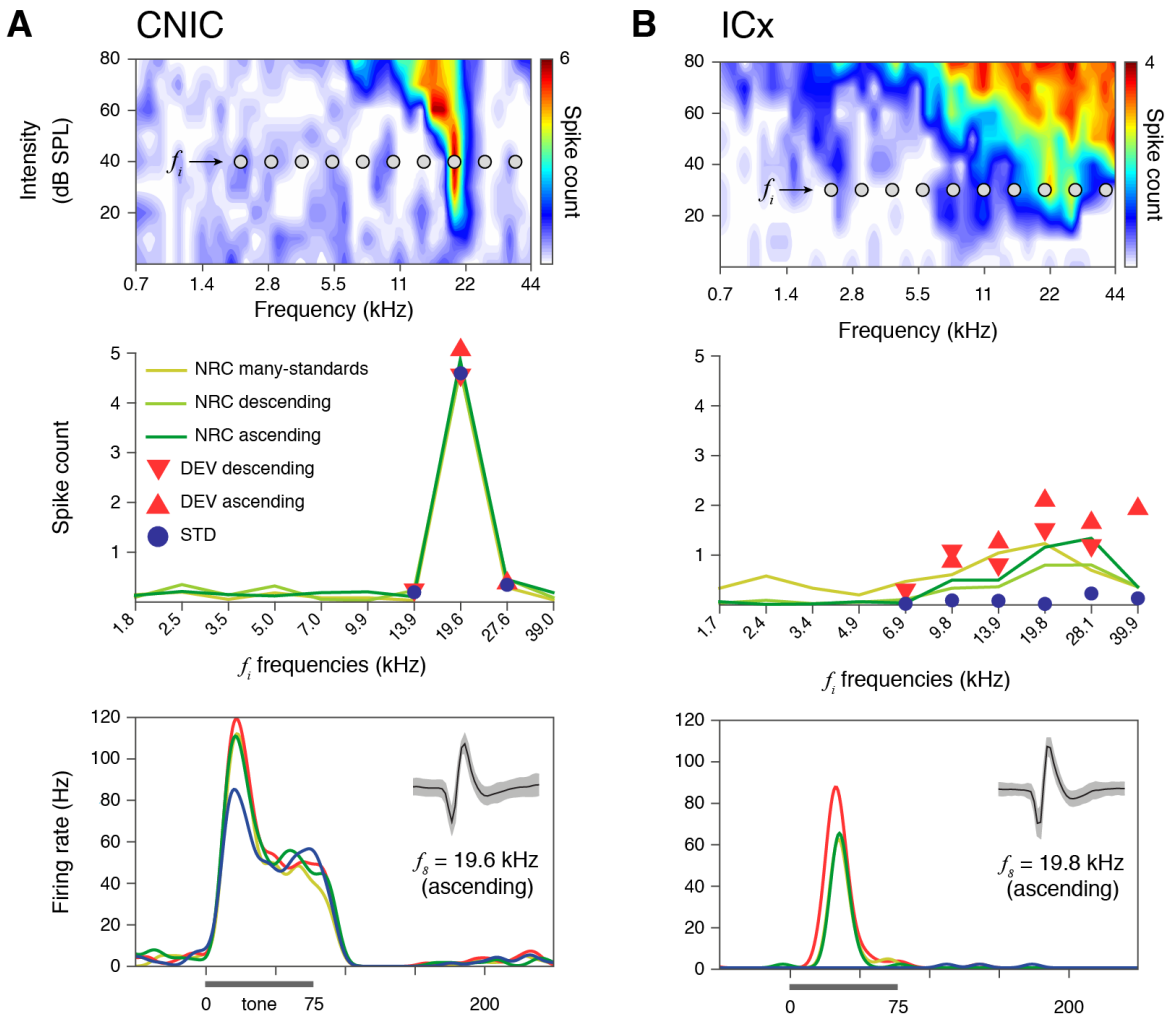

Figure 28. Examples of isolated neurons recorded in the IC of the anesthetized rat. A. CNIC neuron. The top panel shows a narrow, sharply-tuned FRA, typical of lemniscal neurons. Within the FRA, 10 grey dots indicate the 10 tones (f_i) selected to build the experimental sequences (Figure 17A and B). The middle panel displays the measured responses of this CNIC neuron to each f_i tone (baseline-corrected spike counts, averaged within 0–180 ms after tone onset) for all conditions tested. Note that all evoked responses overlap. The bottom panel contains the PSTH of the ascending tone f_8 as example. A thick horizontal line represents stimulus duration. A small inset within the upper right corner features the isolated spike (mean ± SEM) of that single neuron. **B.** ICx neuron. The top panel shows a broadly-tuned FRA, typical of nonlemniscal neurons. The middle panel displays the measured responses of this ICx neuron to each f_i tone for all conditions tested. Note that DEV responses are stronger than NRC responses, which in turn are stronger than STD responses. The bottom panel contains the PSTH of ascending tone f_8 as example. Again, DEV responses are stronger than NRC responses, and there was no response to the STD.

the expected precision of current predictions as STD input accumulates, yielding repetition suppression on the STD response (Auksztulewicz & Friston, 2016; Garrido et al., 2009;

Stefanics et al., 2014). Therefore, stronger PEs would be elicited by the DEV than by the NRC, due to the lack of sequential stimulus repetitions in the many-standards and cascade sequences (Figure 17E; Ruhnau et al., 2012; Stefanics et al., 2014).

Statistical comparisons between responses evoked by the many-standards and cascade sequences did not find any significant differences within the CNIC (p = 0.194) nor the ICx (p = 0.820) of the anesthetized preparations. This is consistent with the lack of differences also reported in human EEG data (Wiens et al., 2019). Consequently, the results using either many-standards or cascades as NRC were largely equivalent (Table 1). Therefore, in order to avoid excessive redundancy in the ensuing text and figures, I will limit my descriptions of the results to those obtained using the cascade sequences as NRC, since this sequence controls for additional factors beyond presentation rate of the DEV and it is usually regarded as a better control for the repetition effects induced by the oddball paradigm (see Section I.2.d; Harms et al., 2014; Ruhnau et al., 2012). Notwithstanding, results using the many-standards sequence as NRC in the anesthetized preparations are summarized in Table 1.

IV.3.a.- Spiking activity of ICx neurons contains PE signals

In order to demonstrate PP activity in the IC, a within-station multiple comparison Friedman test was performed between DEV, STD and NRC responses, such that each pair of conditions within the CNIC (Figure 29A) or the ICx (Figure 29B) was tested for a difference in medians (Table 1). Median DEV responses were stronger than STD responses all over the IC (Figure 29A and B), resulting in a median iMM of 0.19 [0.12, 0.31] in the CNIC (p < 0.001; Figure 29C, in magenta) and a median iMM of 0.53 [0.27, 0.70] in the ICx (p < 0.001; Figure 29D, in magenta). These indices replicate the reports in previous SSA studies from our lab (Duque et al., 2012; Malmierca et al., 2009; Pérez-González et al., 2005).

The Adaptation Hypothesis could hold within the CNIC, as the median normalized NRC spike count was 0.65 [0.59, 0.74], slightly stronger than the 0.61 [0.56, 0.67] yielded by the DEV. Both DEV and NRC normalized responses surpassed the 0.42 [0.23, 0.48] normalized STD spike count (Figure 29A). Hence, the resulting median iRS value of 0.23 [0.13, 0.52] could account for the whole neuronal mismatch signal in the CNIC (p < 0.001), whereas the median iPE value of −0.04 [−0.20, 0.06] was not statistically different from zero (p = 0.240; Figure 29C).

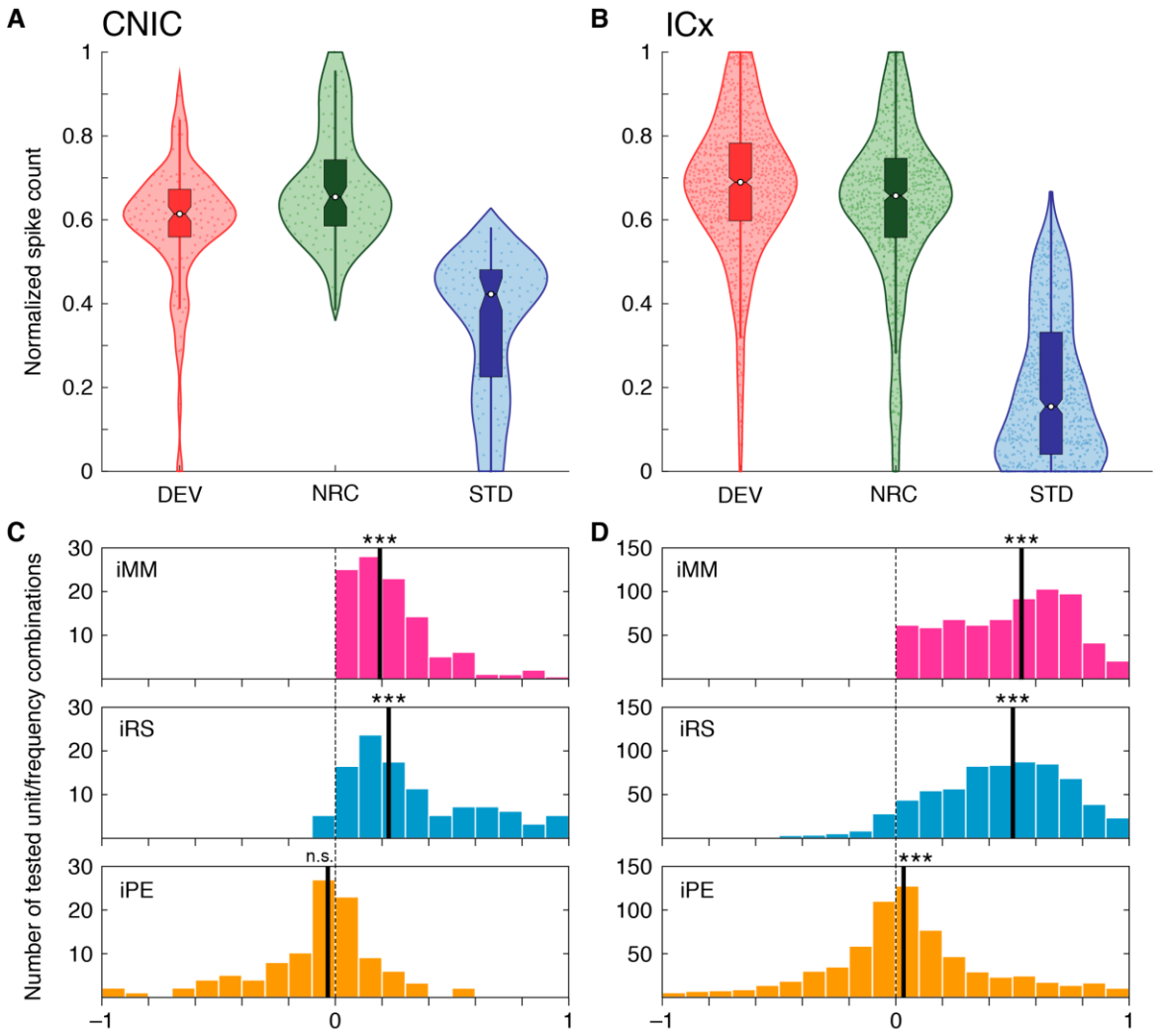

Figure 29. PE signaling at population level in the IC. A. Violin plots of normalized responses in the CNIC. Each color point within the violin represents a measurement for a given unit/frequency combination. A big white point marks the median of each distribution, and the boxplots inside each distribution indicate the interquartile range, with the confidence interval for the median indicated by the notches. **B.** Violin plots of normalized responses in the ICx. **C.** Histograms represent distributions indices in the CNIC. **D.** Distribution of indices in the ICx. Solid black lines indicate medians (n.s. = non-significant, *** $p < 0.001$).

Conversely, the Adaptation Hypothesis could not account for the behavior of ICx neurons. The median normalized DEV spike count of 0.69 [0.78, 0.60] surpassed the 0.66 [0.75, 0.56] registered for the NRC (Figure 29B), as proposed by the Expectation Hypothesis (Figure 17E). This resulted in a significant iPE of 0.03 [−0.12, 0.20], confirming the presence of significant PE signaling activity at sample level within the ICx ($p < 0.001$). In addition, the median normalized STD spike count of 0.15 [0.04, 0.33] in the ICx was almost a third of that observed in the CNIC. Therefore, the resulting median iRS value of 0.50 [0.24, 0.67] was

considerably higher among nonlemniscal neurons than in their lemniscal counterparts ($p < 0.001$), which implies a stronger influence of top-down predictive activity suppressing expected input in the ICx (Figure 29D).

	CNIC		ICx	
	Cascade	Many-standards	Cascade	Many-standards
Number of multiunits	26	36	103	123
Tested frequencies	105	157	673	815
Median raw spike counts				
DEV	1.3743	1.1176	0.9471	0.9451
STD	0.8251	0.5158	0.1487	0.1247
NRC	1.4147	1.1314	0.8769	0.8505
Median normalized spike counts				
DEV	0.6140	0.6326	0.6897	0.6892
STD	0.4226	0.3356	0.1549	0.1279
NRC	0.6545	0.6568	0.6573	0.6670
Raw spike count differences, Friedman test				
DEV − STD	0.5492	0.6018	0.7984	0.8204
p value	**3.5263×10^{-22}**	**1.3864×10^{-34}**	**1.4701×10^{-164}**	**2.7372×10^{-199}**
DEV − NRC	–0.0404	–0.0138	0.0702	0.0946
p value	0.2396	0.8211	**6.5652×10^{-4}**	**0.0080**
NRC − STD	0.5897	0.6156	0.7282	0.7257
p value	**1.7891×10^{-27}**	**8.2907×10^{-36}**	**1.4361×10^{-126}**	**4.1573×10^{-126}**
Normalized spike count differences, Friedman test				
iMM = DEV − STD	0.1915	0.2970	0.5348	0.5613
p value	**3.5263×10^{-22}**	**1.3864×10^{-34}**	**1.4701×10^{-164}**	**2.7372×10^{-199}**
iPE = DEV − NRC	–0.0405	–0.0242	0.0324	0.0221
p value	0.2396	0.8211	**6.5652×10^{-4}**	**0.0080**
iRS = NRC − STD	0.2319	0.3212	0.5024	0.5392
p value	**1.7891×10^{-27}**	**8.2907×10^{-36}**	**1.4361×10^{-126}**	**4.1573×10^{-126}**

Table 1. Summary of spiking activity results in the anesthetized preparation. In addition to the normalized values, raw spike counts are also in display. Indices have been computed using both NRC, i.e., cascade and many-standards sequences. Significant p values are highlighted.

IV.3.b.- PE signaling is stronger in untuned ICx neurons

IC neurons present many different shapes of FRA (Figure 7; Hernández et al., 2005), implying different compatibilities of spectral integration. In order to test a possible relationship between the neuronal tuning bandwidth and PE signaling, I tried to correlate the neuronal tuning bandwidth with the median iPE of each neuron. First, the characteristic frequency within each FRA was identified as the threshold frequency with the best evoked response expressed in kHz. Then, the bandwidth at 30 dB SPL above threshold was measured for each unit by calculating the difference between the base 2 logarithms of the upper and lower frequencies of the tuning curve, expressed in kHz. The most commonly used measure to express the sharpness of frequency tuning is the Q factor. Q_n is defined as the characteristic frequency divided by the bandwidth in kHz at 'n' dB above threshold. Thus, the Q_{30} was calculated and its correlation with the iPE was tested. There was no apparent correlation between these 2 measurements (Spearman correlation coefficient, $\rho = -0.02$, $p = 0.585$, Figure 30).

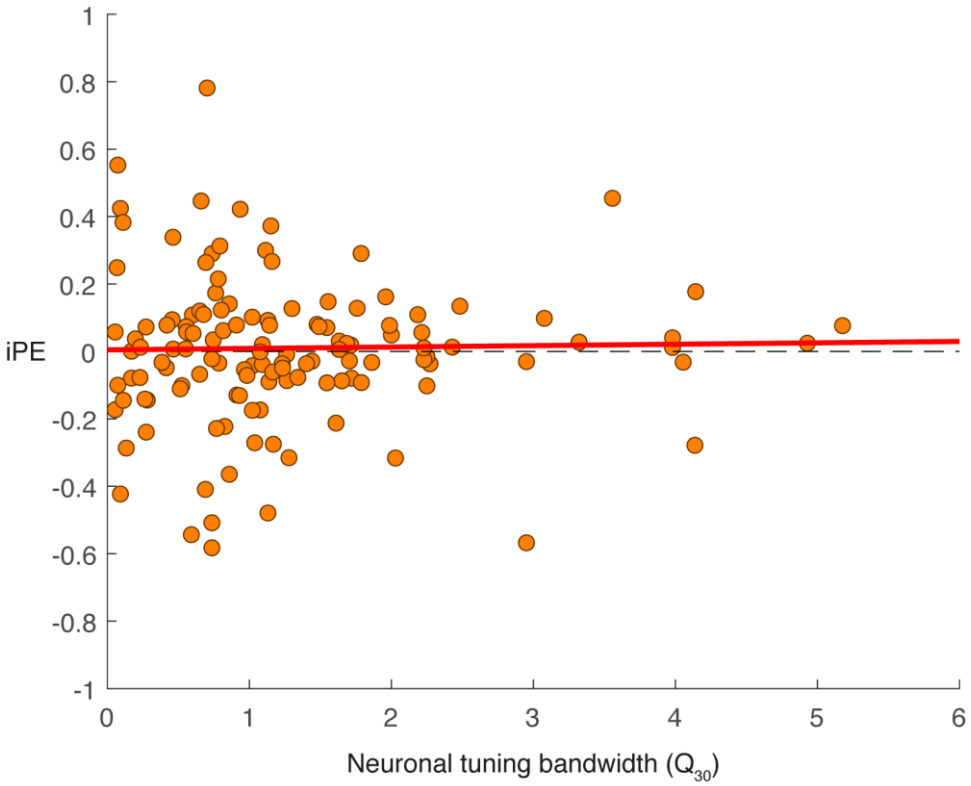

Figure 30. Correlation between PE signaling and the width of the receptive field in the IC. Scatterplot showing the distribution of the median iPE along the Q_{30} factor of each corresponding neuron. There is not an apparent correlation between both variables.

Nevertheless, there was a subset of neurons with highly disorganized FRA for which a Q_{30} factor could not be calculated (n = 13). The median iPE value of 0.39 [−0.10, 0.43] in the group of untuned neurons was significantly higher (p = 0.004) than the median iPE value of 0.01 [−0.07, 0.09] observed in the group of tuned neurons. This indicates that untuned neurons exhibiting disorganized FRAs (Figure 7D) are the prime PE signalers of the ICx.

IV.3.c.- The PE-LFP coincides in time with the iPE in spiking activity

The same microelectrode used for extracellular recordings simultaneously recorded the LFPs within each recoding location (see Section III.7.e). LFPs provide a mesoscopic signal that help to bridge the gap between the mismatch signals observed at the microscopic level, such as in the spiking activity of single neurons, and at the macroscopic level, such as in the ABR (Duque et al., 2018; Harms et al., 2014; Klein et al., 2014; Shiramatsu et al., 2013; von der Behrens et al., 2009). Hence, LFP responses to each condition were averaged in the CNIC and the ICx, as well as the LFP difference waves and the time intervals containing significant modulations, and then the LFP activity was compared with the SFD (Figure 31, see Section III.7.e).

In the CNIC, the mismatch potential comprised 3 significant components. First there was a quick negative deflection spanning from 6 ms to 24 ms, readily followed by a slow positive modulation spanning between 30 ms and 79 ms, and later a final slow negative component appeared from 118 ms to 154 ms post-stimulus onset. Mismatch responses in the spiking activity coincided with the first 2 components of the mismatch LFP, as significantly positive iMM values lasted until 90 ms post-stimulus onset (Figure 31E). Also consistent with the observations of spiking activity, no trace a significant of PE-LFP could be found in the CNIC (Figure 31G).

In the ICx, the mismatch potential comprised at least 4 distinctive components. First came a very quick positive modulation spanning between 4 ms and 8 ms, immediately followed by a quick negative deflection that spanned from 12 ms to 32 ms post-stimulus onset. Right after that, a slow positive deflection followed from 35 ms to 87 ms post-stimulus onset. Finally, at 92 ms post-stimulus onset started a series relatively quick negative modulations that lasted until 165 ms post-stimulus onset. Mismatch responses in the spiking activity coincided with the first 3 components of the mismatch LFP, as significantly positive iMM values lasted until 70 ms post-stimulus onset (Figure 31F). Most importantly, a significant PE-LFP was detectable

in the form of a quick positive deflection between 45 ms and 60 ms post-stimulus onset. This coincided with an early time window between 30 ms and 70 ms post-stimulus onset where iPE values in spiking activity were significantly positive. An additional late window of positive iPE values was revealed between 150 ms and 170 ms post-stimulus onset (Figure 31H).

Figure 31. Comparison between spiking activity and the LFP (⏎ next page). The left column (panels A, C, E and G) represent the results for the CNIC, whereas the right column (panels B, D, F and H) display the results for the ICx. Grey horizontal bars represent a 75-ms tone for reference. **A, B.** The SFD represent the average firing rate profiles of IC division (see Section III.7.a). **C, D.** Average LFP across all tested tones and units from each IC division for different conditions (see Section III.7.e). **E, F.** Mismatch potentials (black trace) are plotted as the difference wave of the DEV- and the STD-evoked LFP. Along the mismatch potentials, the time course of the average iMM is also plotted in purple (mean ± SEM, asterisks indicating significant iMM of $p < 0.05$ for the corresponding time window; Wilcoxon signed-rank test for 12 comparisons, corrected for FDR = 0.1). Below each panel, an instantaneous p value (white trace) of the corresponding mismatch potential (paired t test against equal means, corrected for FDR = 0.1, critical threshold for significance set at $\alpha = 0.05$ represented as a red, thin horizontal bar). The thick, black, horizontal bars mark time intervals for which the average mismatch potential is significant. Note that they tend to coincide with the purple asterisks marking time windows with significant iMM in the spiking activity. **G, H.** PE-LFPs (black trace) are plotted as the difference wave of the DEV- and the NRC-evoked LFP. Along the PE-LFPs, the time course of the average iPE is also plotted in orange (mean ± SEM, asterisks indicating significant iPE of $p < 0.05$ for the corresponding time window; Wilcoxon signed-rank test for 12 comparisons, corrected for FDR = 0.1). Below each panel, an instantaneous p value (white trace) of the corresponding mismatch potential (paired t test against equal means, corrected for FDR = 0.1, critical threshold for significance set at $\alpha = 0.05$ represented as a red, thin horizontal bar). The thick, black, horizontal bar in panel H mark time interval for which the average PE-LFP is significant. Therefore, only the ICx generates a PE-LFP. Note that the PE-LFP coincides with the first 2 orange asterisks marking time windows with significant iPE in the spiking activity.

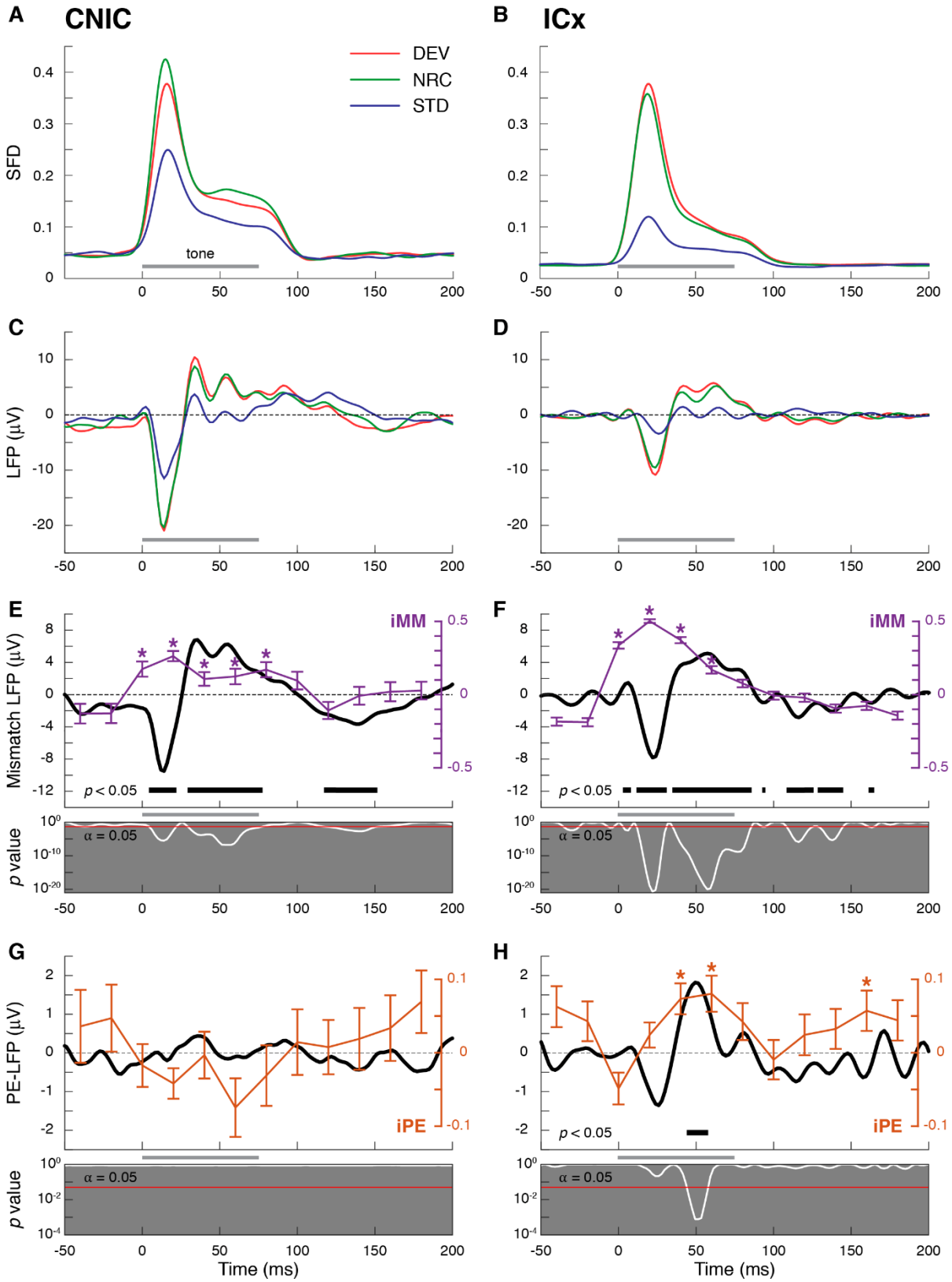
A
CNIC
B
ICx
DEV
NRC
STD
SFD
tone
C
D
LFP (μV)
E
F
Mismatch LFP (μV)
iMM
p < 0.05
p value
α = 0.05
G
H
PE-LFP (μV)
iPE
Time (ms)

IV.3.d.- The ICx signals stronger PEs at lower intensities and for pitch increases

A preliminary analysis of the data revealed that iPE values tended to be higher when the intensity of the stimulation was low, i.e., < 40 dB SPL (Figure 32).

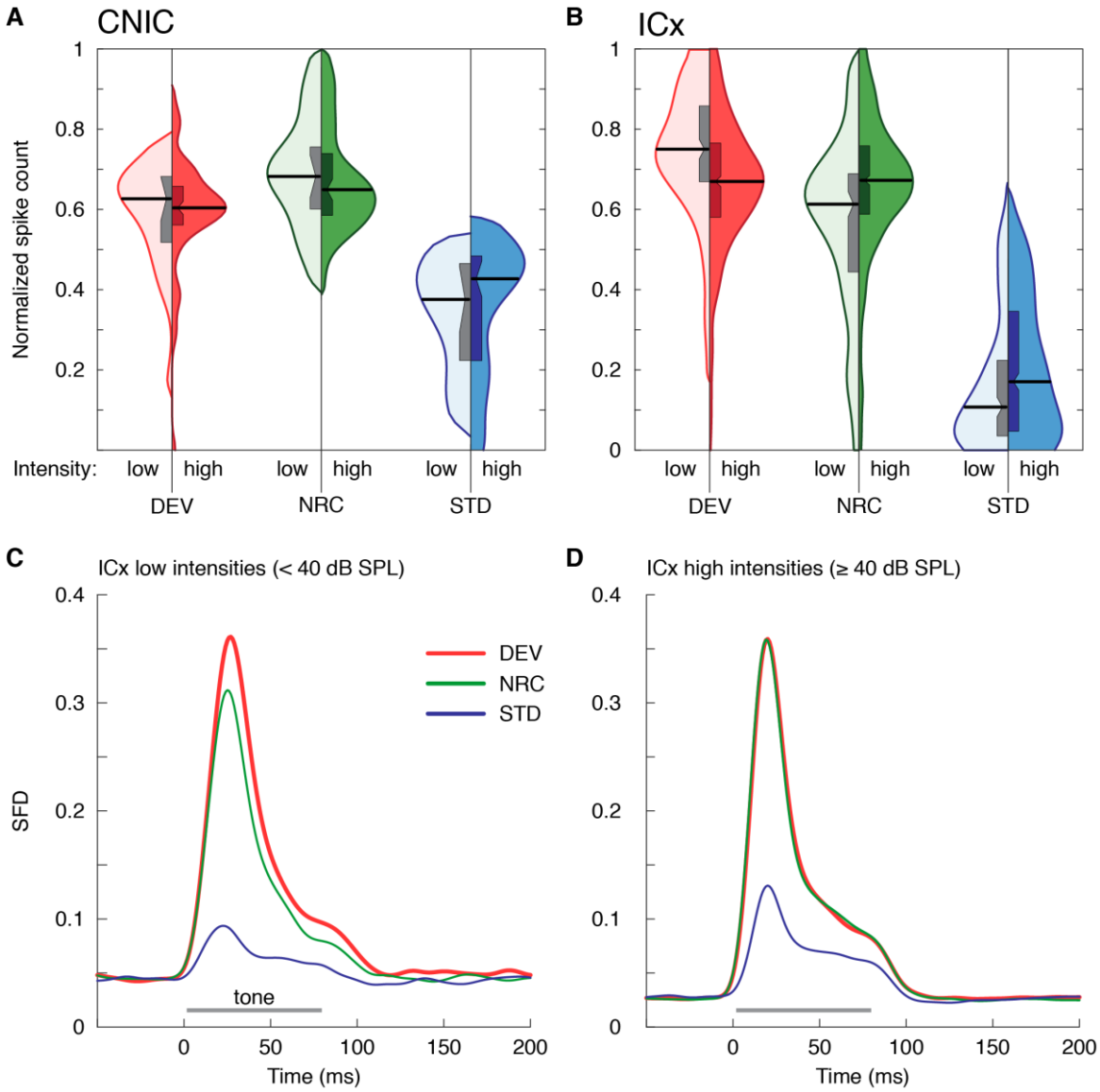

Figure 32. Evoked responses to low and high intensity stimulation. A. Violin plots of the normalized responses in the CNIC. Low intensities (< 40 dB SPL) are represented in the left half of each violin (light color and grey), while high intensities (≥ 40 dB SPL) are on display in the right half. Horizontal thick black lines mark the median of each distribution, and the boxplots inside each distribution indicate the interquartile range, with the confidence interval for the median indicated by the notches. **B.** Violin plots of the normalized responses in the ICx. **C.** SDF for low intensities in the ICx (< 40 dB SPL). Note that the DEV response comfortably surpasses the NRC response. **D.** By contrast, the SDF for stimulation levels ≥ 40 dB SPL in the ICx shows how the DEV and NRC responses equalize at high intensities.

In order to test how the physical features of the sound affected to the resulting iPE value, a linear model fitted the data using *SPL* (in Bels = dB SPL/10) and *direction* of DEV (ascending or descending) as predictor variables (Figure 33A). *Direction* is a categorical variable, so the factor 'ascending' acquired the numeric value of 1 when true or 0 when false, while the factor 'descending' was used as reference to calculate the intercept. The resulting iPE model for the ICx was:

$$\boldsymbol{iPE = 0.144 + 0.211 * ascending - 0.029 * SPL - 0.034 * ascending * SPL}$$

Applying an ANOVA to this linear model revealed significant effects for both direction ($F = 4.972$; $p = 0.026$) and intensity ($F = 32.033$; $p < 0.001$) separately, as well as for their interaction ($F = 4.254$, $p = 0.040$). Conversely, the attempt to define a linear model to account for iRS values in the ICx did not reveal any significant effects of intensity, direction, or the interaction between both factors. Therefore, the changes observed on the CSI (Duque et al., 2012) and the iMM in the ICx due to intensity and frequency shifts seem to be caused by how those factors elicit PE signaling in the auditory midbrain.

Using data from another study in which I participated applying Protocol 2 in the rat MGB and AC (Parras et al., 2017), I tried to fit a linear model of the aforementioned characteristics to each neuroanatomical division where neurons exhibited significantly positive iPE values. The iPE of nonlemniscal MGB (Figure 33B), primary AC (Figure 33C) and nonprimary AC (Figure 33D) could not be accounted for by a linear model that relied on *intensity* and *direction* as predictor variables. Therefore, PE signaling in the ICx is very influenced by the physical features of the sound (Figure 33A), whereas in higher processing levels PE signaling seems to be driven by more abstract factors, in agreement with the predictions of the Expectation Hypothesis (see Section I.3.a).

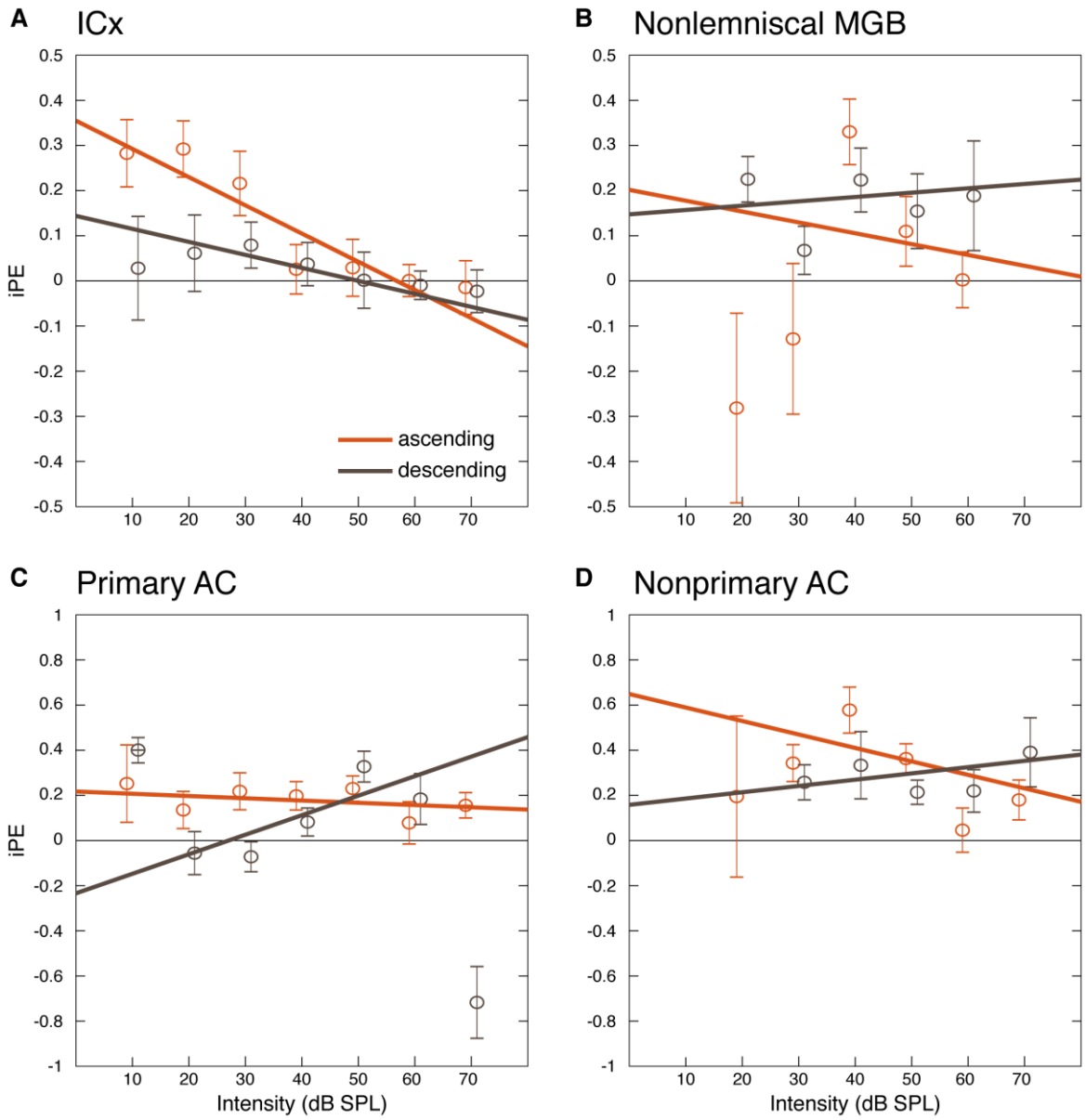

Figure 33. Linear models fitted for the iPE using intensity and direction as predictors. Error bars denote mean and standard error of the mean for each intensity and direction. **A.** The ICx model significantly predicts greater iPE values at low intensities, especially for ascending conditions (in orange). **B-D.** In the rest of auditory processing centers where PE signaling has been reported, this type of model fitted data poorly and did not show a significant relationship between the iPE and the intensity or the direction of the stimulus.

IV.3.e.- Awake preparations confirm robust PE signaling in the ICx

Protocol 2 was also applied on awake mice in order to confirm the results obtained in anesthetized rats on a different species while excluding the potential biasing influence of the anesthesia. 20 MUA were recorded from the CNIC (Figures 21C and 34A) and 27 MUA were

recorded from the ICx (Figures 21D and 34B). Representative sample recordings are shown in Figure 34. As in the SUA recordings performed in the anesthetized preparations, PE signals were evident across the MUA sample obtained from the awake preparations.

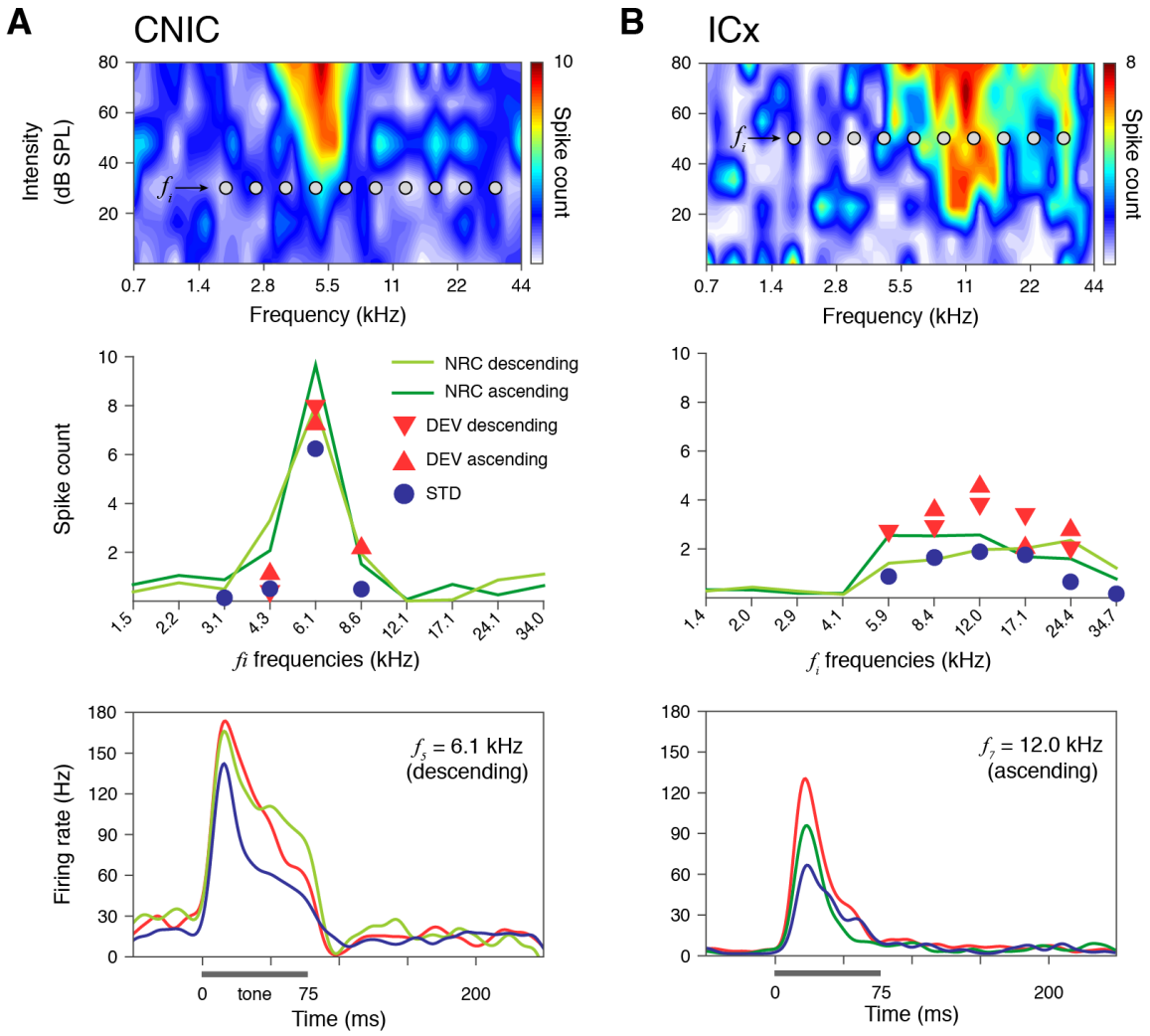

Figure 34. Examples of MUA recorded in the IC of the awake mouse. A. MUA recorded in the CNIC. The top panel shows a narrow, sharply-tuned FRA, typical of lemniscal divisions. Within the FRA, 10 grey dots represent the 10 tones (f_i) selected to build the experimental sequences (Figure 17A and B). The middle panel displays the evoked MUA to each f_i tone (baseline-corrected spike counts, averaged within 0–180 ms after tone onset) for all conditions tested. The bottom panel contains the PSTH of the descending tone f_5 as example. A thick horizontal line represents stimulus duration. **B.** MUA recorded in the ICx. The top panel shows a broadly-tuned FRA, typical of nonlemniscal divisions. The middle panel displays the evoked MUA to each f_i tone for all conditions tested. Note that DEV responses tend to be stronger than NRC responses, which in turn tend to be stronger than STD responses. The third panel contains the PSTH of ascending tone f_7 as example.

Normalized responses and indices for the awake sample are equivalent in meaning to the results obtained from the anesthetized rats. In the CNIC, median iPE value was −0.13 [−0.28, 0.02], significantly smaller than zero (p = 0.023), and therefore the Adaptation Hypothesis could not be discarded. In the ICx, median iPE of 0.12 [−0.06, 0.29] was significantly greater than zero (p = 0.018), which confirmed the Expectation Hypothesis. In addition, median iPE levels were significantly higher in awake than in anesthetized ICx (p = 0.048), which suggests that anesthesia lessens PE signaling in nonlemniscal IC neurons (Figure 35).

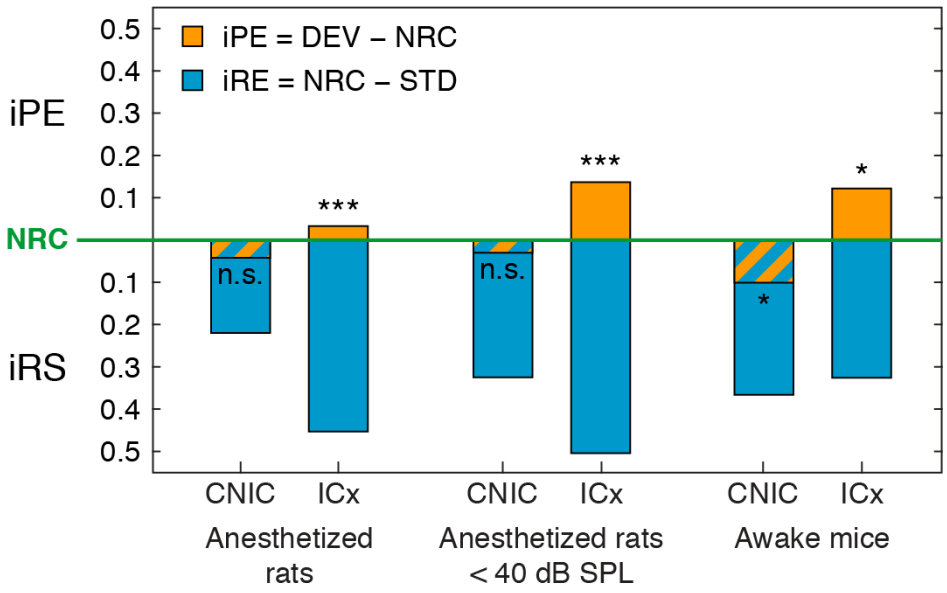

Figure 35. PE signaling in the IC under different conditions. Median indices of iPE (orange) and iRS (cyan), represented with respect to the baseline set by the NRC. Thereby, iPE is upwards-positive while iRS is downwards-positive. Asterisks denote statistical significance of iPE against zero median (n.s. = non-significant, * p < 0.05, *** p < 0.001).

IV.4.- Dopamine application tends to induce iPE reductions

Once PP in nonlemniscal IC neurons had been confirmed, 43 additional units were recorded following Protocol 3 (see Section III.4.c) to test how dopamine modulates PE signaling in the ICx. A bootstrap analysis evaluated the statistical significance of the effect of dopamine on the iMM of each recording (see Section III.7.d), which confirmed that 23 units underwent heterogeneous iMM changes (Figure 36B, purple dots, each representing one tested unit/frequency combination), whereas another 18 remained stable (Figure 36B, gray dots). Results agreed with those obtained using the CSI, as the iMM of the sample fell by 22%, from

a median of 0.57 [0.41, 0.69] in the control condition to a median of 0.45 [0.27, 0.65] under dopaminergic influence (p = 0.002; Fig 35B).

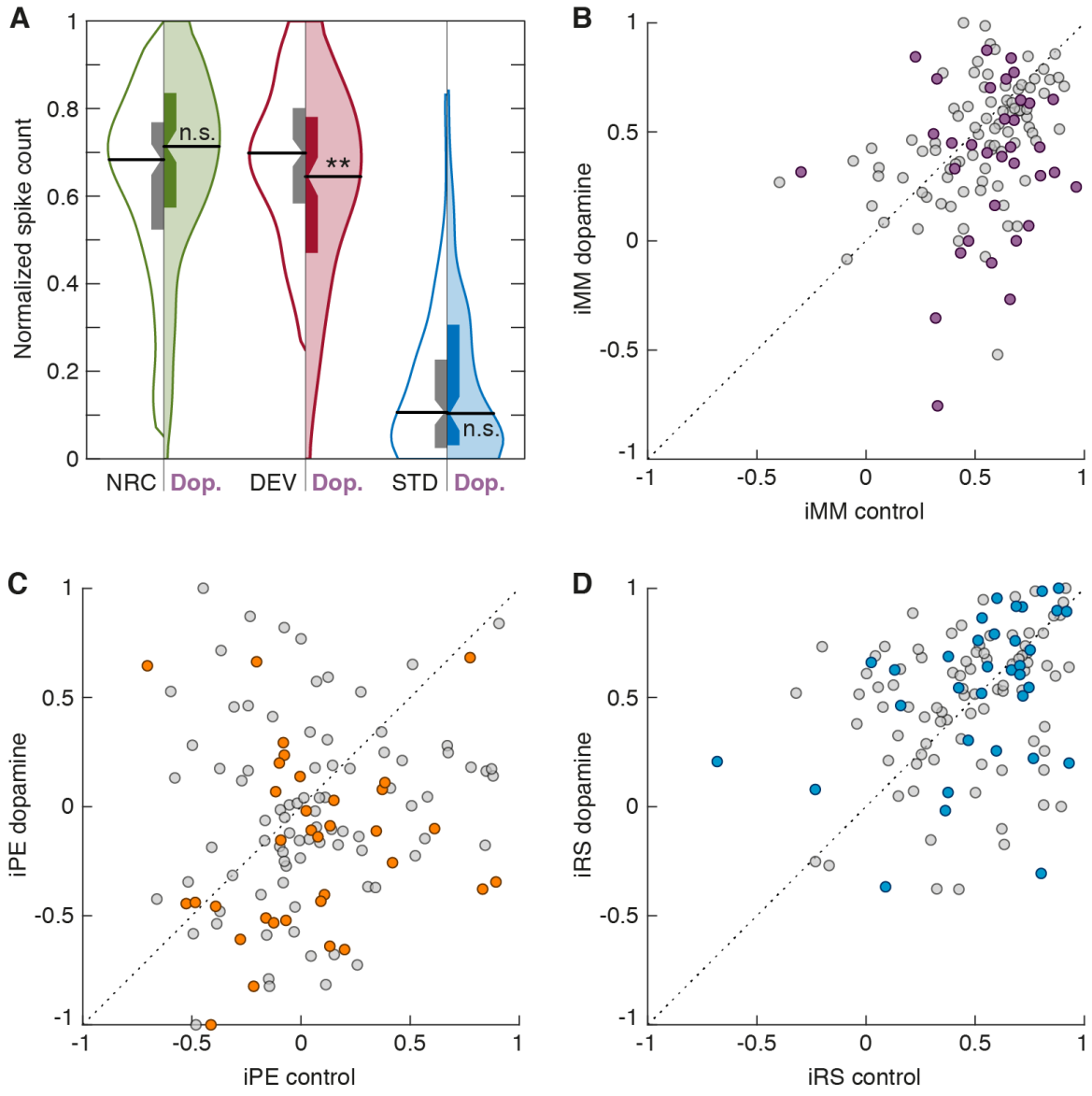

Figure 36. Dopamine effects on unexpected auditory input. A. Violin plots of the ICx normalized responses. Control conditions are represented in the left half of each violin (no color), and dopamine effects are on display in the right half (colored). Horizontal thick black lines mark the median of each distribution, and the boxplots inside each distribution indicate the interquartile range, with the confidence interval for the median indicated by the notches (n.s. = non-significant, ** p < 0.01). **B.** Scatterplot of the iMM where units that underwent significant changes are highlighted in purple and the rest are represented in grey. **C.** Scatterplot of the iPE where units that underwent significant iMM changes are highlighted in orange. **D.** Scatterplot of the iRS where units that underwent significant iMM changes are highlighted in cyan.

The only reason behind the general iMM drop was a significant decrease of the median DEV response (control normalized firing rate: 0.70 [0.58, 0.80]; dopamine normalized firing rate: 0.64 [0.47, 0.78]; p = 0.002). The STD response was not significantly affected (control normalized firing rate: 0.11 [0.02, 0.23]; dopamine normalized firing rate: 0.10 [0.03, 0.31]; p = 0.188). Most interestingly, NRC responses also remained unaffected by dopamine application (control normalized firing rate: 0.68 [0.52, 0.77]; dopamine normalized firing rate: 0.71 [0.57, 0.83]; p = 0.115; Figure 36A).

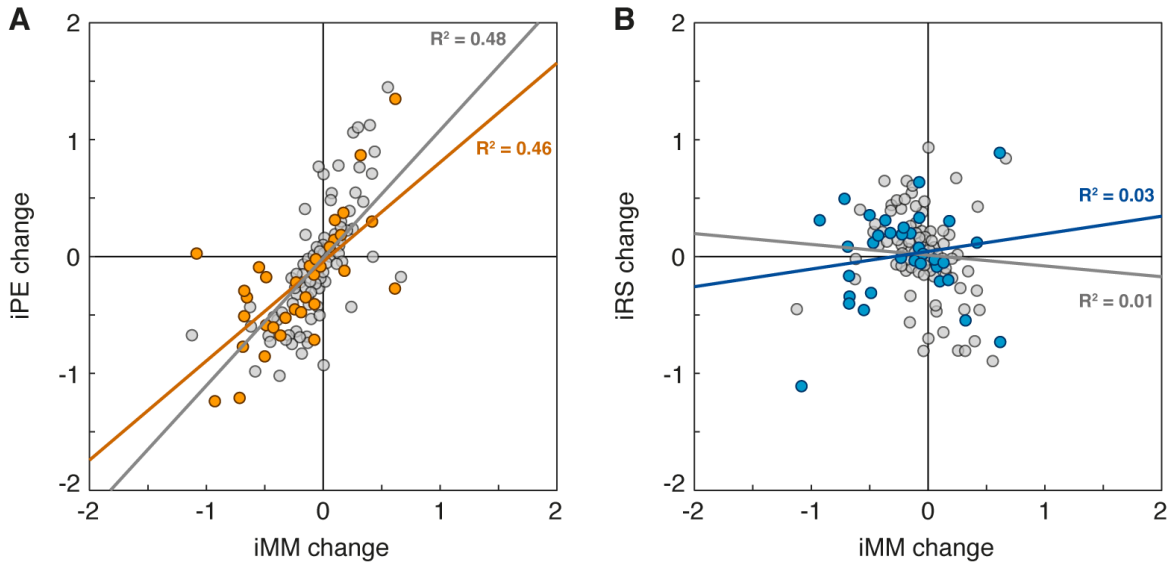

Figure 37. Dopamine effects on unexpected auditory input. A. Scatterplot representing $iMM_{chances} = iMM_{dopamine} - iMM_{control}$ in abscissas against $iPE_{chances} = iPE_{dopamine} - iPE_{control}$ in ordinates. Units that underwent significant iMM changes are highlighted in orange. Linear regressions showed good fitness for the whole sample (orange and grey dots, gray line), as well as for the subpopulation that only included neurons that underwent significant iMM changes (orange dots only, orange line). **B.** Scatter plot representing $iMM_{chances}$ in abscissas versus $iRS_{chances}$ in ordinates, where units that underwent significant iMM changes are highlighted in cyan. Linear regression models fitted poorly, both for the whole sample, and for the subpopulation with significant iMM changes.

As a result, the median iPE for the whole population of neurons went down as well, from 0.04 [−0.22, 0.26] to −0.06 [−0.35, 0.22] after dopamine injection (p = 0.003; Figure 36C, all dots). Conversely, the median iRS did not undergo any significant changes (from 0.53 [0.33, 0.72] to 0.51 [0.25, 0.71]; p = 0.253; Figure 36D, all dots). In fact, there is a positive correlation between the changes found in the iMM and those in the iPE (Figure 37A), whereas changes in the iRS do not correlate with those in the iMM (Figure 37B). These results imply that dopaminergic input to the IC cortices specifically modulates PE signaling.

V.- DISCUSSION

The results that provide the foundation for my thesis have been achieved through the application of 3 extracellular recording protocols. Protocol 1 (see Section III.4.a) consisted of microiontophoretic releases of dopamine or eticlopride in the IC of anaesthetized rats under auditory oddball stimulation (Figure 17A), in order to investigate the involvement of D_2-like dopaminergic receptors in the appearance of early signs of auditory novelty perception in the midbrain at cellular level. Protocol 2 (see Section III.4.b) controlled the oddball paradigm by using the many-standards and cascade sequences (Figure 17B) in anaesthetized rats and awake mice, in order to create a yardstick that allowed to dissociate repetition effects such as suppression of the STD response from possible PE signaling activity within the DEV response (Figure 17C). This could confirm the Expectation Hypothesis (see Section I.3.d) over the Adaptation Hypothesis (see Section I.2.b) and pinned down the anatomical origin of auditory PP in the IC (Figure 35). Finally, Protocol 3 (see Section III.4.c) combined both of the previous protocols in order to test how dopamine modulates PE signaling in the ICx. Thorough data analyses have confirmed in several manners that the PP hierarchy within the auditory system finds its anatomical origin in the midbrain. Furthermore, dopaminergic input to the ICx substantially modulate this early PE signaling (Figure 37). In this block, I will take the aforementioned results and integrate them into the wider context provided by the last half century of neuroscientific literature about auditory novelty perception and dopaminergic function, in order to endow this thesis with a greater scope and richer significance.

V.1.- The IC implements the first level of hierarchical PP in the auditory system

The anatomical origin of auditory novelty perception has traditionally been a rather controversial topic. Probability-biased processing has been oftentimes considered too sophisticated for subcortical nuclei, although signs of selective neuronal habituation to repetitive tones have been reported in the auditory midbrain of animal models for many decades (Malmierca, Carbajal & Escera, 2019). One pioneering study predating the discovery of the MMN described ‘novelty neurons’ in the auditory midbrain of lake frogs, proposing that these signs of novelty perception were generated by multipolar neurons located in the nucleus magnocellularis of the torus semicircularis (Bibikov, 1977). Many years later, another study

found early signs of novelty perception in the gerbil IC, also implicitly assuming that those neuronal responses were generated in situ (Malone & Semple, 2001).

Unfortunately, those pioneering studies were overlooked and their conclusions overwritten when a study recorded neuronal mismatch signals from the primary AC of the cat in response to the oddball paradigm (Ulanovsky et al. 2003). This seminal work was the first to offer compelling evidence suggesting that SSA constituted the neuronal correlate of the MMN, capturing great scientific attention from both human (May et al., 2015; May & Tiitinen, 2004) and animal research (Fishman & Steinschneider, 2012; Jääskeläinen et al., 2004). But this study did not find any significant traces of SSA in the MGB, and given that the anatomical sources of the human MMN had been firmly pinned down to the cortex (see Section I.2.a), the authors concluded that SSA was a purely cortical mechanism. Such conclusion enjoyed wide acceptance, leaving an overarching and enduring impression in the literature for years to come. At this moment in time, the idea of any form of probability-biased processing within subcortical nuclei seemed far-fetched and difficult to accept for most scientist working on the topic of novelty perception, whether physiologists, psychologists or physicists.

One of the main drivers of our research group during the last 15 years has been to disprove the myth that the mechanisms behind novelty perception are confined within the limits of the cerebral cortex. Many studies from our lab (Ayala et al., 2013, 2015; Ayala & Malmierca, 2015, 2018; Duque et al., 2012; Duque & Malmierca, 2015; Malmierca et al., 2009; Parras et al., 2017; Pérez-González et al., 2012, 2005; Pérez-González & Malmierca, 2012; Valdés-Baizabal et al., 2017) and other research groups (Gao et al., 2014; Harpaz et al., 2021; Herrmann et al., 2015; Lumani & Zhang, 2010; Netser et al., 2011; Patel et al., 2012; Reches & Gutfreund, 2008; Shen et al., 2015; Thomas et al., 2012; Zhao et al., 2011) undeniably confirmed that neuronal mismatch responses, regarded as SSA at the time, emerged from the auditory midbrain across several species. However, the corticocentric approach to understanding novelty perception was not completely abandoned at first. In order to accommodate the growing evidence in support a direct subcortical contribution to novelty perception, it was proposed that SSA had a cortical origin, but was then passed down to the midbrain (Nelken & Ulanovsky, 2007). Indeed, one study from our lab could confirm that all IC neurons exhibiting significantly positive CSI values received corticocollicular projections (Ayala et al., 2015), so there was solid ground to think of a top-down generation.

Nevertheless, it is not possible to determine the prime anatomical source of SSA just by investigating connectivity. In order to properly address the question, our lab resourced to a cooling technique to perform reversible deactivations of the AC while recording oddball-evoked responses from the rat IC (Anderson & Malmierca, 2013). The AC proved to modulate the response of IC neurons in a gain-control manner (Malmierca et al., 2015), i.e., increasing the contrast between STD and DEV responses by affecting both proportionally. But the results also demonstrated that the AC was not generating the SSA recorded in the auditory midbrain, inasmuch as it persisted after cortical deactivation (Malmierca et al., 2015). Remarkable alterations were observed in many other response properties of the subcortical neurons during cortical deactivation, such as their FRA, spontaneous activity, and first spike latencies. However, the overall strength and dynamics of subcortical SSA were mostly unaffected by the deactivation of the AC. Only about half of the IC neurons exhibiting SSA underwent significant changes in their CSI values. This confirms a prominent cortical modulation indeed, but it also demonstrates that signs of novelty perception emerges in the midbrain rather independently from corticocollicular input. As a matter of fact, IC neurons exhibiting close to absolute SSA levels (i.e., CSI > 0.8) remained mostly unaffected after the AC was deactivated. Even the partially-adapting IC neurons that underwent CSI reductions did not lose SSA completely (Anderson & Malmierca, 2013). Given that cortical deactivation does not efface SSA from the IC, the AC could not be the origin of auditory novelty perception. It would be far more plausible that the SSA present in the AC were inherited from subcortical auditory nuclei than viceversa. Nevertheless, the possibility of SSA being generated de novo at the intrinsic microcircuitry of each station rather independently, and then undergoing an accumulative effect along the ascending auditory pathway, cannot be ruled out either. In any case, inasmuch as no other auditory nuclei lower than the midbrain manifests SSA (Ayala et al., 2013), the IC is the first the first nuclei within the ascending auditory pathway to generate mismatch responses, thus being the most likely candidate for the neuroanatomical origin of novelty perception. The current work takes our previous knowledge to a decisive step further, demonstrating that mismatch responses observed in the auditory midbrain are not the result of sheer SSA, but rather the physiological footprint of a generative model forging auditory expectations, as described by the PP framework.

V.1.a.- Two hierarchical levels of processing within the IC

My results provide solid evidence to support that the IC hosts the first level of a sophisticated PP hierarchy within the auditory system. Whereas the Adaptation Hypothesis could explain the responses of CNIC neurons, it failed to account for the oddball-evoked activity of their nonlemniscal counterparts. CNIC neurons tended to show similar or even more robust responses to the NRCs, both many-standards and cascade sequences, than to the DEV of the oddball paradigm (Figures 28A, 29A and C, 31A, Table 1). Therefore, I cannot discard that the decrease in DEV responsiveness is in fact due to cross-frequency adaptation induced by the repetitive STD (Mill et al., 2011; Taaseh et al., 2011), as proposed by the Adaptation Hypothesis (Figure 17D, see Section I.2.b). On the other hand, ICx neurons tended to exhibit stronger DEV responses than to any other condition (Figures 28B, 29B and D, 31B, Table 1), thereby confirming the Expectation Hypothesis proposed by the PP framework (Figure 17E, see Section I.3.d). The Expectation Hypothesis argues that DEV responses are enhanced because neurons are signaling precision-weighted PEs to higher levels in the PP hierarchy (Figures 18 and 20), thus deeming the term 'SSA' not the best suited for describing the probability-biased processing performed by ICx neurons (Figure 12). Neuronal mismatch responses containing PE components were first observed under anesthesia (Figures 28B, 29B and D, 31B, Table 1), implying that PE signaling in the ICx does not fully depend on consciousness or the state of awareness. Then, PE signaling was also confirmed in awake animal models (Figure 34), where the genuine PE component found within the DEV-evoked spiking activity of ICx neurons was even larger than in the anesthetized preparations (Figure 35). Furthermore, the obtained data indicate that untuned ICx neurons displaying disorganized FRAs are the prime early signalers of PE in the auditory system (Figure 7D). Thus, the ICx is the first auditory nuclei to generate PE signals in the ascending auditory pathway.

ICx neurons also exhibit much more intense repetition suppression than CNIC neurons, most likely because the ICx functions under heavier inhibitory influence resulting from top-down predictive activity (Figure 20; see Section I.3.d). Expectations could be conveyed down from AC via direct corticocollicular input that innervates local inhibitory circuits, as suggested by previous studies from our lab on the connectivity of SSA neurons in the auditory midbrain (Ayala et al., 2015) and their functioning during cortical deactivation (Anderson & Malmierca, 2013). In fact, since anesthesia affects cortical processing more than subcortical, the partial reduction of PE signaling that ICx neurons show under anesthesia may be due to lessened top-

down influences from the AC. In addition, the prime PE signalers of the ICx exhibit disorganized FRAs (Figure 7D), which are probably the result of inhibitory action over the receptive field of the neuron (Le Beau et al., 2001). Such inhibitory action could be the result of top-down predictive influences from the AC imposed on the untuned ICx neurons via direct corticocollicular projections (Ayala et al., 2015). Nevertheless, the reported persistence of neuronal mismatch responses in the ICx after deactivating AC (Anderson & Malmierca, 2013) suggests that at least part of PE signaling activity in the auditory midbrain could be generated de novo in a local PP network contained within the layers of the ICx, akin to the PP networks proposed for the cerebral cortex (Figure 19; see Section I.3.c). A proper way to confirm empirically that PE signals are indeed generated in situ by the own predictive activity of ICx neurons would be to combine Protocol 2 (see Section III.4.b) with reversible deactivations of the AC. In case the ICx were confirmed to be capable of generating PE signals without any top-down influence from the AC, it would also be more plausible that the origin of the mild mismatch responses observed within the CNIC were indeed due to the predictive activity of the ICx neurons inducing repetition suppression on the STD responses of their lemniscal counterparts, albeit this possibility could not be empirically confirmed with the current methodology. In any case, whether the prediction has a cortical origin or it is generated in situ within the IC circuitry, what my results confirm is that the ICx hosts the earliest PE signalers in the ascending auditory pathway. Since the PP framework expected the first auditory PE signalers to be located in the AC, the discovery of PE signals in the midbrain represents a breakthrough in our understanding of PP implementation within the auditory system.

Moving up to the mesoscopic scale of observations (Figure 31C and D), one previous LFP study in 13 rats had found mismatch potentials between 18 ms and 43 ms after sound onset in the ICx (Patel et al., 2012). My data shows that mismatch potentials emerge in the whole IC as soon as auditory input reached the midbrain, starting around the first 4–6 ms and finishing passed 150 ms, and thereby containing the time window at which spiking activity yielded significantly positive iMM values (Figure 31 E and F). Such an early onset can also comfortably accommodate the early mismatch responses identified in the rodent ABR (Figure 14), where differences between DEV and STD were maximal between 8 ms and 10 ms after sound onset (Duque et al., 2018). One study using blood-oxygen-level-dependent fMRI also showed that auditory mismatch signals can be detected in the IC tissue just few seconds after sound onset (Gao et al., 2014). In regards to PE signaling activity, PE-LFPs were identified in the ICx between 45 ms and 60 ms after stimulus onset, perfectly fitting in the time window at

which the spiking activity shows its highest iPE values (Figure 31G and H). To my best knowledge, there are no reports of PE signals within the rodent ABR as of date. Nevertheless, previous FFR (Slabu et al., 2012) and fMRI (Cacciaglia et al., 2015) studies using the many-standards NRC have found traces of PE signaling from the human auditory midbrain. Therefore, my results allow to connect evidence of mibrain-level mismatch signals from animal models at the microscopic —spiking activity of single neurons—, mesoscopic —LFPs— and macroscopic —ABR— scales of observation, providing valuable cellular insight that is not possible to obtain in human participants.

V.1.b.- Midbrain PE signals report on surprising acoustic changes

Genuine PE signals within spiking activity were considerably more evident at lower sound intensities (Figure 32), and also when the deviant tone was pitched higher than redundant stimuli (Figure 33A). This suggests that the ICx could be implementing some sort of gain compensation to endow subtle but rare and informative auditory events with greater salience. Regarding the sound intensity, modeling work suggests that neurons are expected to be maximally sensitive to change for stimulus ranges where the firing rate of the neuron is below saturation (Abbott et al., 1997), which has been contrasted empirically by a previous SSA study in the IC (Duque et al., 2012). As intensity strengthens, auditory neurons will be driven closer to their saturation level, thereby clipping their dynamic range and exhausting their capacity to increase their firing to signal an additional PE for a deviant feature of a loud sound. This would explain why the iPE is very sensitive to loudness, whereas the iRS seems to be barely affected by intensity changes. Regarding the sound frequency, it could be a purely specific phenomenon, as the auditory system of the rodents may be primed to process high-frequency sounds like the ultrasonic vocalizations that these species use for communication. Notwithstanding, there is also room for a less specific explanation, since asymmetries in the direction of frequency-change sensitivity (ascending vs descending) have been found at the macroscopic level in both animal (Harms et al., 2014) and human MMN studies (Peter et al., 2010). It could be argued that a preference for higher pitches might help to define figure-ground relationships between auditory objects more effectively. Lower frequencies can travel longer distances across different mediums, better overcoming obstacles in their way to our ears. These auditory inputs tend to report on distant events that are often unrelated and useless to us, and could thereby be more prone to be processed as a background noise. Conversely, auditory processing of higher frequencies could be physiologically facilitated, as their difficulty to travel

long distances and their propensity to be blocked by changes of the transmission medium imply that they usually convey auditory input generated in our near surroundings, thereby being potentially more informative and relatable to our states and goals. Thus, an ascending oddball paradigm could be readily interpreted as a 'figure' deviant sound emerging from a 'ground' of standard noise, whereas the deviant tone within the descending oddball paradigm does not benefit from any facilitated processing. The resulting early mechanism of automatized relevance assessment reliant on intensity and pitch is likely to contribute greatly to auditory perception under challenging conditions, e.g., when a relatively loud background noise could otherwise mask a potentially informative deviant sound, as described for the visual system (Hupé et al., 1998). This is especially true in situations where efficient and facilitated auditory discrimination might be critical for survival, as it may help to swiftly detect potential threads based on subtle auditory cues, such as the feeblest snap of a little branch caused by the footfall of a stalking predator amidst the relatively louder jungle noise. In this particular example, note that the saliency of the soft predator cue would be enhanced directly by the facilitated PE signal, but also indirectly, as the neural activity evoked by the predictable background noise will undergo expectation suppression. The resulting contrast between the unexpected, quieter, higher-pitched 'figure' and the repetitive, louder, lower-pitched 'ground' allows the auditory system to form a clear auditory percept of the snap that would be impossible to attain otherwise. According to the presented data, this PE gain mechanism reliant on sound intensity and pitch seems to be exclusively at play within the auditory midbrain (Figure 33). Therefore, the main distinctive characteristic of how the neural circuitry of the ICx implements PP is that PE signaling is rather focused on reporting on unexpected changes regarding the physical features of the sound.

V.1.c.- The IC as the origin of PP in the nonlemniscal pathway

PP capabilities first manifest in the cortical circuitry of the IC most likely due to its unique position and neuroanatomical characteristics within the auditory system (Figures 4 and 8). All ascending auditory pathways converge in the IC before innervating the MGB and the AC, placing the IC as an almost obligatory relay station for auditory information (see Section I.1.d). Besides receiving input from the lower auditory brainstem nuclei, cortical regions and even non-auditory structures also send excitatory, inhibitory and neuromodulatory projections to the IC (Figure 4). This rich connectivity, combined with a neuroarchitecture that differentiates a primary core —i.e., the CNIC— and a peripheral higher-order processor

arranged in a 3-layer structure —i.e., the ICx— (Figures 5 and 6), could provide the IC with all the necessary elements to implement PP within its local network (Figures 19 and 20). Hence, the ICx could be hosting the first processing levels of the hierarchical generative model for audition (Figure 18), in a functional role analogous to that of the primary visual cortex in the case of vision (King & Nelken, 2009; Rao & Ballard, 1999). But most importantly, the IC gives rise to 2 parallel lines of auditory processing (see Section I.1.e). The lemniscal pathway, of rather primary nature, emerges from the CNIC, whereas the the nonlemniscal pathway originates in the ICx (Figure 8). The PP framework posits that PP unfolds hierarchically, so the iPE should grow as the DEV-evoked PE flows up in the ascending auditory pathway (Figure 17E; Carbajal & Malmierca, 2018a). Combining the IC data from this thesis with data from studies that applied the same Protocol 2 (see Section III.4.b) in the MGB, the AC and the PFC, my colleagues and I have been able to describe how the PE signals that first emerge in the ICx then evolve as they are conveyed bottom-up through both lemniscal and nonlemniscal lines of the ascending auditory pathway (Parras et al., 2017) and beyond (Casado-Román, Carbajal et al., 2020).

Beginning with the lemniscal divisions of the subcortical auditory nuclei, we found that the iRS values comfortably account for the whole mismatch response (Figure 38; Parras et al., 2017), in accordance with the Adaptation Hypothesis (Figure 17D). Besides, the iMM is weaker in the CNIC and the MGV than in their nonlemniscal counterparts. Therefore, the CNIC and the MGV may be the prime providers of 'raw' input for their nonlemniscal analogues and for the AC. In plain words, the floor of the hierarchical generative model in charge of perceiving novelty may lay in the subcortical lemniscal pathway that begins in the CNIC. The first level of the hierarchical generative model may be hosted right at the beginning of the nonlemniscal pathway, as significantly positive iPE values first appear in the ICx and increase mildly at the MGD and MGM (Figure 38). The functional heterogeneity of the neuronal mismatch responses at subcortical nuclei is very remarkable. Whereas AC neurons tend to show rather homogeneous and prominent mismatch responses, the IC neuronal data presented here runs the gamut from no mismatch sensitivity (iMM ≈ 0) to absolute ones (iMM ≈ 1; Figure 29C and D, in magenta). Some ICx neurons show an iMM that is similar to their iRS, which indicates that those neurons are fundamentally receiving a top-down expectation of repetition (e.g., Figures 28A and 34A). But other ICx neurons exhibit an iRS considerably lower than their iMM (e.g., Figures 28B and 34B), which implies that they might be carrying out other predictive processes, such as adjustments of the expected precision or even top-down predictive

influences more complex than repetition expectation (Carbajal & Malmierca, 2018a, 2020). In fact, previous studies show that GABAergic (Ayala & Malmierca, 2018; Duque et al., 2014; Pérez-González et al., 2012), cholinergic (Ayala & Malmierca, 2015) and endocannabinoid (Valdés-Baizabal et al., 2017) manipulation of these IC neurons modulate their mismatch responses, which hints at processes of precision adjustment of PE signals, as I will discuss in the next section. The great functional diversity of subcortical auditory neurons suggests they act as differentiated processing nodes, presumably performing distinct roles within the lower levels of the hierarchical generative model that enables auditory novelty perception.

Conversely, at cortical level, all cortical neurons have proven to exhibit strongly positive iMM and iPE values (Casado-Román, Carbajal, et al., 2020; Parras et al., 2017). The primary regions of the AC are the first and only lemniscal division of the auditory pathway where the iMM cannot be fully accounted for by the Adaptation Hypothesis (Figure 17E). The iPE values are particularly prominent in the late component of the neuronal mismatch response (I.-W. Chen et al., 2015; Parras et al., 2017). Nevertheless, the swiftest, largest and most enduring iPE values are observed in the nonprimary regions of AC, persistent even beyond 200 ms (Parras et al., 2017). Hence, the hierarchical disposition between lemniscal and nonlemniscal processing that emerges in the auditory midbrain extends to the cortex (Figure 38), as reported in rodents (Parras et al., 2017) and birds (Gill et al., 2008). The iPE values registered in the spiking activity of the AC correlated in time and strength with the cortical PE-LFPs, which also confirmed a hierarchical distribution of iPE between primary and nonprimary AC (Parras et al., 2017). Thus, PE signaling strength seem to be hierarchically distributed along two axes in the auditory system beginning in the IC: from lemniscal towards nonlemniscal, and from subcortical towards cortical (Figure 38; Carbajal & Malmierca, 2018a; Parras et al., 2017). Furthermore, we have proven that this hierarchical progression of auditory processing continues in the PFC (Casado-Román, Carbajal, et al., 2020), finally bridging the gap between auditory PE signaling observed using extracellular recording in animal models and the frontotemporal network that generates the human MMN (see Section I.2.a). In fact, auditory responses in the PFC were similar to the NRC and the STD, and thereby all the neuronal mismatch responses could be fully regarded as genuine PE signaling. As auditory input flows up the processing hierarchy, the explanatory capacity of the Adaptation Hypothesis dwindles to the point of not being able to account for the slightest portion of the observed neuronal mismatch responses (Figure 38), which is even more true when animals are awake (Parras et al., 2017). On the other hand, the Expectation Hypothesis can effectively explain all neuronal

mismatch responses, from the cortex down to the auditory midbrain (Casado-Román, Carbajal, et al., 2020; Parras et al., 2017), and can easily account for the PE signaling increase observed in awake animals in turns of gain produced by the precision-weighting effects afforded by attention (Moran et al., 2013).

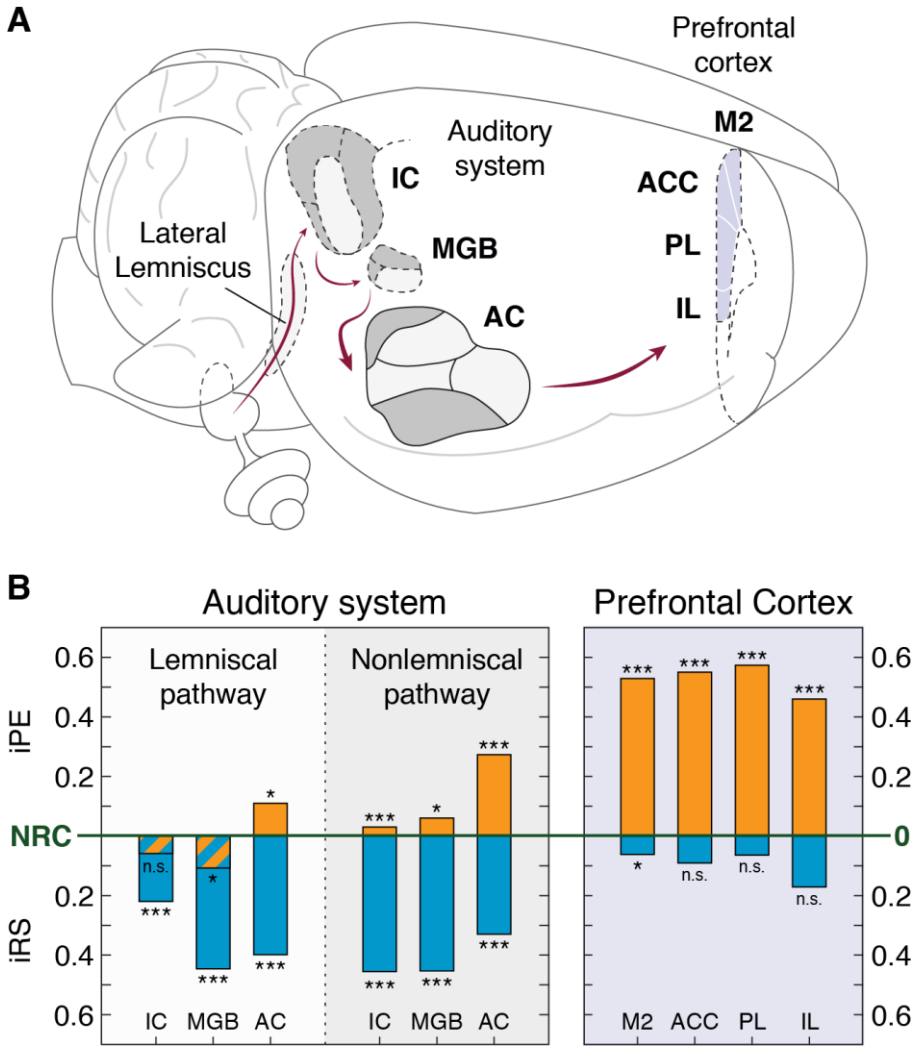

Figure 38. i**PE evolution throughout the anesthetized rat brain**. **A.** Schematic of the auditory system and the medial PFC of a rat brain. Maroon arrows describe the main ascending flow of auditory input. Anatomical divisions comprised within the lemniscal pathway of the auditory system are colored in light grey, whereas divisions comprised within the nonlemniscal pathway are highlighted in dark grey. The 4 divisions of the medial PFC are colored in light violet. **B.** Median indices of iPE (orange) and iRS (cyan), represented with respect to the baseline (green) set by the NRC. Thereby, iPE is upwards-positive while iRS is downwards-positive. Asterisks denote statistical significance of iPE against zero median (n.s. = non-significant, * $p < 0.05$, *** $p < 0.001$). Adapted from Casado-Román, Carbajal, et al. (2020).

In conclusion, contrary to previous belief, the IC is a key player in identifying auditory novelty, perfectly capable of carrying out probability-biases processing. As this work proves, the IC performs PP and signals PEs reporting on unexpected physical features of the auditory input. Furthermore, the auditory midbrain constitutes the neuroanatomical origin of a complex recurrent neural network, extending beyond the limits of the classic auditory pathway, that exchanges top-down predictions and bottom-up PEs in order to develop and update a hierarchical generative model of the auditory scene.

V.2.- Dopaminergic input to the IC configures early auditory PP

My results show that dopamine application causes mismatch responses of ICx neurons to lessen their magnitude by almost 20% on average (Figures 23A and 36B) because DEV responses underwent reductions of up to 30% (Figures 23B and C, 36A and C), while neither STD nor NRC responses were generally affected by dopaminergic manipulation (Figures 23B and D, 36A and D). Since the response to unexpected stimuli dropped while the response to the expected stimuli remained stable, dopamine ejected in the ICx seems to modulate exclusively PE signaling (Figure 37). The net reduction of DEV responses under dopamine influence is unique as compared with the effects of other neurotransmitters and neuromodulators on IC neurons. GABAergic and glutamatergic manipulations alter the general excitability of IC neurons, thereby exerting symmetrical effects on STD and DEV responses, which result in a gain control of the CSI value (Ayala et al., 2016; Ayala & Malmierca, 2018; Pérez-González et al., 2012). Conversely, cholinergic and cannabinoid manipulation yield asymmetrical effects that mostly affect STD responses (Ayala & Malmierca, 2015; Valdés-Baizabal et al., 2017). Activation of M1 muscarinic receptors and CB1 cannabinoid receptors tended to reduce the median CSI by increasing responsiveness to repetitive stimuli. Dopamine application can also yield asymmetrical effects, but in contrast with the aforementioned cases, the activation of dopaminergic receptors tends to reduce mismatch responses by decreasing responsiveness to surprising stimuli (Figure 36A). Moreover, when the D_2-like receptors antagonist was applied, some ICx neurons manifested significant changes in their mismatch responses (Figure 26 and 25A, green circles). These individual changes imply that dopamine is being endogenously released in response to the sound within some parts of the ICx. Thus, dopamine modulates mismatch responses of ICx neurons mainly by decreasing their responsiveness to unexpected auditory events. Furthermore, my data indicates that such dopamine-induced reduction of PE signaling from the ICx is mediated by D_2-like receptors.

V.2.a.- Influence of the intrinsic and synaptic properties of IC neurons

Besides the net population effects described above, dopaminergic effects were heterogeneous across the recorded neurons of the ICx, in the vein of previous reports (Gittelman et al., 2013; Hoyt et al., 2019). Most units underwent significant response changes, although approximately ¼ of the ICx sample remained unaltered by dopaminergic manipulation (Figures 23A, 25A and 36, grey circles). It is possible that those unaffected neurons did not express D_2-like receptors, or not enough to yield significant changes on their mismatch response. The sequential application of dopamine and eticlopride to 5 units of our sample revealed individual antagonistic effects, such that whether the activation of D_2-like receptors by dopamine increased the CSI, their blockade with eticlopride decreased the CSI (Figure 27A), and viceversa (Figure 27B). Such consistency implies that the distinct intrinsic properties and synaptic configuration of each ICx neuron are behind the heterogeneity of dopaminergic effects in our sample, as detailed in the following.

D_2-like receptors are coupled to G proteins that regulate the activity of a variety of voltage-gated ion channels, which in turn can increase or decrease neuronal excitability under dopaminergic influence depending on the particular repertoire of expressed on each IC neuron (Neve et al., 2004). D_2-like receptors coupled to Gi/o proteins can both increase potassium currents and decrease calcium currents via βγ subunit complex, thereby reducing excitability in most brain areas (Neve et al., 2004). The opening probability of calcium channels can also diminish by the activation of D_2-like receptors coupled to Gq proteins (Neve et al., 2004). D_2-like receptor activation influences sodium channels in more heterogeneous ways, augmenting or reducing sodium channels depending on the receptor subtypes expressed on the neuronal membrane (Neve et al., 2004). Furthermore, D_2-like receptor activation can also reduce NMDA synaptic transmission, decreasing the firing rate (Neve et al., 2004). In addition, neurons in the ICx express hyperpolarization-activated cyclic nucleotide-gated channels (Ahuja & Wu, 2007; Koch et al., 2004), which can be modulated by dopamine and yield mixed effects on neuronal excitability (He et al., 2014). Hence, the intrinsic properties of each neuron can explain part of the heterogeneity in the ICx sample. Whether increasing or decreasing the neuronal excitability with dopamine, the intrinsic mechanisms will symmetrically affect both STD and DEV responses, yielding gain effects on neuronal mismatch response. However, given that my data shows asymmetrical dopaminergic effects on STD and DEV responses in the same neuron, intrinsic properties alone cannot account for all the observed effects.

Dopamine and eticlopride may also interact with D_2-like receptors expressed in a presynaptic IC neuron (Gittelman et al., 2013). Both glutamatergic and GABAergic projections converge onto single IC neurons (Ito & Malmierca, 2018; Le Beau et al., 2001; Malmierca, 2015), which may also receive dopaminergic inputs from the thalamic SPF (Batton et al., 2018; Gittelman et al., 2013; Hurd et al., 2001; Nevue, Felix, et al., 2016; Weiner et al., 1991). However, the exact location and neuronal types where D_2-like receptors are expressed in the ICx is currently unknown, so the complex interactions leading to changes in the balance between of excitatory and inhibitory input are difficult to track. Speculatively, dopamine could activate D_2-like receptors expressed in presynaptic glutamatergic neurons, reducing glutamatergic input and thereby the firing rate of the recorded neuron, as previously described in striatal medium spiny neurons (Bamford et al., 2004; Calabresi et al., 1993; Higley & Sabatini, 2010). Another possibility demonstrated in the ventral tegmental area would be that dopamine may activate D_2-like receptors on GABAergic presynaptic neurons, decreasing their GABA release and in turn increasing the firing rate of the recorded neuron (Michaeli & Yaka, 2010). Hence, microiontophoretic applications of dopamine or eticlopride in the neuronal microdomain could alter the balance of excitatory and inhibitory input of the recorded neuron, as observed in other nuclei (Bamford et al., 2004; Calabresi et al., 1993; Higley & Sabatini, 2010; Michaeli & Yaka, 2010). This would not only affect the general excitability of the recorded ICx neuron, but it also has the potential to affect STD and DEV responses asymmetrically by modulating presynaptic STD- or DEV-related input independently (Duque et al., 2012). Given that DEV and STD can undergo dissimilar dopaminergic effects in the same unit (Figures 23C and D, 25C and D; for individual examples, see Figures 24A and 26), the synaptic properties of each ICx neuron must crucially determine the effect of dopaminergic modulation on the neuronal mismatch response.

V.2.b.- A new perspective on dopaminergic function

After discussing the effects of dopaminergic manipulation at both population and neuronal levels, as well as the pharmacological mechanisms that could be involved, one could not but wonder about what sort of natural modulatory process might be mimicked by these microiontophoretic applications of exogenous dopamine. What all these dopamine-induced changes in the neuronal response of the ICx might mean from a functional perspective?

Dopamine is commonly regarded as the modulatory neurotransmitter underlying phenomenological experiences such as pleasure and joy. This 'hedonic' impression derives from classic reinforcement learning approaches emphasizing the role of dopamine in the anticipation and seeking of rewarding outcomes (Fiorillo et al., 2003; Mirenowicz & Schultz, 1996; Schultz et al., 1997). Indeed, mounting empirical evidence supports that dopamine regulates movement, motivation and learning by tracking the violations of our reward expectations, which are encoded as reward PEs (Schultz, 1998, 2007, 2016b). Hence, according to this classic proposal from the reinforcement learning framework, there are 2 types of PE signals. On the one hand, there are sensory PEs, such as the auditory PEs featuring prominently in the previous section, which report the surprise of unexpected sensory inputs in absolute magnitudes. On the other hand, there are reward PEs, characteristic of the dopaminergic system, which indicate whether outcomes are better or worse than expected, thereby resulting in positively and negatively signed PEs (Den Ouden et al., 2012). As a rule of thumb, dopaminergic neurons would report positive PEs by increasing their phasic firing of action potentials, and negative PEs by reducing their tonic discharge rates (Schultz, 1998, 2007, 2016b). Hence, these dopaminergic neurons seem to signal a motivational ambivalence that guides adaptative motor, learning and decision-making processes.

According to the reinforcement learning framework, the microiontophoretic injections of dopamine might be mimicking some sort of reinforcing signal, a positive reward PE, which in natural conditions could be conveyed via dopaminergic projections from the thalamic SPF to the ICx (Batton et al., 2018; Gittelman et al., 2013; Hurd et al., 2001; Nevue, Felix, et al., 2016; Weiner et al., 1991). Speculatively, such dopaminergic input could aim to induce long-term potentiation on ICx neurons to build lasting associations between acoustic cues and rewarding outcomes, thereby contributing to establish reward expectations (Hosomi et al., 1995; Y. Zhang & Wu, 2000). However, I fail to see why these artificially induced positive reward PE would mitigate the transmission of sensory PEs from the ICx, as evidenced by the reduced iPE provoked by dopamine application. Moreover, some experimental evidence defies this classic understanding of dopaminergic function. Aversive outcomes and cues which predict them can elicit dopaminergic activity (Bromberg-Martin et al., 2010; Matsumoto & Hikosaka, 2009; Matsumoto & Takada, 2013; Young et al., 1993; Zweifel et al., 2011), as well as events where the reward PE should theoretically be zero, such as unexpected or surprising stimuli without any hedonic value (Bromberg-Martin et al., 2010; Comoli et al., 2003; Dommett et al., 2005; Horvitz, 2000; Ljungberg et al., 1992; Sadacca et al., 2016; Strecker &

Jacobs, 1985). These dopaminergic responses seem to report sensory stimuli which may have behavioral relevance and should trigger an appropriate coordinated response, thus encoding perceptual salience without any positive or negative value. The existence of signed and unsigned PEs is not mutually exclusive, and nowadays there is relative consensus that dopamine participates in the attribution of physical and surprise salience to sensory stimuli (Diederen & Fletcher, 2020). Some authors suggest that novel and physically salient stimuli might be inherently rewarding, as they provide new information which could be of value for adaptive behavior (Daw et al., 2002; Reed et al., 1996). Other works from the reinforcement learning framework postulate a dual dopaminergic signaling which respectively reports surprise and hedonic value in parallel (Fiorillo, 2013; Schultz, 2016a).

In a different vein, the PP framework advocates for a more integrative account of dopaminergic function, not specifically bound to reward processing (Friston et al., 2012, 2015). Since we cannot directly access the 'true' external world, but only its impression in our sensorium, the brain must *infer* the cause of those sensations (see Section I.3). As previously explained, the brain generates expectations about the 'hidden' states of the world by means of a hierarchical generative model, where higher neural populations try to explain away —i.e., predict and inhibit— input from lower neural populations, and the resulting PE is used to update prior beliefs —i.e., learning—. At each processing level, excitatory neurons receive excitatory input conveying bottom-up sensory evidence, as well as inhibitory input conveying top-down expectations. When these two inputs are congruent, their postsynaptic potentials cancel out; but when they are incongruent, a PE is generated to report the mismatch (Bastos et al., 2012; Friston, 2005, 2010; Friston & Kiebel, 2009b; Keller & Mrsic-Flogel, 2018). Hence, this unsigned PE accounts for both perception and learning, smoothly accommodating dopaminergic responses elicited by surprise. Behavior is optimal, not when reward —i.e., positive PE— is maximized, but when surprise —i.e., unsigned PE— is minimized, as this keeps the organism from potentially harmful interactions with the environment (Friston et al., 2012, 2015). Minimal PE is pursued via *perceptual inference*, i.e., improving the internal model of the world to better explain away incoming sensory input, and via *active inference*, i.e., changing sensory input by engaging in actions with predictable outcomes (Friston et al., 2015, 2017; Parr & Friston, 2017). Classic reinforcement learning tasks may have confused dopaminergic responses with reward PEs because of the more generic role that dopamine plays in PE minimization. Cues predicting rewards minimize PE by resolving the uncertainty about

future outcomes, which is flagged by dopamine release (FitzGerald et al., 2015; Friston et al., 2012, 2015; Schwartenbeck et al., 2015).

Therefore, from the PP standpoint, there are only 2 sorts of things that need to be inferred about the world: the state of the world, and the uncertainty about that state (Friston et al., 2012). Beliefs about the hidden states of the world emerge from the hierarchical exchange of top-down predictions and bottom-up PEs, embodied in the synaptic activity of the nervous system (see Section I.3.a). But every inferential process entails a certain degree of uncertainty due to, e.g., our sensory limitations, ambiguity, noise or volatility in the probabilistic structure of the environment. Such uncertainty is accounted for in terms of posterior confidence or *expected precision* by means of the postsynaptic gain (see Section I.3.b). Synaptic messages are weighted according to their expected precision as they are passed along the processing hierarchy. When expected precision is high, PE signals are deemed reliable and receive postsynaptic amplification to strengthen its updating power. Conversely, when low precision is expected, PE signals undergo attenuation to prevent misrepresentations and the influence of prior beliefs becomes prominent. In plain words, the expected precision is the postsynaptic gain that scales PE to modulate its influence on higher processing levels, such that more is learned from precise PEs than from noisy and unreliable PEs (Friston & Kiebel, 2009b). Neuromodulators, such as dopamine, cannot directly excite or inhibit postsynaptic responses, but only weight the postsynaptic responses to other neurotransmitters, acting as a gain control mechanism (see Section I.3.c). Therefore, the only possible function of the dopaminergic system is to encode the expected precision (Friston et al., 2012, 2015), playing a role in both perceptual and active inference by conferring contextual flexibility to both sensory and motor processing.

Consequently, the PP framework spares the need of 2 distinct types of PE signaling —i.e., reward PEs versus sensory PEs— while more comfortably interpreting my data through the lens of a precision-weighting mechanism. According to this approach, by changing the levels of dopamine at a synaptic domain, I would be altering the gain of the sensory —PE— messages transmitted through there. Thereby, since microiontophoretic applications of dopamine tend to reduce the iPE of ICx neurons, natural dopamine release in the ICx could be signaling low expected precisions of the auditory PEs generated there. In other words, the role of dopaminergic input to the ICx could be to apply a net negative gain that dampens the forward propagation of early auditory PE signals. Such net inhibitory effect over sensory transmission

will especially affect DEV responses to the oddball paradigm, as the unexpected interruptions of an otherwise very regular train of stimuli will elicit the strongest PE signaling activity of all conditions tested in this study.

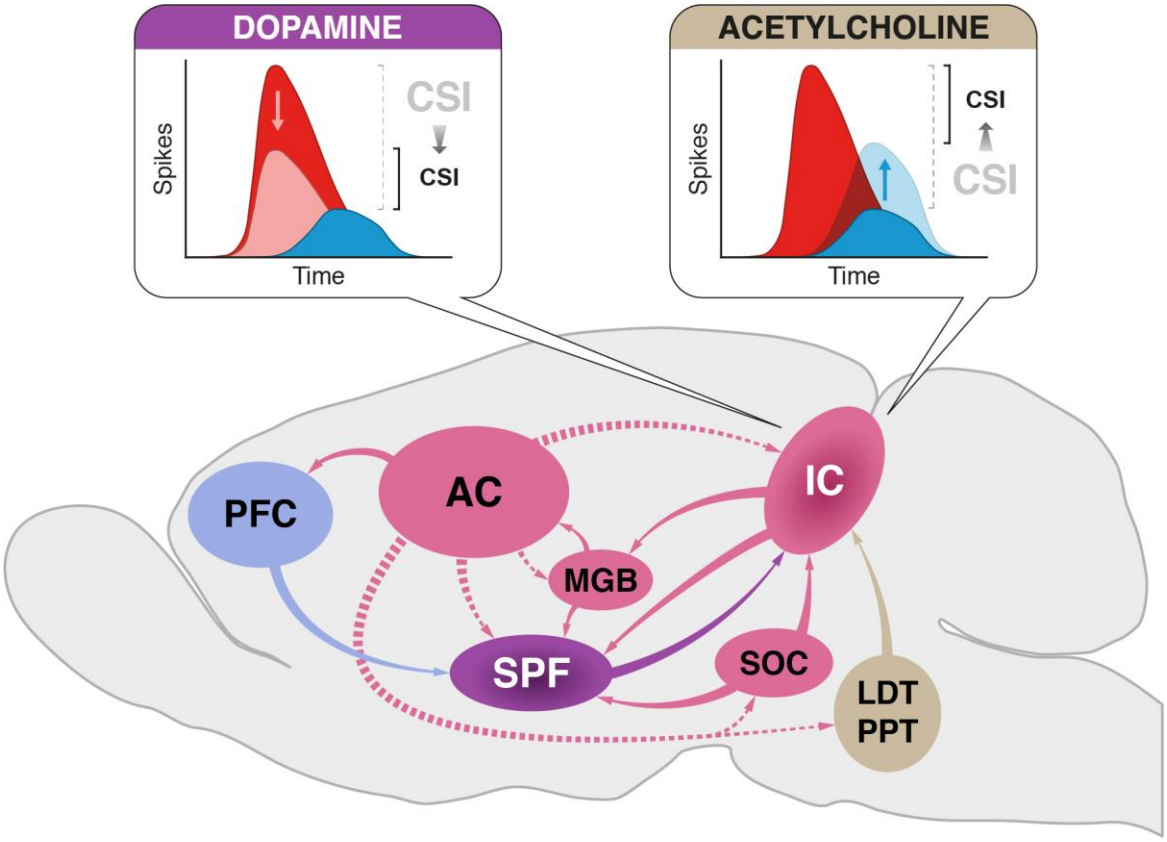

Figure 39. SPF auditory afferences. Schematic diagram of the main connections involved in the CSI modulation and PE precision-weighting in the IC. The auditory pathway (in pink) is composed of ascending (solid arrows) and descending connections (dashed arrows) between cortical and subcortical auditory structures. The hierarchical exchange of bottom-up PEs and top-down predictions postulated by the PP framework could be extended to subcortical auditory neurons by means of these feedback loops. The SPF (purple) receives input from main auditory nuclei (pink) and from the PFC (violet), integrating information from manifold hierarchical processing levels. Such connectivity could allow SPF dopaminergic neurons to estimate the volatility of the probabilistic structure of the auditory context. In turn, the SPF sends dopaminergic projections back to the IC to signal the expected precision of PE signaling at low processing levels. Dopamine release in the nonlemniscal IC reduces the postsynaptic responses to surprising stimuli (red) but has no effect on repetitive ones (blue), consequently reducing SSA indices. By contrast, cholinergic modulation from the LDT and PPT nuclei (brown) of the brainstem increases the responses to repetitive stimuli in the IC (Ayala & Malmierca, 2015). Note that the net effect of both dopamine and acetylcholine is the reduction of CSI, decreasing the relative saliency of surprising input through complementary means. Reproduced from Valdés-Baizabal, Carbajal, et al. (2020).

In natural conditions, such midbrain-level gating of the bottom-up flow of early PE signals could be shaped by SPF dopaminergic neurons projecting to the ICx (Batton et al., 2018; Nevue, Elde, et al., 2016; Yasui et al., 1992). Many auditory nuclei project to the SPF, such as the AC, the MGB, the IC and the SOC, providing the SPF with rich auditory information (Arnault & Roger, 1990; LeDoux et al., 1985; Wang et al., 2006; Yasui et al., 1992; Yasui, Kayahara, Nakano, et al., 1990). Even other centers that perform higher-order functions in the sensory processing and integration of auditory information send projections to the SPF, such as the PFC and the deep layers of the SC (Wang et al., 2006). And as explained in the preceding section, the PFC, the AC, the MGB and the IC are neural structures that implement hierarchical PP of auditory input (Figure 38). Therefore, it is reasonable to think that the dopaminergic activity of the SPF could be an integral component of the hierarchical generative model that allow us to hear efficiently, playing a key early role in the updating process of the internal representation of the auditory scene. The reciprocal connectivity of the SPF with many nuclei at multiple levels of the auditory pathway and beyond could provide the structural basis for an optimal encoding of expected precision, modulating via dopaminergic input the weight of PEs forwarded from the ICx (Figure 39). This dopaminergic neuromodulatory network would allow the auditory system to manage the integration of meaningful and reliable sensory evidence from a very early stage of processing, thereby further reassuring the fundamental implication of the auditory midbrain in enabling an efficient perceptual inference and learning of novel auditory information.

VI.- CONCLUSIONS

Despite being usually neglected by the rather corticocentric insights that oftentimes sway cognitive neuroscience literature, my results provide robust evidence of the direct and key involvement of the IC in the complex neurological network that implements PP for auditory perception. The conclusions of my thesis and their relevance for scientific advancement are the following:

1. The IC is the earliest station in the ascending auditory pathway that generates genuine PE signals, which are transmitted bottom-up via the nonlemniscal pathway.
2. The untuned neurons of the ICx are the prime PE signalers within the auditory midbrain.
3. The ICx generates PEs to signal unexpected physical changes in the sound, whereas PE signaling in hierarchically higher processing levels seem to regard more abstract factors.
4. The state of awareness influences PP in the auditory midbrain, inasmuch as wakefulness strengthens PE signaling most likely by enhancing the expected precision of ICx neurons.
5. Dopamine modulates midbrain PP via D_2-like receptors in heterogeneous manners, which are determined by the intrinsic properties and synaptic configuration of each ICx neuron.
6. The activation of D_2-like receptors in the ICx tends to reduce the net midbrain-level PE forwarding, acting as an early gain mechanism in the auditory system.
7. Dopamine release in the ICx encodes expected precision by adjusting the postsynaptic gain of auditory PE signals, thereby modulating their drive over higher-level processing stages.
8. The dopaminergic projections from the thalamic SPF to the ICx constitute the biological substrate of an early precision-weighting mechanism that regulates the bottom-up transmission of PE signals along the PP hierarchy within the auditory system.

VII.- SINOPSIS EN CASTELLANO

EL ORIGEN MESENCEFÁLICO DEL PROCESAMIENTO PREDICTIVO EN LA AUDICIÓN Y CÓMO LA DOPAMINA MODULA LA PERCEPCIÓN TEMPRANA DE LOS SONIDOS INESPERADOS

¿Por qué algunos sonidos nos sorprenden y atrapan nuestra percepción mientras que otros nos pasan desapercibidos? La neurociencia cognitiva moderna ha perseguido la respuesta a esta pregunta durante al menos medio siglo, abordando la cuestión desde una óptica predominantemente corticocéntrica. Tras 4 años de intenso análisis científico y diversas publicaciones en la materia (Carbajal & Malmierca, 2018a, 2020, 2018b; Casado-Román, Carbajal, et al., 2020; Malmierca, Carbajal & Escera, 2019; Parras et al., 2017; Pérez-González et al., 2020; Valdés-Baizabal, Carbajal, et al., 2020), esta tesis aspira a cambiar la visión establecida acerca de cómo el cerebro identifica la novedad en lo que oímos. Para ello, habremos de apartar el foco de la corteza cerebral para colocarlo sobre los núcleos subcorticales, cuya contribución es sistemáticamente subestimada. Concretamente, este trabajo explorará la función de los colículos inferiores (IC) del mesencéfalo, un par de protuberancias situada en la parte dorsal alta del tronco encefálico, cuyo rol ha sido tradicionalmente reducido a la de mero relé o centro organizador de reflejos. Además, esta tesis involucra a la dopamina en ese proceso que confiere la cualidad de 'sorprendente' a determinadas percepciones auditivas, lo cual contribuirá a expandir la interpretación clásica de la función dopaminérgica, siempre descrita en términos hedónicos de placer y recompensa. Todas estas aspiraciones serán sustanciadas bajo la noción neokantiana del procesamiento predictivo (Friston, 2005; Rao & Ballard, 1999), un marco teórico nacido de la teoría cibernética (Ashby, 1960) que entiende el cerebro como una máquina de Helmholtz (Dayan et al., 1995), movida por la necesidad de generar la representación más precisa posible del mundo exterior por medio de inferencia bayesiana (Clark, 2016; Friston et al., 2006; Hohwy, 2013).

VII.1.- INTRODUCCIÓN TEÓRICA

En cada momento de nuestras vidas, una infinidad de sucesos tienen lugar simultáneamente a nuestro alrededor. La ocurrencia de tales eventos genera una enorme cantidad de cambios físicos en nuestro entorno cercano, los cuales son captados maquinalmente por nuestros órganos sensoriales. Esas señales físicas son transducidas en impulsos electroquímicos operables por nuestro cerebro en un proceso denominado *sensación*. Pero, aparte de los efectos que la selección natural haya ejercido en la evolución de nuestros receptores sensoriales, la importancia que las señales físicas transducidas tengan para nuestros propósitos o nuestra supervivencia es fundamentalmente ignorada por la sensación. Tomemos el caso de la audición, donde un flujo continuo de ondas de presión en el aire, provenientes de innumerables fuentes, golpean nuestro tímpano en cada fracción de segundo de cada situación rutinaria: la conversación que estamos teniendo, las conversaciones que otros tienen a nuestro alrededor, nuestros propios pasos, ruido del tráfico, música de fondo, el zumbido del ordenador o del aire acondicionado, etc. Cada una de esas vibraciones es transducida mecánicamente por el órgano de Corti en potenciales de acción, sin ninguna distinción de utilidad, vertiendo incesantemente información sensorial en nuestro sistema nervioso central incluso a riesgo de sobrecargar su capacidad metabólica.

La función de la *percepción* es organizar, identificar e interpretar la sensación, estableciendo qué potencial de acción se corresponde con cada elemento acústico, y cuáles son los que tienen alguna relevancia para mantener nuestro bienestar o para alcanzar nuestras metas. Así, la tarea principal de todo sistema perceptivo es cribar el aluvión sensorial que recibe nuestro sistema nervioso, escogiendo las porciones esenciales para comprender el mundo que nos rodea y transformándolas en percepciones útiles para dirigir nuestro comportamiento. Dado que nuestras percepciones constituirán la base de operaciones cognitivas y motoras más complejas para adaptar nuestras actuaciones al medio, la percepción debe desarrollarse de la manera más rápida y eficaz posible. En esta necesidad imperiosa de inmediatez, nuestro sistema nervioso central no tiene ni el tiempo ni los recursos requeridos para evaluar meticulosamente el contenido de cada sensación en su totalidad. En cambio, nuestra percepción está sesgada por la probabilidad de las sensaciones. Los cambios poco comunes en nuestro entorno tienden a ser más informativos y críticos para nuestra supervivencia que los eventos más frecuentes y repetitivos. Por lo tanto, la estrategia más eficiente para elaborar percepciones útiles es asignar

automáticamente los limitados recursos de procesamiento a la información sensorial más improbable.

La demostración experimental más sencilla de este principio puede obtenerse a través de la aplicación del paradigma *oddball* (Figura 10A). Este consiste en una secuencia de estímulos, donde la presentación repetitiva de un estímulo se intercala aleatoriamente con otro, poco común, que aparece tan solo el 10% de las presentaciones. Este estímulo anómalo es diferente al repetitivo en unas características físicas determinadas, comúnmente su tonalidad. En el caso de una secuencia *oddball* auditiva, el estímulo anómalo puede variar del repetitivo en su frecuencia, intensidad, duración, modulación de amplitud, intervalo entre estímulos, etc. Después, en una secuencia invertida, los estímulos previamente utilizados intercambian su rol. Esto permitirá comparar cada estímulo consigo mismo en ambas condiciones de presentación, controlando así la influencia de las características físicas del sonido en la respuesta nerviosa evocada. Así, obtendremos la respuesta a cada estímulo en una condición *estándar*, esto es, cuando era presentado repetitivamente, y en una condición *discrepante* o desviada de dicho estándar. Cuando un estímulo auditivo evoca diferentes respuestas en las condiciones estándar y discrepante, tal diferencia solo puede deberse a la probabilidad desigual de cada condición. Durante los registros electrofisiológicos de la actividad nerviosa, las respuestas evocadas por las condiciones discrepantes suelen ser considerablemente más robustas que las evocadas en condiciones estándar, lo que genera una respuesta diferencial al paradigma *oddball*.

La respuesta diferencial al paradigma oddball se manifiesta en 2 escalas de observación. En la escala macroscópica del electroencefalograma, aparece como un componente negativo dentro del potencial evocado auditivo registrado en el cuero cabelludo humano (Figura 10D). Este componente se conoce como *potencial de disparidad* en la literatura científica en castellano, aunque, incluso en esta, lo más habitual es nombrarlo por sus siglas en inglés, *MMN*, de *mismatch negativity* (Figura 10D, línea negra). A efectos de este resumen, el término *potencial de disparidad* hará referencia a cualquier respuesta diferencial de gran escala al paradigma oddball, mientras que *MMN* se referirá exclusivamente al componente cortical negativo del potencial evocado auditivo humano. En la escara microscópica de los registros extracelulares (Figura 12A), la respuesta diferencial surge aparentemente de una adaptación de la respuesta neuronal que afecta específicamente la condición estándar, mientras que la respuesta evocada por la condición discrepante permanece robusta (Figura 12). A pesar de las numerosas semejanzas entre ambos biomarcadores de percepción de novedad, su relación ha

sido objeto de un arduo debate científico, y cada fenómeno ha dado lugar a su propio marco teórico de preferencia.

VII.1.a.- El MMN y la Hipótesis de la Detección

En la actualidad, el MMN se ha convertido en una de las herramientas centrales de la neurociencia cognitiva y clínica, debido a sus incomparables características: Es una técnica de registro accesible, económica, no invasiva, muy versátil, y lo más importante, es un potencial evocado obligatorio, lo cual permite trabajar con poblaciones no colaborativas como pacientes neurológicos graves (Bartha-Doering et al., 2015; Kujala et al., 2007; Sussman et al., 2014). De hecho, las alteraciones en el MMN se han relacionado con diversas afecciones neuropsiquiátricas (Lavoie et al., 2019; Näätänen et al., 2014) como la esquizofrenia (Light & Näätänen, 2013; Michie et al., 2016; Näätänen et al., 2015, 2016; Todd et al., 2013) o los trastornos del espectro autista (Schwartz et al., 2018; Vlaskamp et al., 2017), así como con enfermedades neurodegenerativas como Alzheimer (Horváth et al., 2018; Pekkonen, 2000) o Parkinson (Pekkonen, 2000; Seer et al., 2016), además de trastornos de la comunicación (Bishop, 2007; Kujala & Leminen, 2017). Comprender el origen de estas alteraciones del MMN puede ofrecer información valiosa para la investigación clínica, e incluso abre la posibilidad de crear aplicaciones diagnósticas (Schall, 2016).

En las más de 4 décadas que han transcurrido desde su descubrimiento (Näätänen et al., 1978), el estudio minucioso de las latencias y topografías del MMN ha permitido identificar 2 procesos neuropsicológicos subyacentes que se desarrollan en una red frontotemporal de la corteza cerebral (Figura 10E). Por un lado, los generadores temporales del MMN, situados en la corteza auditiva secundaria, han sido relacionados con una memoria sensorial. Por otro lado, los generadores frontales del MMN se le atribuyen a un proceso ejecutivo de reorientación atencional (Alho, 1995). Conforme a esta hipótesis, un sistema detector preatencional compara la entrada sensorial actual con un registro de memoria sensorial, en la cual se han codificado las regularidades auditivas previas (Figura 11). Ante un estímulo anómalo, dicho sistema detectaría una desviación respecto a la regularidad previamente codificada, lo cual provocaría un cambio de atención involuntario hacia la información discrepante. La suma de toda esa actividad nerviosa quedaría reflejada dentro del potencial auditivo evocado, dando lugar al MMN. Por lo tanto, el MMN sería una señal genuina, generada de manera separada y única respecto a otros componentes del potencial auditivo evocado. Así, el MMN marcaría el

funcionamiento de un mecanismo de detección de la desviación cuyo objetivo sería dirigir recursos cognitivos a procesar detalladamente la información sensorial novedosa (Näätänen, 1990; Näätänen & Winkler, 1999; Winkler et al., 1996). Esta *Hipótesis de la Detección* ha gozado tradicionalmente de gran aceptación y predicamento entre los investigadores de la percepción de novedad.

VII.1.b.- Adaptación específica al estímulo y la Hipótesis de la Adaptación

La identificación de adaptación específica al estímulo repetitivo en las neuronas de la corteza auditiva de modelos animales relanzó y reforzó una interpretación alternativa del MMN (Jääskeläinen et al., 2004; May & Tiitinen, 2004; Ulanovsky et al., 2003). La respuesta diferencial al paradigma *oddball* podría deberse a mecanismos fisiológicos simples que inducen una adaptación sináptica que afectaría de forma selectiva a la condición estándar (Figura 12E-G). Mecanismos de plasticidad a corto plazo, como la depresión y la facilitación sinápticas (Abbott et al., 1997; Tsodyks & Markram, 1997) o la inhibición (L. I. Zhang et al., 2003), podrían afectar de manera diferencial a distintas regiones del árbol dendrítico, induciendo así efectos específicos sobre la respuesta de la neurona a estímulos repetitivos. La *Hipótesis de la Adaptación* ofrece una interpretación más parsimoniosa del MMN, más arraigada en la neurobiología en comparación la interpretación cognitiva. Un sistema detector, basado en la interacción entre procesadores sensoriales, rastreadores de memoria y comparadores en línea, parecía plausible en la escala masiva de un electroencefalograma. Sin embargo, esta propuesta ha encontrado dificultades persistentes al tratar de precisar sus correlatos biológicos en la escala neuronal (Fishman, 2014; May & Tiitinen, 2010). Por el contrario, la Hipótesis de la Adaptación considera que el MMN resulta esencialmente de la suma de muchos procesos adaptación específica al estímulo que tendrían lugar a lo largo la corteza cerebral (Jääskeläinen et al., 2004; Ulanovsky et al., 2003). Si tal relación entre ambos fenómenos fuese correcta, la adaptación específica al estímulo ofrecería un modelo excepcional para investigar los mecanismos fisiológicos afectados en las afecciones neuropatológicas y psiquiátricas que aparecen acompañadas de alteraciones en el MMN.

Tanto la Hipótesis de la Detección como la Hipótesis de la Adaptación ofrecen una explicación sobre la respuesta diferencial al paradigma *oddball*, pero sus interpretaciones funcionales resultan contradictorias. Por un lado, la Hipótesis de la Detección implica un sistema que compara la entrada sensorial actual con una plantilla mnésica de la condición

estándar, donde cualquier discrepancia provoca una actualización de la memoria sensorial y una reorientación de la atención. Bajo esta óptica, un potencial de disparidad constituye una señal genuina emitida a tal efecto, resultado de ese proceso activo de detección de la desviación sensorial. Por otro lado, según la Hipótesis de la Adaptación, las neuronas simplemente adaptan su capacidad de respuesta específicamente a las entradas sensoriales repetitivas de la condición estándar. Esta adaptación específica al estímulo se generaría a través de mecanismos como la depresión sináptica o la inhibición. Por lo tanto, los potenciales de disparidad serían tan solo el resultado de sustraer una respuesta atenuada la condición estándar de la respuesta no adaptada que evocaría la condición discrepante. Así, no se podría hablar de una señal separada propiamente dicha, ni existiría un proceso activo de detección de la desviación, sino tan solo la adaptación pasiva de un canal de procesamiento determinado mientras el resto permanecen frescos. Estas 2 hipótesis entienden la percepción de la novedad de maneras cualitativamente distintas. Ahora bien, cabe destacar que, aunque la Hipótesis de la Adaptación es capaz de explicar de manera muy eficaz y parsimoniosa los datos obtenidos mediante el paradigma *oddball*, su poder explicativo decae considerablemente en diseños experimentales que involucran regularidades más complejas, al contrario de lo que ocurre con la Hipótesis de la Detección (para una revisión reciente, ver Carbajal & Malmierca, 2020).

VII.1.c.- El procesamiento predictivo y la Hipótesis de la Expectativa

En los últimos años, una nueva explicación posible ha surgido bajo el marco del procesamiento predictivo (Hohwy, 2013). Originalmente, el procesamiento predictivo surgió como una estrategia de codificación desarrollada para la compresión de datos, la cual permite a un sistema computacional procesar de manera eficiente información compleja mediante la *predicción* de su contenido. En lugar de codificar toda la información, un sistema de procesamiento predictivo solo codificaría los valores del *error de predicción*, esto es, la diferencia entre el valor esperado de una variable y el valor real de esa variable en la señal de entrada (Clark, 2013). Podemos encontrar un ejemplo muy ilustrativo en la forma en que los ordenadores almacenan archivos de video. Los videos contienen mucha información redundante de un fotograma al siguiente, por lo que, en lugar de codificar cada píxel en cada fotograma, los ordenadores simplemente codifican las diferencias entre los fotogramas adyacentes para comprimir los datos. En la misma línea, nuestro cerebro podría esperar el contenido de una sensación basándose en el contenido ya procesado de sensaciones previas. Cada receptor sensorial que responda de manera inesperada se codificará en un valor de error

de predicción que el sistema perceptivo debe emplear para corregir su modelo del mundo exterior, y así poder predecir adecuadamente la siguiente sensación. Por lo tanto, para representar una secuencia completa de eventos, en lugar de procesar cada uno de los elementos de la secuencia, nuestro cerebro solo tendría que procesar los valores de error de predicción, es decir, la discrepancia entre nuestras *sensaciones* y nuestras *expectativas*. A medida que esos errores de predicción se utilizan para actualizar el modelo perceptual y generar expectativas más ajustadas, la carga de errores a procesar se va reduciendo. Así, valores de error pequeños indican un procesamiento optimizado de la información. Este es el principio central del procesamiento predictivo: la minimización del error de predicción.

El procesamiento predictivo toma un enfoque eminentemente kantiano de la percepción (Kant, 1781), la cual entiende como un continuo proceso inferencial bayesiano (Dayan et al., 1995; Friston, 2003, 2009; Friston & Kiebel, 2009a). Dado que nunca experimentamos directamente el 'auténtico' mundo externo, sino que solo podemos accedemos a la impresión que este deja en nuestros sentidos, el cerebro debe *inferir* la causa de dichas sensaciones para poder representar lo que sucede fuera del sistema nervioso. El cerebro genera expectativas sobre estos 'estados ocultos' del mundo por medio de un modelo generativo jerárquico, donde las poblaciones neuronales superiores intentan predecir e inhibir las entradas de información proveniente de poblaciones neurales inferiores. El error de predicción resultante se utiliza para actualizar el modelo, es decir, nuestra representación interna del mundo, en un proceso de *aprendizaje perceptivo*. En cada nivel de procesamiento, las neuronas excitadoras reciben entradas excitadoras que transmiten información sensorial ascendente, así como entradas inhibidoras que transmiten información descendente sobre las expectativas del modelo perceptivo. Cuando ambas entradas son congruentes, sus potenciales postsinápticos se cancelan; pero cuando son incongruentes, se genera un error de predicción que señal el desajuste al nivel de procesamiento superior. Por tanto, la minimización del error de predicción es de naturaleza jerárquica, y nuestro organismo la persigue a través de 2 procesos: (1) la *inferencia perceptiva*, es decir, mejorando el modelo interno del mundo para explicar mejor la entrada sensorial, y (2) la *inferencia activa*, es decir, cambiando la entrada sensorial participando en acciones con resultados predecibles (Friston, 2005, 2008, 2010; Friston et al., 2006, 2017; Friston & Kiebel, 2009a, 2009b; Parr & Friston, 2017).

Desde el punto de vista del procesamiento predictivo, solo hay 2 clases de cosas que el sistema nervioso debe inferir: el estado del mundo y la incertidumbre sobre ese estado (Friston

et al., 2012). Nuestras representaciones sobre los estados ocultos del mundo surgen del intercambio jerárquico entre información descendente sobre las expectativas e información ascendente sobre los errores de predicción. Este intercambio se produce en la actividad sináptica, excitadora e inhibidora, del sistema nervioso. Pero todo proceso inferencial conlleva un cierto grado de incertidumbre. Esto se debe a que no somos perceptores perfectos. Nuestras capacidades sensoriales y de procesamiento son limitadas, y por tanto vulnerables a la ambigüedad, el ruido y la volatilidad en la estructura probabilística del entorno sensorial. Dicha incertidumbre se codifica en términos de *confianza posterior* o *precisión esperada* por medio de la ganancia postsináptica. Según el procesamiento predictivo, los mensajes sinápticos son ponderados de acuerdo con su precisión esperada conforme se transmiten a lo largo de la jerarquía de procesamiento. Cuando la precisión esperada es alta, las señales de error se consideran confiables y reciben amplificación postsináptica para priorizar su potencial de actualización. Por el contrario, cuando se espera una precisión baja, estas señales de error se atenúan para evitar malinterpretaciones por parte el modelo perceptivo, de tal manera que la influencia de la evidencia previa acumulada se vuelve más prominente. En otras palabras, la precisión esperada es la ganancia postsináptica sobre el error de predicción, modulando su influencia sobre niveles de procesamiento más altos, de tal modo que se aprende más de las señales de error precisas que de las ruidosas y poco fiables (Friston & Kiebel, 2009b). Los neuromoduladores, como la acetilcolina o la dopamina, no pueden excitar o inhibir directamente las respuestas postsinápticas, sino que tan solo ponderan las respuestas postsinápticas a otros neurotransmisores, actuando como un mecanismo de control de la ganancia. Es por eso que el marco teórico del procesamiento predictivo entiende que la única función posible de la neuromodulación es codificar la precisión esperada, desempeñando un papel tanto en la inferencia perceptiva como en la activa al conferir flexibilidad contextual al procesamiento sensorial y motor (FitzGerald et al., 2015; Friston et al., 2012; Moran et al., 2013).

En síntesis, de acuerdo con el marco teórico del procesamiento predictivo, nuestro cerebro minimiza jerárquicamente el error de predicción: (1) al representar los estados de un entorno inmediato rápidamente cambiante, (2) al tener en cuenta las fluctuaciones lentas en parámetros más generales y (3) al aplicar una ganancia positiva a señales confiables. Cada una de estas operaciones tiene un posible correlato neuronal directo: (1) la *actividad sináptica* de los circuitos neuronales proporcionan el intercambio jerárquico de expectativas y señales de error a partir del cual emergen las representaciones o percepciones, en un proceso conocido

como *inferencia perceptual*; (2) la *eficacia sináptica* regula la forma en que las neuronas se conectan mediante mecanismos de plasticidad, lo cual sustenta el *aprendizaje perceptivo*; (3) la *ganancia postsináptica* ajustada a través de la neuromodulación regula la excitabilidad intrínseca de las neuronas de acuerdo con su *precisión esperada*, facilitando o amortiguando la transmisión de mensajes (Hohwy, 2012). En funcionamiento dentro de cada red neuronal y entre cada nivel de procesamiento de nuestro sistema perceptivo, estos mecanismos neuronales de actividad sináptica, plasticidad y neuromodulación se pueden medir tanto a través de electroencefalograma como de registros extracelulares (Carbajal & Malmierca, 2020).

Según la *Hipótesis de la Expectativa* basada en el marco teórico del procesamiento predictivo, nuestro sistema nervioso trata de predecir la entrada sensorial a partir de eventos pasados por medio de un modelo generativo jerárquico, que se actualiza mediante la codificación de señales de error de predicción. Esto se asemeja a la Hipótesis de Detección, donde un sistema de detección de la desviación comparaba la entrada sensorial con una memoria (Figura 11, guiones azules), generando potenciales de disparidad para marcar las discrepancias e inducir actualizaciones de dicha memoria sensorial (Figura 11, flecha roja gruesa). Por tanto, la señalización de errores de predicción en la Hipótesis de la Expectativa juega un papel análogo al de la detección de la desviación en la Hipótesis de la Detección (Schröger et al., 2014, 2015; Winkler et al., 2009; Winkler & Czigler, 2012; Winkler & Schröger, 2015). Contrariamente a la Hipótesis de la Adaptación, las Hipótesis de la Detección y de la Expectativa interpretan las respuestas diferenciales al paradigma *oddball* como señales genuinas, activamente generadas para indicar una desviación de la regularidad previamente establecida. Pero, en contraste con la Hipótesis de la Detección, la Hipótesis de la Expectativa no considera que esas señales de disparidad sean evocadas *de novo* (Figura 11, flecha roja gruesa) y separadamente de la señal de entrada sensorial (Figura 11, flecha negra gruesa). Por el contrario, la Hipótesis de la Expectativa postula que las porciones redundantes de la señal de entrada original se suprimen, mientras que las porciones remanentes con información inesperada conforman el potencial de disparidad (Figura 20), lo cual va más en la línea de la Hipótesis de la Adaptación (Carbajal & Malmierca, 2020).

En consecuencia, las diferencias entre las respuestas a las condiciones estándar y discrepante del paradigma *oddball* resultan de 2 procesos distintos (Figuras 18 y 20): (1) Las expectativas en un nivel de procesamiento dado inhiben parte de la entrada sensorial o señales de error enviadas desde niveles inferiores, suprimiendo parcialmente la respuesta neuronal.

Durante un paradigma *oddball*, tal efecto supresor resultará fortalecido con cada repetición de la condición estándar. Por lo tanto, la adaptación específica al estímulo sería una forma de aprendizaje perceptual, compatible con la generación de potenciales de disparidad. (2) Los elementos inesperados de la señal de entrada sensorial, esto es, aquellos que no pudieron ser inhibidos o previstos por las expectativas en el nivel dado, son transmitidos a niveles de procesamiento más elevados en una señal de error, susceptible de ser amplificada o amortiguada según su precisión esperada. Durante un paradigma *oddball*, toda información sensorial proporcionada por la condición discrepante que contraste con la expectativa de un estímulo estándar se transmite como una señal de error a un nivel de procesamiento más alto, y posiblemente se amplifique en su transmisión postsináptica (Carbajal & Malmierca, 2020). De esta manera, algunos autores dentro del marco teórico del procesamiento predictivo han ofrecido reinterpretaciones del MMN como una suma de señales de error de predicción ponderadas según su precisión (Chennu et al., 2016; Garrido et al., 2008, 2009; Garrido, Kilner, Kiebel, & Friston, 2007; Garrido, Kilner, Kiebel, Stephan, et al., 2007; Phillips et al., 2015, 2016). Además, la Hipótesis de la Expectativa considera al MMN y al fenómeno de la adaptación específica al estímulo como los signos macroscópicos y microscópicos, respectivamente, del mismo proceso de codificación automática de la novedad sensorial, ofreciendo así una explicación unificada de su aparición en ambas escalas de observación (Carbajal & Malmierca, 2018a; Garrido et al., 2009).

VII.2.- LÓGICA DE LA INVESTIGACIÓN

La Hipótesis de la Detección ofrece un enfoque cognitivo del MMN basado en una intrincada interacción entre procesadores sensoriales, rastreadores de memoria y comparadores en línea distribuidos a lo largo de una red frontotemporal situada en la corteza cerebral (Alho, 1995; Näätänen, 1990; Näätänen & Winkler, 1999; Winkler et al., 1996). Una formulación tan compleja puede resultar plausible en la escala macroscópica del electroencefalograma, pero encuentra serias dificultades a la hora de trasladar sus asunciones a la neurobiología. Además, la Hipótesis de la Detección excluye de su modelo cortical la evidencia creciente en favor de la contribución subcortical a la percepción de novedad en el sonido (Malmierca, Carbajal & Escera, 2019). Por el contrario, la Hipótesis de la Adaptación es capaz de integrar estas contribuciones subcorticales a la par que proporciona implementaciones más parsimoniosas de la percepción de novedad en el sustrato microscópico, basándose para ello en los mecanismos que inducen el fenómeno de la adaptación específica al estímulo. Sin embargo, su formulación

simplista se ve sobrepasada a la hora de explicar la evidencia empírica más allá del paradigma *oddball*.

La Hipótesis de la Expectativa es capaz de situarse en un término medio respecto a sus predecesoras, reteniendo así muchas de sus virtudes. Por ejemplo, la Hipótesis de la Expectativa es muy parsimoniosa. Con un principio simple en su núcleo teórico (la minimización del error de predicción), replicado a través de la jerarquía nerviosa, la Hipótesis de la Expectativa puede explicar cómo el cerebro desarrolla la inferencia perceptiva en general (Figura 18), y la percepción de novedad sensorial en particular (Figura 20). Además, los modelos de procesamiento predictivo son capaces de proponer circuitos neuronales ricamente detallados, cuyas operaciones se fundamentan en mecanismos neurofisiológicos concretos de actividad sináptica, plasticidad y neuromodulación. Estos modelos son capaces de explicar las características más sofisticadas del procesamiento automático de las sensaciones novedosas, desde una simple neurona hasta la actividad masiva de grandes áreas de la corteza cerebral (Figuras 19 y 20). Por lo tanto, la Hipótesis de la Expectativa puede competir en poder explicativo con la Hipótesis de Detección, al tiempo que conserva en cierto modo el enfoque parsimonioso de la Hipótesis de Adaptación. Al integrar los aspectos más fuertes de las 2 hipótesis precedentes bajo el marco del procesamiento predictivo, la Hipótesis de la Expectativa considera que el MMN y fenómeno de adaptación específica al estímulo observado en la corteza auditiva son respectivamente los signos macroscópico y microscópico del mismo procesamiento automático de la novedad sensorial, ofreciendo así una explicación unificada de su aparición en ambas escalas (Figura 20). Considerando las múltiples aplicaciones en la investigación neurocognitiva y el diagnóstico del MMN, el vínculo entre ambos fenómenos y escalas de observación es de suma importancia científica, dado que abre la posibilidad de estudiar los potenciales de disparidad a nivel de neuronas individuales (Carbajal & Malmierca, 2018a).

Empero, todavía existe evidencia empírica que no encaja completamente en la Hipótesis de la Expectativa, o al menos no en su formulación actual. Los modelos neurobiológicos propuestos de procesamiento predictivo se refieren exclusivamente a una jerarquía de procesamiento establecida entre columnas y áreas de la corteza cerebral (Bastos et al., 2012; Friston, 2005; Keller & Mrsic-Flogel, 2018; Spratling, 2008a, 2008b, 2010). Una red neuronal más profunda capaz de implementar un procesamiento predictivo contravendría estos modelos (Figura 19). Sin embargo, los estudios de registro extracelular indican claramente que las

primeras neuronas auditivas donde se aprecia adaptación específica al estímulo no se sitúan en el neocórtex, sino tan profundamente como en el mesencéfalo (Malmierca, Carbajal & Escera, 2019). En el sistema auditivo, las primeras respuestas diferenciales al paradigma *oddball* emergen a nivel del colículo inferior, como confirman tanto los estudios en participantes humanos (Figuras 15 y 16; Shiga et al., 2015; Skoe et al., 2014; Slabu et al., 2012) como con modelos animales (Figuras 13 y 14; Ayala et al., 2013; Duque et al., 2018; Gao et al., 2014; Malmierca et al., 2009).

La posibilidad de encontrar un circuito subcortical capaz de implementar procesamiento predictivo jerárquico no resulta tan descabellada cuando se considera la compleja y sofisticada citoarquitectura del colículo inferior (Figura 6). Siendo este el origen neurológico de las vías lemniscal y no lemniscal de procesamiento auditivo (Figura 8), el colículo inferior contiene al menos un nivel de procesamiento de orden inferior en su núcleo central, y al menos otro nivel o niveles de procesamiento de orden superior en los circuitos de 3 capas que conforman su corteza (Figura 6). Ambos niveles están conectados recíprocamente a través de una densa red local de conexiones intrínsecas y comisurales. Además, casi todas las vías auditivas ascendentes y descendentes convergen en el colículo inferior (Malmierca, 2015). Esto crea una conectividad iterativa que integra aferencias excitadoras, inhibidoras y neuromoduladoras ascendentes y descendentes, y donde especialmente la corteza del colículo inferior trabaja bajo una fuerte influencia cortical y neuromoduladora (Figura 4). Esta red tan abundante de conexiones de alimentación y retroalimentación entre estaciones de procesamiento organizadas a distintos niveles contiene todos los elementos requeridos para construir un circuito de procesamiento predictivo jerárquico: el flujo descendente de expectativas, la transmisión ascendente de señales de error de predicción y los mecanismos neuromoduladores necesarios para ajustar la precisión esperada (Figuras 18, 19 y 20).

Aunque la posibilidad de que la circuitería colicular realice procesamiento predictivo nunca se ha investigado directamente, indicios empíricos proporcionados por estudios previos permiten especular en esta dirección. En el debate sobre la detección frente a la adaptación como origen del MMN, el paradigma *oddball* (Figura 17A) aqueja de una limitación metodológica importante: No puede distinguir los efectos de la detección de la desviación de los efectos producidos por el fenómeno de la adaptación específica al estímulo. Con el fin de controlar los efectos de adaptación pasiva que podrían contribuir al surgimiento del MMN, algunos diseños experimentales comenzaron a incorporar controles para la repetición de la

condición estándar. Las denominadas *secuencias de control sin repeticiones* (Figura 17B) estan diseñadas inducir en el sistema auditivo una refracción similar a la provocada por el paradigma *oddball*, pero sin evocar un MMN. Por un lado, la *secuencia multi-estándar* (Schröger & Wolff, 1996) presenta el estímulo de interés incrustado en una secuencia aleatoria de estímulos variados, donde cada tono comparte la misma probabilidad de presentación que la condición discrepante en el paradigma *oddball*. Por otro lado, la *secuencia en cascada* (Ruhnau et al., 2012) ordena los estímulos de manera regular, siguiendo una sucesión de frecuencias creciente o decreciente. Así, el estímulo de interés se ajusta a una regularidad (a diferencia de la condición discrepante), pero no a una regularidad establecida por repetición (contrariamente a la condición estándar). De esta manera, las secuencias de control sin repeticiones sirven para establecer una *condición no discrepante* (Figura 17B), comparable con las condiciones estándar y discrepante del paradigma *oddball* (Figura 17A). La condición no discrepante proporciona un punto de referencia con el que comparar la respuesta diferencial al paradigma *oddball*, segregando así los efectos de la adaptación de un posible potencial de disparidad genuino. Si la respuesta a la condición no discrepante es mayor que a la condición discrepante, entonces la Hipótesis de la Adaptación no puede ser descartada. En cambio, si respuesta a la condición discrepante supera a la de la condición no discrepante, entonces podría confirmarse la presencia de un potencial de disparidad genuino. Lo más interesante es que un estudio de electroencefalograma (Slabu et al., 2012) y otro de imagen por resonancia magnética funcional (Cacciaglia et al., 2015) en participantes humanos encontraron respuestas mesencefálicas a la condición discrepante que superaban la respuesta media a la secuencia multi-estándar. Dado que la Hipótesis de Detección no es aplicable al procesamiento subcortical (Figura 11), tal evidencia podría interpretarse en favor de la Hipótesis de Expectativa (Figura 20).

El fundamento de las secuencias de control sin repeticiones, y de la condición no discrepante que establecen, se puede reinterpretar fácilmente bajo la óptica del procesamiento predictivo (Figura 17C). Durante el paradigma *oddball* (Figura 17A), la repetición de la condición estándar permite establecer una expectativa muy precisa (‘el siguiente tono será el mismo’), que falla cuando acontece la condición discrepante (Figura 20A). Por un lado, la secuencia en cascada ascendente/descendente (Figura 17B) también genera una expectativa relativamente precisa (‘el siguiente tono tendrá un tono más agudo/grave’), pero ni esas predicciones se basan en una expectativa de repetición, como en la condición estándar, ni se frustran con la aparición del estímulo de interés, como en la condición discrepante. Por otro lado, la secuencia multi-estándar crea un contexto de incertidumbre que impide la generación

de expectativas precisas (Figura 20B). En el mejor de los casos, la única predicción que podría establecer el modelo perceptivo sería 'el próximo tono será diferente'. En caso de que la respuesta a la condición discrepante superase la respuesta la condición no discrepante, significaría que la Hipótesis de Adaptación no puede dar cuenta de la respuesta diferencial al paradigma *oddball*. Por tanto, cabría la participación de mecanismos predictivos propuesta por la Hipótesis de la Expectativa (Figura 17E). Según esta, un componente de disparidad en el potencial auditivo evocado no resultaría simplemente del sumatorio de adaptación específica al estímulo en las regiones auditivas del cerebro, sino más bien de la señalización del error de predicción. En ese caso, las diferencias entre las respuestas a la condición no discrepante y la condición estándar no deben atribuirse a mera adaptación, sino a una expectativa de repetición que suprime la respuesta a la condición discrepante (Auksztulewicz & Friston, 2016). La diferencia entre las respuestas a la condición discrepante y no discrepante correspondería la amplificación de la señal de error de predicción por efecto de su precisión esperada, con una posible contribución de otros errores de predicción provocados por el fracaso de expectativas de orden superior distintas a la expectativa de repetición (Figura 17C). En consecuencia, las secuencias de control sin repetición se pueden utilizar durante los registros extracelulares de las neuronas del colículo inferior para establecer condiciones no discrepantes comparables con el paradigma *oddball*. De esta forma, se puede examinar empíricamente la validez de la Hipótesis de Adaptación, así como obtener evidencia en favor de la Hipótesis de la Expectativa (Carbajal & Malmierca, 2020).

El estudio del papel de la neuromodulación en el fenómeno de la adaptación específica al estímulo observado en las neuronas coliculares también podría proporcionar evidencia adicional en favor de la Hipótesis de la Expectativa. Algunos autores del marco teórico del procesamiento predictivo han propuesto que la acetilcolina (Moran et al., 2013) y la dopamina (FitzGerald et al., 2015; Friston et al., 2012, 2014; Nour et al., 2018; Schwartenbeck et al., 2015) modulan la precisión esperada de las señales de error de predicción. Respecto a la modulación colinérgica, un estudio previo de nuestro laboratorio utilizó una técnica de microiontoforesis *in vivo* para aplicar localmente agonistas y antagonistas colinérgicos a las neuronas en el colículo inferior de la rata. La infusión del agonista colinérgico provocó una disminución general de los niveles de SSA, mientras que los antagonistas colinérgicos produjeron el efecto contrario (Ayala & Malmierca, 2015). Sin embargo, los posibles efectos neuromoduladores de la dopamina sobre la respuesta diferencial al paradigma *oddball* de las neuronas coliculares nunca han sido explorados, a pesar de que varios estudios indican que el

colículos inferior recibe sustanciosa inervación dopaminérgica del núcleo subparafascicular del tálamo (Figura 4), el cual proyecta densamente a la corteza del colículo inferior (Batton et al., 2018; C. Chen et al., 2018; Gittelman et al., 2013; Hurd et al., 2001; Nevue, Elde, et al., 2016; Nevue, Felix, et al., 2016; Weiner et al., 1991; Yasui et al., 1992). Además, 2 estudios han detectado ARN mensajero codificante de receptores dopaminérgicos tipo D_2 en el colículo inferior (Nevue, Elde, et al., 2016; Nevue, Felix, et al., 2016) y un tercer estudio ha demostrado su expresión funcional como proteína (Hoyt et al., 2019). Asimismo, otros 2 estudios adicionales han confirmado que la dopamina modula las respuestas auditivas de las neuronas coliculares de manera heterogénea (Gittelman et al., 2013; Hoyt et al., 2019).

En conclusión, existe una base científica sólida para explorar la posible participación de la modulación dopaminérgica de la respuesta diferencial neuronas del colículo inferior al paradigma *oddball*. Esto puede llevarse a cabo aplicando la misma técnica de microiontoforesis que permitió a mis colegas estudiar la influencia colinérgica en el fenómeno de la adaptación específica al estímulo en las neuronas del colículo inferior de la rata. Además, es posible presentar las secuencias de control sin repeticiones junto con el paradigma *oddball* durante el registro extracelular de neuronas coliculares, para establecer una condición no discrepante, y así poder identificar indicios de señalización de errores de predicción. Finalmente, si se pudiese probar que la dopamina modula la respuesta diferencial al paradigma *oddball* de las neuronas del colículo inferior, y que dicha respuesta diferencial mesencefálica contiene un componente genuino de error de predicción, el paso siguiente lógico sería intentar modular directamente dicha señalización de errores de predicción aplicando localmente dopamina mediante microiontoforesis. Si tales condiciones se cumpliesen, los resultados indicarían que la Hipótesis de la Expectativa es perfectamente aplicable al colículo inferior, lo cual implicaría que el procesamiento predictivo auditivo emerge primeramente a nivel mesencefálico, y no cortical como está establecido en la actualidad.

VII.2.a.- Hipótesis

Una vez considerados todos estos factores, las hipótesis planteadas para el estudio son las siguientes:

1. La Hipótesis de Expectativa es más adecuada que las Hipótesis de la Detección y de la Adaptación para explicar la aparición de la respuesta nerviosa diferencial al paradigma *oddball*.

2. El fenómeno de adaptación específica al estímulo repetitivo observado en los registros extracelulares es, en realidad, un biomarcador del procesamiento predictivo jerárquico que realiza el sistema auditivo.
3. A pesar del habitual enfoque corticocéntrico que toman los modelos de procesamiento predictivo disponibles en la actualidad, el procesamiento predictivo auditivo no comienza a nivel cortical, sino a nivel mesencefálico, en el colículo inferior.
4. El núcleo central del colículo inferior actúa como un nivel de entrada primario, tal vez recibiendo expectativas impuestas por niveles de procesamiento de orden superior que induzcan supresión por repetición, pero sin capacidad para elaborar e imponer expectativas sobre otros niveles de procesamiento inferiores.
5. La corteza del colículo inferior posee las propiedades citoarquitectónicas y funcionales necesarias para implementar un circuito de procesamiento predictivo jerárquico dentro de su estructura de 3 capas. Sus neuronas reciben expectativas de niveles de procesamiento más altos en la vía auditiva, y tal vez incluso de otras neuronas y regiones de orden superior dentro de las propias cortezas del colículo inferior. A su vez, la corteza del colículo inferior puede imponer expectativas sobre las neuronas del núcleo central, induciendo en ellas supresión de la respuesta evocada por repetición del estímulo.
6. La liberación de dopamina en la corteza del colículo inferior configura la precisión esperada de las señales de error de predicción generadas por sus neuronas.

VII.2.b.- Objetivos

Por tanto, el objetivo principal de esta tesis es demostrar que el origen neuroanatómico del procesamiento predictivo auditivo no se sitúa en la corteza cerebral auditiva, sino en el colículo inferior. Para ello, se recabarán datos empíricos que apoyen la idoneidad de la Hipótesis de la Expectativa para explicar el procesamiento auditivo mesencefálico. Para poner a prueba las hipótesis antes mencionadas, se plantean los siguientes objetivos para el estudio:

1. Investigar si el sistema dopaminérgico modula la respuesta diferencial al paradigma *oddball* observable en el registro extracelular de las neuronas de la corteza del colículo inferior, emulando la liberación local de dopamina mediante microiontoforesis.
2. Comprobar si la modulación dopaminérgica de la respuesta diferencial al paradigma oddball está mediada por los receptores dopaminérgicos de tipo D_2 presentes en el colículo

inferior, mediante la microiontoforesis de eticlopride, un antagonista selectivo de dichos receptores.

3. Confirmar que las neuronas del colículo inferior participan en un procesamiento predictivo jerárquico mediante la identificación de un componente de error de predicción dentro de la respuesta diferencial al paradigma *oddball*, utilizando para ello las secuencias de control sin repetición.
4. Comparar el procesamiento del núcleo central del colículo inferior con el de la corteza respecto a la señalización de errores de predicción y a su nivel de supresión de respuesta por repetición del estímulo.
5. Controlar los posibles efectos de la anestesia en la señalización de errores de predicción, mediante el registro de respuestas extracelulares al paradigma *oddball* y a las secuencias de control sin repeticiones en el colículo inferior de animales despiertos.
6. Investigar si las proyecciones dopaminérgicas que reciben las neuronas de la corteza del colículo inferior podrían modular la señalización de errores de predicción, mediante la liberación de dopamina a través de microiontoforesis durante la presentación del paradigma *oddball* y de las secuencias de control sin repeticiones.

VII.3.- METODOLOGÍA ABREVIADA

Los consumibles necesarios para el registro extracelular, estos son, los microelectrodos de tungsteno y las pipetas multibarril para la microiontoforesis, en tanto que herramientas críticas para esta investigación, se fabricaron a mano en nuestro laboratorio utilizando la configuración de la estación de trabajo referenciada (Bullock et al., 1988).

Los experimentos fueron realizados en 67 ratas Long-Evans hembra de 150–250 g de peso y 9–17 semanas de edad, así como en 5 ratones CBA/J hembra de 27–30 g de peso y 8–12 semanas de edad. Todos los procedimientos metodológicos fueron aprobados por el Comité de Bioética para el Cuidado Animal de la Universidad de Salamanca (USAL-ID-195) y realizados cumpliendo con los estándares del Convenio Europeo ETS 123, la Directiva de la Unión Europea 2010/63/UE y el Real Decreto 53/2013 para el uso de animales en la investigación científica.

Las ratas fueron anestesiadas con uretano, un anestésico terminal que produce analgesia y anestesia profundas, pero que no altera significativamente las propiedades fisiológicas básicas de las neuronas de la vía auditiva (Duque et al., 2016; Hara & Harris, 2002; Maggi &

Meli, 1986; Sceniak & MacIver, 2006). También se les aplicaron otros fármacos como corticoides (cortexona) para evitar la inflamación y el edema cerebral durante la cirugía, bloqueantes de la secreción bronquial (atropina) y anestésicos locales (lidocaína). Después de anestesiar al animal se le realiza una prueba de umbrales de audición (ABR) para descartar algún déficit auditivo. Durante la cirugía, se expone el hueso occipital izquierdo y se practica una craneotomía de unos 5 mm de diámetro que permita acceder al colículo inferior con un microelectrodo de grabación y una pipeta multibarril.

Previamente a la intervención quirúrgica, los ratones eran convenientemente entrenados y acondicionados durante días para mantenerse en estado de relajación durante las eventuales sesiones de registro electrofisiológico en animal despierto. Para la cirugía, los ratones fueron anestesiados con una combinación de ketamina y xilacina, anestésicos reversibles que inducen analgesia y anestesia profundas durante aproximadamente 1 hora. Durante ese periodo, se realizaba la craneotomía sobre el colículo inferior izquierdo, cubriendo posteriormente la ventana craneal con un elastómero de silicona que pudiese ser cómodamente retirado cuando hubiese que introducir el microelectrodo de registro extracelular. Al terminar la cirugía, los ratones eran devueltos a sus cajas de hábitat enriquecido para una recuperación de al menos 3 días. Para las sesiones de grabación, los ratones se mantuvieron inmovilizados y despiertos durante no más de 3 horas, proporcionándoseles recompensas a intervalos variables (leche condensada) siguiendo las pautas de acondicionamiento previamente marcadas.

En ambas especies, los microelectrodos se introdujeron siguiendo coordenadas estereotácticas para la localización del colículo inferior. El mismo microelectrodo se empleaba para registrar la actividad evocada auditiva en 2 escalas: (1) a escala microscópica, se registró la actividad evocada neuronal, medida como conteo de espigas disparada por estímulo por una neurona aislada, grabada neurona por neurona; y (2) a escala mesoscópica, se registró el potencial de campo local, el cual recoge la actividad de una región nerviosa completa de varios milímetros alrededor de la punta del electrodo. Para buscar la respuesta neuronal al sonido se utilizaron ráfagas intermitentes de ruido blanco a intensidades moderadas. En cada lugar de registro seleccionado se determinó primero el campo receptivo de la neurona aplicando una secuencia pseudoaleatoria de tonos puros a diferentes frecuencias e intensidades. Después, se seleccionaron 10 tonos para construir el paradigma *oddball* y las secuencias de control sin repeticiones. En algunos experimentos con ratas, tras una primera ronda de registros en la condición ‘control’, se aplicaban inyecciones locales de dopamina o eticlopride (antagonista

de los receptores dopaminérgicos D_2) mediante microiontoforesis y se repetía el protocolo de registro en la condición 'droga'. Después, se esperaban en torno a 40 minutos a que las drogas se disipasen para realizar una nueva ronda de registros en la condición 'recuperación'. En 5 casos donde la sesión de registro resultó excepcionalmente estable, se pudo aplicar la otra droga en una condición 'droga 2' y grabar después una condición 'recuperación 2'. En algunos lugares de registro seleccionados se realizó una lesión electrolítica para su posterior localización neuroanatómica precisa mediante el procesamiento histológico del tejido.

Todos los análisis y la visualización de datos se realizaron con el software SigmaPlot™ (Systat Software) y MATLAB™ (MathWorks), utilizando las funciones integradas, la caja de herramientas de Estadísticas y Aprendizaje Automático para MATLAB, así como scripts y funciones personalizadas desarrolladas en nuestro laboratorio.

VII.4.- RESUMEN DE RESULTADOS

A continuación, se expone un compendio sintetizado de las observaciones empíricas más relevantes para los fines de esta tesis doctoral:

1. En el núcleo central del colículo inferior, las respuestas evocadas por la condición discrepante son equivalentes a las evocadas por la condición no discrepante, superando ambas a la condición estándar. Esta observación pudo ser confirmada tanto en los análisis de conteo de espigas (escala microscópica) como en los del potencial de campo local (escala mesoscópica). Por tanto, ni la Hipótesis de la Expectativa puede ser confirmada, ni la Hipótesis de la Adaptación puede ser descartada en esta división del colículo inferior.
2. En la corteza del colículo inferior, las respuestas evocadas por la condición discrepante superaron a las de la condición no discrepante, que a su vez fueron mayores que las de la condición estándar. Esta observación pudo ser confirmada tanto en los análisis de conteo de espigas (escala microscópica) como en los del potencial de campo local (escala mesoscópica). De esta manera, la Hipótesis de la Adaptación puede ser descartada en esta división del colículo inferior, y la interpretación de la Hipótesis de la Expectativa se ve reforzada. Por tanto, el concepto de 'adaptación específica al estímulo' resulta inadecuado para describir la respuesta diferencial al paradigma *oddball*. La respuesta diferencial sería en realidad el resultado de la combinación de, por un lado, la supresión de la respuesta a la condición estándar por la expectativa de repetición, y, por otro lado, por la emisión de señales de error de predicción ante la aparición inesperada de la condición discrepante.

3. Las principales emisoras mesencefálicas de errores de predicción auditivos son las neuronas del colículo inferior que exhiben campos receptivos altamente desorganizados (Figura 7D).
4. La emisión de errores de predicción desde la corteza del colículo inferior está muy condicionada por las características físicas del estímulo, como la intensidad del sonido o la dirección del cambio de tonalidad. Esta característica es propia del mesencéfalo auditivo, pues no se reproduce en el tálamo ni la corteza auditiva. Esto probablemente se deba a que estas estaciones superiores emiten de errores de predicción referentes a propiedades del sonido más abstractas, como prevé el principio de minimización jerárquica del error de predicción.
5. Las neuronas coliculares son capaces de generar errores de predicción auditivos en estados de anestesia profunda. Sin embargo, la emisión de errores de predicción se vuelve más robusta cuando el animal se encuentra despierto, demostrando que el estado de consciencia influye en el procesamiento predictivo de información auditiva.
6. La liberación de dopamina en la corteza del colículo provoca respuestas heterogéneas, pero existe una tendencia a reducir la respuesta evocada por la condición discrepante que no se generaliza al resto de condiciones. Por tanto, la modulación dopaminérgica parece afectar exclusivamente a la transmisión de error de predicción, como formulaba la Hipótesis de la Expectativa.
7. La aplicación local de eticlopride confirma la liberación endógena de dopamina durante el paradigma *oddball* auditivo, y desvela a los receptores D_2 como mediadores de los efectos dopaminérgicos previamente descritos.

VII.5.- DISCUSIÓN

En este bloque, los resultados mencionados serán integrados en el amplio contexto que brinda la literatura neurocientífica del último medio siglo sobre la percepción de novedad auditiva y la función dopaminérgica, con el fin de dotar a esta tesis de un significado más rico y de mayor alcance.

VII.5.a.- El colículo inferior alberga el primer nivel de una jerarquía de procesamiento predictivo de la información auditiva

El origen neuroanatómico de la percepción de novedad en la audición ha sido tradicionalmente un tema bastante debatido y controvertido. El procesamiento de información sesgado por la probabilidad de la entrada sensorial ha sido considerado a menudo como demasiado sofisticado para los núcleos subcorticales. Sin embargo, desde hace décadas se han descrito indicios de habituación neuronal selectiva a tonos repetitivos en el cerebro medio de modelos animales. Un estudio pionero, previo incluso al descubrimiento del MMN, describió 'neuronas de la novedad' en el mesencéfalo auditivo de la rana. Dicho estudio propuso que estos signos de percepción de la novedad auditiva eran generados por las neuronas multipolares ubicadas en el núcleo magnocellular del torus semicircularis (Bibikov, 1977). Años después, otro estudio encontró signos tempranos de percepción de la novedad en el colículo inferior del jerbo. Sus autores también asumieron implícitamente que esas respuestas neuronales eran generadas *in situ* en el mesencéfalo auditivo (Malone & Semple, 2001).

Desafortunadamente, esos estudios pioneros fueron pasados por alto, y sus conclusiones ignoradas, cuando una nueva investigación encontró respuestas diferenciales al paradigma *oddball* en el registro extracelular de corteza auditiva primaria del gato (Ulanovsky et al., 2003). Este influyente trabajo fue el primero en ofrecer pruebas convincentes que sugerían que el fenómeno de adaptación específica al estímulo repetitivo constituía el correlato neuronal del MMN, captando la atención científica tanto de los estudiosos del cerebro humano (May et al., 2015; May & Tiitinen, 2004) como de los investigadores en modelos animales (Fishman & Steinschneider, 2012; Jääskeläinen et al., 2004). Pero este estudio no encontró respuestas diferenciales al paradigma *oddball* en el tálamo auditivo, y dado que los generadores neuroanatómicos del MMN se encuentran en la corteza cerebral, sus autores concluyeron que el fenómeno de la adaptación específica al estímulo repetitivo era una propiedad exclusivamente cortical. Tal conclusión gozó de una amplia aceptación en la literatura científica, donde dejó una honda impresión que perduraría por años.

Una de las principales motivaciones de nuestro grupo de investigación durante los últimos 15 años ha sido desmentir el mito de que los mecanismos neurológicos que sustentan la percepción de novedad auditiva se encuentran confinados en los límites del neocórtex. Numerosos estudios de nuestro laboratorio (Ayala et al., 2013, 2015; Ayala & Malmierca,

2015, 2018; Duque et al., 2012; Duque & Malmierca, 2015; Malmierca et al., 2009; Parras et al., 2017; Pérez-González et al., 2012, 2005; Pérez-González & Malmierca, 2012; Valdés-Baizabal et al., 2017) y de otros grupos de investigación (Gao et al., 2014; Harpaz et al., 2021; Herrmann et al., 2015; Lumani & Zhang, 2010; Netser et al., 2011; Patel et al., 2012; Reches & Gutfreund, 2008; Shen et al., 2015; Thomas et al., 2012; Zhao et al., 2011) han confirmado ya inequívocamente que las respuestas diferenciales al paradigma *oddball*, consideradas en su momento fruto de la adaptación, emergen en el mesencéfalo auditivo de varias especies. Aún con todo, el enfoque corticocéntrico de la percepción de novedad sensorial se resistió a ser abandonado. Para adaptarse a la creciente evidencia empírica en favor de la contribución subcortical, se propuso que la adaptación específica al estímulo repetitivo tenía un origen cortical, pero luego se transmitía a través de proyecciones descendentes al mesencéfalo (Nelken & Ulanovsky, 2007). En efecto, un estudio de nuestro propio laboratorio pudo confirmar que todas las neuronas de colículo inferior de la rata que exhibían altos niveles de adaptación específica al estímulo repetitivo recibían aferencias corticocoliculares (Ayala et al., 2015), por lo que había una base sólida para pensar en una imposición desde el nivel cortical al subcortical.

No obstante, no es posible determinar el origen neuroanatómico de las respuestas diferenciales simplemente investigando la conectividad nerviosa. Por ello, nuestro laboratorio recurrió a una técnica de enfriamiento para realizar desactivaciones reversibles de la corteza auditiva mientras se registraban las respuestas evocadas al paradigma *oddball* en el colículo inferior de la rata (Anderson & Malmierca, 2013). Los resultados demostraron que la adaptación específica al estímulo repetitivo persistía tras la desactivación cortical. Es más, tan solo la mitad de las neuronas coliculares mostraron cambios significativos en sus niveles de adaptación. Esto confirma una modulación cortical prominente, pero también demuestra que la percepción de novedad sensorial comienza a formarse en el mesencéfalo, hasta cierto punto independientemente de la innervación corticocolicular (Malmierca et al., 2015). A la vista de estos resultados, sería mucho más plausible que las respuestas diferenciales al paradigma *oddball* presentes en la corteza auditiva viniesen heredadas de los núcleos auditivos subcorticales que viceversa. Sin embargo, tampoco se puede descartar la posibilidad de que tales respuestas diferenciales se generen *de novo* en la circuitería intrínseca de cada estación de procesamiento, de forma relativamente independiente, y que luego emerja un efecto acumulativo a lo largo de la vía auditiva ascendente. De cualquier manera, dado que ningún otro núcleo auditivo anterior al mesencéfalo presenta respuestas diferenciales (Ayala et al.,

2013), el colículo inferior es el candidato más plausible a ser el origen neuroanatómico de la percepción de novedad en la audición.

El presente trabajo recoge todo este conocimiento previo y lo lleva a un paso más allá, demostrando que las respuestas diferenciales al paradigma *oddball* que se observan en las neuronas auditivas del cerebro medio no son el resultado de un mero proceso de adaptación, sino más bien la huella fisiológica de un modelo generativo que impone expectativas sobre la información auditiva entrante. Los resultados aquí expuestos proporcionan datos empíricos que respaldan que el colículo inferior alberga el primer nivel de una sofisticada jerarquía de procesamiento predictivo dentro del sistema auditivo. Aunque la Hipótesis de la Adaptación podría llegar a explicar las respuestas neuronales observadas en el núcleo central, esta se descubre insuficiente en la corteza del colículo inferior. Por un lado, las condiciones no discrepantes establecidas por las secuencias de control sin repeticiones, tanto multi-estándar como cascadas, tienden a evocar las respuestas más robustas observadas en el núcleo central del colículo inferior. Por lo tanto, no se puede descartar completamente que en las neuronas del núcleo central tenga lugar una disminución en su capacidad de respuesta a las condiciones discrepantes a causa de una adaptación cruzada inducida por la tonalidad repetitiva de la condición estándar, según lo propuesto por la Hipótesis de Adaptación (Mill et al., 2011; Taaseh et al., 2011). Por otro lado, las neuronas de la corteza del colículo tendieron a exhibir respuestas mayores a la condición discrepante que a cualquier otra condición, confirmando así la Hipótesis de la Expectativa surgida del marco teórico del procesamiento predictivo. La Hipótesis de la Expectativa argumenta que las respuestas a estímulos anómalos aumentan porque las neuronas están señalando errores de predicción ponderadas por su precisión esperada. Por ello, el término de ‘adaptación específica al estímulo repetitivo’ no sería el más adecuado para describir el procesamiento auditivo con sesgo de probabilidad realizado por las neuronas del colículo inferior. Las respuestas diferenciales al paradigma *oddball* que contienen componentes de error de predicción pueden observarse en animales anestesiados, lo que implica que la señalización de errores de predicción en el colículo inferior no depende completamente del estado de conciencia. No obstante, también se observó que el componente genuino de error de predicción que se puede identificar dentro de la actividad evocada por sonidos inesperados en la corteza del colículo inferior es mayor en animales despiertos. Además, los datos obtenidos indican que son las neuronas con campos receptivos altamente desorganizados las principales responsables de la señalización temprana de errores de

predicción en el sistema auditivo. Por todo ello, puede concluirse que el colículo inferior es el primer núcleo auditivo que genera señales de error de predicción en la vía auditiva ascendente.

Las neuronas de la corteza del colículo inferior también exhiben una supresión por repetición del estímulo mucho más intensa que las neuronas del núcleo central, muy probablemente porque las primeras funcionan bajo una mayor influencia inhibitoria provocada por la actividad predictiva de niveles de procesamiento superiores. Es muy probable que la transmisión descendente de expectativas se produzca a través de la innervación corticocolicular sobre circuitos inhibitorios intrínsecos de la corteza del colículo, como sugiere un estudio de conectividad de nuestro laboratorio (Ayala et al., 2015). Dado que la anestesia tiende a afectar el procesamiento cortical más que el subcortical, la disminución parcial de la señalización de errores de predicción que muestran las neuronas de la corteza del colículo inferior bajo anestesia puede deberse a la reducción de las influencias descendentes de la corteza auditiva. Además, las principales generadoras de errores de predicción son las neuronas con campos receptivos desorganizados (Figura 7D), los cuales son probablemente resultado de la acción inhibidora (Le Beau et al., 2001). Dicha acción inhibitoria podría ser el resultado de influencias predictivas descendentes de la corteza auditiva impuestas sobre las neuronas coliculares. Sin embargo, debemos recordar que las respuestas diferenciales al paradigma *oddball* en las neuronas del colículo inferior persisten tras desactivar la corteza auditiva (Anderson y Malmierca, 2013). Esto sugiere que al menos parte de la actividad de señalización de errores de predicción en el mesencéfalo auditivo podría generarse completamente *de novo* en una red de procesamiento predictivo local, implementada dentro de las capas de la corteza del colículo inferior de forma parecida a las redes de procesamiento predictivo propuestas para la corteza cerebral (Figura 19). Una forma adecuada de confirmarlo empíricamente sería combinar presentaciones del paradigma *oddball* y de las secuencias de control sin repetición con desactivaciones reversibles de la corteza auditiva. En caso de que la corteza del colículo inferior probase ser capaz de generar señales de error sin ninguna influencia cortical, resultaría más plausible que el origen de las leves respuestas diferenciales del núcleo central se debiesen, efectivamente, a la actividad predictiva de la corteza del colículo inferior, cuyas neuronas estarían suprimiendo las respuestas a la condición estándar por la expectativa de repetición impuesta sobre las neuronas del núcleo central, algo que no pudo ser confirmado con la metodología actual. Ya sea que las expectativas sobre la información auditiva entrante tengan un origen cortical o se generen *in situ* dentro de la circuitería colicular intrínseca, lo que confirman los resultados es que la corteza del colículo inferior alberga los primeros elementos

neuronales en la vía auditiva ascendente capaces de señalar errores de predicción. Dado que los modelos actuales de procesamiento predictivo sitúan las primeras unidades de error en la corteza cerebral (Figura 19), el descubrimiento de señales de error generadas en el colículo inferior representa un gran avance en nuestra comprensión de la implementación neurológica del procesamiento predictivo dentro del sistema auditivo.

Tras debatir los datos microscópicos del registro extracelular, conviene ahora ponerlos en relación con las observaciones a escala mesoscópica. Un estudio previo de los potenciales de campo local de la rata había encontrado potenciales de disparidad entre 18 ms y 43 ms tras el inicio del sonido en la corteza del colículo inferior (Patel et al., 2012). Mis datos muestran que estos potenciales de disparidad emergen de todo el colículo inferior, incluyendo su núcleo central, tan pronto como la información auditiva entra en el mesencéfalo. El potencial de disparidad comienza en torno a los primeros 4-6 ms y termina pasados los 150 ms. Esta amplia ventana de tiempo abarca los periodos en los que el conteo de espigas de las neuronas también refleja respuestas diferenciales. Un desarrollo tan veloz también puede acomodar el potencial de disparidad identificable tempranamente a nivel macroscópico en el potencial auditivo evocado masivo del tronco encefálico, donde las respuestas diferenciales al paradigma *oddball* fueron máximas entre 8 ms y 10 ms tras del inicio del sonido (Duque et al., 2018). Un estudio que empleó imagen por resonancia magnética funcional dependiente del nivel de oxígeno en sangre también mostró que los potenciales de disparidad auditivos se pueden detectar en el tejido del colículo inferior tan solo unos segundos después del inicio del sonido (Gao et al., 2014). Con respecto la señalización de errores de predicción, los datos sobre el potencial de campo local de la corteza del colículo inferior contienen potenciales de error entre 45 ms y 60 ms después del inicio del estímulo. Este potencial mesoscópico coincide en tiempo con el periodo en el que el conteo de espigas revelaba una señalización de errores de predicción más intensa. Hasta la fecha, no se han descrito señales de error de predicción a escala macroscópica dentro del potencial evocado auditivo masivo del tronco encefálico de los roedores. Sin embargo, estudios previos de electroencefalograma (Slabu et al., 2012) e imagen por resonancia magnética funcional (Cacciaglia et al., 2015) que emplearon la secuencia multi-estándar en su diseño, encontraron un componente del potencial evocado auditivo temprano que podría ser interpretado como un potencial de error de predicción generado en el mesencéfalo auditivo humano. Por lo tanto, los resultados permiten relacionar las señales de disparidad y errores de predicción mesencefálicas observadas a escala microscópica (conteo de espigas), mesoscópica (potencial de campo local) y macroscópica (potencial evocado auditivo

del tronco encefálico). De esta forma, el presente estudio completa la panorámica sobre el procesamiento predictivo aportando valiosa información sobre lo que sucede en el nivel celular, algo imposible de obtener actualmente en estudios sobre el cerebro humano.

La señalización de errores de predicción en la corteza del colículo inferior es relativamente más robusta cuando el sonido se presenta a baja intensidad, y también cuando el tono discrepante es más agudo que el estándar. Esto sugiere que la corteza del colículo inferior podría estar implementando algún tipo de mecanismo de ganancia para dotar a los estímulos auditivos sutiles, pero infrecuentes e informativos, de una mayor prominencia en nuestra percepción. Con respecto a la intensidad del sonido, trabajos previos de modelización indican que las neuronas serán más sensibles al cambio estimular para los rangos físicos donde la tasa de disparo de la neurona esté muy por debajo del nivel de saturación (Abbott et al., 1997), lo cual ha sido contrastado empíricamente por un estudio previo de nuestro laboratorio en el colículo inferior (Duque et al., 2012). A medida que el sonido se intensifica, las neuronas auditivas se acercarán más a su nivel de saturación, agotando así su rango dinámico y, por tanto, su capacidad de aumentar su tasa de disparo para señalar un error de predicción sobre una característica inesperada de la entrada sensorial. Esto explicaría por qué las señales de error de predicción son muy sensibles al volumen del sonido, mientras que los niveles de supresión por expectativa de repetición apenas se ven afectados por los cambios de intensidad.

En cuanto a la influencia de los cambios a sonidos más agudos, podría tratarse de un fenómeno puramente específico. El sistema auditivo de los roedores está más preparado para procesar sonidos de alta frecuencia, como las vocalizaciones ultrasónicas que estas especies emplean para comunicarse. No obstante, también hay lugar para una explicación no relativa a la especie, ya que se han encontrado asimetrías en la sensibilidad a la dirección del cambio de frecuencia (a más agudo o a más grave) a nivel macroscópico en estudios del potencial de disparidad tanto en animales (Harms et al., 2014) como en humanos (Peter et al., 2010). Cabría argumentar que una preferencia por tonos más agudos puede contribuir a definir las relaciones fondo-figura entre objetos auditivos de manera más eficaz. Las frecuencias más graves pueden viajar largas distancias a través de diferentes medios de transmisión, ya que superan mejor los obstáculos en su camino hacia nuestros oídos. Por consiguiente, estas entradas auditivas tienden a informarnos sobre sucesos distantes que a menudo no son útiles para determinar nuestros estados en el entorno ni están relacionados con nuestras metas inmediatas. De esta manera, estos cambios a frecuencias graves podrían ser más propensos a ser procesados como

un ruido de fondo. Por el contrario, el procesamiento auditivo de frecuencias más agudas podría verse facilitado fisiológicamente, ya que su dificultad para recorrer largas distancias y su propensión a ser bloqueadas por cambios del medio de transmisión implican que suelen transmitir información auditiva generada en nuestro entorno cercano, siendo por tanto potencialmente más informativas y relacionadas con nuestros estados y metas. Por lo tanto, un paradigma *oddball* ascendente podría interpretarse fácilmente como un sonido 'figura' que surge de un 'fondo' de ruido estándar, mientras que el tono desviado dentro del paradigma *oddball* descendente no se beneficiaría de ningún procesamiento facilitado. Es probable que este mecanismo temprano de evaluación automática de la relevancia, dependiente de la intensidad y la tonalidad, facilite la percepción auditiva en condiciones desafiantes. Esta situación podría darse, por ejemplo, cuando un ruido de fondo relativamente intenso enmascara un sonido inesperado y potencialmente informativo, como se ha descrito en el sistema visual (Hupé et al., 1998).

Este mecanismo de facilitación cobra especial relevancia en situaciones donde una discriminación auditiva eficiente y veloz puede ser crítica para la supervivencia, ya que ayudaría a detectar rápidamente posibles amenazas basadas en señales auditivas sutiles, como puede ser el débil chasquido de una pequeña rama causado por la pisada de un depredador en medio del ruido relativamente más intenso de la jungla. En este ejemplo, la saliencia perceptiva de la débil señal del depredador se vería reforzada directamente por el error de predicción, pero también indirectamente, ya que la actividad neuronal evocada por el ruido de fondo predecible se verá suprimida por la expectativa de repetición. El contraste resultante entre una 'figura' auditiva inesperada, más silenciosa y aguda, y un 'fondo' auditivo redundante, más intenso y grave, permite que el sistema auditivo forme una percepción clara del chasquido que sería imposible de lograr de otra manera. Según los datos empíricos disponibles, este mecanismo de ganancia del error de predicción dependiente de la intensidad y el tono del sonido parece exclusivo de la corteza del colículo inferior. Por lo tanto, la característica más distintiva del procesamiento predictivo auditivo mesencefálico es que las señales de error de predicción informan principalmente sobre cambios inesperados en las características físicas del sonido.

El procesamiento predictivo auditivo se manifiesta por primera vez en los circuitos corticales del colículo inferior, probablemente debido a su posición y características neuroanatómicas únicas dentro del sistema auditivo. Todas las vías auditivas ascendentes convergen en el colículo inferior antes de inervar el tálamo y la corteza auditiva, convirtiendo

al colículo inferior en un nodo de transmisión casi obligatorio para la información auditiva entrante (Malmierca, 2015). Además de recibir información de los núcleos auditivos inferiores del tronco encefálico, las regiones corticales del cerebro e incluso otras estructuras extra-auditivas también envían proyecciones excitadoras, inhibidoras y neuromoduladoras al colículo inferior, especialmente a sus cortezas (Figura 4). Esta rica conectividad, combinada con su circuitería cortical en 3 capas (Figuras 5 y 6), podría dotar al colículo inferior de todos los elementos necesarios para realizar procesamiento predictivo dentro de su red neuronal. Por tanto, la corteza del colículo podría albergar los primeros niveles de procesamiento predictivo jerárquico del sistema auditivo, cumpliendo así un papel funcional análogo al de la corteza visual primaria en el caso del sistema visual (King & Nelken, 2009; Rao & Ballard, 1999).

En conclusión, en contraste con la creencia prevalente, el colículo inferior es un actor clave en la identificación de la novedad auditiva, perfectamente capaz de realizar el procesamiento de sesgos de probabilidad. Como demuestra esta investigación, el colículo inferior realiza procesamiento predictivo y emite errores de predicción que codifican las características físicas inesperadas en la información auditiva entrante.

VII.5.b.- La inervación dopaminérgica del colículo inferior modula la configuración del procesamiento predictivo auditivo temprano

La liberación de dopamina exógena en el microdominio de las neuronas de la corteza del colículo inferior generó efectos heterogéneos, en consonancia con otros estudios previos (Gittelman et al., 2013; Hoyt et al., 2019). Estos efectos demostraron ser consistentes, con efectos contrarios según la aplicación de agonistas o antagonistas de los receptores dopaminérgicos en 5 neuronas individuales (Figura 27). Tal consistencia implica que las diferentes propiedades intrínsecas y configuración sináptica de cada neurona de la corteza del colículo inferior son la causa de la heterogeneidad de los efectos dopaminérgicos de la muestra.

A pesar de la heterogeneidad individual, los datos también describen una tendencia poblacional principal. La aplicación de dopamina induce una disminución en las respuestas a la condición discrepante del paradigma *oddball* de hasta un 30%, mientras que ni las respuestas a la condición estándar ni a la condición no discrepante se vieron significativamente afectadas por la manipulación dopaminérgica. Dado que la respuesta a estímulos inesperados disminuyó mientras que la respuesta a los estímulos predecibles permaneció estable, la dopamina inyectada en el microdominio de las neuronas de la corteza del colículo inferior parece modular

exclusivamente la señalización de errores de predicción. Esta reducción neta de las respuestas a estímulos inesperados bajo la influencia de la dopamina es única en comparación con los efectos de otros neurotransmisores y neuromoduladores en las neuronas del colículo inferior. Las manipulaciones GABAérgicas y glutamatérgicas alteran la excitabilidad general de las neuronas coliculares, ejerciendo efectos simétricos sobre las respuestas a las condiciones discrepantes y estándares (Ayala et al., 2016; Ayala & Malmierca, 2018; Pérez-González et al., 2012). Por el contrario, la manipulación colinérgica y cannabinoide produce efectos asimétricos que afectan principalmente a la respuesta a la condición estándar (Ayala & Malmierca, 2015; Valdés-Baizabal et al., 2017). La activación de los receptores muscarínicos M_1 y los receptores cannabinoides CB_1 tendió a reducir la respuesta diferencial al paradigma *oddball* al aumentar la responsividad a estímulos repetitivos. La aplicación de dopamina también induce efectos asimétricos, pero en contraste con los casos anteriores, la activación de receptores dopaminérgicos tiende a reducir la respuesta diferencial al disminuir la responsividad a estímulos inesperados (Figura 39). Además, cuando se aplicó el antagonista a receptores de tipo D_2, algunas neuronas de la corteza del colículo inferior manifestaron cambios significativos en sus respuestas diferenciales al paradigma *oddball*. Estas alteraciones implican que la dopamina se libera de forma endógena en respuesta al sonido en algunas zonas de la corteza del colículo inferior. Por lo tanto, la dopamina modula las respuestas diferenciales al paradigma *oddball* de las neuronas de la corteza del colículo inferior, principalmente al disminuir su responsividad a estímulos auditivos inesperados. Además, los resultados de la microiontoforesis de eticlopride indican que tal reducción de la magnitud de los errores de predicción está mediada por receptores de tipo D_2.

Una vez descritos los efectos de la manipulación dopaminérgica, cabe preguntarse qué clase de proceso modulador natural podrían estar imitando estas aplicaciones microiontoforéticas de dopamina exógena. ¿Qué podrían significar todos estos cambios inducidos por la dopamina en la respuesta neuronal de la corteza del colículo desde una perspectiva funcional? La dopamina se considera comúnmente como el neurotransmisor modulador que subyace a experiencias fenomenológicas como el placer y la satisfacción. Esta connotación ‘hedónica’ proviene de los enfoques clásicos del condicionamiento operante que enfatizan el papel de la dopamina en la anticipación y búsqueda de refuerzos o resultados gratificantes (Fiorillo et al., 2003; Mirenowicz & Schultz, 1996; Schultz et al., 1997). Abundante evidencia empírica respalda que la dopamina regula el movimiento, la motivación y el aprendizaje al rastrear los fracasos de nuestras expectativas de recompensa, los cuales se

codificarían como *errores de predicción de recompensa* (Schultz, 1998, 2007, 2016b). Así, según esta propuesta clásica del marco teórico del aprendizaje por refuerzo, existirían 2 tipos de señales de error de predicción. Por un lado, están los errores de predicción sensoriales, como los errores de predicción auditivos discutidos en la sección anterior, los cuales informan sobre la *sorpresa* de las entradas sensoriales inesperadas en valores absolutos. Por otro lado, existirían errores de predicción de recompensa, característicos del sistema dopaminérgico, los cuales comunican si los resultados han sido mejores o peores de lo esperado, lo que genera un error de predicción con signo positivo o negativo (Den Ouden et al., 2012). Por regla general, las neuronas dopaminérgicas reportarían errores de predicción de recompensa positivos al aumentar sus tasas de disparo fásicas, y errores de predicción de recompensa negativos al reducir sus tasas de disparo tónicas (Schultz, 1998, 2007, 2016b). Por lo tanto, las neuronas dopaminérgicas señalarían una ambivalencia motivacional, la cual guía los procesos motores, de aprendizaje y de toma de decisiones de manera adaptativa en función de los resultados obtenidos respecto de los resultados esperados.

De acuerdo con el marco teórico del aprendizaje por refuerzo, las inyecciones microiontoforéticas de dopamina podrían estar imitando algún tipo de señal de refuerzo, un error de predicción de recompensa positivo, que en condiciones naturales podría transmitirse a través de proyecciones dopaminérgicas desde el núcleo subparafascicular del tálamo a la corteza del colículo inferior (Batton et al., 2018; Gittelman et al., 2013; Hurd et al., 2001; Nevue, Felix, et al., 2016; Weiner et al., 1991). Hablando en términos especulativos, tal entrada dopaminérgica podría tener por objetivo inducir la potenciación a largo plazo en las neuronas coliculares para construir asociaciones duraderas entre determinadas señales acústicas y unos resultados gratificantes, contribuyendo así a establecer expectativas de recompensa (Hosomi et al., 1995; Y. Zhang & Wu, 2000). Sin embargo, no veo por qué estos errores de predicción de recompensa positivos inducidos artificialmente habrían de mitigar la transmisión de errores de predicción auditivos desde la corteza del colículo inferior, como demuestran los resultados. Además, cabe mencionar que algunos otros estudios ponen en tela de juicio esta comprensión clásica de la función dopaminérgica. Las consecuencias aversivas y los indicios que las predicen pueden provocar aumentos de la actividad dopaminérgica fásica (Bromberg-Martin et al., 2010; Matsumoto & Hikosaka, 2009; Matsumoto & Takada, 2013; Young et al., 1993; Zweifel et al., 2011), al igual que algunas condiciones experimentales donde los errores de predicción de recompensa deberían ser teóricamente cero, como en el caso de estímulos inesperados o sorprendentes sin valor hedónico (Bromberg-Martin et al., 2010; Comoli et al.,

2003; Dommett et al., 2005; Horvitz, 2000; Ljungberg et al., 1992; Sadacca et al., 2016; Strecker & Jacobs, 1985). Estas respuestas dopaminérgicas parecen informar sobre estímulos sensoriales que pueden tener relevancia conductual y que por tanto deberían desencadenar una respuesta coordinada adecuada. De esta manera, estas descargas dopaminérgicas estarían codificando una saliencia perceptiva o notoriedad, sin ningún valor positivo o negativo. En principio, los errores de predicción de recompensa con signo y sin signo no son mutuamente excluyentes, y hoy en día existe un cierto consenso de que la dopamina participa en la atribución de saliencia física y sorpresa a las entradas sensoriales (Diederen & Fletcher, 2020). Algunos autores sugieren que los estímulos novedosos y físicamente salientes pueden ser intrínsecamente gratificantes, ya que proporcionan nueva información que podría resultar valiosa para desarrollar un comportamiento adaptativo (Daw et al., 2002; Reed et al., 1996). Otros trabajos del marco teórico del aprendizaje por refuerzo postulan una señalización dopaminérgica dual, la cual reportaría respectivamente valor 'sorpresa' y valores 'hedónicos' en paralelo (Fiorillo, 2013; Schultz, 2016a).

Siguiendo una lógica distinta, el marco teórico del procesamiento predictivo aboga por una explicación más integradora de la función dopaminérgica, no vinculada específicamente al procesamiento de recompensas. Para el marco del procesamiento predictivo, el error de predicción sin signo explica tanto la percepción como el aprendizaje, acomodando sin problemas las respuestas dopaminérgicas provocadas por la sorpresa. El comportamiento está óptimamente adaptado, no cuando la recompensa (error de predicción de recompensa positivo) se maximiza, sino cuando la sorpresa (error de predicción sin signo) se minimiza, ya que esto evita que el organismo mantenga interacciones potencialmente dañinas con su medio ambiente (Friston et al., 2012, 2015). La minimización del error de predicción se busca mediante 2 procesos: (1) la inferencia perceptiva, mejorando el modelo interno o representación del mundo para explicar mejor la entrada sensorial; y (2) inferencia activa, cambiando la entrada sensorial al iniciar acciones con resultados predecibles (Friston et al., 2015, 2017; Parr & Friston, 2017). Las tareas clásicas de condicionamiento operante pueden haber confundido las respuestas dopaminérgicas con errores de predicción de recompensa debido al papel más genérico que desempeña la dopamina en la minimización del error de predicción. Las señales que predicen recompensas minimizan el error de predicción al resolver la incertidumbre sobre los resultados futuros, lo cual es comunicado por una liberación de dopamina (FitzGerald et al., 2015; Friston et al., 2012, 2015; Schwartenbeck et al., 2015). Desde el punto de vista del procesamiento predictivo, tiene mucho más sentido que el sistema dopaminérgico sea el encargado de

codificar el nivel de incertidumbre en nuestras inferencias. Esto es debido a que los neuromoduladores como la dopamina no pueden excitar o inhibir directamente las respuestas postsinápticas, sino que solo pueden ponderar las respuestas postsinápticas a otros neurotransmisores, actuando como un mecanismo de control de la ganancia. Por lo tanto, la única función posible del sistema dopaminérgico sería la de codificar la precisión esperada, desempeñando un papel tanto en la inferencia perceptiva como en la inferencia activa al conferir flexibilidad contextual al procesamiento sensorial y motor.

En consecuencia, la Hipótesis de la Expectativa evita la necesidad de 2 tipos distintos de señalización de errores de predicción, ofreciendo una interpretación más parsimoniosa de los datos a través de un único mecanismo de ponderación de la precisión esperada. De acuerdo con este enfoque, al cambiar los niveles de dopamina en un dominio sináptico, se estaría alterando la ganancia de los mensajes sensoriales por ahí transmitidos, y en este caso, de los errores de predicción. Por lo tanto, dado que las aplicaciones microiontoforéticas de dopamina en el mesencéfalo auditivo tienden a reducir exclusivamente las respuestas evocadas por sonidos inesperados, la liberación natural de dopamina en la corteza del colículo inferior podría estar codificando una baja precisión esperada de los errores de predicción auditivos allí generados. En otras palabras, el rol de la entrada dopaminérgica a la corteza del colículo inferior podría ser el de aplicar una ganancia postsináptica negativa que amortigüe la propagación de señales tempranas de errores de predicción auditivos.

En condiciones naturales, dicha regulación a nivel mesencefálico del flujo ascendente de las señales tempranas de error de predicción podría ser realizada por las neuronas dopaminérgicas del núcleo subparafascicular del tálamo que se proyectan la corteza del colículo inferior (Batton et al., 2018; Nevue, Elde, et al., 2016; Yasui et al., 1992). Muchos centros de procesamiento auditivo inervan el núcleo subparafascicular, tales como la corteza auditiva, el cuerpo geniculado medial del tálamo, el colículo inferior y el complejo olivar superior, lo cual le dota de una rica entrada de información auditiva (Figura 39; Arnault & Roger, 1990; LeDoux et al., 1985; Wang et al., 2006; Yasui et al., 1990, 1992). El núcleo subparafascicular del tálamo recibe proyecciones incluso de otros centros extra-auditivos que realizan funciones de orden superior en el procesamiento e integración sensorial, como la corteza prefrontal y las capas profundas del colículo superior (Wang et al., 2006). Es más, la participación de algunas de estas estructuras nerviosas en el procesamiento predictivo jerárquico de la información auditiva ya ha sido corroborada empíricamente (Casado-Román,

Carbajal et al., 2020; Parras et al., 2017; Figura 38). Por lo tanto, es razonable pensar que la innervación dopaminérgica del núcleo subparafascicular del tálamo a la corteza del colículo inferior podría ser un componente integral de la jerarquía de procesamiento auditivo que nos permite escuchar de manera eficiente. La actividad dopaminérgica del núcleo subparafascicular del tálamo jugaría así un papel clave en las fases tempranas del proceso de actualización de la representación interna del escenario auditivo. La conectividad recíproca del núcleo subparafascicular con múltiples núcleos a distintos niveles de la vía auditiva y más allá, podría dotar al subparafascicular de la base estructural necesaria para implementar una codificación óptima de la precisión esperada. Mediante la liberación o no de dopamina, el núcleo subparafascicular podría modular el peso específico que tendrán los errores de predicción enviados desde la corteza del colículo sobre niveles superiores de procesamiento auditivo (Figura 38). Esta red neuromoduladora dopaminérgica permitiría al sistema auditivo gestionar la integración de entradas sensoriales inesperadas y confiables desde una etapa muy temprana del procesamiento auditivo, lo cual recalca una vez más la contribución fundamental del mesencéfalo auditivo a una inferencia perceptiva eficiente de la información auditiva novedosa.

VII.6.- CONCLUSIONES

A pesar de que las aportaciones subcorticales a la percepción de novedad sensorial han sido tradicionalmente infravaloradas por la perspectiva más bien corticocéntrica que a menudo predomina en la literatura neurocognitiva, los resultados aquí presentados proporcionan una base empírica sólida en favor de la participación directa y clave del colículo inferior en una red neurológica jerárquica que implementa procesamiento predictivo auditivo. Las principales conclusiones de esta tesis y su relevancia para el avance científico son las siguientes:

1. El colículo inferior es la estación más temprana en la vía auditiva ascendente que genera señales de error de predicción, los cuales se propagan por la vía no lemniscal a niveles de procesamiento auditivo superiores.
2. Las neuronas de la corteza del colículo inferior que exhiben campos receptivos altamente desorganizados son las principales generadoras de errores de predicción dentro del mesencéfalo auditivo.

3. La corteza del colículo inferior genera errores de predicción para señalar cambios físicos inesperados en el sonido, mientras que en los niveles de procesamiento auditivo jerárquicamente más altos parecen señalar cambios más abstractos.
4. El estado de conciencia influye en el procesamiento predictivo del mesencéfalo auditivo, ya que la vigilia fortalece la señalización de errores de predicción, muy probablemente al mejorar la precisión esperada de las neuronas de la corteza del colículo inferior.
5. La dopamina modula el procesamiento predictivo del mesencéfalo auditivo a través de receptores de tipo D_2 de formas heterogéneas, las cuales están determinadas por las propiedades intrínsecas y la configuración sináptica de cada neurona colicular.
6. La activación de receptores de tipo D_2 en la corteza del colículo inferior tiende a reducir la transmisión neta de señales de error de predicción provenientes del nivel mesencefálico, actuando como un mecanismo temprano de ganancia en el sistema auditivo.
7. La liberación de dopamina en la corteza del colículo inferior codifica la precisión esperada de las neuronas coliculares mediante el ajuste de la ganancia postsináptica de las señales de error de predicción auditivo, modulando así su influencia sobre niveles superiores de procesamiento auditivo.
8. Las proyecciones dopaminérgicas del núcleo subparafascicular del tálamo a la corteza del colículo inferior constituyen el sustrato biológico de un mecanismo temprano de ponderación de la precisión esperada, el cual regula la transmisión ascendente de señales de error de predicción a lo largo de la jerarquía de procesamiento predictivo que opera dentro del sistema auditivo.

VII.- REFERENCES

Abbott, L. F., Varela, J. A., Sen, K., & Nelson, S. B. (1997). Synaptic Depression and Cortical Gain Control. *Science, 275*(5297), 221–224. https://doi.org/10.1126/science.275.5297.221

Adams, J. C. (1979). Ascending projections to the inferior colliculus. *Journal of Comparative Neurology*, *183*(3), 519–538. https://doi.org/10.1002/cne.901830305

Adams, J. C., & Wenthold, R. J. (1979). Distribution of putative amino acid transmitters, choline acetyltransferase and glutamate decarboxylase in the inferior colliculus. *Neuroscience*, *4*(12), 1947–1951. https://doi.org/10.1016/0306-4522(79)90067-8

Adams, R. A., Stephan, K. E., Brown, H. R., Frith, C. D., & Friston, K. J. (2013). The computational anatomy of psychosis. *Frontiers in Psychiatry*, *4*, 47. https://doi.org/10.3389/fpsyt.2013.00047

Aghamolaei, M., Zarnowiec, K., Grimm, S., & Escera, C. (2016). Functional dissociation between regularity encoding and deviance detection along the auditory hierarchy. *European Journal of Neuroscience*, *43*(4), 529–535. https://doi.org/10.1111/ejn.13138

Ahuja, T. K., & Wu, S. H. (2007). Intrinsic membrane properties and synaptic response characteristics of neurons in the rat's external cortex of the inferior colliculus. *Neuroscience*, *145*(3), 851–865. https://doi.org/10.1016/j.neuroscience.2006.12.031

Aitchison, L., & Lengyel, M. (2017). With or without you: predictive coding and Bayesian inference in the brain. *Current Opinion in Neurobiology*, *46*, 219–227. https://doi.org/10.1016/j.conb.2017.08.010

Aitkin, L. M., Kenyon, C. E., & Philpott, P. (1981). The representation of the auditory and somatosensory systems in the external nucleus of the cat inferior colliculus. *Journal of Comparative Neurology*, *196*(1), 25–40. https://doi.org/10.1002/cne.901960104

Aitkin, L. M., & Phillips, S. C. (1984). The interconnections of the inferior colliculi through their commissure. *Journal of Comparative Neurology*, *228*(2), 210–216. https://doi.org/10.1002/cne.902280207

Aitkin, L. M., & Webster, W. R. (1971). Tonotopic organization in the medial geniculate body of the cat. *Brain Research*, *26*(2), 402–405. https://doi.org/10.1016/S0006-8993(71)80015-X

Aitkin, L. M., & Webster, W. R. (1972). Medial geniculate body of the cat: organization and responses to tonal stimuli of neurons in ventral division. *Journal of Neurophysiology*, *35*(3), 365–380. https://doi.org/10.1152/jn.1972.35.3.365

Alho, K. (1995). Cerebral generators of mismatch negativity (MMN) and its magnetic counterpart (MMNm) elicited by sound changes. *Ear and Hearing*, *16*(1), 38–51. https://doi.org/10.1097/00003446-199502000-00004

Althen, H., Grimm, S., & Escera, C. (2011). Fast detection of unexpected sound intensity

decrements as revealed by human evoked potentials. *PLoS ONE*, *6*(12). https://doi.org/10.1371/journal.pone.0028522

Althen, H., Grimm, S., & Escera, C. (2013). Simple and complex acoustic regularities are encoded at different levels of the auditory hierarchy. *European Journal of Neuroscience*, *38*(10), 3448–3455. https://doi.org/10.1111/ejn.12346

Althen, H., Huotilainen, M., Grimm, S., & Escera, C. (2016). Middle latency response correlates of single and double deviant stimuli in a multi-feature paradigm. *Clinical Neurophysiology*, *127*(1), 388–396. https://doi.org/10.1016/j.clinph.2015.04.058

Andersen, R. A., Roth, G. L., Aitkin, L. M., & Merzenich, M. M. (1980). The efferent projections of the central nucleus and the pericentral nucleus of the inferior collculus in the cat. *Journal of Comparative Neurology*, *194*(3), 649–662. https://doi.org/10.1002/cne.901940311

Andersen, R. A., Snyder, R. L., & Merzenich, M. M. (1980). The topographic organization of corticocollicular projections from physiologically identified loci in the AI, AII, and anterior auditory cortical fields of the cat. *Journal of Comparative Neurology*, *191*(3), 479–494. https://doi.org/10.1002/cne.901910310

Anderson, L. A., Christianson, G. B., & Linden, J. F. (2009). Stimulus-Specific Adaptation Occurs in the Auditory Thalamus. *Journal of Neuroscience*, *29*(22), 7359–7363. https://doi.org/10.1523/JNEUROSCI.0793-09.2009

Anderson, L. A., & Malmierca, M. S. (2013). The effect of auditory cortex deactivation on stimulus-specific adaptation in the inferior colliculus of the rat. *European Journal of Neuroscience*, *37*(1), 52–62. https://doi.org/10.1111/ejn.12018

Antunes, F. M., Nelken, I., Covey, E., & Malmierca, M. S. (2010). Stimulus-specific adaptation in the auditory thalamus of the anesthetized rat. *PLoS ONE*, *5*(11), e14071. https://doi.org/10.1371/journal.pone.0014071

Arcelli, P., Frassoni, C., Regondi, M. C., Biasi, S. De, & Spreafico, R. (1997). GABAergic neurons in mammalian thalamus: A marker of thalamic complexity? *Brain Research Bulletin*, *42*(1), 27–37. https://doi.org/10.1016/S0361-9230(96)00107-4

Arnault, P., & Roger, M. (1990). Ventral temporal cortex in the rat: Connections of secondary auditory areas Te2 and Te3. *The Journal of Comparative Neurology*, *302*(1), 110–123. https://doi.org/10.1002/cne.903020109

Ashby, W. R. (1960). *Design for a brain: The origin of adaptive behavior* (2nd ed.). Wiley. https://archive.org/details/designforbrainor00ashb

Auksztulewicz, R., & Friston, K. J. (2016). Repetition suppression and its contextual determinants in predictive coding. *Cortex*, *80*, 125–140. https://doi.org/10.1016/j.cortex.2015.11.024

Ayala, Y. A., & Malmierca, M. S. (2013). Stimulus-specific adaptation and deviance detection in the inferior colliculus. *Frontiers in Neural Circuits*, *6*(January), 1–16. https://doi.org/10.3389/fncir.2012.00089

Ayala, Y. A., & Malmierca, M. S. (2015). Cholinergic Modulation of Stimulus-Specific Adaptation in the Inferior Colliculus. *Journal of Neuroscience*, *35*(35), 12261–12272. https://doi.org/10.1523/JNEUROSCI.0909-15.2015

Ayala, Y. A., & Malmierca, M. S. (2018). The effect of inhibition on stimulus-specific adaptation in the inferior colliculus. *Brain Structure and Function*, *223*(3), 1391–1407. https://doi.org/10.1007/s00429-017-1546-4

Ayala, Y. A., Pérez-González, D., Duque, D., Nelken, I., & Malmierca, M. S. (2013). Frequency discrimination and stimulus deviance in the inferior colliculus and cochlear nucleus. *Frontiers in Neural Circuits*, *6*, 119. https://doi.org/10.3389/fncir.2012.00119

Ayala, Y. A., Pérez-González, D., & Malmierca, M. S. (2016). Stimulus-specific adaptation in the inferior colliculus: The role of excitatory, inhibitory and modulatory inputs. *Biological Psychology*, *116*, 10–22. https://doi.org/10.1016/j.biopsycho.2015.06.016

Ayala, Y. A., Udeh, A., Dutta, K., Bishop, D. C., Malmierca, M. S., & Oliver, D. L. (2015). Differences in the strength of cortical and brainstem inputs to SSA and non-SSA neurons in the inferior colliculus. *Scientific Reports*, *5*(April), 10383. https://doi.org/10.1038/srep10383

Bajo, V. M., & Moore, D. R. (2005). Descending projections from the auditory cortex to the inferior colliculus in the gerbil, Meriones unguiculatus. *Journal of Comparative Neurology*, *486*(2), 101–116. https://doi.org/10.1002/cne.20542

Bajo, V. M., Nodal, F. R., Bizley, J. K., Moore, D. R., & King, A. J. (2007). The ferret auditory cortex: Descending projections to the inferior colliculus. *Cerebral Cortex*, *17*(2), 475–491. https://doi.org/10.1093/cercor/bhj164

Bamford, N. S., Robinson, S., Palmiter, R. D., Joyce, J. A., Moore, C., & Meshul, C. K. (2004). Dopamine modulates release from corticostriatal terminals. *The Journal of Neuroscience : The Official Journal of the Society for Neuroscience*, *24*(43), 9541–9552. https://doi.org/10.1523/JNEUROSCI.2891-04.2004

Bartha-Doering, L., Deuster, D., Giordano, V., am Zehnhoff-Dinnesen, A., & Dobel, C. (2015). A systematic review of the mismatch negativity as an index for auditory sensory memory: From basic research to clinical and developmental perspectives. *Psychophysiology*, *52*(9), 1115–1130. https://doi.org/10.1111/psyp.12459

Bartlett, E. L., & Smith, P. H. (1999). Anatomic, intrinsic, and synaptic properties of dorsal and ventral division neurons in rat medial geniculate body. *Journal of Neurophysiology*, *81*(5), 1999–2016. https://doi.org/10.1152/jn.1999.81.5.1999

Bartlett, E. L., Stark, J. M., Guillery, R. W., & Smith, P. H. (2000). Comparison of the fine structure of cortical and collicular terminals in the rat medial geniculate body. *Neuroscience*, *100*(4), 811–828. https://doi.org/10.1016/S0306-4522(00)00340-7

Bastos, A. M., Usrey, W. M., Adams, R. A., Mangun, G. R., Fries, P., & Friston, K. J. (2012). Canonical Microcircuits for Predictive Coding. *Neuron*, *76*(4), 695–711. https://doi.org/10.1016/j.neuron.2012.10.038

Batton, A. D., Blaha, C. D., Bieber, A., Lee, K. H., & Boschen, S. L. (2018). Stimulation of

the subparafascicular thalamic nucleus modulates dopamine release in the inferior colliculus of rats. *Synapse*, 0–2. https://doi.org/10.1002/syn.22073

Bäuerle, P., von der Behrens, W., Kössl, M., & Gaese, B. H. (2011). Stimulus-Specific Adaptation in the Gerbil Primary Auditory Thalamus Is the Result of a Fast Frequency-Specific Habituation and Is Regulated by the Corticofugal System. *Journal of Neuroscience*, *31*(26), 9708–9722. https://doi.org/10.1523/JNEUROSCI.5814-10.2011

Bendor, D. (2015). The role of inhibition in a computational model of an auditory cortical neuron during the encoding of temporal information. *PLoS Computational Biology*, *11*(4), 1004197. https://doi.org/10.1371/journal.pcbi.1004197

Beyerl, B. D. (1978). Afferent projections to the central nucleus of the inferior colliculus in the rat. *Brain Research*, *145*(2), 209–223. https://doi.org/10.1016/0006-8993(78)90858-2

Bibikov, N. G. (1977). ["Novelty" neurons in the frog auditory system]. *Zh Vyssh Nerv Deiat Im I P Pavlova*, *27*(5), 1075–1082. http://www.ncbi.nlm.nih.gov/pubmed/930404

Bishop, D. V. M. (2007). Using Mismatch Negativity to Study Central Auditory Processing in Developmental Language and Literacy Impairments: Where Are We, and Where Should We Be Going? *Psychological Bulletin*, *133*(4), 651–672. https://doi.org/10.1037/0033-2909.133.4.651

Bordi, F., & Ledoux, J. E. (1994). Response properties of single units in areas of rat auditory thalamus that project to the amygdala I. Acoustic discharge patterns and frequency receptive fields. *Experimental Brain Research*, *98*(2), 261–274.

Bordi, F., & LeDoux, J. E. (1994). Response properties of single units in areas of rat auditory thalamus that project to the amygdala - II. Cells receiving convergent auditory and somatosensory inputs and cells antidromically activated by amygdala stimulation. *Experimental Brain Research*, *98*(2), 275–286. https://doi.org/10.1007/BF00228415

Brawer, J. R., Morest, D. K., & Kane, E. C. (1974). The neuronal architecture of the cochlear nucleus of the cat. *Journal of Comparative Neurology*, *155*(3), 251–299. https://doi.org/10.1002/cne.901550302

Bromberg-Martin, E. S., Matsumoto, M., & Hikosaka, O. (2010). Dopamine in Motivational Control: Rewarding, Aversive, and Alerting. *Neuron*, *68*(5), 815–834. https://doi.org/10.1016/j.neuron.2010.11.022

Bullock, D. C., Palmer, A. R., & Rees, A. (1988). Compact and easy-to-use tungsten-in-glass microelectrode manufacturing workstation. *Medical & Biological Engineering & Computing*, *26*(6), 669–672. https://doi.org/10.1007/BF02447511

Cacciaglia, R., Escera, C., Slabu, L., Grimm, S., Sanjuán, A., Ventura-Campos, N., & Ávila, C. (2015). Involvement of the human midbrain and thalamus in auditory deviance detection. *Neuropsychologia*, *68*, 51–58. https://doi.org/10.1016/j.neuropsychologia.2015.01.001

Caicedo, A., & Eybalin, M. (1999). Glutamate receptor phenotypes in the auditory brainstem and mid-brain of the developing rat. *European Journal of Neuroscience*, *11*(1), 51–74.

https://doi.org/10.1046/j.1460-9568.1999.00410.x

Caicedo, A., & Herbert, H. (1993). Topography of descending projections from the inferior colliculus to auditory brainstem nuclei in the rat. *Journal of Comparative Neurology*, *328*(3), 377–392. https://doi.org/10.1002/cne.903280305

Calabresi, P., Mercuri, N. B., Sancesario, G., & Bernardi, G. (1993). Electrophysiology of dopamine-denervated striatal neurons. Implications for Parkinson's disease. *Brain : A Journal of Neurology*, *116 (Pt 2*, 433–452. http://www.ncbi.nlm.nih.gov/pubmed/8096420

Camalier, C. R., Scarim, K., Mishkin, M., & Averbeck, B. B. (2019). A comparison of auditory oddball responses in dorsolateral prefrontal cortex, basolateral amygdala, and auditory cortex of macaque. *Journal of Cognitive Neuroscience*, *31*(7), 1054–1064. https://doi.org/10.1162/jocn_a_01387

Carandini, M., & Ferster, D. (1997). A tonic hyperpolarization underlying contrast adaptation in cat visual cortex. *Science*, *276*(5314), 949–952. https://doi.org/10.1126/science.276.5314.949

Carbajal, G. V., & Malmierca, M. S. (2018a). The Neuronal Basis of Predictive Coding Along the Auditory Pathway: From the Subcortical Roots to Cortical Deviance Detection. *Trends in Hearing*, *22*, 233121651878482. https://doi.org/10.1177/2331216518784822

Carbajal, G. V., & Malmierca, M. S. (2020). Novelty Processing in the Auditory System: Detection, Adaptation or Expectation? In B. Fritzsch & B. Gothe (Eds.), *The Senses: A Comprehensive Reference* (2nd ed., pp. 749–776). Elsevier. https://doi.org/10.1016/B978-0-12-809324-5.24154-0

Carbajal, G. V., & Malmierca, M. S. (2018b). The unique role of the non-lemniscal pathway on stimulus-specific adaptation (SSA) in the auditory system. In S. Santurette, T. Dau, J. Christensen-Dalsgaard, L. Tranebjærg, T. Andersen, & T. Poulsen (Eds.), *Proceedings of the International Symposium on Auditory and Audiological Research* (Vol. 6, pp. 95–106). The Danavox Jubilee Foundation. https://proceedings.isaar.eu/index.php/isaarproc/article/view/2017-12

Carral, V., Huotilainen, M., Ruusuvirta, T., Fellman, V., Näätänen, R., & Escera, C. (2005). A kind of auditory "primitive intelligence" already present at birth. *European Journal of Neuroscience*, *21*(11), 3201–3204. https://doi.org/10.1111/j.1460-9568.2005.04144.x

Casado-Román, L., Carbajal, G. V., Pérez-González, D., & Malmierca, M. S. (2020). Prediction error signaling explains neuronal mismatch responses in the medial prefrontal cortex. *PLoS Biology*, *18*(12 December), e3001019. https://doi.org/10.1371/journal.pbio.3001019

Chen, C., Cheng, M., Ito, T., & Song, S. (2018). Neuronal organization in the inferior colliculus revisited with cell-type-dependent monosynaptic tracing. *Journal of Neuroscience*, *38*(13), 3318–3332. https://doi.org/10.1523/JNEUROSCI.2173-17.2018

Chen, I.-W., Helmchen, F., & Lutcke, H. (2015). Specific Early and Late Oddball-Evoked

Responses in Excitatory and Inhibitory Neurons of Mouse Auditory Cortex. *Journal of Neuroscience*, *35*(36), 12560–12573. https://doi.org/10.1523/JNEUROSCI.2240-15.2015

Chennu, S., Noreika, V., Gueorguiev, D., Shtyrov, Y., Bekinschtein, T. A., & Henson, R. (2016). Silent Expectations: Dynamic Causal Modeling of Cortical Prediction and Attention to Sounds That Weren't. *Journal of Neuroscience*, *36*(32), 8305–8316. https://doi.org/10.1523/JNEUROSCI.1125-16.2016

Chernock, M. L., Larue, D. T., & Winer, J. A. (2004). A periodic network of neurochemical modules in the inferior colliculus. *Hearing Research*, *188*(1–2), 12–20. https://doi.org/10.1016/S0378-5955(03)00340-X

Chew, S. J., Mello, C., Nottebohm, F., Jarvis, E., & Vicario, D. S. (1995). Decrements in auditory responses to a repeated conspecific song are long-lasting and require two periods of protein synthesis in the songbird forebrain. *Proceedings of the National Academy of Sciences*, *92*(8), 3406–3410. https://doi.org/10.1073/pnas.92.8.3406

Clark, A. (2013). Whatever next? Predictive brains, situated agents, and the future of cognitive science. *Behavioral and Brain Sciences*, *36*(3), 181–204. https://doi.org/10.1017/S0140525X12000477

Clark, A. (2016). *Surfing uncertainty: prediction, action, and the embodied mind*. Oxford University Press.

Clark, A. (2017). Predictions, precision, and agentive attention. In *Consciousness and Cognition* (Vol. 56, pp. 115–119). https://doi.org/10.1016/j.concog.2017.06.013

Clarkson, C., Herrero-Turrión, M. J., & Merchán, M. A. (2012). Cortical auditory deafferentation induces long-term plasticity in the inferior colliculus of adult rats: Microarray and qPCR analysis. *Frontiers in Neural Circuits*, *6*(OCTOBER 2012), 1–32. https://doi.org/10.3389/fncir.2012.00086

Clarkson, C., Juíz, J. M., & Merchán, M. A. (2010a). Long-term regulation in calretinin staining in the rat inferior colliculus after unilateral auditory cortical ablation. *Journal of Comparative Neurology*, *518*(20), 4261–4276. https://doi.org/10.1002/cne.22453

Clarkson, C., Juíz, J. M., & Merchán, M. A. (2010b). Transient down-regulation of sound-induced c-Fos protein expression in the inferior colliculus after ablation of the auditory cortex. *Frontiers in Neuroanatomy*, *4*(OCT), 141. https://doi.org/10.3389/fnana.2010.00141

Clerici, W. J., & Coleman, J. R. (1990). Anatomy of the rat medial geniculate body: I. Cytoarchitecture, myeloarchitecture, and neocortical connectivity. *Journal of Comparative Neurology*, *297*(1), 14–31. https://doi.org/10.1002/cne.902970103

Clerici, W. J., McDonald, A. J., Thompson, R., & Coleman, J. R. (1990). Anatomy of the rat medial geniculate body: II. Dendritic morphology. *Journal of Comparative Neurology*, *297*(1), 32–54. https://doi.org/10.1002/cne.902970104

Coleman, J. R., & Clerici, W. J. (1987). Sources of projections to subdivisions of the inferior colliculus in the rat. *Journal of Comparative Neurology*, *262*(2), 215–226.

https://doi.org/10.1002/cne.902620204

Comerchero, M. D., & Polich, J. (1999). P3a and P3b from typical auditory and visual stimuli. *Clinical Neurophysiology*, *110*(1), 24–30. https://doi.org/10.1016/S0168-5597(98)00033-1

Comoli, E., Coizet, V., Boyes, J., Bolam, J. P., Canteras, N. S., Quirk, R. H., Overton, P. G., & Redgrave, P. (2003). A direct projection from superior colliculus to substantia nigra for detecting salient visual events. *Nature Neuroscience*, *6*(9), 974–980. https://doi.org/10.1038/nn1113

Condon, C. D., & Weinberger, N. M. (1991). Habituation Produces Frequency-Specific Plasticity of Receptive Fields in the Auditory Cortex. *Behavioral Neuroscience*, *105*(3), 416–430. https://doi.org/10.1037/0735-7044.105.3.416

Cornella, M., Leung, S., Grimm, S., & Escera, C. (2012). Detection of simple and pattern regularity violations occurs at different levels of the auditory hierarchy. *PLoS ONE*, *7*(8). https://doi.org/10.1371/journal.pone.0043604

Cotillon, N., Nafati, M., & Edeline, J. M. (2000). Characteristics of reliable tone-evoked oscillations in the rat thalamo-cortical auditory system. *Hearing Research*, *142*(1–2), 113–130. https://doi.org/10.1016/S0378-5955(00)00016-2

Cowan, N., Winkler, I., Teder, W., & Näätänen, R. (1993). Memory Prerequisites of Mismatch Negativity in the Auditory Event-Related Potential (ERP). *Journal of Experimental Psychology: Learning, Memory, and Cognition*, *19*(4), 909–921. https://doi.org/10.1037/0278-7393.19.4.909

Curtis, D. R., & Koizumi, K. (1961). Chemical transmitter substances in brain stem of cat. *Journal of Neurophysiology*, *24*, 80–90. https://doi.org/10.1152/jn.1961.24.1.80

Dallos, P. (1992). The active cochlea. *Journal of Neuroscience*, *12*(12), 4575–4585. https://doi.org/10.1523/jneurosci.12-12-04575.1992

Dautan, D., Bay, H. H., Bolam, J. P., Gerdjikov, T. V., & Mena-Segovia, J. (2016). Extrinsic sources of cholinergic innervation of the striatal complex: A whole-brain mapping analysis. *Frontiers in Neuroanatomy*, *10*(JAN), 1. https://doi.org/10.3389/fnana.2016.00001

Daw, N. D., Kakade, S., & Dayan, P. (2002). Opponent interactions between serotonin and dopamine. *Neural Networks*, *15*(4–6), 603–616. https://doi.org/10.1016/S0893-6080(02)00052-7

Dayan, P., Hinton, G. E., Neal, R. M., & Zemel, R. S. (1995). The Helmholtz machine. *Neural Computation*, *7*(5), 889–904. https://doi.org/10.1162/neco.1995.7.5.889

DeFelipe, J., López-Cruz, P. L., Benavides-Piccione, R., Bielza, C., Larrañaga, P., Anderson, S., Burkhalter, A., Cauli, B., Fairén, A., Feldmeyer, D., Fishell, G., Fitzpatrick, D., Freund, T. F., González-Burgos, G., Hestrin, S., Hill, S., Hof, P. R., Huang, J., Jones, E. G., … Ascoli, G. A. (2013). New insights into the classification and nomenclature of cortical GABAergic interneurons. *Nature Reviews Neuroscience*, *14*(3), 202–216. https://doi.org/10.1038/nrn3444

Den Ouden, H. E. M., Kok, P., & de Lange, F. P. (2012). How prediction errors shape perception, attention, and motivation. *Frontiers in Psychology*, *3*(DEC), 548. https://doi.org/10.3389/fpsyg.2012.00548

Diamond, I. T., Jones, E. G., & Powell, T. P. S. (1969). The projection of the auditory cortex upon the diencephalon and brain stem in the cat. *Brain Research*, *15*(2), 305–340. https://doi.org/10.1016/0006-8993(69)90160-7

Diederen, K. M. J., & Fletcher, P. (2020). Dopamine, Prediction Error and beyond. *The Neuroscientist*, 107385842090759. https://doi.org/10.1177/1073858420907591

Dommett, E., Coizet, V., Blaha, C. D., Martindale, J., Lefebvre, V., Walton, N., Mayhew, J. E. W., Overton, P. G., & Redgrave, P. (2005). How visual stimuli activate dopaminergic neurons at short latency. *Science*, *307*(5714), 1476–1479. https://doi.org/10.1126/science.1107026

Donishi, T., Kimura, A., Okamoto, K., & Tamai, Y. (2006). "Ventral" area in the rat auditory cortex: A major auditory field connected with the dorsal division of the medial geniculate body. *Neuroscience*, *141*(3), 1553–1567. https://doi.org/10.1016/j.neuroscience.2006.04.037

Doron, N. N., & Ledoux, J. E. (1999). Organization of projections to the lateral amygdala from auditory and visual areas of the thalamus in the rat. *Journal of Comparative Neurology*, *412*(3), 383–409. https://doi.org/10.1002/(SICI)1096-9861(19990927)412:3<383::AID-CNE2>3.0.CO;2-5

Doron, N. N., LeDoux, J. E., & Semple, M. N. (2002). Redefining the tonotopic core of rat auditory cortex: Physiological evidence for a posterior field. *Journal of Comparative Neurology*, *453*(4), 345–360. https://doi.org/10.1002/cne.10412

Doubell, T. P., Baron, J., Skaliora, I., & King, A. J. (2000). Topographical projection from the superior colliculus to the nucleus of the brachium of the inferior colliculus in the ferret: convergence of visual and auditory information. *European Journal of Neuroscience*, *12*(12), 4290–4308. https://doi.org/10.1111/j.1460-9568.2000.01337.x

Draganova, R., Eswaran, H., Murphy, P., Huotilainen, M., Lowery, C., & Preissl, H. (2005). Sound frequency change detection in fetuses and newborns, a magnetoencephalographic study. *NeuroImage*, *28*(2), 354–361. https://doi.org/10.1016/J.NEUROIMAGE.2005.06.011

Draganova, R., Eswaran, H., Murphy, P., Lowery, C., & Preissl, H. (2007). Serial magnetoencephalographic study of fetal and newborn auditory discriminative evoked responses. *Early Human Development*, *83*(3), 199–207. https://doi.org/10.1016/J.EARLHUMDEV.2006.05.018

Druga, R., & Syka, J. (1984). Ascending and descending projections to the inferior colliculus in the rat. *Physiologia Bohemoslovaca*, *33*(1), 31–42. https://europepmc.org/article/med/6709726

Druga, R., Syka, J., & Rajkowska, G. (1997). Projections of auditory cortex onto the inferior colliculus in the rat. *Physiological Research*, *46*(3), 215–222.

Duncan, C. C., Barry, R. J., Connolly, J. F., Fischer, C., Michie, P. T., Näätänen, R., Polich, J., Reinvang, I., & van Petten, C. (2009). Event-related potentials in clinical research: Guidelines for eliciting, recording, and quantifying mismatch negativity, P300, and N400. *Clinical Neurophysiology*, *120*(11), 1883–1908. https://doi.org/10.1016/J.CLINPH.2009.07.045

Duque, D., & Malmierca, M. S. (2015). Stimulus-specific adaptation in the inferior colliculus of the mouse: anesthesia and spontaneous activity effects. *Brain Structure and Function*, *220*(6), 3385–3398. https://doi.org/10.1007/s00429-014-0862-1

Duque, D., Malmierca, M. S., & Caspary, D. M. (2014). Modulation of stimulus-specific adaptation by GABAA receptor activation or blockade in the medial geniculate body of the anaesthetized rat. *Journal of Physiology*, *592*(4), 729–743. https://doi.org/10.1113/jphysiol.2013.261941

Duque, D., Pais, R., & Malmierca, M. S. (2018). Stimulus-specific adaptation in the anesthetized mouse revealed by brainstem auditory evoked potentials. *Hearing Research*, *370*, 294–301. https://doi.org/10.1016/j.heares.2018.08.011

Duque, D., Pérez-González, D., Ayala, Y. A., Palmer, A. R., & Malmierca, M. S. (2012). Topographic Distribution, Frequency, and Intensity Dependence of Stimulus-Specific Adaptation in the Inferior Colliculus of the Rat. *Journal of Neuroscience*, *32*(49), 17762–17774. https://doi.org/10.1523/JNEUROSCI.3190-12.2012

Duque, D., Wang, X., Nieto-Diego, J., Krumbholz, K., & Malmierca, M. S. (2016). Neurons in the inferior colliculus of the rat show stimulus-specific adaptation for frequency, but not for intensity. *Scientific Reports*, *6*(1), 24114. https://doi.org/10.1038/srep24114

Elgoyhen, A. B., Wedemeyer, C., & Di Guilmi, M. N. (2019). Efferent Innervation to the Cochlea. In *The Oxford Handbook of the Auditory Brainstem* (pp. 58–94). Oxford University Press. https://doi.org/10.1093/oxfordhb/9780190849061.013.3

Faingold, C. L., Boersma Anderson, C. A., & Caspary, D. M. (1991). Involvement of GABA in acoustically-evoked inhibition in inferior colliculus neurons. *Hearing Research*, *52*(1), 201–216. https://doi.org/10.1016/0378-5955(91)90200-S

Faingold, C. L., Gehlbach, G., & Caspary, D. M. (1989). On the role of GABA as an inhibitory neurotransmitter in inferior colliculus neurons: iontophoretic studies. *Brain Research*, *500*(1–2), 302–312. https://doi.org/10.1016/0006-8993(89)90326-0

Faure, P. A., Fremouw, T., Casseday, J. H., & Covey, E. (2003). Temporal masking reveals properties of sound-evoked inhibition in duration-tuned neurons of the inferior colliculus. *Journal of Neuroscience*, *23*(7), 3052–3065. https://doi.org/23/7/3052 [pii]

Faye-Lund, H. (1985). The neocortical projection to the inferior colliculus in the albino rat. *Anatomy and Embryology*, *173*(1), 53–70. https://doi.org/10.1007/BF00707304

Faye-Lund, H., & Osen, K. K. (1985). Anatomy of the inferior colliculus in rat. *Anatomy and Embryology*, *171*(1), 1–20. https://doi.org/10.1007/BF00319050

Feldman, H., & Friston, K. J. (2010). Attention, Uncertainty, and Free-Energy. *Frontiers in Human Neuroscience*, *4*, 215. https://doi.org/10.3389/fnhum.2010.00215

Feliciano, M., & Potashner, S. J. (1995). Evidence for a Glutamatergic Pathway from the Guinea Pig Auditory Cortex to the Inferior Colliculus. *Journal of Neurochemistry*, *65*(3), 1348–1357. https://doi.org/10.1046/j.1471-4159.1995.65031348.x

Felix, R. A., Fridberger, A., Leijon, S., Berrebi, A. S., & Magnusson, A. K. (2011). Sound rhythms are encoded by postinhibitory rebound spiking in the superior paraolivary nucleus. *Journal of Neuroscience*, *31*(35), 12566–12578. https://doi.org/10.1523/JNEUROSCI.2450-11.2011

Felleman, D. J., & van Essen, D. C. (1991). Distributed hierarchical processing in the primate cerebral cortex. *Cerebral Cortex*, *1*(1), 1–47. https://doi.org/10.1093/cercor/1.1.1

Felmy, F. (2019). The Nuclei of the Lateral Lemniscus. In *The Oxford Handbook of the Auditory Brainstem* (pp. 444–472). Oxford University Press. https://doi.org/10.1093/oxfordhb/9780190849061.013.13

Fiorillo, C. D. (2013). Two dimensions of value: Dopamine neurons represent reward but not aversiveness. *Science*, *341*(6145), 546–549. https://doi.org/10.1126/science.1238699

Fiorillo, C. D., Tobler, P. N., & Schultz, W. (2003). Discrete coding of reward probability and uncertainty by dopamine neurons. *Science*, *299*(5614), 1898–1902. https://doi.org/10.1126/science.1077349

Fishman, Y. I. (2014). The mechanisms and meaning of the mismatch negativity. *Brain Topography*, *27*(4), 500–526. https://doi.org/10.1007/s10548-013-0337-3

Fishman, Y. I., & Steinschneider, M. (2012). Searching for the Mismatch Negativity in Primary Auditory Cortex of the Awake Monkey: Deviance Detection or Stimulus Specific Adaptation? *Journal of Neuroscience*, *32*(45), 15747–15758. https://doi.org/10.1523/JNEUROSCI.2835-12.2012

FitzGerald, T. H. B., Dolan, R. J., & Friston, K. J. (2015). Dopamine, reward learning, and active inference. *Frontiers in Computational Neuroscience*, *9*, 136. https://doi.org/10.3389/fncom.2015.00136

Friauf, E. (1992). Tonotopic Order in the Adult and Developing Auditory System of the Rat as Shown by c-fos Immunocytochemistry. *European Journal of Neuroscience*, *4*(9), 798–812. https://doi.org/10.1111/j.1460-9568.1992.tb00190.x

Friauf, E., Krächan, E. G., & Müller, N. I. C. (2019). Lateral Superior Olive. In *The Oxford Handbook of the Auditory Brainstem* (pp. 328–394). Oxford University Press. https://doi.org/10.1093/oxfordhb/9780190849061.013.10

Friston, K. J. (2003). Learning and inference in the brain. *Neural Networks*, *16*(9), 1325–1352. https://doi.org/10.1016/j.neunet.2003.06.005

Friston, K. J. (2005). A theory of cortical responses. *Philosophical Transactions of the Royal Society B: Biological Sciences*, *360*(1456), 815–836. https://doi.org/10.1098/rstb.2005.1622

Friston, K. J. (2008). Hierarchical models in the brain. *PLoS Computational Biology*, *4*(11), e1000211. https://doi.org/10.1371/journal.pcbi.1000211

Friston, K. J. (2009). The free-energy principle: a rough guide to the brain? *Trends in Cognitive Sciences*, *13*(7), 293–301. https://doi.org/10.1016/j.tics.2009.04.005

Friston, K. J. (2010). The free-energy principle: a unified brain theory? *Nature Reviews. Neuroscience*, *11*(2), 127–138. https://doi.org/10.1038/nrn2787

Friston, K. J. (2018). Does predictive coding have a future? *Nature Neuroscience*, *21*(8), 1019–1021. https://doi.org/10.1038/s41593-018-0200-7

Friston, K. J., FitzGerald, T. H. B., Rigoli, F., Schwartenbeck, P., & Pezzulo, G. (2017). Active inference: A process theory. *Neural Computation*, *29*(1), 1–49. https://doi.org/10.1162/NECO_a_00912

Friston, K. J., & Kiebel, S. J. (2009a). Predictive coding under the free-energy principle. *Philosophical Transactions of the Royal Society B: Biological Sciences*, *364*(1521), 1211–1221. https://doi.org/10.1098/rstb.2008.0300

Friston, K. J., & Kiebel, S. J. (2009b). Cortical circuits for perceptual inference. *Neural Networks*, *22*(8), 1093–1104. https://doi.org/10.1016/j.neunet.2009.07.023

Friston, K. J., Kilner, J. M., & Harrison, L. (2006). A free energy principle for the brain. *Journal of Physiology Paris*, *100*(1–3), 70–87. https://doi.org/10.1016/j.jphysparis.2006.10.001

Friston, K. J., Rigoli, F., Ognibene, D., Mathys, C., Fitzgerald, T., & Pezzulo, G. (2015). Active inference and epistemic value. *Cognitive Neuroscience*, *6*(4), 187–214. https://doi.org/10.1080/17588928.2015.1020053

Friston, K. J., Schwartenbeck, P., FitzGerald, T. H. B., Moutoussis, M., Behrens, T., & Dolan, R. J. (2014). The anatomy of choice: Dopamine and decision-making. *Philosophical Transactions of the Royal Society B: Biological Sciences*, *369*(1655). https://doi.org/10.1098/rstb.2013.0481

Friston, K. J., Shiner, T., FitzGerald, T. H. B., Galea, J. M., Adams, R. A., Brown, H. R., Dolan, R. J., Moran, R. J., Stephan, K. E., & Bestmann, S. (2012). Dopamine, affordance and active inference. *PLoS Computational Biology*, *8*(1), e1002327. https://doi.org/10.1371/journal.pcbi.1002327

Fritz, J. B., Elhilali, M., David, S. V., & Shamma, S. A. (2007). Auditory attention-focusing the searchlight on sound. *Current Opinion in Neurobiology*, *17*(4), 437–455. https://doi.org/10.1016/j.conb.2007.07.011

Fyk-Kolodziej, B. E., Shimano, T., Gafoor, D., Mirza, N., Griffith, R. D., Gong, T. W., & Holt, A. G. (2015). Dopamine in the auditory brainstem and midbrain: Co-localization with amino acid neurotransmitters and gene expression following cochlear trauma. *Frontiers in Neuroanatomy*, *9*(July), 88. https://doi.org/10.3389/fnana.2015.00088

Games, K. D., & Winer, J. A. (1988). Layer V in rat auditory cortex: Projections to the inferior colliculus and contralateral cortex. *Hearing Research*, *34*(1), 1–25. https://doi.org/10.1016/0378-5955(88)90047-0

Gao, P. P., Zhang, J. W., Cheng, J. S., Zhou, I. Y., & Wu, E. X. (2014). The inferior

colliculus is involved in deviant sound detection as revealed by BOLD fMRI. *NeuroImage*, *91*, 220–227. https://doi.org/10.1016/j.neuroimage.2014.01.043

Garrido, M. I., Friston, K. J., Kiebel, S. J., Stephan, K. E., Baldeweg, T., & Kilner, J. M. (2008). The functional anatomy of the MMN: a DCM study of the roving paradigm. *NeuroImage*, *42*(2), 936–944. https://doi.org/10.1016/j.neuroimage.2008.05.018

Garrido, M. I., Kilner, J. M., Kiebel, S. J., & Friston, K. J. (2007). Evoked brain responses are generated by feedback loops. *Proceedings of the National Academy of Sciences*, *104*(52), 20961–20966. https://doi.org/10.1073/pnas.0706274105

Garrido, M. I., Kilner, J. M., Kiebel, S. J., Stephan, K. E., & Friston, K. J. (2007). Dynamic causal modelling of evoked potentials: a reproducibility study. *NeuroImage*, *36*(3), 571–580. https://doi.org/10.1016/j.neuroimage.2007.03.014

Garrido, M. I., Kilner, J. M., Stephan, K. E., & Friston, K. J. (2009). The mismatch negativity: a review of underlying mechanisms. *Clinical Neurophysiology*, *120*(3), 453–463. https://doi.org/10.1016/j.clinph.2008.11.029

Gaza, W. C., & Ribak, C. E. (1997). Immunocytochemical localization of AMPA receptors in the rat inferior colliculus. *Brain Research*, *774*(1–2), 175–183. https://doi.org/10.1016/S0006-8993(97)81701-5

Gill, P., Woolley, S. M. N., Fremouw, T., & Theunissen, F. E. (2008). What's That Sound? Auditory Area CLM Encodes Stimulus Surprise, Not Intensity or Intensity Changes. *Journal of Neurophysiology*, *99*(6), 2809–2820. https://doi.org/10.1152/jn.01270.2007

Gimenez, T. L., Lorenc, M., & Jaramillo, S. (2015). Adaptive categorization of sound frequency does not require the auditory cortex in rats. *Journal of Neurophysiology*, *114*(2), 1137–1145. https://doi.org/10.1152/jn.00124.2015

Gittelman, J. X., Perkel, D. J., & Portfors, C. V. (2013). Dopamine modulates auditory responses in the inferior colliculus in a heterogeneous manner. *JARO - Journal of the Association for Research in Otolaryngology*, *14*(5), 719–729. https://doi.org/10.1007/s10162-013-0405-0

González-Hernández, T., Mantolán-Sarmiento, B., González-González, B., & Pérez-González, H. (1996). Sources of GABAergic input to the inferior colliculus of the rat. *Journal of Comparative Neurology*, *372*(2), 309–326. https://doi.org/10.1002/(SICI)1096-9861(19960819)372:2<309::AID-CNE11>3.0.CO;2-E

Grimm, S., Escera, C., & Nelken, I. (2016). Early indices of deviance detection in humans and animal models. *Biological Psychology*, *116*, 23–27. https://doi.org/10.1016/j.biopsycho.2015.11.017

Grimm, S., Escera, C., Slabu, L., & Costa-Faidella, J. (2011). Electrophysiological evidence for the hierarchical organization of auditory change detection in the human brain. *Psychophysiology*, *48*(3), 377–384. https://doi.org/10.1111/j.1469-8986.2010.01073.x

Grimm, S., Recasens, M., Althen, H., & Escera, C. (2012). Ultrafast tracking of sound location changes as revealed by human auditory evoked potentials. *Biological*

Psychology, *89*(1), 232–239. https://doi.org/10.1016/j.biopsycho.2011.10.014

Grothe, B., Leibold, C., & Pecka, M. (2019). The Medial Superior Olivary Nucleus. In *The Oxford Handbook of the Auditory Brainstem* (pp. 300–328). Oxford University Press. https://doi.org/10.1093/oxfordhb/9780190849061.013.9

Guillery, R. W., & Sherman, S. M. (2002). Thalamic relay functions and their role in corticocortical communication: Generalizations from the visual system. *Neuron*, *33*(2), 163–175. https://doi.org/10.1016/S0896-6273(01)00582-7

Gutfreund, Y. (2012). Stimulus-specific adaptation, habituation and change detection in the gaze control system. *Biological Cybernetics*, *106*(11–12), 657–668. https://doi.org/10.1007/s00422-012-0497-3

Habbicht, H., & Vater, M. (1996). A microiontophoretic study of acetylcholine effects in the inferior colliculus of horseshoe bats: Implications for a modulatory role. *Brain Research*, *724*(2), 169–179. https://doi.org/10.1016/0006-8993(96)00224-7

Hara, K., & Harris, R. A. (2002). The anesthetic mechanism of urethane: The effects on neurotransmitter-gated ion channels. *Anesthesia and Analgesia*, *94*(2), 313–318. https://doi.org/10.1213/00000539-200202000-00015

Harms, L., Fulham, W. R., Todd, J., Budd, T. W., Hunter, M., Meehan, C., Penttonen, M., Schall, U., Zavitsanou, K., Hodgson, D. M., & Michie, P. T. (2014). Mismatch negativity (MMN) in freely-moving rats with several experimental controls. *PLoS ONE*, *9*(10), e110892. https://doi.org/10.1371/journal.pone.0110892

Harms, L., Michie, P. T., & Näätänen, R. (2016). Criteria for determining whether mismatch responses exist in animal models: Focus on rodents. *Biological Psychology*, *116*, 28–35. https://doi.org/10.1016/j.biopsycho.2015.07.006

Harpaz, M., Jankowski, M. M., Khouri, L., & Nelken, I. (2021). Emergence of abstract sound representations in the ascending auditory system. *Progress in Neurobiology*, 102049. https://doi.org/10.1016/j.pneurobio.2021.102049

Harrison, J. M., & Feldman, M. L. (1970). Anatomical aspects of the cochlear nucleus and superior olivary complex. *Contributions to Sensory Physiology*, *4*, 95–142. https://doi.org/10.1016/b978-0-12-151804-2.50010-3

Harrison, J. M., & Irving, R. (1965). The anterior ventral cochlear nucleus. *Journal of Comparative Neurology*, *124*(1), 15–41. https://doi.org/10.1002/cne.901240103

Harrison, J. M., & Irving, R. (1966). The organization of the posterior ventral cochlear nucleus in the rat. *Journal of Comparative Neurology*, *126*(3), 391–401. https://doi.org/10.1002/cne.901260303

Harrison, J. M., & Warr, W. B. (1962). A study of the cochlear nuclei and ascending auditory pathways of the medulla. *Journal of Comparative Neurology*, *119*(3), 341–379. https://doi.org/10.1002/cne.901190306

Hazama, M., Kimura, A., Donishi, T., Sakoda, T., & Tamai, Y. (2004). Topography of corticothalamic projections from the auditory cortex of the rat. *Neuroscience*, *124*(3),

655–667. https://doi.org/10.1016/j.neuroscience.2003.12.027

He, C., Chen, F., Li, B., & Hu, Z. (2014). Neurophysiology of HCN channels: From cellular functions to multiple regulations. *Progress in Neurobiology*, *112*, 1–23. https://doi.org/10.1016/J.PNEUROBIO.2013.10.001

Heilbron, M., & Chait, M. (2018). Great expectations: is there evidence for predictive coding in auditory cortex? *Neuroscience*, *389*, 54–73. https://doi.org/10.1016/j.neuroscience.2017.07.061

Helmholtz, H. (1867). *Handbuch der physiologischen Optik*.

Herbert, H., Aschoff, A., & Ostwald, J. (1991). Topography of projections from the auditory cortex to the inferior colliculus in the rat. *Journal of Comparative Neurology*, *304*(1), 103–122. https://doi.org/10.1002/cne.903040108

Hernández, O., Espinosa, N., Pérez-González, D., & Malmierca, M. S. (2005). The inferior colliculus of the rat: A quantitative analysis of monaural frequency response areas. *Neuroscience*, *132*(1), 203–217. https://doi.org/10.1016/j.neuroscience.2005.01.001

Herrmann, B., Parthasarathy, A., Han, E. X., Obleser, J., & Bartlett, E. L. (2015). Sensitivity of rat inferior colliculus neurons to frequency distributions. *Journal of Neurophysiology*, *114*(5), 2941–2954. https://doi.org/10.1152/jn.00555.2015

Higley, M. J., & Sabatini, B. L. (2010). Competitive regulation of synaptic Ca2+ influx by D2 dopamine and A2A adenosine receptors. *Nature Neuroscience*, *13*(8), 958–966. https://doi.org/10.1038/nn.2592

Hohwy, J. (2012). Attention and conscious perception in the hypothesis testing brain. *Frontiers in Psychology*, *3*(APR), 96. https://doi.org/10.3389/fpsyg.2012.00096

Hohwy, J. (2013). *The predictive mind*. Oxford University Press. https://doi.org/10.5860/choice.169393

Hormigo, S., e Horta, J. de A. de C., Gómez-Nieto, R., & López, D. E. (2012). The selective neurotoxin DSP-4 impairs the noradrenergic projections from the locus coeruleus to the inferior colliculus in rats. *Frontiers in Neural Circuits*, *6*(JUNE 2012), 41. https://doi.org/10.3389/fncir.2012.00041

Horváth, A. A., Szucs, A., Csukly, G., Sakovics, A., Stefanics, G., & Kamondi, A. (2018). EEG and ERP biomarkers of Alzheimer's disease: a critical review. *Frontiers in Bioscience (Landmark Edition)*, *23*, 183–220. http://www.ncbi.nlm.nih.gov/pubmed/28930543

Horvitz, J. C. (2000). Mesolimbocortical and nigrostriatal dopamine responses to salient non-reward events. *Neuroscience*, *96*(4), 651–656. https://doi.org/10.1016/S0306-4522(00)00019-1

Hosomi, H., Hirai, H., Okadaa, Y., & Amatsu, M. (1995). Long-term potentiation of neurotransmission in the inferior colliculus of the rat. *Neuroscience Letters*, *195*(3), 175–178. https://doi.org/10.1016/0304-3940(95)11811-A

Howard, J., Roberts, W. M., & Hudspeth, A. J. (1988). Mechanoelectrical transduction by hair cells. *Annual Review of Biophysics and Biophysical Chemistry*, *17*, 99–124. https://doi.org/10.1146/annurev.bb.17.060188.000531

Hoyt, J. M., Perkel, D. J., & Portfors, C. V. (2019). Dopamine acts via D2-like receptors to modulate auditory responses in the inferior colliculus. *ENeuro*, *6*(5), ENEURO.0350-19.2019. https://doi.org/10.1523/ENEURO.0350-19.2019

Hu, B. (2003). Functional organization of lemniscal and nonlemniscal auditory thalamus. *Experimental Brain Research*, *153*(4), 543–549. https://doi.org/10.1007/s00221-003-1611-5

Hudspeth, A. J. (1997). Mechanical amplification of stimuli by hair cells. *Current Opinion in Neurobiology*, *7*(4), 480–486. https://doi.org/10.1016/S0959-4388(97)80026-8

Hudspeth, A. J. (2014). Integrating the active process of hair cells with cochlear function. *Nature Reviews Neuroscience*, *15*(9), 600–614. https://doi.org/10.1038/nrn3786

Hullfish, J., Sedley, W., & Vanneste, S. (2019). Prediction and perception: insights for (and from) tinnitus. *Neuroscience & Biobehavioral Reviews*, *102*, 1–12. https://doi.org/10.1016/j.neubiorev.2019.04.008

Hupé, J. M., James, A. C., Payne, B. R., Lomber, S. G., Girard, P., & Bullier, J. (1998). Cortical feedback improves discrimination between figure and background by V1, V2 and V3 neurons. *Nature*, *394*(6695), 784–787. https://doi.org/10.1038/29537

Hurd, Y. L., Suzuki, M., & Sedvall, G. C. (2001). D1 and D2 dopamine receptor mRNA expression in whole hemisphere sections of the human brain. *Journal of Chemical Neuroanatomy*, *22*(1–2), 127–137. https://doi.org/10.1016/S0891-0618(01)00122-3

Hurley, L. M. (2007). Activation of the serotonin 1A receptor alters the temporal characteristics of auditory responses in the inferior colliculus. *Brain Research*, *1181*(1), 21–29. https://doi.org/10.1016/j.brainres.2007.08.053

Hurley, L. M. (2018). Neuromodulatory Feedback to the Inferior Colliculus. In K. Kandler (Ed.), *The Oxford Handbook of the Auditory Brainstem*. Oxford University Press. https://doi.org/10.1093/oxfordhb/9780190849061.013.15

Hurley, L. M., Devilbiss, D. M., & Waterhouse, B. D. (2004). A matter of focus: Monoaminergic modulation of stimulus coding in mammalian sensory networks. *Current Opinion in Neurobiology*, *14*(4), 488–495. https://doi.org/10.1016/j.conb.2004.06.007

Hurley, L. M., & Pollak, G. D. (1999). Serotonin differentially modulates responses to tones and frequency- modulated sweeps in the inferior colliculus. *Journal of Neuroscience*, *19*(18), 8071–8082. https://doi.org/10.1523/jneurosci.19-18-08071.1999

Hurley, L. M., & Pollak, G. D. (2001). Serotonin effects on frequency tuning of inferior colliculus neurons. *Journal of Neurophysiology*, *85*(2), 828–842. https://doi.org/10.1152/jn.2001.85.2.828

Hurley, L. M., & Pollak, G. D. (2005a). Serotonin modulates responses to species-specific

vocalizations in the inferior colliculus. *Journal of Comparative Physiology A: Neuroethology, Sensory, Neural, and Behavioral Physiology*, *191*(6), 535–546. https://doi.org/10.1007/s00359-005-0623-y

Hurley, L. M., & Pollak, G. D. (2005b). Serotonin shifts first-spike latencies of inferior colliculus neurons. *Journal of Neuroscience*, *25*(34), 7876–7886. https://doi.org/10.1523/JNEUROSCI.1178-05.2005

Hurley, L. M., & Sullivan, M. R. (2012). From behavioral context to receptors: Serotonergic modulatory pathways in the IC. In *Frontiers in Neural Circuits* (Vol. 6, Issue SEPTEMBER, p. 58). Frontiers. https://doi.org/10.3389/fncir.2012.00058

Imaizumi, K., & Lee, C. C. (2014). Frequency transformation in the auditory lemniscal thalamocortical system. *Frontiers in Neural Circuits*, *8*(JULY), 75. https://doi.org/10.3389/fncir.2014.00075

Imig, T. J., & Morel, A. (1985). Tonotopic organization in ventral nucleus of medial geniculate body in the cat. *Journal of Neurophysiology*, *53*(1), 309–340. https://doi.org/10.1152/jn.1985.53.1.309

Irvine, D. R. F. (1986a). *Auditory Brainstem Processing: Integration and Conclusions* (pp. 212–228). https://doi.org/10.1007/978-3-642-71057-5_8

Irvine, D. R. F. (1986b). *Cochlear Nucleus: Anatomy and Physiology* (pp. 40–78). https://doi.org/10.1007/978-3-642-71057-5_4

Irvine, D. R. F. (1986c). *Superior Olivary Complex: Anatomy and Physiology* (pp. 79–121). https://doi.org/10.1007/978-3-642-71057-5_5

Irvine, D. R. F. (1992). *Physiology of the Auditory Brainstem* (pp. 153–231). Springer, New York, NY. https://doi.org/10.1007/978-1-4612-2838-7_4

Ito, T., & Malmierca, M. S. (2018). Neurons, Connections, and Microcircuits of the Inferior Colliculus. In D. Oliver, N. Cant, R. Fay, & A. Popper (Eds.), *The Mammalian Auditory Pathways* (pp. 127–167). Springer, Cham. https://doi.org/10.1007/978-3-319-71798-2_6

Ito, T., Ono, M., Oliver, D. L., Ito, T., Ono, M., & Oliver, D. L. (2018). Neuron Types, Intrinsic Circuits, and Plasticity in the Inferior Colliculus. In K. Kandler (Ed.), *The Oxford Handbook of the Auditory Brainstem*. Oxford University Press. https://doi.org/10.1093/oxfordhb/9780190849061.013.25

Jääskeläinen, I. P., Ahveninen, J., Bonmassar, G., Dale, A. M., Ilmoniemi, R. J., Levänen, S., Lin, F.-H., May, P. J. C., Melcher, J., Stufflebeam, S., Tiitinen, H., & Belliveau, J. W. (2004). Human posterior auditory cortex gates novel sounds to consciousness. *Proceedings of the National Academy of Sciences*, *101*(17), 6809–6814. https://doi.org/10.1073/pnas.0303760101

Jacobsen, T., Horenkamp, T., & Schröger, E. (2003). Preattentive memory-based comparison of sound intensity. *Audiology and Neuro-Otology*, *8*(6), 338–346. https://doi.org/10.1159/000073518

Jacobsen, T., & Schröger, E. (2001). Is there pre-attentive memory-based comparison of

pitch? *Psychophysiology*, *38*(4), 723–727. https://doi.org/10.1017/s0048577201000993

Jacobsen, T., & Schröger, E. (2003). Measuring duration mismatch negativity. *Clinical Neurophysiology*, *114*(6), 1133–1143. https://doi.org/10.1016/S1388-2457(03)00043-9

Jia, G., Li, X., Liu, C., He, J., & Gao, L. (2021). Stimulus-Specific Adaptation in Auditory Thalamus Is Modulated by the Thalamic Reticular Nucleus. *ACS Chemical Neuroscience*, *12*(9), 1688–1697. https://doi.org/10.1021/acschemneuro.1c00137

Jung, F., Stephan, K. E., Backes, H., Moran, R. J., Gramer, M., Kumagai, T., Graf, R., Endepols, H., & Tittgemeyer, M. (2013). Mismatch Responses in the Awake Rat: Evidence from Epidural Recordings of Auditory Cortical Fields. *PLoS ONE*, *8*(4), e63203. https://doi.org/10.1371/journal.pone.0063203

Kaan, E., Harris, A., Gibson, E., & Holcomb, P. (2000). The P600 as an index of syntactic integration difficulty. *Language and Cognitive Processes*, *15*(2), 159–201. https://doi.org/10.1080/016909600386084

Kaas, J. H. (2011). The evolution of auditory cortex: The core areas. In *The Auditory Cortex* (pp. 407–427). Springer US. https://doi.org/10.1007/978-1-4419-0074-6_19

Kaas, J. H., Hackett, T. A., & Tramo, M. J. (1999). Auditory processing in primate cerebral cortex. *Current Opinion in Neurobiology*, *9*(2), 164–170. https://doi.org/10.1016/S0959-4388(99)80022-1

Kadner, A., & Berrebi, A. S. (2008). Encoding of temporal features of auditory stimuli in the medial nucleus of the trapezoid body and superior paraolivary nucleus of the rat. *Neuroscience*, *151*(3), 868–887. https://doi.org/10.1016/j.neuroscience.2007.11.008

Kadner, A., Kulesza, R. J., & Berrebi, A. S. (2006). Neurons in the medial nucleus of the trapezoid body and superior paraolivary nucleus of the rat may play a role in sound duration coding. *Journal of Neurophysiology*, *95*(3), 1499–1508. https://doi.org/10.1152/jn.00902.2005

Kant, I. (1781). *Critik der reinen Vernunft*.

Keller, G. B., & Mrsic-Flogel, T. D. (2018). Predictive processing: a canonical cortical computation. *Neuron*, *100*(2), 424–435. https://doi.org/10.1016/j.neuron.2018.10.003

Kelly, J. B., & Caspary, D. M. (2005). Pharmacology of the inferior colliculus. In *The Inferior Colliculus* (pp. 248–281). Springer New York. https://doi.org/10.1007/0-387-27083-3_9

Kelly, J. B., & Kavanagh, G. L. (1986). Effects of Auditory Cortical Lesions on Pure-Tone Sound Localization by the Albino Rat. *Behavioral Neuroscience*, *100*(4), 569–575. https://doi.org/10.1037/0735-7044.100.4.569

Kelly, J. B., Van Adel, B. A., & Ito, M. (2009). Anatomical projections of the nuclei of the lateral lemniscus in the Albino rat (Rattus norvegicus). *Journal of Comparative Neurology*, *512*(4), 573–593. https://doi.org/10.1002/cne.21929

Kelly, J. B., & Zhang, H. (2002). Contribution of AMPA and NMDA receptors to excitatory

responses in the inferior colliculus. *Hearing Research*, *168*(1–2), 35–42. https://doi.org/10.1016/S0378-5955(02)00372-6

Khouri, L., & Nelken, I. (2015). Detecting the unexpected. *Current Opinion in Neurobiology*, *35*, 142–147. https://doi.org/10.1016/j.conb.2015.08.003

Kimura, A., Donishi, T., Okamoto, K., & Tamai, Y. (2005). Topography of projections from the primary and non-primary auditory cortical areas to the medial geniculate body and thalamic reticular nucleus in the rat. *Neuroscience*, *135*(4), 1325–1342. https://doi.org/10.1016/j.neuroscience.2005.06.089

Kimura, A., Donishi, T., Sakoda, T., Hazama, M., & Tamai, Y. (2003). Auditory thalamic nuclei projections to the temporal cortex in the rat. *Neuroscience*, *117*(4), 1003–1016. https://doi.org/10.1016/S0306-4522(02)00949-1

Kimura, A., Imbe, H., Donishi, T., & Tamai, Y. (2007). Axonal projections of single auditory neurons in the thalamic reticular nucleus: Implications for tonotopy-related gating function and cross-modal modulation. *European Journal of Neuroscience*, *26*(12), 3524–3535. https://doi.org/10.1111/j.1460-9568.2007.05925.x

King, A. J., & Nelken, I. (2009). Unraveling the principles of auditory cortical processing: can we learn from the visual system? *Nature Neuroscience*, *12*(6), 698–701. https://doi.org/10.1038/nn.2308

Klein, C., von der Behrens, W., & Gaese, B. H. (2014). Stimulus-specific adaptation in field potentials and neuronal responses to frequency-modulated tones in the primary auditory cortex. *Brain Topography*, *27*(4), 599–610. https://doi.org/10.1007/s10548-014-0376-4

Klepper, A., & Herbert, H. (1991). Distribution and origin of noradrenergic and serotonergic fibers in the cochlear nucleus and inferior colliculus of the rat. *Brain Research*, *557*(1–2), 190–201. https://doi.org/10.1016/0006-8993(91)90134-H

Koch, U., Braun, M., Kapfer, C., & Grothe, B. (2004). Distribution of HCN1 and HCN2 in rat auditory brainstem nuclei. *The European Journal of Neuroscience*, *20*(1), 79–91. https://doi.org/10.1111/j.0953-816X.2004.03456.x

Koelsch, S., Heinke, W., Sammler, D., & Olthoff, D. (2006). Auditory processing during deep propofol sedation and recovery from unconsciousness. *Clinical Neurophysiology*, *117*(8), 1746–1759. https://doi.org/10.1016/j.clinph.2006.05.009

Kok, A. (2001). On the utility of P3 amplitude as a measure of processing capacity. *Psychophysiology*, *38*(3), 557–577. https://doi.org/10.1017/S0048577201990559

Kraus, N., McGee, T., Littman, T., Nicol, T. G., & King, C. (1994). Nonprimary auditory thalamic representation of acoustic change. *Journal of Neurophysiology*, *72*(3), 1270–1277. http://jn.physiology.org/content/72/3/1270.long%5Cnpapers3://publication/uuid/06F26B87-7714-4C5B-8C12-52EAD353A59F

Krieg, W. J. S. (1946a). Connections of the cerebral cortex. I. The albino rat. A. Topography of the cortical areas. *Journal of Comparative Neurology*, *84*(2), 221–275. https://doi.org/10.1002/cne.900840205

Krieg, W. J. S. (1946b). Connections of the cerebral cortex. I. The albino rat. B. Structure of the cortical areas. *Journal of Comparative Neurology*, *84*(3), 277–323. https://doi.org/10.1002/cne.900840302

Krieg, W. J. S. (1947). Connections of the cerebral cortex I. The Albino Rat. C. Extrinsic connections. *Journal of Comparative Neurology*, *86*(3), 267–394. https://doi.org/10.1002/cne.900860302

Kujala, T., & Leminen, M. (2017). Low-level neural auditory discrimination dysfunctions in specific language impairment—A review on mismatch negativity findings. *Developmental Cognitive Neuroscience*, *28*, 65–75. https://doi.org/10.1016/j.dcn.2017.10.005

Kujala, T., Tervaniemi, M., & Schröger, E. (2007). The mismatch negativity in cognitive and clinical neuroscience: Theoretical and methodological considerations. *Biological Psychology*, *74*(1), 1–19. https://doi.org/10.1016/j.biopsycho.2006.06.001

Kutas, M., & Hillyard, S. A. (1980). Reading senseless sentences: Brain potentials reflect semantic incongruity. *Science*, *207*(4427), 203–205. https://doi.org/10.1126/science.7350657

Lavoie, S., Polari, A. R., Goldstone, S., Nelson, B., & McGorry, P. D. (2019). Staging model in psychiatry: Review of the evolution of electroencephalography abnormalities in major psychiatric disorders. *Early Intervention in Psychiatry*. https://doi.org/10.1111/eip.12792

Le Beau, F. E. N., Malmierca, M. S., & Rees, A. (2001). Iontophoresis in vivo demonstrates a key role for GABA(A) and glycinergic inhibition in shaping frequency response areas in the inferior colliculus of guinea pig. *The Journal of Neuroscience : The Official Journal of the Society for Neuroscience*, *21*(18), 7303–7312. https://doi.org/21/18/7303 [pii]

Le Beau, F. E. N., Rees, A., & Malmierca, M. S. (1996). Contribution of GABA- and glycine-mediated inhibition to the monaural temporal response properties of neurons in the inferior colliculus. *Journal of Neurophysiology*, *75*(2), 902–919. https://doi.org/10.1152/jn.1996.75.2.902

LeDoux, J. E., Ruggiero, D. A., Forest, R., Stornetta, R., & Reis, D. J. (1987). Topographic organization of convergent projections to the thalamus from the inferior colliculus and spinal cord in the rat. *Journal of Comparative Neurology*, *264*(1), 123–146. https://doi.org/10.1002/cne.902640110

LeDoux, J. E., Ruggiero, D. A., & Reis, D. J. (1985). Projections to the subcortical forebrain from anatomically defined regions of the medial geniculate body in the rat. *Journal of Comparative Neurology*, *242*(2), 182–213. https://doi.org/10.1002/cne.902420204

Lee, C. C. (2015). Exploring functions for the non-lemniscal auditory thalamus. *Frontiers in Neural Circuits*, *9*, 69. https://doi.org/10.3389/fncir.2015.00069

Lee, C. C., & Sherman, S. M. (2011). On the classification of pathways in the auditory midbrain, thalamus, and cortex. *Hearing Research*, *276*(1–2), 79–87. https://doi.org/10.1016/j.heares.2010.12.012

Lee, T. S., & Mumford, D. (2003). Hierarchical Bayesian inference in the visual cortex. *Journal of the Optical Society of America A*, *20*(7), 1434. https://doi.org/10.1364/JOSAA.20.001434

Lesicko, A. M. H., Hristova, T. S., Maigler, K. C., & Llano, D. A. (2016). Connectional Modularity of Top-Down and Bottom-Up Multimodal Inputs to the Lateral Cortex of the Mouse Inferior Colliculus. *Journal of Neuroscience*, *36*(43), 11037–11050. https://doi.org/10.1523/JNEUROSCI.4134-15.2016

Leung, S., Recasens, M., Grimm, S., & Escera, C. (2013). Electrophysiological index of acoustic temporal regularity violation in the middle latency range. *Clinical Neurophysiology*, *124*(12), 2397–2405. https://doi.org/10.1016/j.clinph.2013.06.001

Li, J., Liao, X., Zhang, J., Wang, M., Yang, N., Zhang, J., Lv, G., Li, H., Lu, J., Ding, R., Li, X., Guang, Y., Yang, Z., Qin, H., Jin, W., Zhang, K., He, C., Jia, H., Zeng, S., … Chen, X. (2017). Primary Auditory Cortex is Required for Anticipatory Motor Response. *Cerebral Cortex*, *27*(6), 3254–3271. https://doi.org/10.1093/cercor/bhx079

Light, G. A., & Näätänen, R. (2013). Mismatch negativity is a breakthrough biomarker for understanding and treating psychotic disorders. *Proceedings of the National Academy of Sciences*, *110*(38), 15175–15176. https://doi.org/10.1073/pnas.1313287110

Ljungberg, T., Apicella, P., & Schultz, W. (1992). Responses of monkey dopamine neurons during learning of behavioral reactions. *Journal of Neurophysiology*, *67*(1), 145–163. https://doi.org/10.1152/jn.1992.67.1.145

Llano, D. A., & Sherman, S. M. (2008). Evidence for nonreciprocal organization of the mouse auditory thalamocortical-corticothalamic projection systems. *Journal of Comparative Neurology*, *507*(2), 1209–1227. https://doi.org/10.1002/cne.21602

Loftus, W. C., Malmierca, M. S., Bishop, D. C., & Oliver, D. L. (2008). The cytoarchitecture of the inferior colliculus revisited: A common organization of the lateral cortex in rat and cat. *Neuroscience*, *154*(1), 196–205. https://doi.org/10.1016/j.neuroscience.2008.01.019

López-Caballero, F., Zarnowiec, K., & Escera, C. (2016). Differential deviant probability effects on two hierarchical levels of the auditory novelty system. *Biological Psychology*, *120*, 1–9. https://doi.org/10.1016/j.biopsycho.2016.08.001

Lorente de No, R. (1926). Etude sur l'anatomie et la physiologie du labyrinthe de lóreille et du VIIIe nerf. *Travaux Du Laboratoire de Recherches Biologiques de l'Université de Madrid*, *25*, 53–153. https://ci.nii.ac.jp/naid/10030781929

Lorente de No, R. (1933). Anatomy of the eighth nerve: III.—General plan of structure of the primary cochlear nuclei. *The Laryngoscope*, *43*(4), 327–349. https://doi.org/10.1288/00005537-193304000-00014

Lumani, A., & Zhang, H. (2010). Responses of neurons in the rat's dorsal cortex of the inferior colliculus to monaural tone bursts. *Brain Research*, *1351*, 115–129. https://doi.org/10.1016/j.brainres.2010.06.066

Maggi, C. A., & Meli, A. (1986). Suitability of urethane anesthesia for

physiopharmacological investigations in various systems. Part 1: General considerations. *Experientia*, *42*(2), 109–114. https://doi.org/10.1007/BF01952426

Malmierca, M. S. (2004). The inferior colliculus: A center for convergence of ascending and descending auditory information. *Neuroembryology and Aging*, *3*(4), 215–229. https://doi.org/10.1159/000096799

Malmierca, M. S. (2015). Chapter 29 – Auditory System. In G. Paxinos (Ed.), *The Rat Nervous System* (pp. 865–946). Academic Press. https://doi.org/10.1016/B978-0-12-374245-2.00029-2

Malmierca, M. S., Anderson, L. A., & Antunes, F. M. (2015). The cortical modulation of stimulus-specific adaptation in the auditory midbrain and thalamus: a potential neuronal correlate for predictive coding. *Frontiers in Systems Neuroscience*, *9*(March), 19. https://doi.org/10.3389/fnsys.2015.00019

Malmierca, M. S., & Auksztulewicz, R. (2021). Stimulus-specific adaptation, MMN and predictive coding. In *Hearing Research* (Vol. 399). Elsevier B.V. https://doi.org/10.1016/j.heares.2020.108076

Malmierca, M. S., Blackstad, T. W., & Osen, K. K. (2011). Computer-assisted 3-D reconstructions of Golgi-impregnated neurons in the cortical regions of the inferior colliculus of rat. *Hearing Research*, *274*(1–2), 13–26. https://doi.org/10.1016/j.heares.2010.06.011

Malmierca, M. S., Blackstad, T. W., Osen, K. K., Karagülle, T., & Molowny, R. L. (1993). The central nucleus of the inferior colliculus in rat: A Golgi and computer reconstruction study of neuronal and laminar structure. *Journal of Comparative Neurology*, *333*(1), 1–27. https://doi.org/10.1002/cne.903330102

Malmierca, M. S., Carbajal, G. V., & Escera, C. (2019). Deviance Detection and Encoding Acoustic Regularity in the Auditory Midbrain. In K. Kandler (Ed.), *The Oxford Handbook of the Auditory Brainstem* (pp. 706–740). Oxford University Press. https://doi.org/10.1093/oxfordhb/9780190849061.013.19

Malmierca, M. S., Cristaudo, S., Pérez-González, D., & Covey, E. (2009). Stimulus-Specific Adaptation in the Inferior Colliculus of the Anesthetized Rat. *Journal of Neuroscience*, *29*(17), 5483–5493. https://doi.org/10.1523/JNEUROSCI.4153-08.2009

Malmierca, M. S., & Hackett, T. A. (2010). Structural organization of the ascending auditory pathway. In D. R. Moore, A. Rees, & A. R. Palmer (Eds.), *The Oxford handbook of auditory science: The Auditory Brain* (pp. 9–42). Oxford University Press.

Malmierca, M. S., Izquierdo, M. A., Cristaudo, S., Hernández, O., Pérez-González, D., Covey, E., & Oliver, D. L. (2008). A Discontinuous Tonotopic Organization in the Inferior Colliculus of the Rat. *Journal of Neuroscience*, *28*(18), 4767–4776. https://doi.org/10.1523/JNEUROSCI.0238-08.2008

Malmierca, M. S., Le Beau, F. E. N., & Rees, A. (1996). The topographical organization of descending projections from the central nucleus of the inferior colliculus in guinea pig. *Hearing Research*, *93*(1–2), 167–180. https://doi.org/10.1016/0378-5955(95)00227-8

Malmierca, M. S., Leergaard, T. B., Bajo, V. M., Bjaalie, J. G., & Merchán, M. A. (1998). Anatomic evidence of a three-dimensional mosaic pattern of tonotopic organization in the ventral complex of the lateral lemniscus in cat. *Journal of Neuroscience*, *18*(24), 10603–10618. https://doi.org/10.1523/jneurosci.18-24-10603.1998

Malmierca, M. S., Merchán, M. A., Henkel, C. K., & Oliver, D. L. (2002). Direct projections from cochlear nuclear complex to auditory thalamus in the rat. *Journal of Neuroscience*, *22*(24), 10891–10897. https://doi.org/10.1523/jneurosci.22-24-10891.2002

Malmierca, M. S., Rees, A., Le Beau, F. E. N., & Bjaalie, J. G. (1995). Laminar organization of frequency-defined local axons within and between the inferior colliculi of the guinea pig. *Journal of Comparative Neurology*, *357*(1), 124–144. https://doi.org/10.1002/cne.903570112

Malmierca, M. S., & Ryugo, D. K. (2011). Descending connections of auditory cortex to the midbrain and brain stem. In Jeffery A; Winer & C. E. Schreiner (Eds.), *The Auditory Cortex* (1st ed., pp. 189–208). Springer US. https://doi.org/10.1007/978-1-4419-0074-6

Malmierca, M. S., Saint Marie, R. L., Merchán, M. A., & Oliver, D. L. (2005). Laminar inputs from dorsal cochlear nucleus and ventral cochlear nucleus to the central nucleus of the inferior colliculus: Two patterns of convergence. *Neuroscience*, *136*(3), 883–894. https://doi.org/10.1016/j.neuroscience.2005.04.040

Malone, B. J., Scott, B. H., & Semple, M. N. (2002). Context-dependent adaptive coding of interaural phase disparity in the auditory cortex of awake macaques. *The Journal of Neuroscience : The Official Journal of the Society for Neuroscience*, *22*(11), 4625–4638. https://doi.org/20026408

Malone, B. J., & Semple, M. N. (2001). Effects of auditory stimulus context on the representation of frequency in the gerbil inferior colliculus. *Journal of Neurophysiology*, *86*(3), 1113–1130. http://www.ncbi.nlm.nih.gov/pubmed/11535662

Markin, V. S., & Hudspeth, A. J. (1995). Gating-spring models of mechanoelectrical transduction by hair cells of the internal ear. *Annual Review of Biophysics and Biomolecular Structure*, *24*, 59–83. https://doi.org/10.1146/annurev.bb.24.060195.000423

Matsumoto, M., & Hikosaka, O. (2009). Two types of dopamine neuron distinctly convey positive and negative motivational signals. *Nature*, *459*(7248), 837–841. https://doi.org/10.1038/nature08028

Matsumoto, M., & Takada, M. (2013). Distinct Representations of Cognitive and Motivational Signals in Midbrain Dopamine Neurons. *Neuron*, *79*(5), 1011–1024. https://doi.org/10.1016/j.neuron.2013.07.002

May, P. J. C., & Tiitinen, H. (2004). The MMN is a derivative of the auditory N100 response. *Neurology and Clinical Neurophysiology*, *2004*.

May, P. J. C., & Tiitinen, H. (2010). Mismatch negativity (MMN), the deviance-elicited auditory deflection, explained. *Psychophysiology*, *47*(1), 66–122. https://doi.org/10.1111/j.1469-8986.2009.00856.x

May, P. J. C., Westö, J., & Tiitinen, H. (2015). Computational modelling suggests that temporal integration results from synaptic adaptation in auditory cortex. *European Journal of Neuroscience*, *41*(5), 615–630. https://doi.org/10.1111/ejn.12820

McCown, T. J., & Breese, G. R. (1991). The role of the inferior collicular cortex in the neonatal rat: sensorimotor modulation. *Developmental Brain Research*, *59*(1), 1–5. https://doi.org/10.1016/0165-3806(91)90022-B

McKenna, T. M., Weinberger, N. M., & Diamond, D. M. (1989). Responses of single auditory cortical neurons to tone sequences. *Brain Research*, *481*(1), 142–153. https://doi.org/10.1016/0006-8993(89)90494-0

Merchán, M. A., Aguilar, L. A., Lopez-Poveda, E. A., & Malmierca, M. S. (2005). The inferior colliculus of the rat: Quantitative immunocytochemical study of GABA and glycine. *Neuroscience*, *136*(3), 907–925. https://doi.org/10.1016/j.neuroscience.2004.12.030

Merchán, M. A., & Berbel, P. (1996). Anatomy of the ventral nucleus of the lateral lemniscus in rats: A nucleus with a concentric laminar organization. *Journal of Comparative Neurology*, *372*(2), 245–263. https://doi.org/10.1002/(SICI)1096-9861(19960819)372:2<245::AID-CNE7>3.0.CO;2-3

Merchán, M. A., Saldaña, E., & Plaza, I. (1994). Dorsal nucleus of the lateral lemniscus in the rat: Concentric organization and tonotopic projection to the inferior colliculus. *Journal of Comparative Neurology*, *342*(2), 259–278. https://doi.org/10.1002/cne.903420209

Merrill, E. G., & Ainsworth, A. (1972). Glass-coated platinum-plated tungsten microelectrodes. *Medical & Biological Engineering*, *10*(5), 662–672. https://doi.org/10.1007/BF02476084

Merzenich, M. M., Knight, P. L., & Roth, G. L. (1975). Representation of cochlea within primary auditory cortex in the cat. *Journal of Neurophysiology*, *38*(2), 231–249. https://doi.org/10.1152/jn.1975.38.2.231

Merzenich, M. M., & Reid, M. D. (1974). Representation of the cochlea within the inferior colliculus of the cat. *Brain Research*, *77*(3), 397–415. https://doi.org/10.1016/0006-8993(74)90630-1

Michaeli, A., & Yaka, R. (2010). Dopamine inhibits GABA(A) currents in ventral tegmental area dopamine neurons via activation of presynaptic G-protein coupled inwardly-rectifying potassium channels. *Neuroscience*, *165*(4), 1159–1169. https://doi.org/10.1016/j.neuroscience.2009.11.045

Michie, P. T., Malmierca, M. S., Harms, L., & Todd, J. (2016). The neurobiology of MMN and implications for schizophrenia. *Biological Psychology*, *116*, 90–97. https://doi.org/10.1016/j.biopsycho.2016.01.011

Mill, R. W., Coath, M., Wennekers, T., & Denham, S. L. (2011). A neurocomputational model of stimulus-specific adaptation to oddball and markov sequences. *PLoS Computational Biology*, *7*(8), e1002117. https://doi.org/10.1371/journal.pcbi.1002117

Miller, K. E., Casseday, J. H., & Covey, E. (2005). Relation between intrinsic connections and isofrequency contours in the inferior colliculus of the big brown bat, Eptesicus fuscus. *Neuroscience*, *136*(3), 895–905. https://doi.org/10.1016/j.neuroscience.2005.04.032

Mirenowicz, J., & Schultz, W. (1996). Preferential activation of midbrain dopamine neurons by appetitive rather than aversive stimuli. *Nature*, *379*(6564), 449–451. https://doi.org/10.1038/379449a0

Mitani, A., Shimokouchi, M., & Nomura, S. (1983). Effects of stimulation of the primary auditory cortex upon colliculogeniculate neurons in the inferior colliculus of the cat. *Neuroscience Letters*, *42*(2), 185–189. https://doi.org/10.1016/0304-3940(83)90404-4

Moran, R. J., Campo, P., Symmonds, M., Stephan, K. E., Dolan, R. J., & Friston, K. J. (2013). Free Energy, Precision and Learning: The Role of Cholinergic Neuromodulation. *Journal of Neuroscience*, *33*(19), 8227–8236. https://doi.org/10.1523/JNEUROSCI.4255-12.2013

Morest, D. K., & Oliver, D. L. (1984). The neuronal architecture of the inferior colliculus in the cat: Defining the functional anatomy of the auditory midbrain. *Journal of Comparative Neurology*, *222*(2), 209–236. https://doi.org/10.1002/cne.902220206

Moriizumi, T., & Hattori, T. (1992). Anatomical and functional compartmentalization of the subparafascicular thalamic nucleus in the rat. *Experimental Brain Research*, *90*(1), 175–179. https://doi.org/10.1007/BF00229269

Morlet, D., & Fischer, C. (2014). MMN and novelty P3 in coma and other altered states of consciousness: A review. *Brain Topography*, *27*(4), 467–479. https://doi.org/10.1007/s10548-013-0335-5

Motts, S. D., & Schofield, B. R. (2009). Sources of cholinergic input to the inferior colliculus. *Neuroscience*, *160*(1), 103–114. https://doi.org/10.1016/j.neuroscience.2009.02.036

Mountcastle, V. B. (1997). The columnar organization of the neocortex. *Brain*, *120*(4), 701–722. https://doi.org/10.1093/brain/120.4.701

Mulders, W. H. A. M., & Robertson, D. (2001). Origin of the noradrenergic innervation of the superior olivary complex in the rat. *Journal of Chemical Neuroanatomy*, *21*(4), 313–322. https://doi.org/10.1016/S0891-0618(01)00118-1

Müller, U. (2008, October 1). Cadherins and mechanotransduction by hair cells. In *Current Opinion in Cell Biology*. Elsevier Current Trends. https://doi.org/10.1016/j.ceb.2008.06.004

Näätänen, R. (1990). The role of attention in auditory information processing as revealed by event-related potentials and other brain measures of cognitive function. *Behavioral and Brain Sciences*, *13*(2), 201–233. https://doi.org/10.1017/S0140525X00078407

Näätänen, R., & Alho, K. (1995). Mismatch negativity-a unique measure of sensory processing in audition. *International Journal of Neuroscience*, *80*(1–4), 317–337. https://doi.org/10.3109/00207459508986107

Näätänen, R., Astikainen, P., Ruusuvirta, T., & Huotilainen, M. (2010). Automatic auditory intelligence: An expression of the sensory-cognitive core of cognitive processes. *Brain Research Reviews*, *64*(1), 123–136. https://doi.org/10.1016/j.brainresrev.2010.03.001

Näätänen, R., Gaillard, A. W. K., & Mäntysalo, S. (1978). Early selective-attention effect on evoked potential reinterpreted. *Acta Psychologica*, *42*(4), 313–329. https://doi.org/10.1016/0001-6918(78)90006-9

Näätänen, R., Jacobsen, T., & Winkler, I. (2005). Memory-based or afferent processes in mismatch negativity (MMN): A review of the evidence. *Psychophysiology*, *42*(1), 25–32. https://doi.org/10.1111/j.1469-8986.2005.00256.x

Näätänen, R., & Michie, P. T. (1979). Early selective-attention effects on the evoked potential: A critical review and reinterpretation. *Biological Psychology*, *8*(2), 81–136. https://doi.org/10.1016/0301-0511(79)90053-X

Näätänen, R., Paavilainen, P., Rinne, T., & Alho, K. (2007). The mismatch negativity (MMN) in basic research of central auditory processing: A review. *Clinical Neurophysiology*, *118*(12), 2544–2590. https://doi.org/10.1016/j.clinph.2007.04.026

Näätänen, R., Shiga, T., Asano, S., & Yabe, H. (2015). Mismatch negativity (MMN) deficiency: A break-through biomarker in predicting psychosis onset. *International Journal of Psychophysiology*, *95*(3), 338–344. https://doi.org/10.1016/j.ijpsycho.2014.12.012

Näätänen, R., Sussman, E. S., Salisbury, D. F., & Shafer, V. L. (2014). Mismatch negativity (MMN) as an index of cognitive dysfunction. *Brain Topography*, *27*(4), 451–466. https://doi.org/10.1007/s10548-014-0374-6

Näätänen, R., Tervaniemi, M., Sussman, E. S., Paavilainen, P., & Winkler, I. (2001). "Primitive intelligence" in the auditory cortex. *Trends in Neurosciences*, *24*(5), 283–288. https://doi.org/10.1016/S0166-2236(00)01790-2

Näätänen, R., Todd, J., & Schall, U. (2016). Mismatch negativity (MMN) as biomarker predicting psychosis in clinically at-risk individuals. *Biological Psychology*, *116*, 36–40. https://doi.org/10.1016/j.biopsycho.2015.10.010

Näätänen, R., & Winkler, I. (1999). The concept of auditory stimulus representation in cognitive neuroscience. *Psychological Bulletin*, *125*(6), 826–859. https://doi.org/10.1037/0033-2909.125.6.826

Nashida, T., Yabe, H., Sato, Y., Hiruma, T., Sutoh, T., Shinozaki, N., & Kaneko, S. (2000). Automatic auditory information processing in sleep. *Sleep*, *23*(6), 821–828. http://www.ncbi.nlm.nih.gov/pubmed/11007449

Neisser, U. (1976). *Cognition and reality: Principles and implications of cognitive psychology*. W H Freeman/Times Books/ Henry Holt & Co.

Nelken, I. (2004). Processing of complex stimuli and natural scenes in the auditory cortex. *Current Opinion in Neurobiology*, *14*(4), 474–480. https://doi.org/10.1016/j.conb.2004.06.005

Nelken, I., & Ulanovsky, N. (2007). Mismatch negativity and stimulus-specific adaptation in animal models. *Journal of Psychophysiology*, *21*(3–4), 214–223. https://doi.org/10.1027/0269-8803.21.34.214

Netser, S., Zahar, Y., & Gutfreund, Y. (2011). Stimulus-specific adaptation: can it be a neural correlate of behavioral habituation? *Journal of Neuroscience*, *31*(49), 17811–17820. https://doi.org/10.1523/JNEUROSCI.4790-11.2011

Neve, K. A., Seamans, J. K., & Trantham-Davidson, H. (2004). Dopamine receptor signaling. *Journal of Receptors and Signal Transduction*, *24*(3), 165–205. https://doi.org/10.1081/RRS-200029981

Nevue, A. A., Elde, C. J., Perkei, D. J., & Portfors, C. V. (2016). Dopaminergic input to the inferior colliculus in mice. *Frontiers in Neuroanatomy*, *9*(JAN2016), 168. https://doi.org/10.3389/fnana.2015.00168

Nevue, A. A., Felix, R. A., & Portfors, C. V. (2016). Dopaminergic projections of the subparafascicular thalamic nucleus to the auditory brainstem. *Hearing Research*, *341*, 202–209. https://doi.org/10.1016/j.heares.2016.09.001

Nieto-Diego, J., & Malmierca, M. S. (2016). Topographic Distribution of Stimulus-Specific Adaptation across Auditory Cortical Fields in the Anesthetized Rat. *PLoS Biology*, *14*(3), e1002397. https://doi.org/10.1371/journal.pbio.1002397

Nobili, R., Mammano, F., & Ashmore, J. (1998). How well do we understand the cochlea? *Trends in Neurosciences*, *21*(4), 159–167. https://doi.org/10.1016/S0166-2236(97)01192-2

Nour, M. M., Dahoun, T., Schwartenbeck, P., Adams, R. A., FitzGerald, T. H. B., Coello, C., Wall, M. B., Dolan, R. J., & Howes, O. D. (2018). Dopaminergic basis for signaling belief updates, but not surprise, and the link to paranoia. *Proceedings of the National Academy of Sciences*, *115*(43), 201809298. https://doi.org/10.1073/pnas.1809298115

Nwabueze-Ogbo, F. C., Popelář, J., & Syka, J. (2003). Changes in Neuronal Activity of the Inferior Colliculus in Rat after Temporal Inactivation of the Auditory Cortex. *Physiological Research*, *52*(5), 615–628. http://www.biomed.cas.cz/physiolres

Ohishi, H., Shigemoto, R., Nakanishi, S., & Mizuno, N. (1993). Distribution of the messenger RNA for a metabotropic glutamate receptor, mGluR2, in the central nervous system of the rat. *Neuroscience*, *53*(4), 1009–1018. https://doi.org/10.1016/0306-4522(93)90485-X

Oliver, D. L. (1984a). Neuron types in the central nucleus of the inferior colliculus that project to the medial geniculate body. *Neuroscience*, *11*(2), 409–424. https://doi.org/10.1016/0306-4522(84)90033-2

Oliver, D. L. (1984b). Dorsal cochlear nucleus projections to the inferior colliculus in the cat: A light and electron microscopic study. *Journal of Comparative Neurology*, *224*(2), 155–172. https://doi.org/10.1002/cne.902240202

Oliver, D. L. (1987). Projections to the inferior colliculus from the anteroventral cochlear nucleus in the cat: Possible substrates for binaural interaction. *Journal of Comparative*

Neurology, *264*(1), 24–46. https://doi.org/10.1002/cne.902640104

Oliver, D. L. (2005). Neuronal organization in the inferior colliculus. In *The Inferior Colliculus* (pp. 69–114). Springer New York. https://doi.org/10.1007/0-387-27083-3_2

Oliver, D. L., & Huerta, M. F. (1992). *Inferior and Superior Colliculi* (pp. 168–221). Springer, New York, NY. https://doi.org/10.1007/978-1-4612-4416-5_5

Oliver, D. L., Kuwada, S., Yin, T. C. T., Haberly, L. B., & Henkel, C. K. (1991). Dendritic and axonal morphology of HRP-injected neurons in the inferior colliculus of the cat. *Journal of Comparative Neurology*, *303*(1), 75–100. https://doi.org/10.1002/cne.903030108

Oliver, D. L., Winer, J. A., Beckius, G. E., & Marie, R. L. S. (1994). Morphology of GABAergic neurons in the inferior colliculus of the cat. *Journal of Comparative Neurology*, *340*(1), 27–42. https://doi.org/10.1002/cne.903400104

Osen, K. K. (1969). Cytoarchitecture of the cochlear nuclei in the cat. *Journal of Comparative Neurology*, *136*(4), 453–483. https://doi.org/10.1002/cne.901360407

Ottersen, O. P., & Ben-Ari, Y. (1979). Afferent connections to the amygdaloid complex of the rat and cat. I. Projections from the thalamus. *Journal of Comparative Neurology*, *187*(2), 401–424. https://doi.org/10.1002/cne.901870209

Ottersen, O. P., & Storm-Mathisen, J. (1984). Glutamate- and GABA-containing neurons in the mouse and rat brain, as demonstrated with a new immunocytochemical technique. *Journal of Comparative Neurology*, *229*(3), 374–392. https://doi.org/10.1002/cne.902290308

Palombi, P. S., & Caspary, D. M. (1996). GABA inputs control discharge rate primarily within frequency receptive fields of inferior colliculus neurons. *Journal of Neurophysiology*, *75*(6), 2211–2219. https://doi.org/10.1152/jn.1996.75.6.2211

Papesh, M. A., & Hurley, L. M. (2016). Modulation of auditory brainstem responses by serotonin and specific serotonin receptors. *Hearing Research*, *332*, 121–136. https://doi.org/10.1016/j.heares.2015.11.014

Parr, T., & Friston, K. J. (2017). Uncertainty, epistemics and active Inference. *Journal of the Royal Society Interface*, *14*(136). https://doi.org/10.1098/rsif.2017.0376

Parr, T., & Friston, K. J. (2019). Attention or salience? *Current Opinion in Psychology*, *29*, 1–5. https://doi.org/10.1016/j.copsyc.2018.10.006

Parr, T., Rees, G., & Friston, K. J. (2018). Computational neuropsychology and Bayesian inference. *Frontiers in Human Neuroscience*, *12*, 61. https://doi.org/10.3389/fnhum.2018.00061

Parras, G. G., Nieto-Diego, J., Carbajal, G. V., Valdés-Baizabal, C., Escera, C., & Malmierca, M. S. (2017). Neurons along the auditory pathway exhibit a hierarchical organization of prediction error. *Nature Communications*, *8*(1), 2148. https://doi.org/10.1038/s41467-017-02038-6

Patel, C. R., Redhead, C., Cervi, A. L., & Zhang, H. (2012). Neural sensitivity to novel sounds in the rat's dorsal cortex of the inferior colliculus as revealed by evoked local field potentials. *Hearing Research*, *286*(1–2), 41–54. https://doi.org/10.1016/j.heares.2012.02.007

Paula-Barbosa, M. M., & Sousa-Pinto, A. (1973). Auditory cortical projections to the superior colliculus in the cat. *Brain Research*, *50*(1), 47–61. https://doi.org/10.1016/0006-8993(73)90593-3

Paxinos, G., & Watson, C. (2007). *The rat brain in stereotaxic coordinates*. Academic Press.

Pekkonen, E. (2000). Mismatch Negativity in Aging and in Alzheimer's and Parkinson's Diseases. *Audiology & Neurotology*, *5*(3–4), 216–224. https://doi.org/10.1159/000013883

Pérez-González, D., Hernández, O., Covey, E., & Malmierca, M. S. (2012). GABA A-mediated inhibition modulates stimulus-specific adaptation in the inferior colliculus. *PLoS ONE*, *7*(3), e34297. https://doi.org/10.1371/journal.pone.0034297

Pérez-González, D., & Malmierca, M. S. (2012). Variability of the time course of stimulus-specific adaptation in the inferior colliculus. *Frontiers in Neural Circuits*, *6*, 107. https://doi.org/10.3389/fncir.2012.00107

Pérez-González, D., Malmierca, M. S., & Covey, E. (2005). Novelty detector neurons in the mammalian auditory midbrain. *European Journal of Neuroscience*, *22*(11), 2879–2885. https://doi.org/10.1111/j.1460-9568.2005.04472.x

Pérez-González, D., Parras, G. G., Morado-Díaz, C. J., Aedo-Sánchez, C., Carbajal, G. V., & Malmierca, M. S. (2020). Deviance detection in physiologically identified cell types in the rat auditory cortex. *Hearing Research*, *399*, 107997. https://doi.org/10.1016/j.heares.2020.107997

Peruzzi, D., Sivaramakrishnan, S., & Oliver, D. L. (2000). Identification of cell types in brain slices of the inferior colliculus. *Neuroscience*, *101*(2), 403–416. https://doi.org/10.1016/S0306-4522(00)00382-1

Peter, V., McArthur, G., & Thompson, W. F. (2010). Effect of deviance direction and calculation method on duration and frequency mismatch negativity (MMN). *Neuroscience Letters*, *482*(1), 71–75. https://doi.org/10.1016/j.neulet.2010.07.010

Petersen, C. L., & Hurley, L. M. (2017). Putting it in context: Linking auditory processing with social behavior circuits in the vertebrate brain. *Integrative and Comparative Biology*, *57*(4), 865–877. https://doi.org/10.1093/icb/icx055

Phillips, H. N., Blenkmann, A., Hughes, L. E., Bekinschtein, T. A., & Rowe, J. B. (2015). Hierarchical Organization of Frontotemporal Networks for the Prediction of Stimuli across Multiple Dimensions. *Journal of Neuroscience*, *35*(25), 9255–9264. https://doi.org/10.1523/JNEUROSCI.5095-14.2015

Phillips, H. N., Blenkmann, A., Hughes, L. E., Kochen, S., Bekinschtein, T. A., Cam-CAN, & Rowe, J. B. (2016). Convergent evidence for hierarchical prediction networks from human electrocorticography and magnetoencephalography. *Cortex*, *82*, 192–205.

https://doi.org/10.1016/j.cortex.2016.05.001

Pickles, J. O., & Corey, D. P. (1992). Mechanoelectrical transduction by hair cells. *Trends in Neurosciences*, *15*(7), 254–259. https://doi.org/10.1016/0166-2236(92)90066-H

Picton, T. W. (2010). *Human Auditory Evoked Potentials*. Plural Publishing. https://books.google.es/books?hl=es&lr=&id=-N22CwAAQBAJ&oi=fnd&pg=PR5&dq=Picton+TW+(2010)+Human+auditory+evoked+potentials&ots=JkilubiSoN&sig=7Iq8TVomMM4vUWSi2YnhNDkyvq0#v=onepage&q=Picton TW (2010) Human auditory evoked potentials&f=false

Pienkowski, M., & Eggermont, J. J. (2009). Effects of adaptation on spectrotemporal receptive fields in primary auditory cortex. *NeuroReport*, *20*(13), 1198–1203. https://doi.org/10.1097/WNR.0b013e32832f812c

Pierson, M., & Snyder-Keller, A. (1994). Development of frequency-selective domains in inferior colliculus of normal and neonatally noise-exposed rats. *Brain Research*, *636*(1), 55–67. https://doi.org/10.1016/0006-8993(94)90175-9

Pincze, Z., Lakatos, P., Rajkai, C., Ulbert, I., & Karmos, G. (2001). Separation of mismatch negativity and the N1 wave in the auditory cortex of the cat: A topographic study. *Clinical Neurophysiology*, *112*(5), 778–784. https://doi.org/10.1016/S1388-2457(01)00509-0

Polley, D. B., Read, H. L., Storace, D. A., & Merzenich, M. M. (2007). Multiparametric Auditory Receptive Field Organization Across Five Cortical Fields in the Albino Rat. *Journal of Neurophysiology*, *97*(5), 3621–3638. https://doi.org/10.1152/jn.01298.2006

Ponnath, A., Hoke, K. L., & Farris, H. E. (2013). Stimulus change detection in phasic auditory units in the frog midbrain: Frequency and ear specific adaptation. *Journal of Comparative Physiology A: Neuroethology, Sensory, Neural, and Behavioral Physiology*, *199*(4), 295–313. https://doi.org/10.1007/s00359-013-0794-x

Prešern, J., Triblehorn, J. D., & Schul, J. (2015). Dynamic dendritic compartmentalization underlies stimulus-specific adaptation in an insect neuron. *Journal of Neurophysiology*, *113*(10), 3787–3797. https://doi.org/10.1152/jn.00945.2014

Quaedflieg, C. W., Münte, S., Kalso, E., & Sambeth, A. (2014). Effects of remifentanil on processing of auditory stimuli: A combined MEG/EEG study. *Journal of Psychopharmacology*, *28*(1), 39–48. https://doi.org/10.1177/0269881113512036

Rajan, R. (1990). Electrical stimulation of the inferior colliculus at low rates protects the cochlea from auditory desensitization. *Brain Research*, *506*(2), 192–204. https://doi.org/10.1016/0006-8993(90)91251-B

Ramón y Cajal, S. (1902). Estructura del tubérculo cuadrigémino posterior: Cuerpo geniculado interno y vías acústicas centrales. *Trabajos Del Laboratorio de Investigaciones Biológicas de La Universidad de Madrid*, *1*, 207–227.

Ramón y Cajal, S. (1904). *Histología del Sistema Nervioso del Hombre y los Vetebrados*. Imprenta N. Moya.

Ranganath, C., & Rainer, G. (2003). Cognitive neuroscience: Neural mechanisms for detecting and remembering novel events. *Nature Reviews Neuroscience*, *4*(3), 193–202. https://doi.org/10.1038/nrn1052

Rao, R. P. N., & Ballard, D. H. (1999). Predictive coding in the visual cortex: a functional interpretation of some extra-classical receptive-field effects. *Nature Neuroscience*, *2*(1), 79–87. https://doi.org/10.1038/4580

Read, H. L., Winer, J. A., & Schreiner, C. E. (2002). Functional architecture of auditory cortex. *Current Opinion in Neurobiology*, *12*(4), 433–440. https://doi.org/10.1016/S0959-4388(02)00342-2

Reale, R. A., & Imig, T. J. (1980). Tonotopic organization in auditory cortex of the cat. *Journal of Comparative Neurology*, *192*(2), 265–291. https://doi.org/10.1002/cne.901920207

Recasens, M., Grimm, S., Capilla, A., Nowak, R., & Escera, C. (2014). Two sequential processes of change detection in hierarchically ordered areas of the human auditory cortex. *Cerebral Cortex*, *24*(1), 143–153. https://doi.org/10.1093/cercor/bhs295

Recasens, M., Grimm, S., Wollbrink, A., Pantev, C., & Escera, C. (2014). Encoding of nested levels of acoustic regularity in hierarchically organized areas of the human auditory cortex. *Human Brain Mapping*, *35*(11), 5701–5716. https://doi.org/10.1002/hbm.22582

Reches, A., & Gutfreund, Y. (2008). Stimulus-Specific Adaptations in the Gaze Control System of the Barn Owl. *Journal of Neuroscience*, *28*(6), 1523–1533. https://doi.org/10.1523/JNEUROSCI.3785-07.2008

Reed, P., Mitchell, C., & Nokes, T. (1996). Intrinsic reinforcing properties of putatively neutral stimuli in an instrumental two-lever discrimination task. *Animal Learning and Behavior*, *24*(1), 38–45. https://doi.org/10.3758/BF03198952

Rees, A., & Orton, L. D. (2019). Unifying the Midbrain: The Commissure of the Inferior Colliculus. In *The Oxford Handbook of the Auditory Brainstem* (pp. 548–576). Oxford University Press. https://doi.org/10.1093/oxfordhb/9780190849061.013.21

Rees, A., Sarbaz, A., Malmierca, M. S., & Le Beau, F. E. N. (1997). Regularity of firing of neurons in the inferior colliculus. *Journal of Neurophysiology*, *77*(6), 2945–2965. https://doi.org/10.1152/jn.1997.77.6.2945

Reetz, G., & Ehret, G. (1999). Inputs from three brainstem sources to identified neurons of the mouse inferior colliculus slice. *Brain Research*, *816*(2), 527–543. https://doi.org/10.1016/S0006-8993(98)01230-X

Riquelme, R., Saldaña, E., Osen, K. K., Ottersen, O. P., & Merchán, M. A. (2001). Colocalization of GABA and glycine in the ventral nucleus of the lateral lemniscus in rat: An in situ hybridization and semiquantitative immunocytochemical study. *Journal of Comparative Neurology*, *432*(4), 409–424. https://doi.org/10.1002/cne.1111

Roberts, R. C., & Ribak, C. E. (1987). An electron microscopic study of GABAergic neurons and terminals in the central nucleus of the inferior colliculus of the rat. *Journal of Neurocytology*, *16*(3), 333–345. https://doi.org/10.1007/BF01611345

Robles, L., & Ruggero, M. A. (2001). Mechanics of the mammalian cochlea. In *Physiological Reviews* (Vol. 81, Issue 3, pp. 1305–1352). American Physiological Society. https://doi.org/10.1152/physrev.2001.81.3.1305

Rockel, A. J., & Jones, E. G. (1973). The neuronal organization of the inferior colliculus of the adult cat. I. The central nucleus. *Journal of Comparative Neurology*, *147*(1), 11–59. https://doi.org/10.1002/cne.901470103

Rodríguez, R. A., Bussière, M., Froeschl, M., & Nathan, H. J. (2014). Auditory-evoked potentials during coma: Do they improve our prediction of awakening in comatose patients? *Journal of Critical Care*, *29*(1), 93–100. https://doi.org/10.1016/j.jcrc.2013.08.020

Romanski, L. M., & Ledoux, J. E. (1993). Information cascade from primary auditory cortex to the amygdala: Corticocortical and corticoamygdaloid projections of temporal cortex in the rat. *Cerebral Cortex*, *3*(6), 515–532. https://doi.org/10.1093/cercor/3.6.515

Rubin, J., Ulanovsky, N., Nelken, I., & Tishby, N. (2016). The Representation of Prediction Error in Auditory Cortex. *PLoS Computational Biology*, *12*(8), e1005058. https://doi.org/10.1371/journal.pcbi.1005058

Ruhnau, P., Herrmann, B., & Schröger, E. (2012). Finding the right control: The mismatch negativity under investigation. *Clinical Neurophysiology*, *123*(3), 507–512. https://doi.org/10.1016/j.clinph.2011.07.035

Rummell, B. P., Klee, J. L., & Sigurdsson, T. (2016). Attenuation of responses to self-generated sounds in auditory cortical neurons. *The Journal of Neuroscience*, *36*(47), 12010–12026. https://doi.org/10.1523/jneurosci.1564-16.2016

Russell, I. J. (1983). Origin of the receptor potential in inner hair cells of the mammalian cochlea - Evidence for Davis' theory. *Nature*, *301*(5898), 334–336. https://doi.org/10.1038/301334a0

Rutkowski, R. G., Miasnikov, A. A., & Weinberger, N. M. (2003). Characterisation of multiple physiological fields within the anatomical core of rat auditory cortex. *Hearing Research*, *181*(1–2), 116–130. https://doi.org/10.1016/S0378-5955(03)00182-5

Ryugo, D. K., & Killackey, H. P. (1974). Differential telencephalic projections of the medial and ventral divisions of the medial geniculate body of the rat. *Brain Research*, *82*(1), 173–177. https://doi.org/10.1016/0006-8993(74)90903-2

Sadacca, B. F., Jones, J. L., & Schoenbaum, G. (2016). Midbrain dopamine neurons compute inferred and cached value prediction errors in a common framework. *ELife*, *5*(MARCH2016). https://doi.org/10.7554/eLife.13665

Saldaña, E., Feliciano, M., & Mugnaini, E. (1996). Distribution of descending projections from primary auditory neocortex to inferior colliculus mimics the topography of intracollicular projections. *Journal of Comparative Neurology*, *371*(1), 15–40. https://doi.org/10.1002/(SICI)1096-9861(19960715)371:1<15::AID-CNE2>3.0.CO;2-O

Saldaña, E., & Merchán, M. A. (1992). Intrinsic and commissural connections of the rat inferior colliculus. *Journal of Comparative Neurology*, *319*(3), 417–437.

https://doi.org/10.1002/cne.903190308

Sánchez-Vives, M. V., Nowak, L. G., & McCormick, D. A. (2000a). Cellular mechanisms of long-lasting adaptation in visual cortical neurons in vitro. *The Journal of Neuroscience*, *20*(11), 4286–4299. https://doi.org/10.1523/JNEUROSCI.20-11-04286.2000

Sánchez-Vives, M. V., Nowak, L. G., & McCormick, D. A. (2000b). Membrane mechanisms underlying contrast adaptation in cat area 17 in vivo. *Journal of Neuroscience*, *20*(11), 4267–4285. https://doi.org/10.1523/JNEUROSCI.20-11-04267.2000

Sceniak, M. P., & MacIver, M. B. (2006). Cellular Actions of Urethane on Rat Visual Cortical Neurons In Vitro. *Journal of Neurophysiology*, *95*(6), 3865–3874. https://doi.org/10.1152/jn.01196.2005

Schall, U. (2016). Is it time to move mismatch negativity into the clinic? *Biological Psychology*, *116*, 41–46. https://doi.org/10.1016/j.biopsycho.2015.09.001

Schinkel-Bielefeld, N., David, S. V., Shamma, S. A., & Butts, D. A. (2012). Inferring the role of inhibition in auditory processing of complex natural stimuli. *Journal of Neurophysiology*, *107*(12), 3296–3307. https://doi.org/10.1152/jn.01173.2011

Schmid, S., Guthmann, A., Ruppersberg, J. P., & Herbert, H. (2001). Expression of AMPA receptor subunit flip/flop splice variants in the rat auditory brainstem and inferior colliculus. *Journal of Comparative Neurology*, *430*(2), 160–171. https://doi.org/10.1002/1096-9861(20010205)430:2<160::AID-CNE1022>3.0.CO;2-3

Schofield, B. R., & Beebe, N. L. (2019). Descending Auditory Pathways and Plasticity. In *The Oxford Handbook of the Auditory Brainstem* (pp. 610–638). Oxford University Press. https://doi.org/10.1093/oxfordhb/9780190849061.013.17

Schröger, E., Bendixen, A., Denham, S. L., Mill, R. W., Bohm, T. M., & Winkler, I. (2014). Predictive regularity representations in violation detection and auditory stream segregation: From conceptual to computational models. *Brain Topography*, *27*(4), 565–577. https://doi.org/10.1007/s10548-013-0334-6

Schröger, E., Marzecová, A., & SanMiguel, I. (2015). Attention and prediction in human audition: A lesson from cognitive psychophysiology. *European Journal of Neuroscience*, *41*(5), 641–664. https://doi.org/10.1111/ejn.12816

Schröger, E., & Wolff, C. (1996). Mismatch response of the human brain to changes in sound location. *Neuroreport*, *7*(18), 3005–3008. https://doi.org/10.1097/00001756-199611250-00041

Schul, J., Mayo, A. M., & Triblehorn, J. D. (2012). Auditory change detection by a single neuron in an insect. *Journal of Comparative Physiology A: Neuroethology, Sensory, Neural, and Behavioral Physiology*, *198*(9), 695–704. https://doi.org/10.1007/s00359-012-0740-3

Schultz, W. (1998). Predictive reward signal of dopamine neurons. *Journal of Neurophysiology*, *80*(1), 1–27. https://doi.org/10.1152/jn.1998.80.1.1

Schultz, W. (2007). Multiple Dopamine Functions at Different Time Courses. *Annual Review*

of Neuroscience, *30*(1), 259–288. https://doi.org/10.1146/annurev.neuro.28.061604.135722

Schultz, W. (2016a). Dopamine reward prediction-error signalling: A two-component response. *Nature Reviews Neuroscience*, *17*(3), 183–195. https://doi.org/10.1038/nrn.2015.26

Schultz, W. (2016b). Dopamine reward prediction error coding. *Dialogues in Clinical Neuroscience*, *18*(1), 23–32. https://doi.org/10.1038/nrn.2015.26

Schultz, W., Dayan, P., & Montague, P. R. (1997). A Neural Substrate of Prediction and Reward. *Science*, *275*(5306), 1593–1599. https://doi.org/10.1126/science.275.5306.1593

Schwartenbeck, P., FitzGerald, T. H. B., Mathys, C. D., Dolan, R., & Friston, K. J. (2015). The dopaminergic midbrain encodes the expected certainty about desired outcomes. *Cerebral Cortex*, *25*(10), 3434–3445. https://doi.org/10.1093/cercor/bhu159

Schwartz, S., Shinn-Cunningham, B. G., & Tager-Flusberg, H. (2018). Meta-analysis and systematic review of the literature characterizing auditory mismatch negativity in individuals with autism. *Neuroscience and Biobehavioral Reviews*, *87*, 106–117. https://doi.org/10.1016/j.neubiorev.2018.01.008

Sedley, W., Gander, P. E., Kumar, S., Kovach, C. K., Oya, H., Kawasaki, H., Howard, M. A., & Griffiths, T. D. (2016). Neural signatures of perceptual inference. *ELife*, *5*. https://doi.org/10.7554/elife.11476

Seer, C., Lange, F., Georgiev, D., Jahanshahi, M., & Kopp, B. (2016). Event-related potentials and cognition in Parkinson's disease: An integrative review. *Neuroscience & Biobehavioral Reviews*, *71*, 691–714. https://doi.org/10.1016/J.NEUBIOREV.2016.08.003

Shen, L., Zhao, L., & Hong, B. (2015). Frequency-specific adaptation and its underlying circuit model in the auditory midbrain. *Frontiers in Neural Circuits*, *9*, 55. https://doi.org/10.3389/fncir.2015.00055

Sherman, S. M. (2007). The thalamus is more than just a relay. *Current Opinion in Neurobiology*, *17*(4), 417–422. https://doi.org/10.1016/j.conb.2007.07.003

Sherman, S. M., & Guillery, R. W. (2011). Distinct functions for direct and transthalamic corticocortical connections. *Journal of Neurophysiology*, *106*(3), 1068–1077. https://doi.org/10.1152/jn.00429.2011

Shi, C. J., & Cassell, M. D. (1997). Cortical, thalamic, and amygdaloid projections of rat temporal cortex. *Journal of Comparative Neurology*, *382*(2), 153–175. https://doi.org/10.1002/(SICI)1096-9861(19970602)382:2<153::AID-CNE2>3.0.CO;2-2

Shiga, T., Althen, H., Cornella, M., Zarnowiec, K., Yabe, H., & Escera, C. (2015). Deviance-related responses along the auditory hierarchy: Combined FFR, MLR and MMN evidence. *PLoS ONE*, *10*(9), 1–14. https://doi.org/10.1371/journal.pone.0136794

Shiramatsu, T. I., Kanzaki, R., Takahashi, H., Sams, M., & Näätänen, R. (2013). Cortical Mapping of Mismatch Negativity with Deviance Detection Property in Rat. *PLoS ONE*,

8(12), e82663. https://doi.org/10.1371/journal.pone.0082663

Shneiderman, A., & Henkel, C. K. (1987). Banding of lateral superior olivary nucleus afferents in the inferior colliculus: A possible substrate for sensory integration. *Journal of Comparative Neurology*, *266*(4), 519–534. https://doi.org/10.1002/cne.902660406

Shosaku, A., & Sumitomo, I. (1983). Auditory neurons in the rat thalamic reticular nucleus. *Experimental Brain Research*, *49*(3), 432–442. https://doi.org/10.1007/BF00238784

Sillito, A. M., Cudeiro, J., & Jones, H. E. (2006). Always returning: feedback and sensory processing in visual cortex and thalamus. *Trends in Neurosciences*, *29*(6), 307–316. https://doi.org/10.1016/j.tins.2006.05.001

Sivaramakrishnan, S., & Oliver, D. L. (2001). Distinct K currents result in physiologically distinct cell types in the inferior colliculus of the rat. *Journal of Neuroscience*, *21*(8), 2861–2877. https://doi.org/10.1523/jneurosci.21-08-02861.2001

Skoe, E., Chandrasekaran, B., Spitzer, E. R., Wong, P. C. M., & Kraus, N. (2014). Human brainstem plasticity: The interaction of stimulus probability and auditory learning. *Neurobiology of Learning and Memory*, *109*, 82–93. https://doi.org/10.1016/j.nlm.2013.11.011

Slabu, L., Escera, C., Grimm, S., & Costa-Faidella, J. (2010). Early change detection in humans as revealed by auditory brainstem and middle-latency evoked potentials. *European Journal of Neuroscience*, *32*(5), 859–865. https://doi.org/10.1111/j.1460-9568.2010.07324.x

Slabu, L., Grimm, S., & Escera, C. (2012). Novelty detection in the human auditory brainstem. *The Journal of Neuroscience*, *32*(4), 1447–1452. https://doi.org/32/4/1447 [pii]\r10.1523/JNEUROSCI.2557-11.2012

Slepecky, N. B. (1996). Structure of the Mammalian Cochlea. In P. Dallos, A. N. Popper, & R. R. Fay (Eds.), *The Cochlea* (pp. 44–129). Springer. https://doi.org/10.1007/978-1-4612-0757-3_2

Smith, P. H. (1992). Anatomy and physiology of multipolar cells in the rat inferior collicular cortex using the in vitro brain slice technique. *Journal of Neuroscience*, *12*(9), 3700–3715. https://doi.org/10.1523/jneurosci.12-09-03700.1992

Smith, Philip H., Uhlrich, D. J., Manning, K. A., & Banks, M. I. (2012). Thalamocortical projections to rat auditory cortex from the ventral and dorsal divisions of the medial geniculate nucleus. *Journal of Comparative Neurology*, *520*(1), 34–51. https://doi.org/10.1002/cne.22682

Sonnadara, R. R., Alain, C., & Trainor, L. J. (2006). Occasional changes in sound location enhance middle latency evoked responses. *Brain Research*, *1076*(1), 187–192. https://doi.org/10.1016/j.brainres.2005.12.093

Spratling, M. W. (2008a). Predictive coding as a model of biased competition in visual attention. *Vision Research*, *48*(12), 1391–1408. https://doi.org/10.1016/j.visres.2008.03.009

Spratling, M. W. (2008b). Reconciling predictive coding and biased competition models of cortical function. *Frontiers in Computational Neuroscience*, *2*, 4. https://doi.org/10.3389/neuro.10.004.2008

Spratling, M. W. (2010). Predictive coding as a model of response properties in cortical area V1. *Journal of Neuroscience*, *30*(9), 3531–3543. https://doi.org/10.1523/jneurosci.4911-09.2010

Spreafico, R., Hayes, N. L., & Rustioni, A. (1981). Thalamic projections to the primary and secondary somatosensory cortices in cat: Single and double retrograde tracer studies. *Journal of Comparative Neurology*, *203*(1), 67–90. https://doi.org/10.1002/cne.902030107

Srivastava, H. K., & Bandyopadhyay, S. (2020). Parallel lemniscal and non-lemniscal sources control auditory responses in the orbitofrontal cortex (OFC). *Eneuro*, ENEURO.0121-20.2020. https://doi.org/10.1523/eneuro.0121-20.2020

Stefanics, G., Kremláček, J., & Czigler, I. (2014). Visual mismatch negativity: a predictive coding view. *Frontiers in Human Neuroscience*, *8*, 666. https://doi.org/10.3389/fnhum.2014.00666

Stockard, J. J., Stockard, J. E., & Sharbrough, F. W. (1979). Brain-stem auditory-evoked responses. *Archives of Neurology*, *36*(9), 597–598. https://doi.org/10.1001/archneur.1979.00500450091025

Storace, D. A., Higgins, N. C., & Read, H. L. (2010). Thalamic label patterns suggest primary and ventral auditory fields are distinct core regions. *Journal of Comparative Neurology*, *518*(10), 1630–1646. https://doi.org/10.1002/cne.22345

Storace, D. A., Higgins, N. C., & Read, H. L. (2011). Thalamocortical pathway specialization for sound frequency resolution. *Journal of Comparative Neurology*, *519*(2), 177–193. https://doi.org/10.1002/cne.22501

Stornetta, R. L., Macon, C. J., Nguyen, T. M., Coates, M. B., & Guyenet, P. G. (2013). Cholinergic neurons in the mouse rostral ventrolateral medulla target sensory afferent areas. *Brain Structure and Function*, *218*(2), 455–475. https://doi.org/10.1007/s00429-012-0408-3

Strauss, M., Sitt, J. D., King, J.-R., Elbaz, M., Azizi, L., Buiatti, M., Naccache, L., van Wassenhove, V., & Dehaene, S. (2015). Disruption of hierarchical predictive coding during sleep. *Proceedings of the National Academy of Sciences*, *112*(11), E1353–E1362. https://doi.org/10.1073/pnas.1501026112

Strecker, R. E., & Jacobs, B. L. (1985). Substantia nigra dopaminergic unit activity in behaving cats: Effect of arousal on spontaneous discharge and sensory evoked activity. *Brain Research*, *361*(1–2), 339–350. https://doi.org/10.1016/0006-8993(85)91304-6

Suga, N., Gao, E., Zhang, Y., Ma, X., & Olsen, J. F. (2000). The corticofugal system for hearing: Recent progress. *Proceedings of the National Academy of Sciences of the United States of America*, *97*(22), 11807–11814. https://doi.org/10.1073/pnas.97.22.11807

Sussman, E. S., Chen, S., Sussman-Fort, J., & Dinces, E. (2014). The five myths of MMN: Redefining how to Use MMN in basic and clinical research. *Brain Topography*, *27*(4), 553–564. https://doi.org/10.1007/s10548-013-0326-6

Sutter, M. L., & Shamma, S. A. (2011). The relationship of auditory cortical activity to perception and behavior. In *The Auditory Cortex* (pp. 617–641). Springer US. https://doi.org/10.1007/978-1-4419-0074-6_29

Taaseh, N., Yaron, A., & Nelken, I. (2011). Stimulus-Specific Adaptation and Deviance Detection in the Rat Auditory Cortex. *PLoS ONE*, *6*(8), e23369. https://doi.org/10.1371/journal.pone.0023369

Tan, A. Y. Y., Atencio, C. A., Polley, D. B., Merzenich, M. M., & Schreiner, C. E. (2007). Unbalanced synaptic inhibition can create intensity-tuned auditory cortex neurons. *Neuroscience*, *146*(1), 449–462. https://doi.org/10.1016/j.neuroscience.2007.01.019

Thomas, J. M., Morse, C., Kishline, L., O'Brien-Lambert, A., Simonton, A., Miller, K. E., & Covey, E. (2012). Stimulus-specific adaptation in specialized neurons in the inferior colliculus of the big brown bat, Eptesicus fuscus. *Hearing Research*, *291*(1–2), 34–40. https://doi.org/10.1016/j.heares.2012.06.004

Thompson, G. C., Thompson, A. M., Britton, B. H., & Garrett, K. M. (1994). Serotonin and serotonin receptors in the central auditory system. *Otolaryngology–Head and Neck Surgery*, *110*(1), 93–102. https://doi.org/10.1177/019459989411000111

Thompson, W. H. (1901). Degenerations resulting from Lesions of the Cortex of the Temporal Lobe. *Journal of Anatomy*, *35*(Pt 2), 147–165. http://www.ncbi.nlm.nih.gov/pubmed/17232464

Todd, J., Harms, L., Schall, U., Schal l, U., & Michie, P. T. (2013). Mismatch negativity: Translating the potential. *Frontiers in Psychiatry*, *4*(DEC), 171. https://doi.org/10.3389/fpsyt.2013.00171

Tokunaga, A., Sugita, S., & Otani, K. (1984). Auditory and non-auditory subcortical afferents to the inferior colliculus in the rat. *Journal Fur Hirnforschung*, *25*(4), 461–472. https://europepmc.org/article/med/6481158

Triblehorn, J. D., & Schul, J. (2013). Dendritic mechanisms contribute to stimulus-specific adaptation in an insect neuron. *Journal of Neurophysiology*, *110*(9), 2217–2226. https://doi.org/10.1152/jn.00057.2013

Tsodyks, M. V., & Markram, H. (1997). The neural code between neocortical pyramidal neurons depends on neurotransmitter release probability. *Proceedings of the National Academy of Sciences*, *94*(2), 719–723. https://doi.org/10.1073/pnas.94.2.719

Ulanovsky, N., Las, L., Farkas, D., & Nelken, I. (2004). Multiple time scales of adaptation in auditory cortex neurons. *J.Neurosci.*, *24*(46), 10440–10453. https://doi.org/10.1523/JNEUROSCI.1905-04.2004

Ulanovsky, N., Las, L., & Nelken, I. (2003). Processing of low-probability sounds by cortical neurons. *Nature Neuroscience*, *6*(4), 391–398. https://doi.org/10.1038/nn1032

Valdés-Baizabal, C., Carbajal, G. V., Pérez-González, D., & Malmierca, M. S. (2020). Dopamine modulates subcortical responses to surprising sounds. *PLoS Biology*, *18*(6), e3000744. https://doi.org/10.1371/journal.pbio.3000744

Valdés-Baizabal, C., Casado-Román, L., Bartlett, E. L., & Malmierca, M. S. (2020). In vivo whole-cell recordings of stimulus-specific adaptation in the inferior colliculus. *Hearing Research*, *xxxx*, 107978. https://doi.org/10.1016/j.heares.2020.107978

Valdés-Baizabal, C., Parras, G. G., Ayala, Y. A., & Malmierca, M. S. (2017). Endocannabinoid Modulation of Stimulus-Specific Adaptation in Inferior Colliculus Neurons of the Rat. *Scientific Reports*, *7*(1), 6997. https://doi.org/10.1038/s41598-017-07460-w

Vaudano, E., Legg, C. R., & Glickstein, M. (1991). Afferent and Efferent Connections of Temporal Association Cortex in the Rat: A Horseradish Peroxidase Study. *European Journal of Neuroscience*, *3*(4), 317–330. https://doi.org/10.1111/j.1460-9568.1991.tb00818.x

Vaughn, M. D., Pozza, M. F., & Lingenhöhl, K. (1996). Excitatory acoustic responses in the inferior colliculus of the rat are increased by GABA(B) receptor blockade. *Neuropharmacology*, *35*(12), 1761–1767. https://doi.org/10.1016/S0028-3908(96)00143-8

Vetter, D. E., Saldaña, E., & Mugnaini, E. (1993). Input from the inferior colliculus to medial olivocochlear neurons in the rat: A double label study with PHA-L and cholera toxin. *Hearing Research*, *70*(2), 173–186. https://doi.org/10.1016/0378-5955(93)90156-U

Vlaskamp, C., Oranje, B., Madsen, G. F., Møllegaard Jepsen, J. R., Durston, S., Cantio, C., Glenthøj, B., & Bilenberg, N. (2017). Auditory processing in autism spectrum disorder: Mismatch negativity deficits. *Autism Research*, *10*(11), 1857–1865. https://doi.org/10.1002/aur.1821

von Békésy, G. (1960). *Experiments in Hearing*. McGraw-Hill. https://doi.org/10.1121/1.399656

von der Behrens, W., Bäuerle, P., Kössl, M., & Gaese, B. H. (2009). Correlating Stimulus-Specific Adaptation of Cortical Neurons and Local Field Potentials in the Awake Rat. *Journal of Neuroscience*, *29*(44), 13837–13849. https://doi.org/10.1523/JNEUROSCI.3475-09.2009

Wacongne, C., Changeux, J.-P. J.-P., & Dehaene, S. (2012). A Neuronal Model of Predictive Coding Accounting for the Mismatch Negativity. *Journal of Neuroscience*, *32*(11), 3665–3678. https://doi.org/10.1523/JNEUROSCI.5003-11.2012

Wallace, M. N., Shackleton, T. M., & Palmer, A. R. (2012). Morphological and physiological characteristics of laminar cells in the central nucleus of the inferior colliculus. *Frontiers in Neural Circuits*, *6*(JULY 2012), 55. https://doi.org/10.3389/fncir.2012.00055

Wang, J., Palkovits, M., Usdin, T. B., & Dobolyi, A. (2006). Afferent connections of the subparafascicular area in rat. *Neuroscience*, *138*(1), 197–220. https://doi.org/10.1016/j.neuroscience.2005.11.010

Warr, W. B., & Beck, J. E. (1996). Multiple projections from the ventral nucleus of the trapezoid body in the rat. *Hearing Research*, *93*(1–2), 83–101. https://doi.org/10.1016/0378-5955(95)00198-0

Weinberger, N. M. (2004). Specific long-term memory traces in primary auditory cortex. *Nature Reviews Neuroscience*, *5*(4), 279–290. https://doi.org/10.1038/nrn1366

Weiner, D. M., Levey, A. I., Sunahara, R. K., Niznik, H. B., O'Dowd, B. F., Seeman, P., & Brann, M. R. (1991). D1 and D2 dopamine receptor mRNA in rat brain. *Proceedings of the National Academy of Sciences of the United States of America*, *88*(5), 1859–1863. https://doi.org/10.1073/PNAS.88.5.1859

Wiens, S., Szychowska, M., Eklund, R., & van Berlekom, E. (2019). Cascade and no-repetition rules are comparable controls for the auditory frequency mismatch negativity in oddball tasks. *Psychophysiology*, *56*(1), e13280. https://doi.org/10.1111/psyp.13280

Winer, Jeffery A. (2005). Decoding the auditory corticofugal systems. *Hearing Research*, *207*(1–2), 1–9. https://doi.org/10.1016/j.heares.2005.06.007

Winer, Jeffery A., Chernock, M. L., Larue, D. T., & Cheung, S. W. (2002). Descending projections to the inferior colliculus from the posterior thalamus and the auditory cortex in rat, cat, and monkey. *Hearing Research*, *168*(1–2), 181–195. https://doi.org/10.1016/S0378-5955(02)00489-6

Winer, Jeffery A., Kelly, J. B., & Larue, D. T. (1999). Neural architecture of the rat medial geniculate body. *Hearing Research*, *130*(1–2), 19–41. https://doi.org/10.1016/S0378-5955(98)00216-0

Winer, Jeffery A., & Larue, D. T. (1987). Patterns of reciprocity in auditory thalamocortical and corticothalamic connections: Study with horseradish peroxidase and autoradiographic methods in the rat medial geniculate body. *Journal of Comparative Neurology*, *257*(2), 282–315. https://doi.org/10.1002/cne.902570212

Winer, Jeffery A., & Larue, D. T. (1988). Anatomy of glutamic acid decarboxylase immunoreactive neurons and axons in the rat medial geniculate body. *Journal of Comparative Neurology*, *278*(1), 47–68. https://doi.org/10.1002/cne.902780104

Winer, Jeffery A., Larue, D. T., Diehl, J. J., & Hefti, B. J. (1998). Auditory cortical projections to the cat inferior colliculus. *Journal of Comparative Neurology*, *400*(2), 147–174. https://doi.org/10.1002/(SICI)1096-9861(19981019)400:2<147::AID-CNE1>3.0.CO;2-9

Winer, Jeffery A., Larue, D. T., & Huang, C. L. (1999). Two systems of giant axon terminals in the cat medial geniculate body: Convergence of cortical and GABAergic inputs. *Journal of Comparative Neurology*, *413*(2), 181–197. https://doi.org/10.1002/(SICI)1096-9861(19991018)413:2<181::AID-CNE1>3.0.CO;2-7

Winer, Jeffery A., & Lee, C. C. (2007). The distributed auditory cortex. *Hearing Research*, *229*(1–2), 3–13. https://doi.org/10.1016/j.heares.2007.01.017

Winer, Jeffery A., Saint Marie, R. L., Larue, D. T., & Oliver, D. L. (1996). GABAergic feedforward projections from the inferior colliculus to the medial geniculate body.

Proceedings of the National Academy of Sciences of the United States of America, *93*(15), 8005–8010. https://doi.org/10.1073/pnas.93.15.8005

Winer, Jeffery A., Sally, S. L., Larue, D. T., & Kelly, J. B. (1999). Origins of medial geniculate body projections to physiologically defined zones of rat primary auditory cortex. *Hearing Research*, *130*(1–2), 42–61. https://doi.org/10.1016/S0378-5955(98)00217-2

Winkler, I., & Czigler, I. (2012). Evidence from auditory and visual event-related potential (ERP) studies of deviance detection (MMN and vMMN) linking predictive coding theories and perceptual object representations. *International Journal of Psychophysiology*, *83*(2), 132–143. https://doi.org/10.1016/j.ijpsycho.2011.10.001

Winkler, I., Denham, S. L., & Nelken, I. (2009). Modeling the auditory scene: predictive regularity representations and perceptual objects. *Trends in Cognitive Sciences*, *13*(12), 532–540. https://doi.org/10.1016/j.tics.2009.09.003

Winkler, I., Karmos, G., & Näätänen, R. (1996). Adaptive modeling of the unattended acoustic environment reflected in the mismatch negativity event-related potential. *Brain Research*, *742*(1–2), 239–252. https://doi.org/10.1016/S0006-8993(96)01008-6

Winkler, I., Kushnerenko, E., Horváth, J., Ceponiene, R., Fellman, V., Huotilainen, M., Näätänen, R., & Sussman, E. S. (2003). Newborn infants can organize the auditory world. *Proceedings of the National Academy of Sciences*, *100*(20), 11812–11815. https://doi.org/10.1073/pnas.2031891100

Winkler, I., & Schröger, E. (2015). Auditory perceptual objects as generative models: Setting the stage for communication by sound. *Brain and Language*, *148*, 1–22. https://doi.org/10.1016/j.bandl.2015.05.003

Yaron, A., Hershenhoren, I., & Nelken, I. (2012). Sensitivity to Complex Statistical Regularities in Rat Auditory Cortex. *Neuron*, *76*(3), 603–615. https://doi.org/10.1016/j.neuron.2012.08.025

Yasui, Y., Kayahara, T., Kuga, Y., & Nakano, K. (1990). Direct projections from the globus pallidus to the inferior colliculus in the rat. *Neuroscience Letters*, *115*(2–3), 121–125. https://doi.org/10.1016/0304-3940(90)90441-B

Yasui, Y., Kayahara, T., Nakano, K., & Mizuno, N. (1990). The subparafascicular thalamic nucleus of the rat receives projection fibers from the inferior colliculus and auditory cortex. *Brain Research*, *537*(1–2), 323–327. https://doi.org/10.1016/0006-8993(90)90378-O

Yasui, Y., Nakano, K., & Mizuno, N. (1992). Descending projections from the subparafascicular thalamic nucleus to the lower brain stem in the rat. *Experimental Brain Research*, *90*(3), 508–518. https://doi.org/10.1007/BF00230933

Young, A. M. J., Joseph, M. H., & Gray, J. A. (1993). Latent inhibition of conditioned dopamine release in rat nucleus accumbens. *Neuroscience*, *54*(1), 5–9. https://doi.org/10.1016/0306-4522(93)90378-S

Yu, X. J., Meng, X. K., Xu, X. X., & He, J. (2011). Individual auditory thalamic reticular

neurons have large and cross-modal sources of cortical and thalamic inputs. *Neuroscience*, *193*, 122–131. https://doi.org/10.1016/j.neuroscience.2011.07.040

Yu, X. J., Xu, X. X., He, S., & He, J. (2009). Change detection by thalamic reticular neurons. *Nature Neuroscience*, *12*(9), 1165–1170. https://doi.org/10.1038/nn.2373

Yvert, B., Crouzeix, A., Bertrand, O., Seither-Preisler, A., & Pantev, C. (2001). Multiple Supratemporal Sources of Magnetic and Electric Auditory Evoked Middle Latency Components in Humans. *Cerebral Cortex*, *11*(5), 411–423. https://doi.org/10.1093/cercor/11.5.411

Yvert, B., Fischer, C., Bertrand, O., & Pernier, J. (2005). Localization of human supratemporal auditory areas from intracerebral auditory evoked potentials using distributed source models. *NeuroImage*, *28*(1), 140–153. https://doi.org/10.1016/j.neuroimage.2005.05.056

Zhang, H., & Kelly, J. B. (2001). AMPA and NMDA receptors regulate responses of neurons in the rat's inferior colliculus. *Journal of Neurophysiology*, *86*(2), 871–880. https://doi.org/10.1152/jn.2001.86.2.871

Zhang, H., & Kelly, J. B. (2003). Glutamatergic and GABAergic regulation of neural responses in inferior colliculus to amplitude-modulated sounds. *Journal of Neurophysiology*, *90*(1), 477–490. https://doi.org/10.1152/jn.01084.2002

Zhang, L. I., Tan, A. Y. Y., Schreiner, C. E., & Merzenich, M. M. (2003). Topography and synaptic shaping of direction selectivity in primary auditory cortex. *Nature*, *424*(6945), 201–205. https://doi.org/10.1038/nature01796

Zhang, Y., & Wu, S. H. (2000). Long-term potentiation in the inferior colliculus studied in rat brain slice. *Hearing Research*, *147*(1–2), 92–103. https://doi.org/10.1016/S0378-5955(00)00123-4

Zhao, L., Liu, Y., Shen, L., Feng, L., & Hong, B. (2011). Stimulus-specific adaptation and its dynamics in the inferior colliculus of rat. *Neuroscience*, *181*, 163–174. https://doi.org/10.1016/j.neuroscience.2011.01.060

Zweifel, L. S., Fadok, J. P., Argilli, E., Garelick, M. G., Jones, G. L., Dickerson, T. M. K., Allen, J. M., Mizumori, S. J. Y., Bonci, A., & Palmiter, R. D. (2011). Activation of dopamine neurons is critical for aversive conditioning and prevention of generalized anxiety. *Nature Neuroscience*, *14*(5), 620–628. https://doi.org/10.1038/nn.2808

FINANTIAL INFORMATION

Financial support to elaborate this thesis was provided by the Spanish Ministry of Economy (project reference: SAF2016-75803-P), a PhD fellowship from the Spanish Ministry of Science and Innovation (BES-2017-080030), and a mobility fellowship from the European Commission's Erasmus Mundus Student Exchange Network in Auditory Cognitive Neuroscience.